



Swansea University
Prifysgol Abertawe



Swansea University E-Theses

Rapid species identification and antimicrobial susceptibility testing using Raman spectroscopy.

Kapel, Natalia

How to cite:

Kapel, Natalia (2013) *Rapid species identification and antimicrobial susceptibility testing using Raman spectroscopy.* thesis, Swansea University.

<http://cronfa.swan.ac.uk/Record/cronfa42219>

Use policy:

This item is brought to you by Swansea University. Any person downloading material is agreeing to abide by the terms of the repository licence: copies of full text items may be used or reproduced in any format or medium, without prior permission for personal research or study, educational or non-commercial purposes only. The copyright for any work remains with the original author unless otherwise specified. The full-text must not be sold in any format or medium without the formal permission of the copyright holder. Permission for multiple reproductions should be obtained from the original author.

Authors are personally responsible for adhering to copyright and publisher restrictions when uploading content to the repository.

Please link to the metadata record in the Swansea University repository, Cronfa (link given in the citation reference above.)

<http://www.swansea.ac.uk/library/researchsupport/ris-support/>

Rapid species identification and antimicrobial susceptibility testing using Raman spectroscopy

by

Natalia Kapel



**Swansea University
Prifysgol Abertawe**

Submitted to Swansea University in fulfilment of the requirements for the degree of
Doctor of Philosophy

Swansea University

2013



ProQuest Number: 10797921

All rights reserved

INFORMATION TO ALL USERS

The quality of this reproduction is dependent upon the quality of the copy submitted.

In the unlikely event that the author did not send a complete manuscript and there are missing pages, these will be noted. Also, if material had to be removed, a note will indicate the deletion.



ProQuest 10797921

Published by ProQuest LLC (2018). Copyright of the Dissertation is held by the Author.

All rights reserved.

This work is protected against unauthorized copying under Title 17, United States Code
Microform Edition © ProQuest LLC.

ProQuest LLC.
789 East Eisenhower Parkway
P.O. Box 1346
Ann Arbor, MI 48106 – 1346



SUMMARY

Infectious diseases remain a serious threat to human life and health as well as having important economical factor. One way of successful combating diseases is designing the most appropriate treatment plan following the correct diagnosis. Therefore, there is a need for a method combining reproducibility, precision and speed.

The aim of this work was to evaluate the potential of micro-Raman spectroscopy for identifying bacteria at different taxonomic levels, strains revealing different antibiotic resistance profiles, and for phylogenetic investigation.

The project was based on a selection of bacteria: *Staphylococcus aureus* (6571, Cowan1), *Staphylococcus epidermidis* (1457, 9142), *Escherichia coli* including wild-types (strain B, K12, Top10), transformants expressing ampicillin and kanamycin resistance (Top10^{Amp}, Top10^{Kan}) and clinical isolates expressing extended-spectrum beta-lactamases (ESBL).

Following a precise and detailed protocol, Raman spectra were recorded from bacterial colonies grown overnight on a Colombia Blood Agar. In order to remove background fluorescence, rolling-circle filter procedure was applied. The most critical peaks for differentiation between organisms as well as for characterising each microorganism were determined. The spectral data were analyzed using principal component and cluster analysis techniques.

As expected, the degree of separation decreased in the order genus → species → strain. It was determined that DNA/RNA, proteins and amino-acids are responsible for the differentiation between strains on a lower level of similarity with more influence of the constituents of the bacterial envelope between more closely related organisms. Raman spectroscopy was capable of differentiating between susceptible and resistant strains as well as monitoring whether the organism has been grown under antibiotic pressure.

Based on triplex PCR, clinical isolates of ESBL strains were assigned to one of the phylogenetic group characterising *Escherichia* genus and it was revealed that within CTX-M TEM-1 there were two distinct clusters of D and B2 groups.

Overall we have demonstrated that the combination of micro-Raman spectroscopy, mi-

crobiology and bioinformatics has the potential for the successful discrimination of bacteria species and strains, for the determination of antibiotic resistance profiles and investigating phylogenetic grouping in a clinical environment.

DECLARATION

This work has not previously been accepted in substance for any degree and is not being concurrently submitted in candidature for any degree.

Signed:(candidate)

Date: 06/02/15

STATEMENT 1

This thesis is the result of my own investigations, except where otherwise stated. Where correction services have been used, the extent and nature of the correction is clearly marked in a footnote(s).

Other sources are acknowledged by footnotes giving explicit references. A bibliography is appended.

Signed:(candidate)

Date: 06/02/15

STATEMENT 2

I hereby give consent for my thesis, if accepted, to be available for photocopying and for inter-library loan, and for the title and summary to be made available to outside organisations.

Signed:(candidate)

Date: 06/02/15



Tacie, za to, że exuwała;
Mamie, za to, że kochała;
Oli, za to, że wspierała;
Mitoszewoi, za to, że wierzyła;
Małgosi, za to, że jesteś.

ACKNOWLEDGEMENTS

This work is dedicated to my family and my closest friends, who are considered family. Even though being over 1,800km away from me I have always felt their support and love, they helped me psychologically and, at certain point, also financially because I know they believed in me. Even though my Dear Dad passed away before I started this project I am sure He would have been there for me and I would have made him proud.

This is why those wonderful, always close to my heart people, deserve this work and all the effort, sweat and tears that came with it, to be dedicated to them. Without them, I would not be where I am right now, because without them, I would not be who I am.

I also would like to express my deepest appreciation to everyone who contributed directly to this work: starting with most obviously all my supervisors; Dr Tom Wilkinson, who was by me during the whole process, always willing to help and support. Who was a teacher, a mentor and during the most difficult times, a friend. Who survived all my confusion, all my gaps in knowledge, my 'PhD blues' and my complaints. Who sheltered me from the meanders of academia, offered advice and assistance. I would like to apologise for all those hair turning grey because of me.

I would like to thank Professor Dietrich Mack and Professor Helmut Telle for sharing the duty of being my second supervisors. Professor Mack introduced me to more clinical approach, while Professor Telle was guiding me through the new and rather unfamiliar world of physis and created collaboration (internally called 'The Ramaneiros Team') with, now Dr, Jamal Al-Marashi making an important background for this project. Probably one of the most international and culturally diverse mini-groups to have ever existed and deserving special acknowledgement for both: professionalism and great time outside the university.

Many thanks go to Dr Caron Jones for her ESBL strains and their thorough description giving basis for Chapter 6.

I would like to express my gratitude towards Dr Angharad Davies who kindly gave me a tour of the hospital microbiology unit leading towards deeper understanding of the processes of clinical diagnostics.

Many thanks to all of my work colleagues from the 5th floor of Institute of Life Sciences for their warm welcome and constant support, especially during my writing-up period. Thank you for all of the kind words and all the harsher, honest ones. Thanks to Dr Josie Parker playing her tiny violin for me and generally being a real role model for strength, power, will for going on and not letting go. I definitely owe Josie at least several pages written directly after some of those motivation-boost conversations we had.

I would like to thank Professor Steven Kelly and Professor Diane Kelly for offering me my first post-doctoral position proving that this work made me worthy of becoming a real scientist. Thanks to Dr Claire Price for all the re-assurance talks.

I cannot miss out thanking Bozena Sojka, sharing not only a flat with me but also the burden of thesis-writing and for looking after me in all these times of despair. Thank you for all the fun-evenings, for writing breaks, for watching sentimental programmes, for introducing me to some quality music and of course working very hard in our 'Copacabana' study.

Last but not the least; I would like to thank my Dearest Dr Christopher Beaverstock. Even though I met him at the very last stage of this project, I cannot emphasise enough how much help and support he offered me. Thank you, Chris, for helping me with all the formatting, for staying up all night when I needed you, for supplying food when I did not have enough time to get it myself, for bringing me back from all my states of panic and most of all for your constant care and for having my back.

I am an author of this thesis but it was written leaning on shoulders of people who, in my eyes, are giants.

CONTENTS

Summary	i
Declaration	iii
Acknowledgements	vii
Contents	ix
List of Figures	xv
List of Tables	xix
Abbreviations	xxi
1. Introduction	1
1.1. Infectious Diseases	2
1.2. Antibiotics	3
1.3. Antibiotic resistance	4
1.4. Multi Drug Resistance	4
1.5. β -lactamases	4
1.6. <i>Escherichia coli</i>	5
1.7. Clinical Microbiology	6
1.7.1. Microscopy related methods	7
1.7.2. Microbial culture-based methods	7
1.7.3. Biochemical tests	8
1.7.4. Immunoassays	8
1.7.5. Molecular diagnostic methods	9
1.7.6. Automated Systems	10
1.7.7. The flow in the modern diagnostic laboratory	12

1.8.	Raman Spectroscopy - the novel approach to diagnosis	13
1.8.1.	Introduction to the spectroscopic methods	13
1.8.2.	Modifications and Types of Raman Spectroscopy	16
1.8.3.	Raman spectra processing	19
1.8.4.	Applications of Raman Spectroscopy in various fields	20
2.	Materials and Methods	31
2.1.	Materials	32
2.1.1.	Laboratory instruments and equipment	32
2.1.2.	Miscellaneous materials	32
2.1.3.	Membranes	33
2.1.4.	Chemicals and reagents	33
2.1.5.	Common buffers and solutions	34
2.1.6.	Agar plates	34
2.1.7.	Antibiotics used in this study	35
2.1.8.	Stains and markers	36
2.1.9.	Enzymes	36
2.1.10.	Primers	36
2.1.11.	Plasmids	37
2.1.12.	Bacterial Strains	38
2.1.13.	Routine culture of bacterial strains	39
2.1.14.	Preparation and storage of bacterial stocks	40
2.1.15.	Software	41
2.2.	Methods	42
2.2.1.	Determination of bacterial concentration	42
2.2.2.	Transformation	42
2.2.3.	Determination of minimal inhibitory concentration (MIC) by limiting dilution	43
2.2.4.	Temporal response to the action of antibiotics	43
2.2.5.	Isolation of Plasmid DNA	44
2.2.6.	Polymerase Chain Reaction (PCR) according to Clermont et al. (Clermont et al., 2000)	45
2.2.7.	Agarose Gel Electrophoresis	45
2.2.8.	API 20E®	46
2.2.9.	Raman Spectroscopy	46

3. Development of Raman spectroscopy procedures for reproducible identification of bacteria	47
3.1. Introduction	48
3.2. Methods and Results	50
3.2.1. Calibration	50
3.2.2. Individual spectra parameters	51
3.2.3. Determination of sample repeats	51
3.2.4. Effect of the substrate	53
3.2.5. Spectra processing	58
3.2.6. Variation within and between experiments	64
3.2.7. Synergistic effect of the agar signal	69
3.2.8. Assessing the correct sample size.	72
3.2.9. Selection of the regions of differences.	75
3.3. Discussion	78
4. Discrimination between bacterial species and strains using Raman spectroscopy	83
4.1. Introduction	84
4.2. Methods	86
4.2.1. Bacterial strains	86
4.2.2. Obtaining Raman spectra	86
4.2.3. Multiple strains comparison	86
4.2.4. Assessing the influence of storage conditions on Raman spectroscopy measurements	87
4.3. Results	88
4.3.1. Identifying the most crucial peaks for each bacterial strain	88
4.3.2. Similarity within experimental repeats	96
4.3.3. Comparison of organisms on different taxonomic levels	97
4.4. Discussion	118
5. Discrimination between susceptible strains and isogenic transformants expressing antibiotic resistance using Raman spectroscopy	121
5.1. Introduction	122
5.2. Methods	124
5.2.1. Transformation with electroporation	124

CONTENTS

5.2.2.	Gel electrophoresis with restriction enzymes	124
5.2.3.	Determination of Minimal Inhibitory Concentration (MIC)	124
5.2.4.	Temporal response to the action of antibiotics	124
5.2.5.	API 20E®	124
5.2.6.	Quantification of <i>E. coli</i> viability using fluorescent microscopy	124
5.2.7.	Raman spectroscopy measurement	125
5.2.8.	Modifications of the standard Raman spectroscopy procedures	125
5.3.	Results	128
5.3.1.	Generation of antibiotic resistant <i>E. coli</i> control strains	128
5.3.2.	API 20E®	133
5.3.3.	Comparison of Raman spectra from resistant and susceptible control strains	133
5.3.4.	Multiple strains comparison	141
5.3.5.	Real time monitoring of the bacterial response to antibiotics by Raman spectroscopy.	142
5.4.	Discussion	149
6.	Characterisation of clinical isolates of <i>Escherichia coli</i> expressing Extended Spectrum β-lactamases, using Raman spectroscopy	153
6.1.	Introduction	154
6.2.	Methods	155
6.2.1.	Polymerase Chain Reaction	155
6.2.2.	Phylogenetic classification	155
6.2.3.	Raman spectroscopy measurements	155
6.3.	Results	156
6.3.1.	Polymerase Chain Reaction	156
6.3.2.	Raman spectroscopy	158
6.4.	Discussion	161
7.	Final discussion and future perspectives	163
A.	Supplementary Information	A-1
B.	R-Code	B-1
B.1.	Subtracting agar	B-2
B.2.	Calculating t-tests from PCA scores	B-2

B.3. Subtracting mean spectra intensities in a form of a graph	B-2
C. Publication based on results included in this thesis	C-1
Bibliography	Bib-1

LIST OF FIGURES

1.1. Selected events in the history of infectious diseases, including the most adverse events and the most breakthrough discoveries and theories.	3
1.2. Diagram comparing different types of spectroscopy	13
1.3. Schematic representation of Raman System coupled with microscope. . .	16
2.1. Map of pUC19 plasmid (Nari)	37
2.2. Map for pET-26 plasmid (Novagen)	38
3.1. A single spectrum from the internal silicon sample.	50
3.2. A single spectrum from the internal silicon sample.	50
3.3. Representation of single sample repeats preparation	52
3.4. Representation of whole experimental repeats preparation	53
3.5. Comparison of Raman substrates;	55
3.6. <i>S. epidermidis</i> 1457 on different substrates	57
3.7. Set of 30 spectra from 30 colonies taken during a single measurement of Top10	59
3.8. Single spectra of Top10 and 1457	60
3.9. Subtraction of mean intensities	61
3.10. Principal component analysis results in a form of clusters, of one whole experimental repeat consisting of 30 single sample repeat for each Top10 and 1457	62
3.11. Hierarchical cluster analysis for PC scores from a single whole experimental repeat (containing 15 single sample repeats of each sample) for <i>E. coli</i> Top10 and <i>S. epidermidis</i> 1457.	63
3.12. Comparison of clustering for four whole experimental repeats for pre- and post- agar spectra removal on Top10.	69
3.13. Comparison of clustering between two different organisms pre- and post- agar spectra removal on 4 experimental sets of Top10wt vs. 1457.	70

LIST OF FIGURES

3.14. Influence of sample size on separation and size and spatial distribution of clusters between Top10 and 1457.	73
3.15. Influence of sample size on separation, shape, and spatial distribution of clusters between Top10 and K12	74
3.16. Comparison of two single experiments of 30 repeats for each Top10 and K12	76
3.17. Comparison of single whole experimental repeats containing 30 single sample repeats for each	77
4.1. Plot and a table of most significant peaks with assigned molecules and bonds based on the mean spectra from all Raman measurements	95
4.2. PCA of whole experimental repeats performed for single strains used in the project	97
4.3. The comparison of 1457 and Top10.	99
4.4. The comparison of K12 and 9142	100
4.5. The comparison of 10418 and 6571	101
4.6. The comparison of Strain B and Cowan 1	102
4.7. The comparison of 1457 and 6571	103
4.8. The comparison of 9142 and Cowan1.	104
4.9. The comparison of 1457 and 9142.	106
4.10. The comparison of 6571 and Cowan1.	107
4.11. The comparison of K12 and Top10	109
4.12. The comparison of K12 and Strain B	110
4.13. The comparison of Top10 and Strain B	112
4.14. The hierarchical cluster analysis tree of mean values calculated for each single sample repeat within all whole experimental repeats for the strains used in this chapter	113
4.15. Comparison of the influence of the temperature of storage in time on the clustering of Raman spectra for Top10 in 4°C and 25°C after 0; 1; 2; 4; 8 hours, including three experimental repeats	115
4.16. Comparison of the influence of the temperature of storage in time on the clustering of Raman spectra for K12 in 4°C and 25°C after 0; 1; 2; 4; 8 hours, including three experimental repeats	116

4.17. Comparison of the influence of the temperature of storage in time on the differentiation between K12 and Top10 spectra in 4°C and 25°C after 0; 1; 2; 4; 8 hours, including three experimental repeats for each organism	117
5.1. Schematic representation of the replica plating method	126
5.2. Schematic representation of replication using membranes	127
5.3. Gel electrophoresis of plasmid DNA containing ampicillin resistance.	129
5.4. Gel electrophoresis of plasmid DNA for three clones containing kanamycin resistance	130
5.5. Graph comparing the growth of bacteria after adding ampicillin and kanamycin in transformed and wild-type strains.	132
5.6. Principal component analysis plot representing 6 single sample repeats from each: CBA and CBA containing ampicillin.	134
5.7. The comparison of Top10 and Top10 ^A	135
5.8. The comparison of Top10 and Top10 ^{AA}	136
5.9. The comparison of Top10 and Top10 ^{AA} on ampicillin containing plate	138
5.10. The comparison of Top10 and Top10 ^K	139
5.11. The comparison of Top10 and Top10 ^{KK}	140
5.12. The comparison of Top10 and Top10 ^{KK} on kanamycin containing plate	141
5.13. Hierarchical analysis tree based on means from all the whole experimental repeats performed	142
5.14. Principal component analysis scores of Raman spectra from Top10wt colonies subjected to different solutions and repeated on two consecutive days	143
5.15. Principal component analysis scores of Raman spectra from Top10 colonies subjected to 2ml of 100µg/ml ampicillin for different periods of time	143
5.16. Raman spectra from Top10wt colonies subjected for 3 hours to 1µl performed on two consecutive days	144
5.17. Principal component analysis scores of Raman spectra from Top10wt colonies flooded with 1µl of 1000µg/ml of ampicillin	145
5.18. Principal component analysis scores of Raman spectra from Top10 ^{AA} plated on an original plate and moved to: 1RA - new plate containing antibiotic; 2RN-control plate without antibiotic.	146
5.19. Raman spectra (n=6) from the membranes on CBA plates	146

LIST OF FIGURES

5.20. Principal component analysis scores of: Top10wt plated on CBA plates containing MCE membrane; Top10wt plated on a CBA without the membrane; membrane itself.	147
5.21. Principal component analysis scores of Top10wt plated on CBA plates containing MCE membrane	147
5.22. Comparison of the influence of antibiotic dose on the CBA plates on the spectra of Top10wt grown on nitrocellulose membrane and moved onto the new plates	148
6.1. The results of triplex PCR	157
6.2. The collection of clinical isolates expressing ESBLs with phylogenetic groups assigned to them.	158
6.3. Results based Raman spectra for the collection of clinical strains expressing CTX-M-15, TEM-1	159
6.4. PCA clusters based on Raman spectra for the collection of clinical strains expressing CTX-M-15IS26 positive	160

LIST OF TABLES

2.1. Laboratory instruments and equipment used in this study	32
2.2. Miscellaneous materials used in this study.	32
2.3. Membranes used in this study	33
2.4. Chemicals and reagents used in this study	33
2.5. Antibiotics used in this study	35
2.6. Stains and markers used in this study	36
2.7. Enzymes used in this study	36
2.8. Primers used in this study	36
2.9. Reference laboratory strains used in this study	38
2.10. Reference hospital isolates used in this study	39
2.11. Laboratory transformed strains expressing antibiotic resistance	39
2.12. Archived <i>E. coli</i> hospital isolates of different antibiotic profiles	39
2.13. Laboratory <i>E.coli</i> strains used as standard for phylogenetic classification .	39
2.14. Software used in this study	41
3.1. Results for t-test based on PC scores from the first four principal components calculated for comparison of four whole experimental repeats, each containing thirty single sample repeats of each Top10 and 1457.	64
3.2. Comparison of the natural variation within the consecutive experimental sets of 30 spectra of Top10 (A) and 1457 (B).	65
3.3. Selected reasons for rejection of single spectra.	67
3.4. Comparison of results of t-tests performed on PCA scores of single experimental sets of Top10 and 1457 post- agar intensities removal.	70
3.5. Possible reasons for rejecting the complete experiments	71
4.1. The summary of the Raman signal from all the reference (antibiotic susceptible) strains used in the project and showed separately in Figure 4.1 .	95

LIST OF TABLES

5.1. Comparison of OD readings for untransformed Top10 with Top10 ^A and Top10 ^{AA} based on the results obtained from the plate-reader.	130
5.2. Comparison of OD readings for untransformed Top10 with Top10 ^K and Top10 ^{KK} based on the results obtained from the plate-reader.	131
A.1. Approaches have been used for studying microorganisms with Raman spectroscopy	A-2
A.2. Different microorganisms studied using Raman spectroscopy.	A-3
A.3. Characteristic peaks obtained from Raman spectroscopy of biological samples according to: (De Gelder, 2007; Ivleva et al., 2008; Maquelin et al., 2002; Samek et al., 2008, 2010b; Schuster et al., 2000)	A-4

ABBREVIATIONS

Amp	Ampicillin
AFM	Atomic Force Microscopy
ASGRCF	Applied Savitzky Golay smoothing Rolling Circle Filter
bp	Base pair(s)
CaF₂CARS	Calcium fluoride
CBA	Coherent anti-Stokes Raman Spectroscopy
cm	Columbia Blood Agar/ Centimetre(s)
CTX	Cefotaxime
ESBL	Extended-spectrum β -lactamase
DNA	Deoxyribonucleic acid
dNTP	Deoxynucleotide 5.-triphosphate
dH₂O	Deionised water
EDTA	Ethylenediaminetetraacetic acid
ELISA	Enzyme-linked Immunoassay
g	Grams
h	Hour(s)
HC	Hierarchical Cluster
HCl	Hydrochloric acid
IS	Insertion sequence

ABBREVIATIONS

Kan/^K	Kanamycin
Kbp	Kilobase pairs
L	Litres
LB(A)	Luria Bertani (Agar)
LTRS	Laser Tweezers Raman Spectroscopy
MALDI-TOF/MS	Matrix-assisted laser desorption ionization time-of-flight/mass spectrometry
MDR	Multi drug resistance
MIC	Minimum inhibitory concentration
m-	Milli-
μ	Micro-
M	Molar
n-	Nano-
NaCl	Sodium chloride
PCA	Principle Component Analysis
PCR	Polymerase chain reaction
RCF	Rolling Circle Filter
RNA	Ribonucleic acid
SERS	Surface enhanced Raman spectroscopy
SOP	Standard Operating Procedures
TAE	Tris-Acetate-EDTA
TE	Tris-EDTA buffer
TERS	Tip Enhanced Raman Spectroscopy

Tris	Tris(hydroxymethyl)aminomethane
UVRRS	Ultra-violet resonant Raman spectroscopy



1. INTRODUCTION

1.1. Infectious Diseases

Bacterial infections remain a serious threat to human health causing morbidity and mortality worldwide. The oldest evidence of infectious diseases include: Egyptian mummies carrying signs of smallpox, papyrus paintings depicting conditions such as poliomyelitis (Brachman, 2003) and biblical passages mentioning leprosy and pharaonic plague. Infectious diseases have been responsible for the extinction of whole civilisations for example the Athens Plague which marked the end of Greece's Golden Age or the spread of smallpox across Mexico during the geographical conquests in 16th century causing 10-15 million deaths and therefore the end of Aztec civilisation (Morens et al., 2004).

Epidemics and pandemics have always been considered serious problems; three major outbreaks of plague, between 14th and 17th century were responsible for the death of more than 200 million people across the world (Tatem et al., 2006).

The Indian pandemics of cholera from 1817 onwards have since spread to seven major subsequent outbreaks in China, Japan and Indonesia, reaching towards Russia, Arabic countries and Americas. In the 1990s successive cholera epidemics in Africa and Latin America raised concerns that this disease was becoming endemic to these regions (Codeço, 2001).

Newly identified infections have also emerged in the last 100 years. Human immunodeficiency virus (HIV) causing acquired immune deficiency syndrome (AIDS) was identified in the 1970s which initiated a pandemic that remains and affects people on at least five continents (Tatem et al., 2006). Other newly recognised infectious diseases of the 20th century include Legionnaire's disease, toxic shock syndrome, Lyme disease, campylobacteriosis, infections by *Escherichia coli* O157:H7, *Vibrio vulnificus*, *Vibrio cholera* O139, *Helicobacter* infections, *Bartonella*, Ebola, and Hantavirus infections and spongiform encephalopathies. Furthermore, in addition to emerging diseases, there is the serious issues are re-emerging diseases, including epidemics of: diphtheria in early 1990s attacking many of the nations of former Soviet Union; *Listeria* affecting mainly pregnant women in early 1980s; and serogroup A *Neisseria meningitidis* causing 150,000 cases in 1996 (Cohen, 1998).

Infectious diseases impact on human lives and cause disease resulting in significant morbidity and mortality however there are significant economic factors; the costs of treatment therapies have been estimated to £6 billion per year in England itself (Troop, 2005).

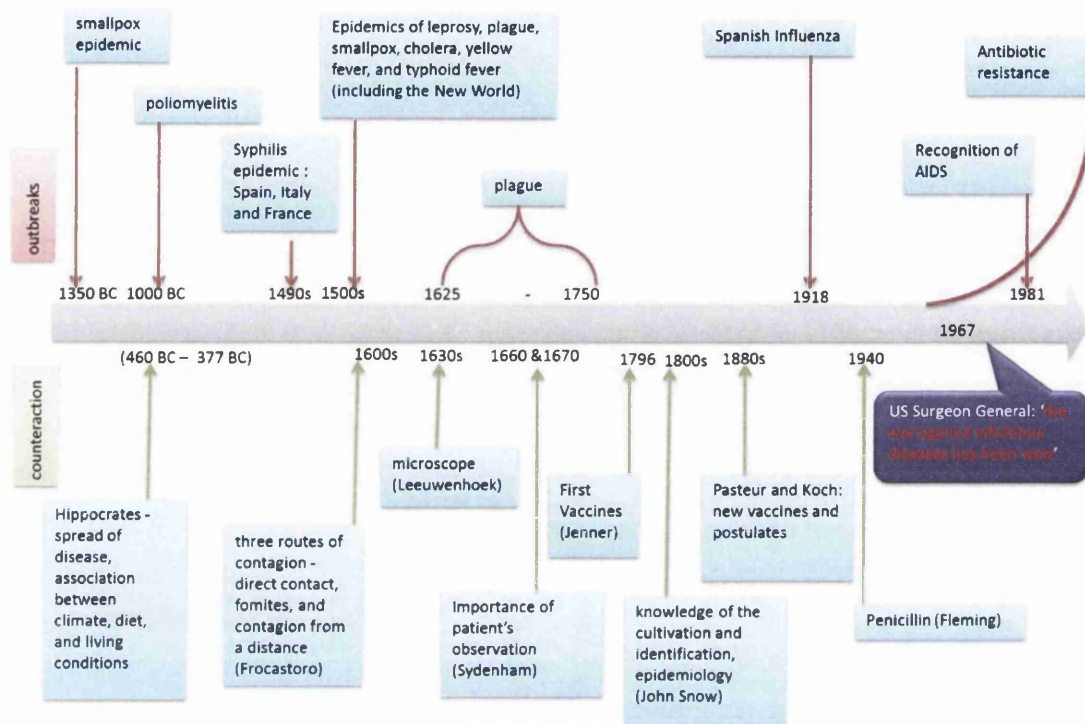


Figure 1.1.: Selected events in the history of infectious diseases, including the most adverse events and the most breakthrough discoveries and theories.

1.2. Antibiotics

In 1904 Paul Ehrlich, developed the idea of a ‘magic bullet’ that would target pathogenic bacteria, without influencing host microbes in his work to find a drug against syphilis, almost incurable at the time. In 1909 together with chemist Alfred Bertheim and bacteriologist, Sahachiro Hata, Ehrlich developed Salvarsan and later, its less toxic derivative: Neosalvarsan, which have been used successfully until they were replaced by penicillin in the 1940s (Aminov, 2010).

The antimicrobial activity of mould has been appreciated since ancient times, however the mass production and distribution of its active components, for instance, penicillin began after its discovery by Alexander Flemming in 1928 (Fleming & Maclean, 1930) (Aminov, 2010). The vast number of new antibiotics discovered in the golden age of antibiotic production between 1950s and 1970s resulted in false perception of controlling infectious disease and in later decades to the present day the number of novel antimicrobial agents released on the market has decreased considerably (Peláez, 2006).

1.3. Antibiotic resistance

Antibiotic resistance is the ability of microorganisms to become resistant to therapies used against them and results in larger doses of antibiotic needed to achieve the same effect or indeed that the effect is lost completely. It is now recognised as a major public concern due to higher mortality and morbidity among patients, as well as having an enormous economic impact (Smith & Coast, 2002). Antibiotic resistance was first observed through the action of bacterial penicillinase in 1940 by researchers working on the penicillin discovery team, even before the newly-discovered penicillin was introduced as a successful therapeutic (Davies & Davies, 2010). Several factors cause antimicrobial resistance development. One of the most common issue is the over-use and miss-use of antibiotics facilitated by: availability of over-the-counter antimicrobials distributed without proper supervision, medicines poorly manufactured causing low effectiveness and potency, access to drugs sold on non-authorized permissions distributed by people with insufficient knowledge (Smith & Hinson-Smith, 2000).

1.4. Multi Drug Resistance

Multiple drug resistance (MDR) is the biggest problem facing medicine in the foreseeable future and is recognised as the biggest threat with respect to morbidity and mortality worldwide. Due to the MDR, the therapeutic options are reduced, extending the time of hospital care, adding to the costs of the treatment (Davies & Davies, 2010). Multiple drug resistance is caused when microorganisms exhibit multiple mutations, responsible for high levels of resistance to antibiotic classes, normally assigned for treating these microbes. In addition, bacteria possessing MDR often express increased virulence and transmissibility.

1.5. β -lactamases

The leading cause of resistance to β -lactam antibiotics (e.g penicillin, cephalosporins, monobactams and carbapenems) is the action of antibiotic-inactivating enzymes, β -lactamases, efficiently catalysing the irreversible hydrolysis of the amide bond of the β -lactam ring resulting in deactivation of the drug (Essack, 2001). The genes for β -lactamase enzyme are some of the most abundant, distributed worldwide, have ancient

origin and have been detected in remote or desolate environments (Davies & Davies, 2010) Tem-1, also called type 1 β -lactamase, is the most common β -lactamase found in high copy number in naturally occurring plasmids (Yamamoto et al., 1982)

An important class of β -lactamases are the extended-spectrum β -lactamases (ESBLs) which are able to efficiently hydrolyse oximino- β -lactams (Tzouvelekis et al., 2000). ESBLs are predominantly mutants of TEM and SHV enzymes, however CTX-M enzymes are gaining importance (Woodford et al., 2004) as a novel group of class-A plasmid-encoded enzymes (Tzouvelekis et al., 2000). Although CTX-M β -lactamases have been claimed to constitute to one of the minor families of ESBLs (Gniadkowski et al., 1998), they gaining dominance over TEM and SHV groups in many European and Eastern Asian countries (Livermore et al., 2007).

CTX-M enzymes have been found in many bacteria, including species within *Klebsiella*, *Citrobacter* and *Protus* genera (Tzouvelekis et al., 2000) however most were reported to be expressed by *E. coli* isolates (Cantón & Coque, 2006).

1.6. *Escherichia coli*

Escherichia coli was discovered in the late 1800s by Theodore von Escherich in the gut and was originally named *Bacterium coli commune* (Rubino et al., 2011). This facultative, gram-negative bacterium belonging to the Enterobacteriaceae family is a normal inhabitant of the intestines of most animals and is most prevalent in human faecal flora. Certain strains can be virulent and are responsible for a wide variety of intestinal and extra-intestinal diseases, including diarrhea, urinary tract infections, septicaemia and neonatal meningitis (Clermont et al., 2000; Johnson, 1991)

In the 1940, *E. coli* was the first species recognised to be expressing β -lactamase activity (Cantón et al., 2008). *E. coli* clinical isolates have also been reported as the main organisms with CTX-M β -lactamases activity (Cantón & Coque, 2006; Tzouvelekis et al., 2000)

Phylogenetic analysis showed that *E. coli* strains are distributed between four main phylogenetic groups: A, B1, B2 and D. The virulent, extra-intestinal strains fall predominantly into B2 group and less often to the group D, while most commensals can be found belonging to the group A (Clermont et al., 2000).

Within the B2 group, virulent, uropathogenic lineage ST131 can be found, of which most isolates in the United Kingdom produce ESBL CTX-M-15, However strains ex-

pressing CTX-M-3 or AmpC were also reported.

Phylogroup D, with lineages including ST69, ST405 and O15:K52:H1 has shown to be able to produce TEM-, SHV- and CTX-M (Cantón & Coque, 2006), namely CTX-M-15, CTX-M-14 ESBLs (Woodford et al., 2004) and to a smaller extent CTX-M-9 (Cantón & Coque, 2006).

Phylogroups A and B1 are mostly non-virulent, there have been reports claiming their capability of producing ESBLs with CTX-M-9 being predominant in group A and hyper-expression of AmpC (Cantón & Coque, 2006).

Within a widespread clone, single members may obtain and develop different resistance profiles resulting from various genes (Woodford et al., 2004).

1.7. Clinical Microbiology

The problem of emerging and re-emerging infectious diseases, coupled with the development of antimicrobial resistance and lack of new advances or discoveries in the fields of vaccines or antibiotics is considered one of the most urgent and serious global threats.

The goals of cutting edge Microbiology are accurate identification and discrimination of microorganisms and furthermore the determination of antimicrobial susceptibility. Indeed fast and effective identification of microbes has been proven as a method of limiting morbidity, mortality and time of hospitalization (Richardson & Small, 1998). Furthermore a delay in initiation of antimicrobial therapy, especially in severe cases, like the onset of a septic shock-related hypotension or meningitis, may contribute towards mortality and morbidity among patients (Rivers et al., 2005; Tunkel et al., 2004). The rate of deaths can be significantly increased even by a 1 hour delay and therefore empirical, broad-spectrum antibiotic therapy is advised (Kumar et al., 2006). However, applying non-specific antibiotics can have adverse effects for the patients, like weakening the beneficial microbial flora contributing towards fungal infections or increasing the risk of liver failure. Moreover, using an inappropriate antimicrobial agent can be a serious factor in the problem of raising antibiotic resistance among bacteria.

The experience gained from treating various other diseases, including cancer, allows for speculating that applying a correct and accurate diagnostic technique for fast and effective determination of the causative infectious agent might be the correct approach. This will allow for initiation of the most appropriate treatment reducing the effects of an infectious disease, and risks associated with misuse of broad-spectrum antibiotics (Bonomo, 2000).

There are various diagnostic methods currently available involving detection of the infectious agent either directly, or indirectly and can be used in combination or independently (Tallury et al., 2010).

1.7.1. Microscopy related methods

Simple visual examination through light microscopy involves microbiological stains, such as Gram and calcofluor white and is based on comparison of the observed results with a set of standard organisms described as controls. Several modifications are currently available, involving using fluorescent microscopy for sample stained with specific dyes of particular excitation.

The advantages include the fact that the sample can be derived straight from the patient in a form of sputum, blood, urine, stool, etc. (Tallury et al., 2010), therefore the identification if successful, could be achieved instantly, without any time delays. In reality, microscopic examination is hardly ever fully conclusive on its own for diagnostic purposes.

1.7.2. Microbial culture-based methods

The most common approach allows the pathogen to grow in a specific growth medium and is characterised based on size, shape, colour of the colony formed and the changes brought by their growth (Tallury et al., 2010). There is a wide range of media available, including liquid and solid, which can be prepared or pre-made. Among the most commonly used agar plates are blood, chocolate, and MacConkey and chromometric plates. More recent innovation are chromometric plates changing colour upon the growth of the organism of interest.

Culturing methods can also offer susceptibility testing when the antimicrobial agent is added onto or into the medium.

One example is serial dilution method when series of tubes, or wells on microdilution plates, containing different dilutions concentration of antibiotics in the liquid growth medium is prepared allowing for determination of minimal inhibitory concentration (MIC), i.e. the concentration of antibiotic preventing the growth of bacteria. The advantage is obtaining a quantitative result however manual preparation of the assay is tedious, burdened by errors as well as time-consuming, requiring plenty of storage space and single-use reagents (Jorgensen & Ferraro, 2009; Stefaniuk et al., 2005)

The antimicrobial gradient method is based on a gradient of antibiotic in an agar medium, which can be achieved by placing commercially available plastic strips impregnated on the underside with a dried antibiotic concentration gradient and marked on the upper surface with a concentration scale. MIC is determined by the intersection of the lower part of elliptical growth inhibition area with the test strip placed for an overnight incubation on a previously inoculated plate. This method serves best when limited antibiotics are used, it is reasonably fast and very simple, nevertheless certain bacteria-antibiotic combinations prove difficult to work with in this assay.

Disk diffusion test requires inoculating bacteria on a Muller-Hinton plate and placing round, commercially prepared, fixed concentration, paper antibiotic discs. After an overnight incubation, the zones of growth inhibition are measured to the nearest millimetre. This test is very cheap with no additional equipment required and has been standardised for a few organisms. The disadvantages include lack of automation and problems with the fastidious or slow growing organisms (Jorgensen & Ferraro, 2009).

1.7.3. Biochemical tests

The identification of some organisms can be based on the detection of a metabolic or enzymatic products characteristic for that organism (Tallury et al., 2010). One of the most popular biochemical tests is a commercially available API[®] kit, subjecting microorganism to a series of biochemical identification tests and based on the results of the reactions the tested sample is compared against a database. Biochemical tests are regarded as reliable, however they may not provide full information at the species level, while decisions involving strains is not possible. The process is also time-consuming and introduces a requirement for cell culturing, in order to obtain sufficient biomass of around 10^6 - 10^8 cells for subsequent tests (Carbonnelle et al., 2011).

1.7.4. Immunoassays

Immunodiagnosics is possible due to the fact that bacterial cell surfaces display a variety of antigenic molecules including protein and polysaccharides. The polyclonal antisera are designed as mixture of antibodies with multiple specificities to interact with various molecules expressed by the bacteria. Currently available assays using polyclonal antisera and monoclonal antibodies include: agglutination assays, enzyme linked immunosorbent assays (ELISA), Western blots, immunofluorescence or immunofluorescence colony

staining, and lateral flow devices. Many modifications and various applications allow for achieving high specificity in this field, however there is still possibility of cross-reactions with unrelated species (Alvarez, 2004) lowering therefore the sensitivity and negative predictive value. In addition they also include the culturing step a major disadvantage for an instant diagnosis (Richardson & Small, 1998).

1.7.5. Molecular diagnostic methods

Advances in the field of genetics lead to the involvement of monitoring the changes in genomic and proteomic structure for identification of the pathogen of interest (Davis et al., 2010; Tang et al., 1997).

Nucleic acid testing can be divided into amplified and non-amplified methods. The latter group can either be based on DNA- or RNA-labelling with probes that generate a recognised signal upon specific base pair binding. The advantages of this method include no risk of contamination of the subsequent samples with amplified material.

The amplification based techniques can be subdivided into: signal amplification, focusing on generating multiple copies of signalling molecules either through branched DNA or hybrid capture assays; and target amplification including polymerase chain reaction (PCR) and transcription-mediated amplification (TMA) (Muldrew, 2009; Pfaller & Herwaldt, 1997). In addition an important step in amplification-based molecular methods is post-amplification analysis, including sequencing (Muldrew, 2009).

DNA-amplification methods are prone to false-negative results, because of the possibility of introducing inhibitors; as well as false positive results due to contaminating sample with foreign DNA during sample collection or preparation. Furthermore, high costs, complexity, no peer-reviewed database and lack of clear, straightforward interpretation of result, all make sequencing methods less than ideal for meeting novel diagnostic requirements (Carbonnelle et al., 2011).

In the clinical environment, molecular methods did not achieve the anticipated status and for the disadvantages listed above, are not commonly used. Mainly due to the fact that hospital testing, in order to avoid any inappropriate results, requires using a '3 room purity' rule: 1st room serving as prep-room, 2nd - clean room where the original, whole sample is not allowed, so the space may be free from any amplicons and finally 3rd where the PCR is conducted.

All these negative points leave molecular diagnostics as the second line of diagnostic techniques playing a role in confirmation following initial microbial identification.

1.7.6. Automated Systems

The advances of technology offered applications of automated and semi-automated tools, like matrix-assisted laser desorption ionisation-time of flight mass spectrometry (MALDI-TOF) (Ferreira et al., 2010) or several systems offering susceptibility testing; eg. Phoenix (Carroll et al., 2006b) (Horstkotte et al., 2004), VITEK1 (Hall & Fluit, 2002), VITEK 2 and MicroScan (Wiegand et al., 2007).

1.7.6.1. Phoenix system

The Phoenix system offers determination of both Gram+ and - bacteria and assesses their antimicrobial minimal inhibitory concentrations (MICs) through an automated test and is used in many hospitals. Its main advantages, besides automation, are: relatively short incubation times, ability to test up to 100 identification and susceptibility test combination panels in a single measurement. In this method, identification of microorganisms is performed based on a variety of colorimetric and fluorometric bacterial indicators, while the susceptibility test uses optimised Mueller-Hinton broth base with a redox-indicator involving red, green, blue and fluorescence readings. Once all the data is collected, it is then comparatively analysed and compared with the Phoenix database (Reuben et al., 1999). However many publications claim satisfying results obtained with this system, there are certain reports of poor performance when a combination of unusual and more clinically common organisms are tested (Carroll et al., 2006a).

One of the most significant drawbacks of this system is the fact that panels are relatively expensive. Taking into account, how many tests are done routinely in a hospital laboratory each day, it would not be plausible to test every sample using the Phoenix.

1.7.6.2. Vitek 2

The Vitek 2 System (bioMérieux), which is a modernised version of Vitek 1 (the difference in holding less samples for a single run and lack of *Streptococcus pneumoniae* test), is highly automated and uses microliter quantities of antibiotic and test media for turbidimetric monitoring of bacterial growth during shortened incubation period. The system can be optimised for 30-240 simultaneous tests for common, rapidly growing, gram-positive and gram-negative aerobic bacteria, and *S.pneumoniae* in 4-10 hours (Jorgensen & Ferraro, 2009). Despite the speed and large sample size available, the system has been reported as burdened with certain inaccuracies, especially for *S.epidermidis* (Kim et al.,

2008).

1.7.6.3. Matrix-assisted laser desorption/ionisation-time of flight (MALDI-TOF) mass spectrometry

MALDI-TOF-MS is based primarily on detection of the mass-to-charge ratio of the analysed sample, which is presented in a form of a spectrum serving as a unique fingerprint. It has been used for profiling proteins from cell extracts and has been proven functional on the grounds of differentiation between bacteria. This technique requires bacterial lysates to be converted from their normal condensed phase, into intact separated ionized molecules in the gas phase. The molecules then migrate in an electric field and are described by: their molecular mass and charge, mass/charge ratio and relative intensity of the signal. (Carbonnelle et al., 2011). The results are then compared with the database. Laboratories using this technique can create their own library of organisms and thus expand the applications of this method (Eydmann et al., 2011). One of the most important features of this technique is the time of the procedure. The stainless steel plate can hold up to 96 organisms and the total time needed for sample of this size would take under 2 hours (Eydmann et al., 2011). It is of a great importance to carefully control the growth conditions and standardise the sample preparation procedures, as the same species can give different mass spectra. MALDI-TOF-MS analyses phenotypic characteristics, which may vary with culture media and incubation times as well as with different chemical extraction methods (Carbonnelle et al., 2011). Although the costs of the consumable matrix and extraction solutions are very low, the cost of purchasing an instrument and service costs, may still be out of reach for most clinical laboratories at present (Eydmann et al., 2011).

Another drawback is the fact that this technique has not been officially confirmed to be effective in antimicrobial susceptibility testing to date. There are on-going research attempts to involve this factor in optimising MALDI-TOF-MS (Carbonnelle et al., 2011).

Generally, despite numerous advantages, there are several considerations arising from using automated systems for clinical testing. Among the most common and important obstacles are: 1) strains within one species may differ in terms of particular characteristic which may not be recognised 2) isolates that are not fresh, may fail to exhibit expected biochemical features 3) subjecting the host to a long antimicrobial therapy may affect the biochemical patterns of the isolates 4) there may be lack of reproducibility within the same strain 5) the limitations of number of species in the database 6) phenotypic

variations may induce inaccuracy of identification on a species level 7) systems based on phenotypic identification often suggest 2 or more designations of similar probability levels (Kim et al., 2008).

1.7.7. The flow in the modern diagnostic laboratory

Medical microbiology assists physicians in caring for patients, by examining appropriate specimens, directly relevant in the diagnostic process (Richardson & Small, 1998). For this reason, hospital diagnostic laboratories have standard operating procedures for processing biological specimens safely, efficiently and confidentially.

Following sample collection from a patient, key details are reported including personal details such as name, health care number/NHS number, date of birth, ward, GP name and number, type of specimen, time the sample was taken, tests required, and other relevant clinical data including any antibiotic treatment and possible risk status. Such information could influence the final diagnosis (Waghorn, 1995). To ensure confidentiality, the details are saved into a computer and the sample is given a specific number instead of being marked with personal details.

Biological samples can be varied and complex therefore hospital laboratories are usually divided into departments processing different materials.

Modern clinical microbiology laboratories need to deliver rapid and robust decisions to physicians regarding the identity and antibiotic susceptibility of microorganisms isolated from patients suspected of an infectious disease. Furthermore the need for rapid identification and determination of the potential consequences of the microorganism for the hospital population and the community (Isenberg & Berkman, 1962), together with the disadvantages of currently available techniques, require investment in testing further novel options for fast reproducible methods of diagnosis.

There are certain desirable qualities that a novel diagnostic method should possess including but not limited to; i) rapid characterisation with the access to a stable database; ii) easy to use; iii) automated analysis of series samples; iv) low costs; v) , reproducibility and accuracy vi) minimal sample preparation on a single cell level; vii) omitting the pre-culturing step while retaining the antimicrobial susceptibility testing; viii) tailoring personalised therapy in one single rapid measurement. Currently approved techniques, do not offer all these requirements however further methods require confirmation as to their potential role in the diagnostic process.

1.8. Raman Spectroscopy - the novel approach to diagnosis

1.8.1. Introduction to the spectroscopic methods

Spectroscopy is a broad field that can be utilised in various different ways, in particular for studying molecular compositions.

Nuclear Magnetic Resonance (NMR) is a spectroscopic technique that has been widely used in medical and biological studies, including diagnostics. The downside is the usually too rich information content, requiring time-consuming post-analysis performed by highly specialised personnel, as well as the low cost-efficiency.

Vibrational spectroscopy provides much higher and well-defined spectral information than electron-level spectroscopy but does not require specific labelling. Additionally, the equipment is simpler, cheaper and more mobile than required by NMR. The two main types of vibrational spectroscopy are: infrared absorption spectroscopy (IR and Fourier transformed infrared - FTIR) and Raman Spectroscopy. IR represents very high intrinsic sensitivity and relatively low cost equipment and its qualities gained high interest in the field of analytical chemistry (Efrima & Zeiri, 2009). Raman Spectroscopy stems from the discovery of the done in 1928 by Chandrasekhara Venkata Raman, awarded with a Nobel prize only two years later.

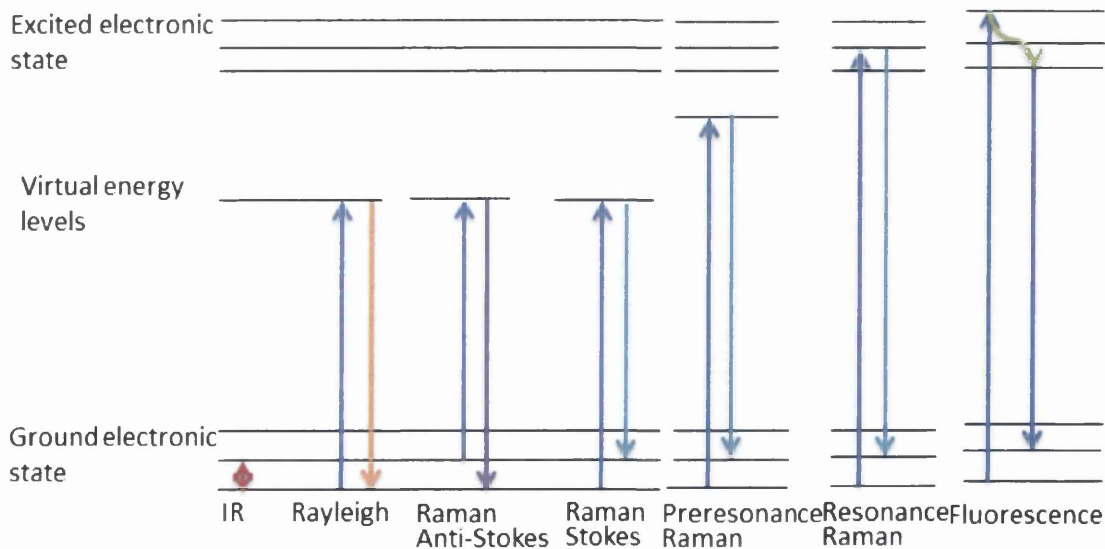


Figure 1.2.: Diagram comparing different types of spectroscopy

1. INTRODUCTION

Raman Spectroscopy is based on the fundamental principle of the exchange of energy between the light and matter. The Raman effect involves transfer scattered and not absorbed light, of the frequency equal to the vibrational frequency of the scattered molecules (Hanlon et al., 2000).

Raman Spectroscopy is often compared to infrared spectroscopy. However, while IR detects vibrational modes from asymmetrical vibrations, Raman spectroscopy bands arise from symmetrical vibration (Jarvis & Goodacre, 2008). Thus since water molecules are asymmetrical, they have very low Raman signal and therefore do not interfere with peaks from other molecules of interest within a sample. Effectively, Raman spectroscopy can be used to investigate aqueous solutions which is a quality particularly useful for biological systems. Further advantages of Raman over IR include: improved spatial resolution, as infrared wavelengths (3-15 μm) are insufficient for useful cells imaging (10 μm diameter) (Downes & Elfick, 2010). In addition Raman spectroscopy can be coupled to confocal microscopy systems employing shorter wavelengths of incident light to its diffraction limit. Furthermore Raman peaks are usually narrower than IR, and therefore detailed, so that chemical information from a wide range of excitation wavelengths can be easily generated. IR generally uses lower power sources and detectors producing complex background noise. Raman Spectroscopy benefits from applications enabling experimental measurements to be taken for prolonged periods without damaging samples such as bacterial specimens (Samek et al., 2010b,c). The sensitivity of this method also allows for shortening the time required for sample preparation, which benefits the speed of spectral acquisition (Samek et al., 2010b,c). Raman Spectroscopy is therefore considered a non-invasive, label-independent technique.

Raman systems usually include four basic elements: light source, disperse element, detector and a computer. A monochromatic, polarised light (laser beam) is focused on the sample. The light scattered from the sample is focussed on the entrance slit of a monochromator and dispersed. The disperse element differentiates between stronger scattered light by elastic scattering (the Rayleigh scattering) of frequency matching the laser beam and much weaker inelastic scattered light (the Raman scattering) of different frequency and related to bond vibrations. The photoelectric system then detects the intensity of the scattered, frequency-shifted light and the resulting signal of the detector is amplified and converted to be appropriate for plotting against frequency (Fabian & Anzenbacher, 1993).

Raman Spectroscopy most often involves a laser wavelength of 523 nm (diode-pumped

frequency doubled Nd:V) or 785 nm (AlGaAs diode), therefore a lateral resolution higher than half the wavelength (230-350 nm) can be achieved. This sub-cellular resolution is comparable to what fluorescence microscopy offers and is much higher than the minimum resolution (~ 0.1 -10nm) available from current medical diagnostic tools involving ultrasound, Magnetic Resonance Imaging, Positron Emission Tomography or X-ray. After losing its energy through exciting a molecular vibration the laser light is then red-shifted to a lower energy and is passed through a spectrometer, which disperses the light into a spectrum, recorded with a cooled CCD camera.

The difference between the frequency of the incident laser light and the red-shifted light is equal to the frequency of the vibrational bond. Each molecule has a unique 'fingerprint' of Raman peaks at precisely determined frequency. Biomolecules contain numerous molecular bonds, which can be excited in the range of ~ 600 -3,000 cm^{-1} . The spectrum then shows the properties of numerous bonds in the sample of interest rather than identifying molecules.

A single spectrum can be acquired from a small sub-cellular volume or averaged over a larger area. The time of spectral acquisition is usually between 1 and 10s, with the longer wavelengths giving a shorter time, while shorter wavelengths are absorbed more strongly, resulting in temperature rises during the exposure of sample to the laser light (Downes & Elfick, 2010).

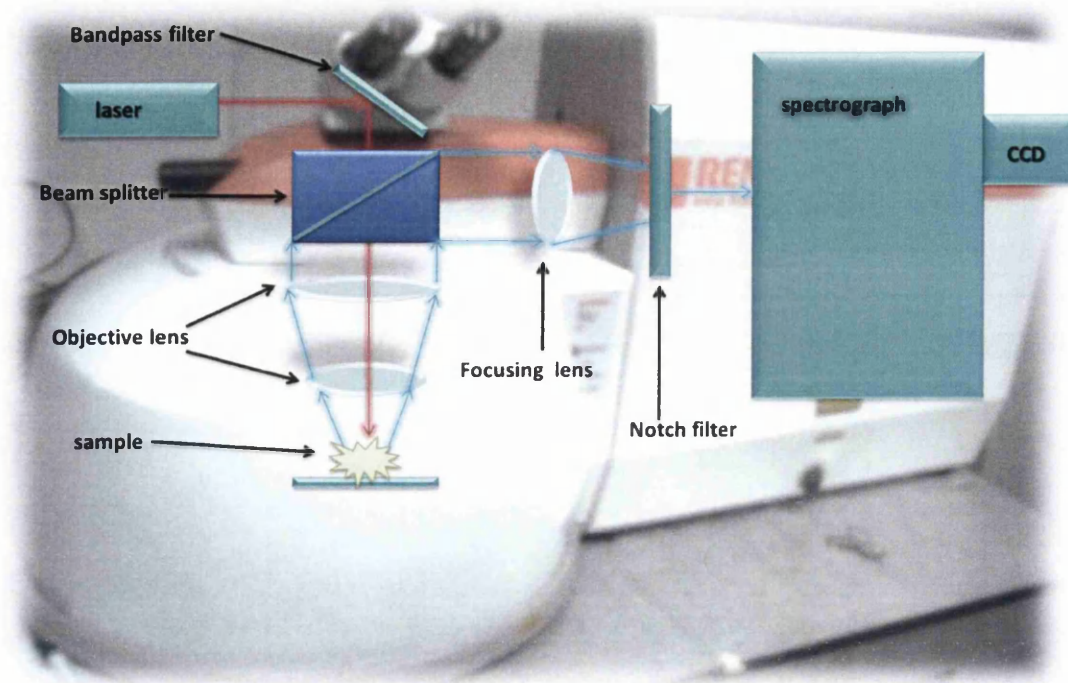


Figure 1.3.: Schematic representation of Raman System coupled with microscope.

1.8.2. Modifications and Types of Raman Spectroscopy

Several disadvantages associated with normal Raman spectroscopy and include; i) inherent weak intensity and; ii) corresponding low sensitivity; iii) problems with selectivity in terms of very high variability of biological milieu. These problems have resulted in modifications and enhancements to the technique.

1.8.2.1. Micro-Raman Spectroscopy

An important advance in applying Raman spectroscopy for broad use was coupling the traditional system setup with a microscope. This allowed the region of interest to be targeted with the use of objectives providing an appropriate numerical aperture. Further incorporation of confocal microscopy allowed for much higher spatial resolution of the studied samples. Biological studies became simplified and 3-dimensional image translation was finally possible. Indeed as the confocal pinhole implements geometry this results in only selected photons being collected after scattering before reaching the detector and thus high precision is achieved and additional, spatio-temporal information is given for identification and quantification. When the laser is guided through an objective

lens, a near-diffraction limited spatial resolution and increased collection efficacy can be achieved. Choosing the right wavelength and objective can provide a very good spatial resolution, but also remain non-invasive, maintaining sample integrity and allowing for direct measurements in either air or aqueous solution, which is especially important for biological samples. Micro-Raman spectroscopy has therefore enabled molecular structure and composition analysis on multiple focal plans (Mariani et al., 2010).

Micro-Raman spectroscopy can also benefit from fluorescent staining, however the technique is not as straightforward as using plain fluorescence microscopy, since the fluorescence effect can often mask the much weaker Raman process. This may enable differentiation between biotic and abiotic or living and dead cells, therefore Raman spectroscopy can be selectively used to only the relevant elements within the sample (Krause & Radt, 2007), especially when the laser excitation wavelength is chosen outside the fluorophore adsorption band (Krause et al., 2008).

1.8.2.2. Fibre-optics

To record spectra from remotely situated samples another important Raman Spectroscopy enhancement was developed and is based on using fibre-optic probes. This modification has found use for the monitoring of environmental pollutants in a range of aqueous solutions, solids and slurries in hostile environments (Gerrard, 1994).

1.8.2.3. Surface Enhanced Raman Spectroscopy (SERS)

Since Raman Spectroscopy uses only very rare incidents of photon-matter interactions, the signal can be rather weak. Surface-enhanced Raman Spectroscopy gives rise to a significant enhancement of the electromagnetic field which results in amplifying the power of the laser wavelength like an antenna and acts like a transmitter to enhance the Raman-shifted signal. Amplification can be achieved due to either adsorption or proximity of the sample to a metal substrate including: roughened metal surfaces, colloidal solutions or roughened electrodes. The enhancement can be from several orders of magnitude to as high as 10^{14} (Jarvis et al., 2004). The chemicals regularly used to form substrate colloids, are gold or silver nanoparticles. In order to avoid the molecules clumping they can be coated with a surfactant or encapsulated in a polymer which itself acts as an additional enhancement. Apart from significant signal strength enhancement, studies suggest that SERS can quench fluorescence (Jarvis et al., 2006) and therefore improve the signal to noise ratio during Raman measurements (Efrima & Zeiri, 2009).

Limitations associated with this particular enhancement are related to the melting of particles, even below 1mW laser power, in a diffraction-limited focal spot. Furthermore the non-uniform nature of nanoparticles can often present spot-to-spot variations. Therefore in order to ensure their quality an additional step is required, which, together with the time required for preparation of the substrate suggest that this technique is less suitable for clinical diagnostic laboratory.

1.8.2.4. Tip-Enhanced Raman Spectroscopy (TERS)

This innovative technique is based on an enhancement effect produced at the apex of a sharp gold-coated atomic force microscope tip. The resolution reaches 10nm and has been used for scanning carbon nanotubes, which produce robust Raman scattering (Cançado et al., 2009). When applied to biological molecules with weaker Raman scattering it is likely more time for spectral acquisition may be required (Stockle et al., 2000). However, heating of the gold tip by absorption, limits the usable power to $< \mu\text{W}$ because of boiling of the water film around the tip apex (Deckert, 2009).

1.8.2.5. Resonant Raman spectroscopy

Resonant Raman spectroscopy (RRS) is characterised by excitation at $\sim 250\text{nm}$ and allows for intense, almost fluorescence-free spectra. RRS produces a particularly intense effect for conjugated aromatic molecular moieties, suggesting the advantage of simplicity but this can also distort the ability of distinguishing based on the presence of nucleic acid bases in all organisms. In addition the high cost and complexity of the equipment required may limit the usefulness of this technique (Robert, 2009).

1.8.2.6. Ultra-Violet Resonance Raman Spectroscopy (UVRRS)

Resonance Raman spectroscopy enables choosing the excitation wavelength to match an absorption maximum, especially in the near ultra-violet range ($\sim 200\text{-}300\text{ nm}$). UVRRS can serve as a tool for the determination of secondary structures of biologically relevant molecules (Jarvis & Goodacre, 2008). UV laser excitation however can have a very adverse effect on live cells due to very strong absorption (Tang et al., 2007) (Manoharan et al., 1990).

1.8.2.7. Coherent anti-Stokes Raman scattering (CARS)

CARS, instead of using high-frequency electromagnetic radiation for exciting a low frequency molecular vibration, like it happens with the visible light, applies two different laser frequencies. The difference between those frequencies can be matched with the vibrational frequency of the scanned molecule. Enhancement of 5 orders of magnitude can be achieved and images of high quality can be generated in very short time. CARS uses wavelengths shorter than any of the pump wavelengths, hence it is unaffected by fluorescent background (Dudovich et al., 2002).

The drawbacks of this method are related to the high-intensity laser pulses which can promote two-photon fluorescence and even lead to cell damage. High levels of the CARS signal do not necessarily guarantee better signal-to-noise ratio because of laser fluctuations and the presence of a strong non-resonant background (Petrov et al., 2007).

1.8.2.8. Laser Tweezers Raman Spectroscopy (LTRS)

Optical tweezers and confocal tweezers Raman Spectroscopy overcome the need for immobilising motile samples (such as cells) which could have an effect on the final spectra focused laser beam. Instead, the particle is captured by a laser trap for sufficient time to generate a spectra. A large Raman signal from the trapped cell is generated since the cell is trapped in the focus of the excitation beam, which permits optimum excitation and collection for Raman scattering in confocal configuration. Meanwhile, stray light and fluorescence background from the cell culture plate can be effectively reduced since the cell can be manipulated well above the cover plate (Xie & Li, 2003). Therefore using optical tweezers has become a powerful tool which is able to capture and manipulate particles including single biological cells, spores, discrimination and sorting microorganisms, viruses, mitochondria, red blood cells, analysis of human lipoproteins and chromosomes as well as dynamic accumulation of recombinant proteins produced in a single living cell in a solution (Xie et al., 2007). There is however a possibility of damaging samples through optical trapping unless low power and appropriate wavelengths are used (Xie & Li, 2003).

1.8.3. Raman spectra processing

The interpretation of Raman spectroscopic results can be obstructed by many factors. The data can often be hindered by the broad background signal mostly due to fluorescence

from organic molecules and contaminants. The intensity of fluorescent background is usually much higher than the weak Raman signal in biological samples, and therefore the subtraction of background is an essential process to extract reliable analytical information from biomedical Raman data (Hutsebaut et al., 2006; Kourkoumelis et al., 2012). In addition the information gained from Raman spectroscopy, especially when related to very complicated samples, including biological specimens, can result in very complex spectra. Comparing a high number of Raman peaks in multiple samples is therefore a significant process that is a critical step towards obtaining final results. Numerous methods exist for spectra analysis which need to be carefully chosen to avoid losing any information available, however it should also be straightforward and rapid.

One of the most widely used methods for analysing Raman spectra is Principal Component Analysis (PCA) (Hutsebaut et al., 2006; Jarvis et al., 2004). The spectra are represented as data groupings of similar variability, allowing the identification and differentiation of investigated samples. This approach is widely used to evaluate the possibility of discriminating different data sets using scatter plots. PCA as a method of multivariate analysis which allows the reduction of the number of variables in a multidimensional dataset, while still retaining most of the variation within the dataset (Fan et al., 2011). The order of the principal components (PCs) denotes their importance to the dataset. PC1 describes the highest amount of variation, PC2 the second highest, and so on. Generally, the first three PCs represent the highest variance present in the data sets, up to 99%, giving the best visualisation of the differentiation of the different clusters. (Bonnier & Byrne, 2012)

Further processing of the results obtained from PCA can be done with several different techniques. One of them is based on applying an F-test to individual components to select the most significant PC's ($p < 0.05$) which then can be subjected to linear discriminant analysis (LDA) (Hutsebaut et al., 2006; Maquelin et al., 2000, 2002). These results may also be presented as dendrograms of a hierarchical cluster analysis (Maquelin et al., 2000, 2002) where the level of relatedness between samples is shown.

1.8.4. Applications of Raman Spectroscopy in various fields

There are many applications for Raman Spectroscopy across numerous disciplines. (Kneipp et al., 1999).

1.8.4.1. Sample purity and composition

1.8.4.1.1 Analytical chemistry

Raman spectroscopy was developed and used for chemical and analytical purposes. It enabled the examination of materials, for their lattice strain, particle size, and impurities inclusions. Hence it can be used as a qualitative technique for characterisation of samples like diamond (Haque et al., 1998) or various other crystals (Basiev et al., 1999).

Interestingly Raman spectroscopy can separate polymorphs through recognising differences between symmetries within the crystals. In addition, when using high spatial resolution, crystallites, including single crystals can be analysed, making this technique a very valuable tool in mineralogy (Triebold et al., 2010). Furthermore, Raman spectroscopy can be used for analysis of chemical compounds, such as TiO_2 which is present in paint pigments, toothpaste and many rock formations (Triebold et al., 2010); or SiC used in extreme (high temperatures and power) semiconductor. Raman Spectroscopy may be a very valuable tool for investigating nanocrystalline and amorphous phases of materials that are subjected to highly localised stresses (Kailer et al., 1999).

1.8.4.1.2 Forensic Sciences

Raman spectroscopy has proved useful in forensic science as it does not require any sample preparation, is non-destructive, and can examine samples through plastic packaging or even in glass containers. In this application samples may be almost any size, and will often be aqueous solutions. Raman spectroscopy is therefore convenient for detection of drugs, explosives, fibres, paints, pigments, inks, gunshot residues, fibres, forgeries and fakes (Lepot et al., 2008). Another application is scanning pathology specimens for the differentiation of foreign materials in tissues (Samek et al., 2010b,c).

1.8.4.1.3 Pharmaceutical

There are many ways Raman spectroscopy can benefit pharmaceutical analysis (Fini, 2004). Scanning for polymorphism is a very common use in this field, since unanticipated polymorphic changes of a drug substance can influence chemical and physical stability, solubility and bioavailability (Starbuck et al., 2002).

Raman spectroscopy can be applied for monitoring spatial distribution of drugs in solid dispersions and recognising possible changes like recrystallisation, which may seriously

affect the effectiveness of a drug. Investigation may involve distinguishing between layers, areas and quality of mixing during the manufacturing procedure (Vankeirsbilck et al., 2002).

Tablet coating is an essential process that is carefully monitored where Raman Spectroscopy has proven successful, non-invasive and rapid. Thus the Process Analytical Technology tool for in-line quantitative monitoring of tablet coating directly, rather than relying on indirect physical evidence, like the weight gain has been shown to be particularly effective (De Beer et al., 2011; Hagrasy et al., 2006). Spectral data have even been obtained from drugs directly inside blister packs. Some very subtle differences have been identified between different crystal forms of a compound or crystalline and amorphous forms. It is possible that Raman spectroscopy, after several adjustments and normalisation, could also serve as a quantitative analysis of drugs (Vankeirsbilck et al., 2002).

1.8.4.1.4 Art and archeology

Raman spectroscopy can be used for identifying materials found within particular artefact or a piece of art, this was used for instance to create pigment databases which are currently available online (Vandenabeele et al., 2007a,b). Such information can serve different purposes including dating, future restoration processes or act against forgeries (Chaplin et al., 2002). Raman spectroscopy can also give an insight into the mechanisms of atmospheric corrosion, as the structural imaging enables clear description of material micro-heterogeneity and organisation (Bellot-Gurlet et al., 2006).

1.8.4.2. Physical properties

1.8.4.2.1 Semiconductivity

Raman spectroscopy used at ambient pressure can be used as an alternative technique for thermoelectric measurements at high pressure for semiconductor microsamples. Its sensitivity allows for performing 'nano-identification' of surfaces and for conducting simultaneous co-existence of different phases within the sample. These properties are useful for important testing, characterisation and quality control (Ovsyannikov et al., 2004).

Raman spectroscopy can serve for investigation of 'strain' in bent nanowires (Chen et al., 2010) while characterisation of crystalline nanostructures in silicon nanowires (SiNW) can show confinement signatures typical of quantum wires (Piscanec et al., 2003). Raman spectroscopy was also used to examine SiNWs grown on different materials to

exhibit characteristic thermal conductivities (Lopez et al., 2011) (Khorasaninejad et al., 2012).

1.8.4.3. Bio-Medicine

There are several characteristics qualifying Raman spectroscopy as particularly useful for biology and medicine. Apart from high precision and preservation of the sample it also offers significantly decreased time of measurement, as living cells and tissues sections are of high sensitivity. Additionally, when the excitation frequency chosen is near the frequency of electronic transition of the molecule, Raman intensities may be enhanced by several orders of magnitude, which allows for examining even relatively diluted samples.

The main disadvantage of using Raman for biological samples is fluorescence, which even in small amounts can significantly obscure the spectra (Petry et al., 2003). One way of overcoming this problem is longer irradiation of the sample with the laser, which does carry a risk of sample damage. If the problem is related to fluorescence causing impurities, those can be removed prior to the measurement, and if fluorescence is intrinsic to the sample, a background correction analysis may be of help. Raman spectroscopy can determine the content of a biological sample through measuring the ratio of protein, enzymes, lipids and nucleic acids. Such results inform on structure and dynamics of biological samples. Scanning essential life molecules can be used as a library and references for any further research (Fabian & Anzenbacher, 1993).

Micro-Raman, in particular, has provided a wide range of benefits for biological use due to its high level of technical flexibility. Using a microscope offers flexibility to change objective lenses and readily apply different wavelengths making this technique applicable to wide varieties of studies, while fully automated xy maps and line scans can maintain the spatial and temporal resolution. The results are Raman spectral images giving direct insight into the composition of the analyte with resolution on a molecular level, resulting in very objective view of pathology or even cell functionality. Single point and imaged samples can therefore provide a complete chemical snapshot of the sample, including the presence of DNA, RNA, protein, lipid and carbohydrate content. Quantitative and qualitative results are obtained when emission or adsorption patterns, distinct for all functional groups and organic compounds, are measured.

The ease of use and numerous applications of Raman spectroscopy permits for samples to be fixed, dried, analysed alive or even measured *in vivo*, reducing the need for biopsies. Minimum sample processing allows also for further sample analysis like IR spectroscopy,

traditional histology and gene expression analysis for result comparison. This combination of methods, provides even more understanding of the measured sample (Mariani et al., 2010).

The study by Pereira et al. showed the use of Fourier-transform Raman spectroscopy for identification of phycocolloid produced by seaweed (Pereira et al., 2003), while Huang et al. and Samek et al. proved that Raman spectroscopy can be successfully used for characterisation of lipid storage within algal cells (Huang et al., 2010; Samek et al., 2010b,c). Raman spectroscopy has proven useful especially in diagnosis and has given successful results in cancer research for intestinal, breast, uterine, laryngeal, skin and brain malignancies as well as studies of skin, detection of malignant and pre-malignant lesions or in arteriosclerotic research through characterisation of atherosclerotic plaques by quantification of cholesterol and cholesteryl esters (Choo-Smith et al., 2002).

1.8.4.4. Raman spectroscopy in the field of Infectious Diseases

1.8.4.4.1 Colonies and biomass

Studies suggest that Raman micro-spectroscopy possesses the ability for recognising specific structures within microbial organisms and can therefore discriminate between bacteria at the genus and species levels.

Micro-Raman is particularly useful for monitoring bacterial samples in the form of colonies on agar plates. It was possible to distinguish between *Micrococcus luteus*, *Bacillus subtilis* and *Pseudomonas fluorescens* (Rsch et al., 2003) as well as between *E. coli*, *S. aureus* and between strains of *S. epidermidis* relevant to medical device-associated infections (Samek et al., 2008). In addition, further differentiation between the properties of biofilm forming *S. epidermidis* 1457 and non-biofilm forming 1457-M10 mutant was also possible (Samek et al., 2010b,c).

An important quality offered by Raman spectroscopy is limiting the time of culturing to increase the speed of diagnosis. Thus instead of growing full size colonies, microcolonies can be scanned. This has proven successful through examination of *E. coli*, *S. aureus*, *S. epidermidis* and *Enterococcus faecium* strains cultivated on solid media for only 6h (Maquelin et al., 2000) and also for the large collection of bacterial and fungal organisms collected from patients (Maquelin & Kirschner, 2003).

In contrast to using colonies or microcolonies sample preparation by smearing bacterial biomass, obtained after cultivation, on a chosen substrate, has been examined in several studies. Spectra taken from several different strains of *Enterococci* applied on a CaF₂

window from various sources, including isolates from food, patient material and strain collection (Kirschner et al., 2001). Using a similar approach differentiation of 68 strains, within 8 species of *Bacillus* genus was achieved and compared to a reference database resulting in over 80% success rate (Hutsebaut et al., 2006). Clinical isolates of urinary tract infections isolates in a form of biomass smeared onto the CaF₂ window, have been scanned with the use of UVRRS (Jarvis & Goodacre, 2004b) and with SERS (Jarvis & Goodacre, 2004a). In order to achieve more thorough analysis of applying SERS for bacterial strains, SEM has been employed prior to scanning *Bacillus subtilis* and *E. coli* on a silver colloid substrate (Jarvis et al., 2004) and for detection of food and waterborne bacteria, including *E. coli* O157:H7, when additional monitoring of the silver-based substrate was performed using TEM (Fan et al., 2011). The need for analysing SERS substrates prior to bacterial measurement stimulated new methods of generating colloidal suspensions for application to *E. coli*. (Kahraman et al., 2008) and further investigation of the SERS substrate for its qualities (Efrima & Zeiri, 2009).

SERS has proved effective when applying Fourier transformed Raman to overnight suspensions of *Listeria monocytogenes*, *Salmonella typhimurium* and *E. coli* where only small volumes of bacterial suspensions and short preparation time of bacteria-colloid mixture was required prior to measurement (Y. Liu, et al., 2008). In addition a study using strains of the *Bacillus* group in the form of log stage cultures applied to either KBr plates or SERS using Au-nanoparticle-covered SiO₂ substrates (Patel & Premasiri, 2008).

Near infrared laser in a line mode has been applied to samples on SERS active substrate for identification and discrimination of bacterial organisms within bacterial and bacteria-yeast mixtures, including *Shigella sonnei*, *Erwinia amylovora*, *Proteus vulgaris* and the DH5 α strain of *E. coli* Cam et al. (2009).

SERS has proven useful for quantitative and semi-quantitative analysis of bacterial organisms. A promising detection limit of $\sim 10^3$ has been achieved in a simple straightforward measurement free from any additional labels or antibodies but adding nanocolloidal silver nanoparticles to aqueous suspension of *E. coli* and *P. aeruginosa* grown for 17h (Sengupta et al., 2006) as well as prospective studies of quantifying waterborne bacteria (Escoriza et al., 2006). Another useful application allows for determination of microorganism ratios directly from the samples without being transferred onto a growth medium. These findings concluded that environmental samples had similar bacterial content to that of dental plaque including *S. sanguis*, *S. mutans*, and *S. gordonii* strains. The relative populations of those bacteria were predicted with the accuracy of few percent

using confocal Raman spectral analysis (Zhu et al., 2004) (Xie et al., 2007).

Comparison of single cells from bacterial smears with bulk samples (Harz et al., 2005) show that variability may arise from using different culturing methods (Rösch et al., 2003). Studies performed on *K. pneumonia*, *E. coli*, *P. aeruginosa*, *E. faecalis*, and two strains of *S. aureus*, demonstrated that spectra of the same organism grown in different media exhibit the same vibrational spectral features (Premasiri et al., 2011).

Metabolic information about bacterial cells and their function as well as their interactions with the environment can also be determined by Raman spectroscopy. SERS was used to monitor the hydrolysis of triglycerides in lipid mixtures of *Propionibacterium acnes*, including wax esters, squalene, triolein and triostearin (Weldon et al., 1998). Raman micro-spectroscopy was also used to evaluate ratios of C:N:P resource stoichiometry within macromolecular composition of *Verrucomicrobium spinosum* and *Pectobacterium carotovorum* grown in log and stationary growth phases (Hall et al., 2011). Further investigation of bacterial metabolism with the use of Raman spectroscopy, included the uptake and retention of xylitol in *E. coli* and viridians group streptococcus (Palchauthuri et al., 2011). Metabolic activity was also investigated in the *Protochalmydia amoebophila*, a non-pathogenic, model organism for symbiotic *Chlamydiae* and was compared with host-free activity of the human pathogen *C. trachomatis* (Haider et al., 2010). Using optical fibres as SERS probes enabled the scanning of single molecules such as lysozyme and cytochrome c with the detection limit of 0.2 µg/ml and also detects *Shewanella oneidensis* at 10⁶ cells/ml Yang et al. (2011). The abundance of cytochrome c within *Geobacter sulfurreducens* allowed SERS to monitor redox reactions of silver and constrained nanoparticles of gold inside the bacteria (Jarvis et al., 2008). Another possible improvement of the present SERS technology could involve construction of a portable system that could be useful for identification of pathogens, involving the food-borne harmful organisms including *L. monocytogenes*, *E. coli* O157:H7 and *S. typhirium* (Luo & Lin, 2008).

Combining Raman spectroscopy with Atomic Force microscopy can help to investigate biomechanical, as well as biochemical properties of living cells under physiological conditions. Using this approach *Pseudomonas putida* were scanned to achieve information about molecular structure, cell architecture and biomechanical properties (Zhou et al., 2010).

Raman spectroscopy has also proved useful when investigating bacterial biofilms. Multispecies biofilm matrix could be characterised with microbial constituents and extracellular polymeric substance. Raman microscopy was able to correlate different structural

features of the biofilm to changes in its chemical composition and therefore deliver information about particular components of the complex biofilm matrix (Ivleva et al., 2009). It was also possible to perform discrimination of different bacterial species in a biofilms. Samples of *Streptococcus mutans* and *Streptococcus sanguinis* were examined in isolation and in pseudo-mixed biofilms with very high validation and lateral resolution of $\sim 2\mu\text{m}$, which could be sufficient for structural studies of intact, multispecies biofilms (Beier et al., 2010). Raman micro-spectroscopy was applied for *in vivo* analysis of the first $80\mu\text{m}$ of undisturbed biofilms in water as well as the bacterial distribution, tracking and identification were taken into account on the level of single cells. The outer layer, containing microparticles was analysed when taking into account the mineral phase and surrounding bacterial microcolonies (Kniggendorf & Meinhardt-Wollweber, 2011). Further investigations scanning biofilms to determine their biochemistry and distribution within the biofilm in order to gain an insight on whether and how the water presence is affected by the nature of the microbial strain or species forming the biofilm. The study was performed on *Pseudomonas aeruginosa* and mucoid marine bacteria: *Pseudoalteromonas* sp. (Samek et al., 2010b,c). Further biochemistry of biofilms has been confirmed through the mapping of chromate, sulphate and nitrate using *Shewanella oneidensis* as a model (Ravindranath et al., 2012).

1.8.4.5. Single cells

Recent progress has allowed Raman spectroscopy to examine bacterial single cells. The organisms commonly responsible for gastroenteritis, namely *E. coli*, *Salmonella choleraesuis*, and *Shigella flexneri* grown for 10h were used to prepare bacterial suspensions that gave 100% correct classification (Mello et al., 2005). Strains of *Staphylococcus cohnii*, *S. epidermidis* and *S. warnei* could be differentiated from both: bulk samples and single cells (Harz et al., 2005) of *Streptococcus pneumoniae*, *Streptococcus agalactiae*, *Neisseria meningitidis*, *S. epidermidis* and *Listeria monocytogenes* following 18h growth in the form of suspensions spotted on fused silica plates, in order to identify pathogens causing meningitis. Furthermore *S. epidermidis* was chosen as a model organism in a cerebrospinal fluid (CSF) matrix using a similar experimental approach (Harz et al., 2009). Raman microspectroscopy could be used for real-time monitoring of methacillin resistant and sensitive strains of *Staphylococcus aureus* grown for 20h and placed on a quartz slide (Willemse-Erix et al., 2010). In order to differentiate between live and dead samples, 2-days old suspensions of *Bacillus* and *Staphylococcus* strains were stained with

Syto9 and Propidium iodide prior to subjecting them to Raman measurements in the form of drops on a fused-silica surface (Krause et al., 2008). When ZnO nanoparticles were used as an enhancement substrate for SERS, successful observation of single cells of *E. coli* was also possible (Dutta et al., 2009).

Investigating single cells for metabolic changes was performed in *Cupravidia metalidurnas* during five different stages of growth, focusing mainly on primary metabolites and their state during the life stages of the cell (De Gelder, 2007; De Gelder et al., 2007a,b,c). Diagnostic properties of Raman spectroscopy for discrimination and investigation of bacterial biochemical content were also shown for *Mycoplasma pneumonia* (Maquelin et al., 2009), while strains of *Bacillus megaterium*, *Bacillus thuringiensis*, *Azohydromonas lata*, and *Cupriavidus necator* were tested for the use of polyhydroxyalkanoates (PHA) as carbon and energy storage materials (Ciobot et al., 2010).

Confocal resonance Raman spectroscopy was used to investigate the effects of fixation methods with different chemicals, including paraformaldehyde and ethanol as the most popular means and applied poly-L-lysine for coating slides. Raman microscopy was proven compatible with both fixing methods during short fixing exposure and when slides were uncoated (Kniggendorf et al., 2011).

Extending Raman spectroscopy applications further has incorporated optical tweezers. Optical trapping allows lifting a single living cell captured in a solution, so that the fluorescence interference from a substrate or plate can be effectively reduced. In the study conducted on *E. coli*, yeast cells, and red blood cells, fluorescence interference was removed further by shifting the excitation Raman difference in the confocal mode (Xie & Li, 2003). This approach has been also used when studying possibilities to detect recombinant somatolactin β protein in single live *E. coli* and *Pichia Pastoris* yeast in aqueous solutions (Xie et al., 2007). Further advances include label-free SERS detection of microorganism in a microarray flow-through system including single-cell imaging of *E. coli* as a proof of concept and quantification of bacteria in a aqueous sample (Knauer et al., 2012).

When Raman spectroscopy was applied for differentiating single cells in a complex mixture of *Bacillus anthracis Sterne* spores and vegetative cells of *Bacillus cereus*, both Raman chemical imaging microspectroscopy and SERS generated spectra from single bacterial cells and spores (Guicheteau et al., 2010). Separate research using spores of *B. anthracis*, *Bacillus subtilis*, *Bacillus mycoides*, *Bacillus sphaericus*, *Bacillus thuringiensis*, and *B. thuringiensis* implied that Raman spectroscopy could be functional for real-

world isolates after inactivation for on-site diagnosis (Stöckel et al., 2010). Bacterial spores were also investigated for their composition through studying changes in Raman spectra during *Bacillus licheniformis* growth and sporulation (De Gelder et al., 2007c). It was shown spectra of *Bacillus subtilis* single endospores taken by CARS were in agreement with traditional Raman spectroscopy however CARS proved to be at least two orders of magnitude more efficient. This suggested 100 times faster remote sensing and detection of possible biohazards (Petrov et al., 2007).

1.8.4.6. Preparation-free approach

One of the first studies performed with a culture-free approach was based on UVRRS for identification *Brochothrix thermosphacta* and *Pseudomonas fluorescens*. Those strains were used as model foodborne bacteria and the beef carcass was involved in the measurement as well (Harhay & Siragusa, 1999).

A sample of CFS containing *Neisseria meningitidis* was obtained directly from the hospital patient and was successfully scanned on a fused silica slides (Harz et al., 2009).

Aims and Objectives

Less is known in terms of a complete summary of application of Raman spectroscopy for a routine use for diagnosing bacterial caused diseases in hospital wards, especially when antibiotic screening is involved. Therefore this project solely focuses on the application of Raman Spectroscopy for real, everyday testing that could be utilised with clinical samples.

In Chapter 3, strict methods of application of Raman spectroscopy were assessed, including sample size, materials that are the most appropriate, system overview and spectra processing. This part of work sets up the procedure that was followed in the all the experiments performed.

Hypothesis: it is possible to design an easy, cost and labour-efficient set of methods to obtain repeatable and accurate Raman spectra from microorganisms.

In Chapter 4, the ability of Raman Spectroscopy for distinguishing of bacterial organism was assessed and therefore the diagnostic potential of the technique was proved.

Hypothesis: Raman spectroscopy can differentiate between microorganisms belonging to various genera, species and groups exhibiting subtle sub-species characteristics

In Chapter 5, the possibility of Raman Spectroscopy to involve screening of different bacterial antibiotic susceptibility profiles is investigated. The chapter includes the complete microbiological experiments performed to assess the functionality of the bacterial transformants that were created for the purpose of this project, as well as spectral analysis performed on those organisms extending the comparison abilities of Raman Spectroscopy to isogenic strains expressing different antibiotic resistance properties.

Hypothesis: Raman spectroscopy can be used for differentiation between microorganisms with various susceptibility profiles.

In Chapter 6 clinical isolates selected for the expression of extended spectrum β -lactamases are being investigated. Spectra are compared in terms of the resistance profiles the organisms express. Furthermore the clinical strains were also grouped according to the phylogenetic classification.

Hypothesis: Raman spectroscopy can be used for differentiation between microorganisms expressing different extended spectrum β -lactamases genes belonging to different phylogenetic classes.

2. MATERIALS AND METHODS

2.1. Materials

2.1.1. Laboratory instruments and equipment

Table 2.1.: Laboratory instruments and equipment used in this study

Equipment	Source
Incubator	Genlab, Uk HT Inforse Minitron Satorius Certomat BS-1
Shaking incubator	Lab Therm LT-X - shaker by Kuhner
Biological safe cabinet (category 2)	Scanlaf
Bench-top autoclave	Prestige Medical
Front load autoclave	Priorclave
FLUOstar Optima plate reader	BMG Labtech
Shandon Cytospin [®] 3	Thermo Electron Corporation
NanoDrop Spectrophotometer	Labtech
Bio-Doc It UV Transilluminator system	Bio-Rad
Laser Scanning Confocal Microscope (710)	Zeiss
Bench spectrophotometer 7310	Jenway
Raman InVia System	Renishaw
PCR Tetrad2 Thermal Cycler	Bio-Rad
Gel electrophoresis PowerPac System	Bio-Rad
pH meter 3310	Jenway

2.1.2. Miscellaneous materials

Table 2.2.: Miscellaneous materials used in this study.

Material	Source
Petri plates (90x15mm)	Greiner Bio-One, UK
96-well microtitre plate	ThermoScientific
API E20 [®]	Biomérieux
Wizard [®] Plus SV Miniprep	Promega
Plastic cuvettes	FisherBrand
Electroporation cuvettes (2mm)	Molecular BioProducts, USA
Clear microscopic glass slides	FisherBrand
Frosted microscopic glass slides	VWR
8-welled slides (Nunc [®] Lab-Tek [®])	ThermoScientific

2.1.3. Membranes

Table 2.3.: Membranes used in this study

Membrane	Source
Nitrocellulose	Schleicher & Schuell
Immobilon	Millipore
MCE	Millipore
Nylon	Millipore
PES	Millipore
PTEF	Millipore
PVDF S-Pak™	Millipore

2.1.4. Chemicals and reagents

Table 2.4.: Chemicals and reagents used in this study

Chemical	Source
Agarose	Melford
TSB powder	Oxoid
Agar (number 3)	Oxoid
EC powder	Oxoid
Tryptone	Formedium
Yeast Extract	Formedium
NaCl	FisherScientific
Glycerol	FisherScientific
5X Green GoTaq® Flexi Buffer	Promega
5X Colourless GoTaq® Flexi Buffer	Promega
Magnesium Chloride Solution (25mM)	Promega
Deoxynucleotide Triphosphates (dNTPs): dATP, dCTP, dGTP, dTTP (10mM each)	Promega
Silver Nitrate	Acros Organics
Trisodium citrate	Fisher Scientific
Tris Base	Fisher Scientific
Ethylenediaminetetraacetic acid (EDTA)	Fisher Scientific
Glacial acetic acid	Fisher Scientific
Buffer D	Promega

2. MATERIALS AND METHODS

2.1.5. Common buffers and solutions

50x Tris-acetate-EDTA (TAE) buffer

Tris base	242g
EDTA	22.6g
Glacial acetic acid	57ml

Made up to 1L with dH₂O, pH adjusted to 8.0

Tryptose Soy Broth (TSB)

TSB powder	30g/L
15g/L agar	was used for TSB agar

Made up to 1L with dH₂O and autoclaved for 45 minutes at 121°C and 1 bar pressure.

EC Broth/agar

EC powder	37g/L
10g/L a	was used for EC agar

Made up to 1L with dH₂O and autoclaved for 45 minutes at 121°C and 1 bar pressure.

Luria-Bertani (LB) Broth/agar

Difco Bacto Tryptone	10g/L
Difco Bacto Yeast Extract	5g/L
NaCl	10g/L
10g/L agar	was used for LB agar

Made up to 1L with dH₂O, pH adjusted to 7.4 and autoclaved for 45 minutes at 121°C and 1 bar pressure.

2.1.6. Agar plates

EC and LB agar plates were prepared after cooling the autoclaved agar solution to ~56°C and aseptically pouring 25ml per single plastic Petri dish before leaving to solidify in a biological safe cabinet.

Columbia (horse) Blood Agar plates were purchased from E&O Lab Limited.

Fresh agar plates were stored at 2 to 8°C in separate refrigerators or in the laboratory cold room.

2.1.7. Antibiotics used in this study

Table 2.5.: Antibiotics used in this study

Antibiotic (in the powder form)	Source
Ampicillin	Melford
Kanamycin	Kanamycin

2.1.7.1. Antibiotics stocks:

Antibiotic stocks were prepared using powder diluted with dH₂O to obtain the final concentration of:

Ampicillin	100mg/ml
Kanamycin	100mg/ml or 50mg/ml

All antibiotic stocks were kept in a -20°C freezer.

2.1.7.2. Antibiotic suspensions:

Antibiotic suspensions were prepared by using antibiotic stocks dissolved in appropriate broth (EC for K12 and LB for Top10) to the final concentration of:

Ampicillin	100µg/ml
Kanamycin	50µg/ml

2.1.7.3. Antibiotic containing agar plates

After bringing autoclaved EC or LB agar to the temperature of 56°C, antibiotics stocks were added mixed and 25ml was poured per single plastic Petri plate before leaving to solidify as previously described.

Antibiotic containing CBA plates were prepared by adding the desired antibiotic to the surface of the CBA agar, spreading it and allowing it to dry.

The final concentrations of antibiotics on all the plates were:

2. MATERIALS AND METHODS

Ampicillin containing plates: 100 μ g/ml
Kanamycin containing plates: 50 μ g/ml

2.1.8. Stains and markers

Table 2.6.: Stains and markers used in this study

Stain	Source
Propidium Iodide (1mg/ml)	Sigma-Aldrich
Syto [®] 9 (5mM)	Invitrogen
Sybr Safe [®] (10,000X)	Invitrogen
6X loading dye	Promega
1,000 bp molecular DNA marker	Promega
100 bp molecular DNA marker	Promega

2.1.9. Enzymes

Table 2.7.: Enzymes used in this study

Stain	Source
GoTaq DNA Polymerase (5u/ μ l)	Promega
<i>Xba</i> I (10U/ μ l) restriction enzyme	Promega
<i>Xho</i> I (10U/ μ l) restriction enzyme	Promega
<i>Bam</i> HI (10U/ μ l) restriction enzyme	Promega

2.1.10. Primers

Table 2.8.: Primers used in this study

Primer	Sequence (5'→3')	Source
ChuA.1	GACGAACCAACGGTCAGGAT	Eurofins
ChuA.2	TGCCGCCAGTACCAAAGACA	Eurofins
YjaA.1	TGAAGTGTCAGGAGACGCTG	Eurofins
YjaA.2	ATGGAGAATGCGTTCCTCAAC	Eurofins
TspE4C2.1	GAGTAATGTCGGGGCATTCA	Eurofins
TspE4C2.2	CGCGCCAACAAAGTATTACG	Eurofins

2.1.11. Plasmids

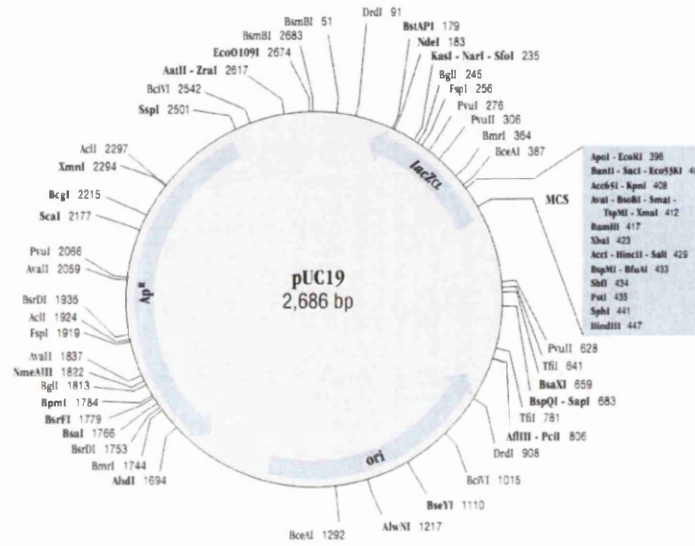


Figure 2.1.: Map of pUC19 plasmid (Nari)

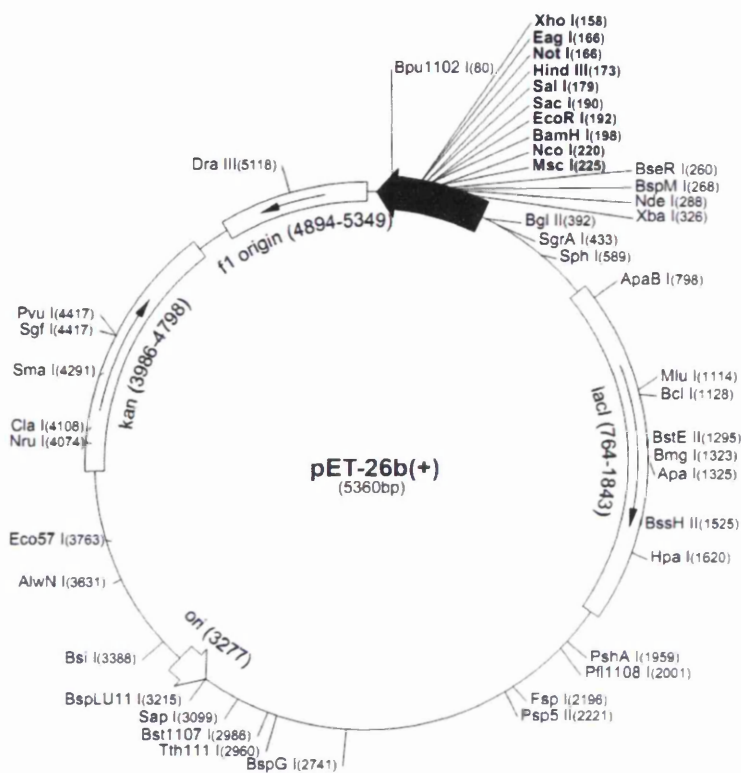


Figure 2.2.: Map for pET-26 plasmid (Novagen)

2.1.12. Bacterial Strains

Table 2.9.: Reference laboratory strains used in this study

Species	Strain	Source	Reference
<i>E.coli</i>	K12	Laboratory	Kind gift from Prof. D.Mack
	Top10	Invitrogen	Purchased
	Strain B	Laboratory	Kind gift from Prof. D.Mack
<i>S. epidermidis</i>	1457	Laboratory	(Mack et al., 1992)
	9142	Laboratory	(Mack et al., 1992)
<i>S. aureus</i>	Cowan1	Laboratory	(Mack et al., 1992)

Table 2.10.: Reference hospital isolates used in this study

Species	Strain	Source
<i>E. coli</i>	10418	Singleton Hospital
<i>S. aureus</i>	6571	Singleton Hospital

Table 2.11.: Laboratory transformed strains expressing antibiotic resistance

Species	Strain	Antibiotic resistance	Source
<i>E. coli</i>	Top10 ^A (and Top10 ^{AA})	Ampicillin	This study
	Top10 ^K (and Top10 ^{KK})	Kanamycin	This study

Table 2.12.: Archived *E. coli* hospital isolates of different antibiotic profiles

Antibiotic resistance profile	Number of strains	Reference
CTX-M15 IS26 positive	38	(Jones, 2012)
CTX-M-15 IS26 positive, TEM1	3	(Jones, 2012)
CTX-M-15 IS26 positive, TEM-116	2	(Jones, 2012)
CTX-M-15	4	(Jones, 2012)
CTX-M-1	2	(Jones, 2012)
CTX-M-15, TEM1	8	(Jones, 2012)
CTX-M group1	1	(Jones, 2012)
CTX-M-14b, TEM1	1	(Jones, 2012)
CTX-M-32, TEM1	2	(Jones, 2012)
CTX-M-14, TEM1	1	(Jones, 2012)
TEM-52	1	(Jones, 2012)
SHV-2	1	(Jones, 2012)
AmpC	1	(Jones, 2012)

Table 2.13.: Laboratory *E. coli* strains used as standard for phylogenetic classification

Name	Phylogenetic group	Reference
ECOR33	B1	(Méric et al., 2013)
ECOR59	B2	(Méric et al., 2013)
ECOR50	D	(Méric et al., 2013)

2.1.13. Routine culture of bacterial strains

All strains were grown under aerobic conditions at 37°C.

Solid medium cultures were prepared by spreading: i) a portion of glycerol stock; ii) several colonies; or iii) 100µl of overnight culture onto an appropriate agar plate. For

2. MATERIALS AND METHODS

microbiological experiments *S. epidermidis* were grown on TSB plates, *E. coli* K12 strains were grown on EC plates, *E. coli* Top10 were grown on LB plates. Antibiotic containing agar plates were used for the transformed strains expressing antibiotic resistance. Bacteria on plates were grown for 18-24h in a stationary incubator unless otherwise stated. Bacteria on agar plates were stored at 2-8°C for no longer than 3 months. For Raman spectroscopic measurements all strains were grown on CBA plates unless otherwise stated.

Bacterial suspensions were prepared by inoculating a single colony or a portion of bacterial glycerol stock in 5ml broth. *S. epidermidis* strains were grown in TSB broth, *E. coli* K12 strains were grown in EC broth and *E. coli* Top10 strains were grown in LB broth. Bacteria in suspensions were grown for 18-24h in a shaking incubator unless otherwise stated.

2.1.14. Preparation and storage of bacterial stocks

All bacterial strains were preserved in glycerol stocks prepared by adding 500 μ l of 80% glycerol solution to 500 μ l of an overnight bacterial suspension or mixing 250 μ l of 80% glycerol solution with 750 μ l of an overnight bacterial suspension. Working stocks were stored at -20°C for periods of no longer than 3 months and in a -80°C freezer for the entire period of this study.

2.1.15. Software

Table 2.14.: Software used in this study

Program	Use	Version	Source
WiRE InVia	Raman Spectrophotometer	v. 3.0	Renishaw
ASGRCF (running on LabView engine)	Spectra processing background removal	v.1.0.0	G. Gonzlvez et al. 2012
Applied Savitzky Golay smoothing Rolling Circle Filter)			
Matlab	Code for spectra processing	7.10.0.499	The MathWorks
R	Various codes	2.14.0	http://cran.r-project.org
Origin	Various use	8.5.0 SRO 8.6.0	OriginLab Corporation
PyChem	Spectra processing - Principal Component Analysis	3.5.0g Beta	Roger Jarvis
GraphPad Prism Confocal Microscope Software	Statistical analysis Confocal Microscope	6 Zen 2009 Light Edition	GraphPad Software Carl Zeiss
ImageJ	Processing confocal microscope images	1.47	MicroImaging GmbH Rasband, W.S., ImageJ, U. S. National Institutes of Health, Bethesda, Maryland, USA, http://imagej.nih.gov/ij/ , 1997-2012.
QuantifyOne	Bio-Doc It UV transilluminator system	4.6.3	Bio-Rad
NanoDrop 1000	NanoDrop Spectrophotometer	3.8.1	Labtech

2.2. Methods

2.2.1. Determination of bacterial concentration

Bacterial concentration was assessed for experiments including *E. coli*, by determining the optical density (OD) at 600nm using a spectrophotometer. Sterile growth media was used as blank prior to testing bacterial suspensions. The estimated bacterial count at $OD_{600} = 1.0$ was $\sim 1 \times 10^8$ cfu/ml for *E. coli*.

2.2.2. Transformation

2.2.2.1. Preparing electrocompetent K12 cells

An overnight bacterial suspension (250ml) of K12 was decanted into five 50ml tubes and centrifuged for 10min at 4000rpm at 4°C. Supernatants were discarded from all bottles and all five pellets combined and resuspended in 50ml of ice-cold glycerol. The sample obtained was centrifuged for 10min at 4000rpm at 4°C, the supernatant discarded and the pellet resuspended in 50ml of ice-cold glycerol. This procedure was repeated twice more. The resulting pellet was finally resuspended in 1ml of ice-cold glycerol. Electrocompetent cells were stored in 50 μ l aliquots at -80°C until use.

2.2.2.2. Transformation by electroporation

Fifty microlitres of electrocompetent cells were aliquoted to a pre-cooled (on ice) electroporation cuvette (0.2cm gap). Then 1 μ l of 1 μ g/ μ l plasmid DNA (pUC19 or p-ET26) was added to the electrocompetent cells, mixed gently and incubated on ice for 5 minutes. The cuvette was then placed in the electroporator before using the '*E. coli* 2mm 250' pre-set protocol. The cuvette was then placed on ice and the contents of the cuvettes transferred to 250 μ l of recovery media (without antibiotics): EC for K12 and LB for Top10; and placed in a vertical position in a shaking incubator at 37°C for 3h. After the recovery, 50 μ l of suspension was spread on a selective agar plate and incubated overnight at 37°C. The remaining suspension was stored in the fridge until growth was determined on the initial set of plates. Control transformations without added DNA were prepared in a similar manner.

2.2.2.2.1 Calculating transformation efficiency

Transformation efficiency was calculated using the formula:

$$\text{Efficiency (cfu/}\mu\text{g DNA)} = \frac{\text{Number of colonies on a plate (cfu)}}{\text{Amount of DNA used for transformation (}\mu\text{g)}}$$

Routinely we found transformation efficiencies of 1×10^8 cfu/ μ g DNA for Top 10 and 3×10^4 cfu/ μ g DNA for K12.

2.2.3. Determination of minimal inhibitory concentration (MIC) by limiting dilution

MIC was determined using the limiting dilution method. Overnight suspensions of K12 and Top10 including transformed strains, were corrected to $\text{OD}_{600} = 0.1$ ($\sim 10^7$ /ml) and 100 μ l were added to each well of a 96-well. Antibiotic solutions were prepared at by serial dilution of stock solution with the appropriate broth (EC for K12 and LB for Top10), in order to obtain 11 defined final concentrations (1024; 512; 256; 128; 64; 32; 16; 8; 4; 2; 1 μ g/ml) and a negative control containing media alone. Then 100 μ l of antibiotic solution was transferred to onto the bacterial suspensions. After overnight incubation at 37°C in a stationary incubator, plates were assessed for growth by measurement of OD_{600} in the plate reader. Growth was defined as $\text{OD}_{600} > 0.15$.

2.2.4. Temporal response to the action of antibiotics

An overnight bacterial culture (5ml) was adjusted to $\text{OD}_{600}=1$, and 100 μ l for each: experimental and control samples were aliquoted. The experimental sample was added with antibiotic to a final concentration of 100 μ g/ml for ampicillin and 50 μ g/ml for kanamycin while the control samples did not include antibiotic. All samples were incubated at 37°C and then at defined time points (0, 60, 120 and 240min for Ampicillin and 0, 30, 60 and 120min for Kanamycin) 100 μ l of bacterial suspension was transferred from each: experimental and control solutions, adjusted to the required concentration by 1:10 serial dilutions with growth medium and two selected dilutions plated onto agar plates. These plates were incubated at 37°C overnight and viable counts determined by counting colonies the following day. The concentration of bacteria in the original solution was determined from:

2. MATERIALS AND METHODS

$$\text{Bacteria/ml} = \text{Dilution} \times 10 \times \text{Colony count}$$

The significance of the experiments was calculated by testing the CFU counts with one-way ANOVA with the $P < 0.05$ using the option available from Prism GraphPad.

2.2.5. Isolation of Plasmid DNA

Preparation of plasmid DNA was performed according manufacturer's instructions with slight modifications. All solutions used for the isolation of DNA were supplied with the Preparation Kit.

After overnight growth of bacterial suspension, 2.5ml was centrifuged for 10min at 14000rpm. Supernatant was decanted and excess drips were blotted on a paper towel. To produce a clear lysate, 250 μ l of Cell Resuscitation Solution was added to the pellet, resuspended thoroughly and transferred to a microcentrifuge tube. Subsequently, 250 μ l of Cell Lysis Solution was added and tube was mixed by inverting four times. This solution was then incubated for 1-5 minutes at room temperature until clear. Then, 10 μ l of Alkaline Protease Solution was added, mixed and incubated at room temperature for 5 minutes followed by adding 350 μ l of Neutralisation Solution. After being mixed, the resulting suspension was centrifuged at 7°C for 10 minutes at 14000rpm. Then, 750 μ l of the clear lysate, avoiding pellet, was transferred to a Spin Column inserted into a Collection Tube (both available with the Wizard® *Plus SV* Minipreps kit). The column and tubes were centrifuged for 1min at maximum speed. The flow-through was discarded from the Collection Tube, and the Spin Column replaced before adding 750 μ l of Column Wash Solution containing 95% ethanol. Columns were centrifuged for 1 minute with maximum speed at room temperature. The flow was discarded from the Collection Tube, and the Spin Column replaced before 250 μ l of the Column Wash Solution was added. Columns were centrifuged for 2 minutes with maximum speed at room temperature. The Spin Column was removed and placed in a 1.5ml tube. Plasmid DNA was eluted by adding 75 μ l of Nuclease-Free water to the Spin Column and centrifuging for 1 minute at maximum speed at room temperature.

2.2.5.1. DNA quantification

The concentration of DNA was determined using the NanoDrop ND-1000 spectrophotometer. The instrument was calibrated using water before the OD at 260nm and 280nm of 2 μ l samples of isolated plasmid DNA was determined.

2.2.6. Polymerase Chain Reaction (PCR) according to Clermont et al. (Clermont et al., 2000)

A single colony was taken directly from the agar plate and placed in 1ml of nuclease-free water to be vortexed and 10 μ l was transferred to a PCR tube.

PCR master-mix was prepared using: 1.4 μ l of 25 μ M MgCl₂, 0.5 μ l of each of 10 μ M primer (ChuA.1, ChuA.2, YjaA.1, YjaA.2, YjaA.2, YjaA.2, TspE4C2.1, TspE4C2.2), 0.2 μ l dNTP, 4 μ l of 5xTaq Buffer, 0.2 μ l of Taq Polymerase and 11.2 μ l of nuclease-free water to make the volume up to 20 μ l per each sample that the master-mix was prepared for. After mixing thoroughly, 10 μ l was transferred to a PCR tube containing bacterial sample.

Samples were subjected to a multiplex PCR consisting of: i) initial incubation at 94°C for 3min; ii) 3 step-cycle including: 94°C for 30s, 57°C for 30s and 72°C for 30s repeated 36 times; and iii) final extension at 72°C for 5min.

Amplified products were subjected to Agarose Gel Electrophoresis.

2.2.7. Agarose Gel Electrophoresis

Fifty millilitres of 1% agarose was prepared by adding 1 gram agarose to 50ml of 1xTAE buffer before heating in a microwave. After cooling, 5 μ l of SybrSafe was added. Once mixed, the molten agarose with added stain was poured onto a casting tray system with comb inserted and left to solidify. Combs were removed from the gel, which was then transferred into the electrophoresis tank ensuring that the gel was covered with 1xTAE buffer.

Loading dye (6X) was added to each sample, including molecular weight (MW) DNA markers, in 1:5 ratio. At least 8 μ l of each sample and 6 μ l of the MW DNA marker was added per well and the gel run for 30-45 minutes at 90V. Gels were visualised in the Gel Doc system under UV light.

2.2.7.1. Preparation of Restriction Enzyme Digests

The reaction mixes for restriction digestion of DNA were prepared in a total volume of $12\mu\text{l}$ per sample. This included $4.8\mu\text{l}$ water, $1.2\mu\text{l}$ 10X restriction buffer, $1\mu\text{l}$ restriction enzyme, and $5\mu\text{l}$ plasmid DNA, respectively, unless otherwise stated. Control samples contained equal volume of distilled water instead of restriction enzyme.

2.2.8. API 20E[®]

The identification of *E. coli* strains using API 20E[®] test was performed according to the manufacturers instructions. The API chamber was humidified with the addition of water to the honeycomb structure of the box prior to introducing the reaction strip. A single colony from an agar plate grown overnight was suspending in 4ml of API suspension medium and mixed thoroughly. The bacterial emulsion obtained was added to each microtubule on the reaction strip. CIT, VP and GEL tests were filled onto the cupule, while the ADH, LCD, ODC, H₂S and URE tests were supplemented with the mineral oil to provide an anaerobic environment. Strips containing bacterial emulsion were placed inside the humidified chamber and incubated overnight at 37°C. Results were obtained by assigning the proper numerical value to the reaction depending on the colour change in the microtubule. Final numbers and identification was confirmed on the API database.

2.2.9. Raman Spectroscopy

All Raman measurements were performed on a Renishaw *InVia* system with a charge-coupled device (CCD) detector and a Leica DM2500 microscope. All Raman spectroscopy experiments are described in detail in Chapter 3, including the calibration 3.2.1, obtaining individual spectra 3.2.2, assessing the reproducibility of the sample 3.2.3, choosing the correct substrate 3.2.4, spectra processing 3.2.5 and investigating possible limitation of this technique 3.2.6

3. DEVELOPMENT OF RAMAN SPECTROSCOPY PROCEDURES FOR REPRODUCIBLE IDENTIFICATION OF BACTERIA

3.1. Introduction

Raman spectroscopy has proved to be a useful technique in microbiology (Downes & Elfick, 2010) (Kastanos et al., 2012).

Various different approaches have been used for studying microorganisms with Raman spectroscopy, including study on fully grown colonies (Samek et al., 2008) (Rösch et al., 2003), microcolonies (Maquelin et al., 2000) (Maquelin et al., 2002) (Maquelin & Kirschner, 2003) (Goodwin, 2006), bacterial biomass (Kirschner et al., 2001) (Choo-Smith, 2001) (Hutsebaut et al., 2006) (De Gelder et al., 2007a) (Ivleva et al., 2009) (Hall et al., 2011) (Willemse-Erix et al., 2009) (Escoriza et al., 2006) or even single cells (Schuster et al., 2000) (Guicheteau et al., 2010) (Harz et al., 2009) (Rösch et al., 2005) Above references can be found in an easier to read format in Table A.1 in Appendix A.

Each of the previous studies has identified steps essential for generating Raman spectra of sufficient quality for discriminating organisms. The variation between the presented experimental arrangements is different not only in terms of the systems and Raman modification used but also in the spectral processing. Several authors, especially in the early stages of Raman spectroscopy investigation into bacteria, when taxonomically distant organisms were compared, studied only the visible differences between spectra resulting from clearly distinguishable peaks (Grow et al., 2003) (Jehlička et al., 2012) (Rösch et al., 2003). Assigning peaks identified by Raman spectroscopy to specific molecules has become an important part of research related to biological applications (De Gelder, 2007) (Maquelin et al., 2002) (Ivleva et al., 2009) (Samek et al., 2008). The more detailed and complicated the results, the higher the difficulty with extracting the information from unprocessed spectra.

Natural drawback of scanning biological samples is associated with high fluorescence related to sample and/or the substrate (Downes & Elfick, 2010). In order to avoid the crucial information being lost or neglected, various spectral processing methods have been suggested, including: Principal Component Analysis (Nicolaou et al., 2011), (Hutsebaut et al., 2006) (Patel & Premasiri, 2008), Hierarchical Cluster Analysis (Maquelin et al., 2009) (Harz et al., 2009) (Buijtels et al., 2008) (Willemse-Erix et al., 2009) and Support Vector Machine (Rösch et al., 2005). However, these methods vary significantly and occasionally involve only single experiments or complicated procedures which could be difficult to repeat in the hospital environment.

3. DEVELOPMENT OF RAMAN SPECTROSCOPY PROCEDURES FOR REPRODUCIBLE IDENTIFICATION OF BACTERIA

In order to assess the potential of Raman micro-spectroscopy for use as a new diagnostic technique, its reproducibility has to be carefully examined. This chapter was structured into five sections containing the key aims for system optimisation and assessment of reproducibility:

- i) calibration of the system used for Raman experiments;
- ii) obtaining individual Raman spectra controls;
- iii) comparison and discrimination between spectra;
- iv) assessment of the possible limitations of the technique;
- v) determination of the optimal sample size.

3.2. Methods and Results

3.2.1. Calibration

To confirm reproducibility and precision, the *inVia* Raman spectrophotometer was calibrated prior to each experiment using a silicon (Si) sample. The Raman spectroscopy measurement of Si produces a single distinctive peak at 520 cm^{-1} and therefore can be used as a standard to ensure system functionality.

The *inVia* Raman system is supplied with the internal built-in Si sample for instant calibration using default settings. For additional quality control, Raman spectra from an external sample of Si mounted on an aluminium slide was also determined, setting the exposure time for 10 seconds of 1 accumulation, using the 50x objective and with laser power of 5%, using the 785nm red laser.

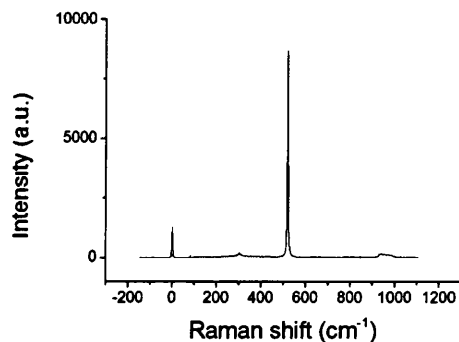


Figure 3.1.: A single spectrum from the internal silicon sample.

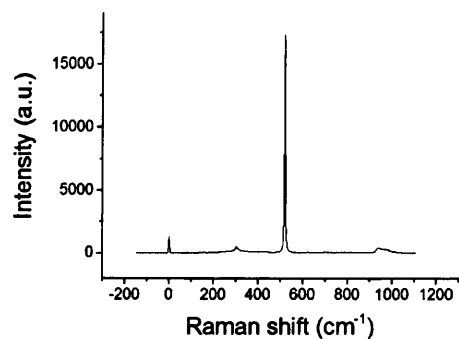


Figure 3.2.: A single spectrum from the internal silicon sample.

The expected results are in the range of 520.00 and 520.9 cm^{-1} , and intensities of 8000 and 15000 for the internal (Figure 3.1) and external Si samples (Figure 3.2) respectively. In cases when the results were not within the appropriate parameters, a 'quick calibration' operation, available from the WiRE 3.2 menu, was performed and Si measurements were repeated.

3.2.2. Individual spectra parameters

For all the experimental samples the inVia Raman system has been set to 10 seconds of 1 accumulation, with laser power of 50%, using the 785nm red laser. The range chosen for the experiments was 600-1600 cm^{-1} . In the case of easily-recognisable cosmic rays (Takeuchi et al., 1993) appearing in the spectra, a 'zap' operation was selected from the WiRE menu and applied to the selected region before saving the spectrum.

3.2.3. Determination of sample repeats

3.2.3.1. Single sample repeats

In order to obtain reproducible results and assess natural variation for biological samples, up to 30 spectra were taken from the same sample, providing that the time of the entire experiment did not exceed 3 hours, which resulted in damaging the sample with exposure to the higher temperature caused by the microscope module light. Therefore up to 30 spectra defined one single sample set (Figure 3.3).

3. DEVELOPMENT OF RAMAN SPECTROSCOPY PROCEDURES FOR REPRODUCIBLE IDENTIFICATION OF BACTERIA

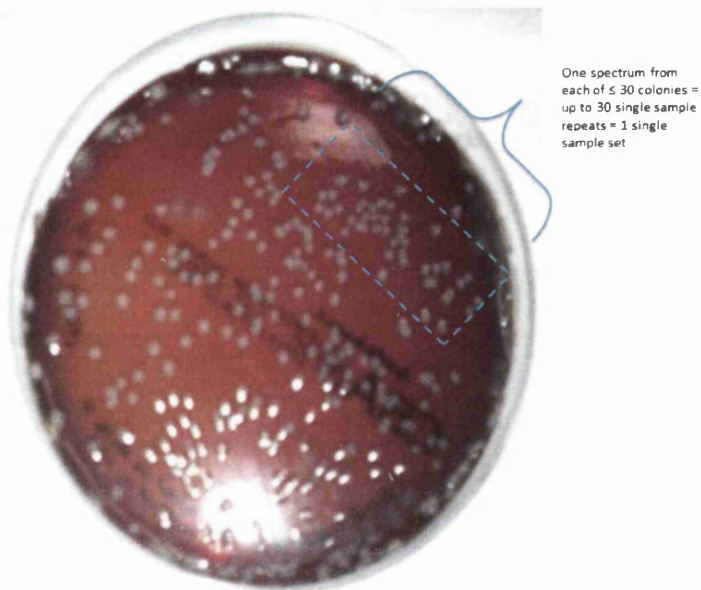


Figure 3.3.: Representation of single sample repeats preparation

3.2.3.2. Whole experimental repeats

To assess the day-to-day variation that can arise from the natural properties of live organisms, single sample repeats were done on consecutive days (up to 4 days) and compared. Whole experiment repeat sets could therefore contain as much as 120 single spectra (Figure 3.4).

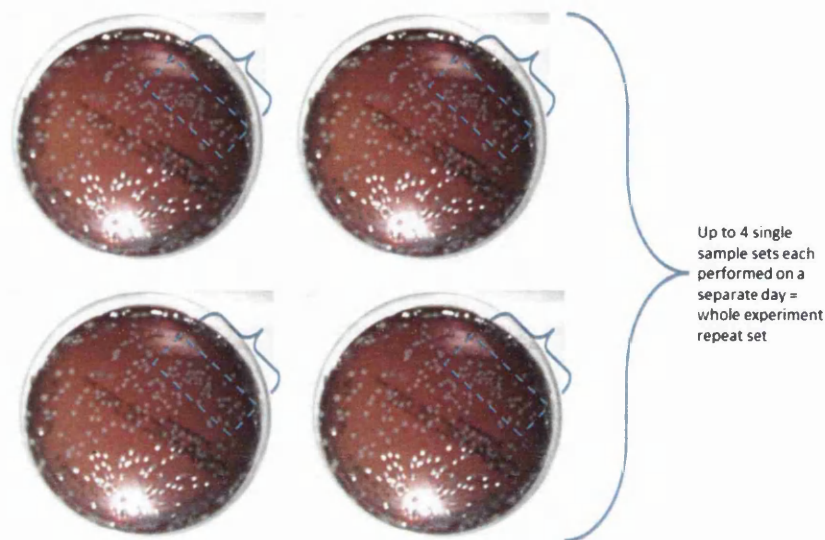


Figure 3.4.: Representation of whole experimental repeats preparation

3.2.4. Effect of the substrate

3.2.4.1. Quality control

To generate Raman spectra from static microorganisms they must be attached to an underlying substrate. In order to choose the most appropriate substrate for the experiments, a series of materials were tested, including:

- i) microscopic glass;
- ii) microscopic glass covered with layer of gold of 10-100nm thick;
- iii) frosted microscopic glass covered with 100nm gold;
- iv) Klarite;
- v) bacteriological agars including: Luria-Bertani agar and Columbia (horse) Blood agar

The results are shown in Figure 3.5 A-J.

3. DEVELOPMENT OF RAMAN SPECTROSCOPY PROCEDURES FOR REPRODUCIBLE IDENTIFICATION OF BACTERIA

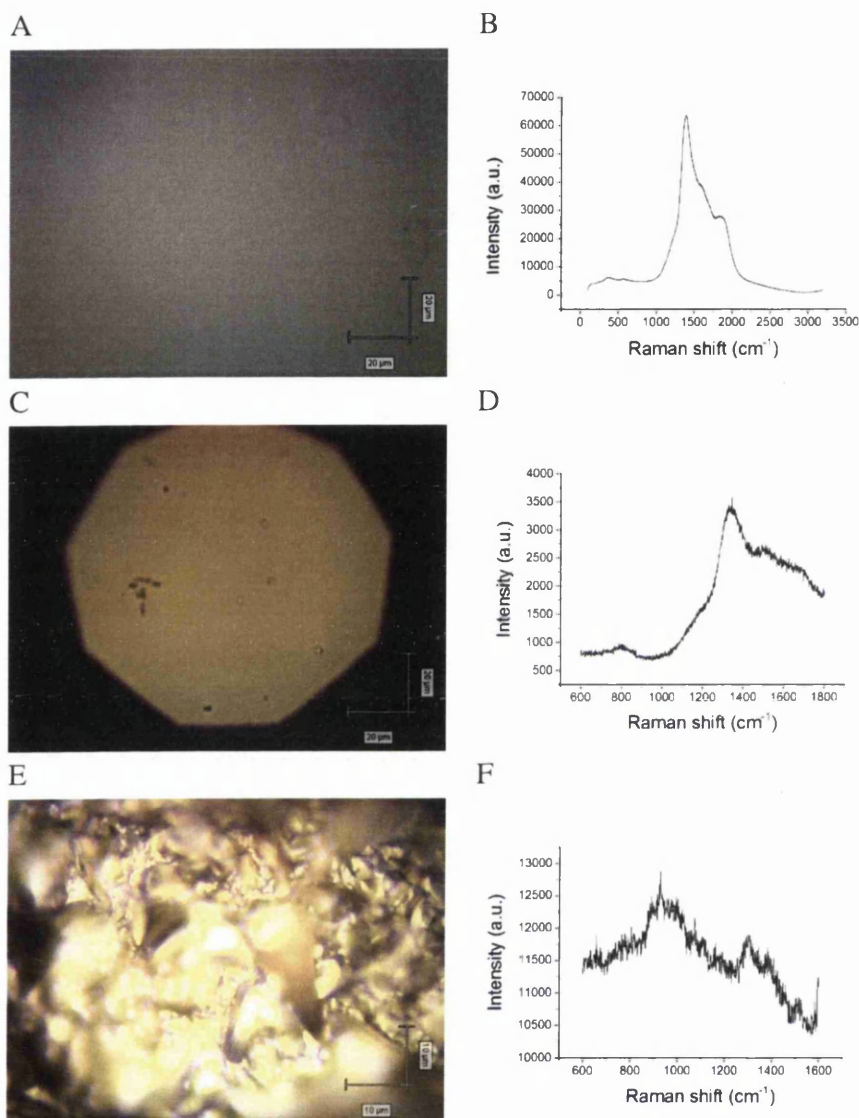


Figure 3.5.: Comparison of Raman substrates; (A) image and (B) spectrum from microscopic glass; (C) image and (D) spectrum from microscopic glass covered with 100nm layer of gold; (E) image and (F) spectrum from gold coated (70nm) frosted microscopic glass; (G) image and (H) spectrum from Klarite; (I) six consecutive spectra from LB agar; (J) six consecutive spectra from Columbia (horse) Blood agar. The Y scale was adjusted to the intensity of the highest peak within the experiment in order to visualise the features of spectra.

3. DEVELOPMENT OF RAMAN SPECTROSCOPY PROCEDURES FOR REPRODUCIBLE IDENTIFICATION OF BACTERIA

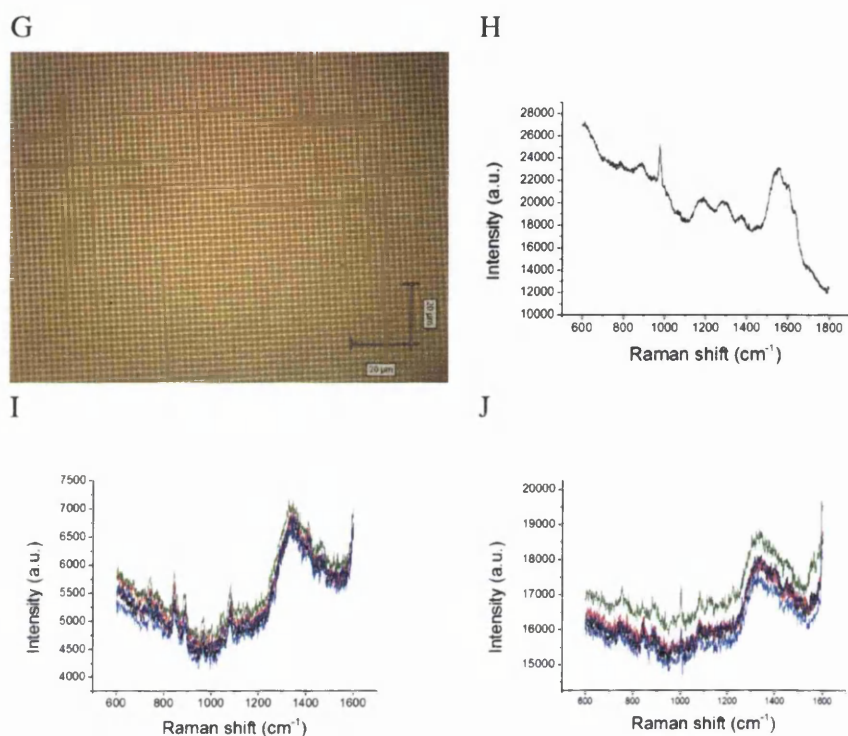


Figure 3.5.: (cont.) Comparison of Raman substrates; (A) image and (B) spectrum from microscopic glass; (C) image and (D) spectrum from microscopic glass covered with 100nm layer of gold; (E) image and (F) spectrum from gold coated (70nm) frosted microscopic glass; (G) image and (H) spectrum from Klarite; (I) six consecutive spectra from LB agar; (J) six consecutive spectra from Columbia (horse) Blood agar. The Y scale was adjusted to the intensity of the highest peak within the experiment in order to visualise the features of spectra.

When microscopic glass was tested on its own, it has presented a very intense fluorescence feature that covered most of the region of interest (Figure 3.5.B).

It was found that changing the amount of gold had little effect on the quality of spectra. Even with the thickest layer tested (100nm) there was still high intensity of the fluorescence in the region of 1300-1400 /cm⁻¹ (Figure 3.5.D), which would interfere with the investigated region of biological samples.

The image of the gold coated frosted glass shows how rough the surface is (Figure 3.5.E), which can create difficulties with proper focusing. The signal was very strong with peak(s) located at 1100, 1300 and 1500 /cm⁻¹ (Figure 3.5.F)

Klarite presented a signal of high background intensity with several strong peaks around 980, 1200, 1300, 1380 and 1600 /cm⁻¹ (Figure 3.5.H)

Spectra taken from both LB and CB agars as controls (Figure 3.5.I and J respectively) showed reproducible signal with small numbers of peaks, and with hardly any glass fluo-

rescence visible, making it the favoured substrate for micro-Raman measurements.

3.2.4.2. Compatibility with microorganisms

In order to verify the compatibility of bacterial sample with the chosen substrate, experiments involving microorganisms were performed in variety of different set ups including:

- i) pellets obtained after centrifugation of an overnight suspension of *S. epidermidis* 1457 and *E. coli* K12 liquid cultures grown in TSB, pipetted onto the gold coated microscopic glass 70nm;
- ii) an overnight culture of *S. epidermidis* 1457 grown overnight in TSB, cytospun on the gold-coated (70nm) microscopic glass
- iii) pellet obtained after centrifugation of an overnight suspension of each: *S. epidermidis* 1457 and *E. coli* K12 liquid cultures, each grown in TSB and pipetted onto the gold coated (100nm) frosted microscopic glass;
- iv) an overnight culture of *S. epidermidis* pipetted directly onto the gold-coated (100nm) frosted microscopic glass and cytospun;
- v) pellet obtained after centrifugation of an overnight suspension of each: *S. epidermidis* 1457 and *E. coli* K12 liquid cultures, each grown in TSB and pipetted onto Klarite;
- vi) bacterial colonies grown directly on the agars

Neither the pellet nor the cytospun form of the sample allowed for successful single cell spectra collection from the gold coated microscopic glass. Bacterial cells have smaller diameters than the set up laser line, causing the signal to be collected from the surrounding area and obstructing the result. Smaller laser lines caused weaker signal. When bigger cell aggregates, resulting from higher concentration of bacterial suspension, were used, the image was too heterogeneous to allow for proper focussing and therefore resulting in poor signal.

Thick layers of gold applied on the microscopic glass, resulted in only small numbers of peaks from the bacteria visible. The most intense peak was at 1400 cm^{-1} therefore in the same position as observed when gold coated microscopic glass was scanned without the presence of any organism (Figure 3.6.B).

3. DEVELOPMENT OF RAMAN SPECTROSCOPY PROCEDURES FOR REPRODUCIBLE IDENTIFICATION OF BACTERIA

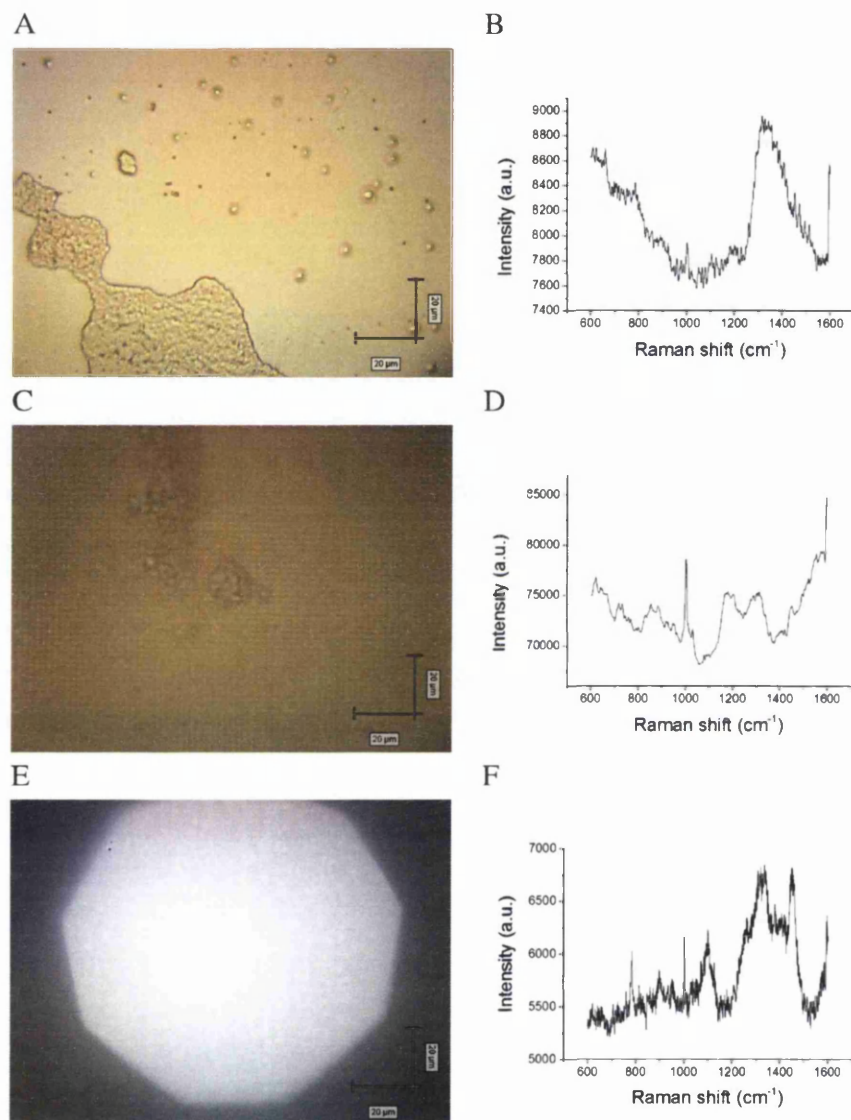


Figure 3.6.: *S. epidermidis* 1457 on different substrates: (A) microscopic image and (B) single Raman spectrum of the sample pipetted on gold coated (70nm) microscopic glass; : (C) microscopic image and (D) single Raman spectrum of the sample pipetted on Klarite; : (E) microscopic image and (F) single Raman spectrum of a bacterial colony (zoomed in).

The surface of the frosted glass is very rough, so even when coated with gold and using very concentrated bacterial sample, the organisms were not accessible and no spectra from cells or biomass could be obtained.

The surface of Klarite consists of a series of groves with diameter bigger than a single bacterial cell, causing the microorganisms to fall in between the groves or stick to the diagonal wall making it impossible to focus properly and therefore obtain reproducible

results. The signal collected is almost identical to the spectrum collected from the Klarite without the sample, suggesting that the laser was focused on the substrate and not on enough bacteria to give satisfying sufficiently robust signal (Figure 3.6.C and D)

When bacterial colonies were grown on agar they proved to be easy to focus on and gave very strong spectra with distinguishable peaks, which seemed to quench the signal from the agar as the size of the colonies allowed for laser line and the reflected light to be limited to the areas of interest and not the surroundings (Figure 3.6.E and F).

3.2.5. Spectra processing

3.2.5.1. Optimum background correction

In order to reduce the influence of the background, it was necessary to select a single and unified method of background correction. Among various available techniques, three were chosen and compared: i) Background Correction built in the PyChem software; ii) AirPLS code written in Matlab language; iii) Rolling Circle Filter (RCF) coupled with Savitzky-Golay smoothing developed into ASGRFC application written for the LabView engine. The background correction built in the PyChem software uses the baseline correction class by setting the first bin to zero method in the pre-processing step. The AirPLS code, written for Matlab offers an instant correction by automatically applying partial least square technique to the uploaded files. The ASGRFC application allowed for correction using RCF method with Savitzky Golay smoothing and had adjustable circle radius and baseline level parameters. The radius was set for 100, while the other option was left at 0.

In order to compare the effects of background correction (Figure 3.7), a typical spectral set of repeats for *E. coli* Top10 was subjected to each method and compared with the raw spectra. For validation (Figure 3.8) of the ability of RCF to enhance the separation between samples, a single spectrum from the *S. epidermidis* 1457 and *E. coli* Top10 subjected to RCF was compared to the unprocessed spectrum.

3. DEVELOPMENT OF RAMAN SPECTROSCOPY PROCEDURES FOR REPRODUCIBLE IDENTIFICATION OF BACTERIA

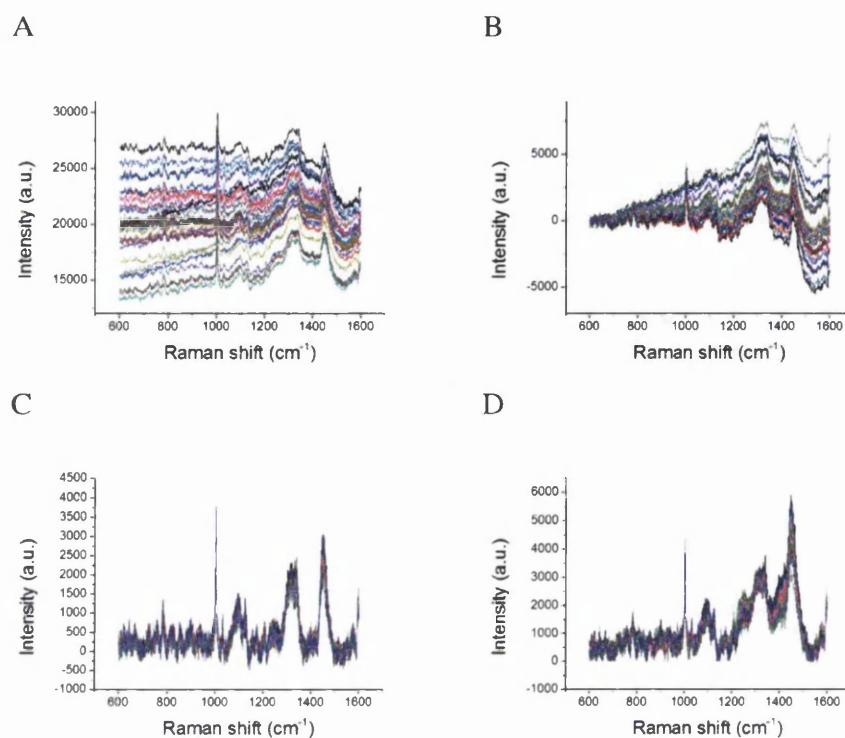


Figure 3.7.: Set of 30 spectra from 30 colonies taken during a single measurement of Top10 (A) unprocessed; (B) subjected to Background Correction procedure built in the PyChem software; (C) subjected to AirPLS procedure written in Matlab; (D) subjected to Rolling Circle Filter developed into SCARF, coupled with Savitzky-Golay smoothing through an application written for the LabView engine

Unprocessed spectra (Figure 3.7.A) confirmed that even single sets of repeats taken during one experiment can exhibit different background intensities. After applying the baseline correction available from PyChem, the background is not equally corrected over the whole set of data (Figure 3.7.B) showing high variation with increasing Raman shifts. The AirPLS code (Figure 3.7.C) and the RCF (Figure 3.7.D) had similar efficiency, however the latter allows for the control of several parameters like the radius of the circle, giving increased versatility for future applications. For this reason, RCF was chosen for future experiments.

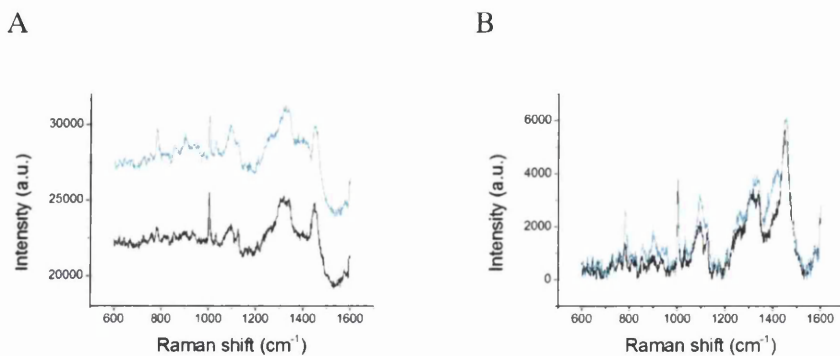


Figure 3.8.: Single spectra of Top10 (black) and 1457 (cyan): (A) not subjected to any processing; (B) subjected to RCF.

When the influence of background subtraction on separation of microorganism was assessed (Figure 3.8), the advantage of removing the background over using raw spectra was uncovered. Background signals cause the spectra to have significantly different intensities (Figure 3.8.A), making it difficult to compare peak heights, In addition some minor peaks may be neglected when the background is not removed.

3.2.5.2. Determination of the most characteristic peaks

A whole set of spectral repeats, with background intensities treated with RCF, taken during one experiment was used to calculate a mean value for each wavelength. The mean signal was plotted to determinate the critical peak positions.

Peaks were selected using the ‘Quick Peaks’ option available from the ‘Gadgets’ tab in Origin 8.6. The baseline was set to ‘none’, peaks were found in both directions, method was set to ‘Window Search’ and Percent of Raw Data was set to 10% for both ‘Height’ and ‘Width’. Filtering of peaks was done by height with 10% threshold. The most significant peaks can be assigned to the biomolecules using signal databases like the one in Table A.3.

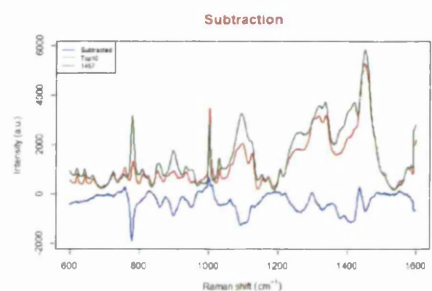
Peaks were identified based on ± 1 wavelength principle, since slight variations in the shifts have been observed. If the wavelength belonged to a wider group of peaks, all the possible molecules listed were assigned. If there were no precisely identified peaks in the \pm region, the identification was extended to maximum of ± 10 and it was clearly stated, that these peaks were approximated identification (the closest identified peaks). In cases when the peak did not match any of the above criterion, it was stated that the signal has not been identified in the literature.

3.2.5.3. Spectra subtraction

The mean result calculated for one organism was subtracted from the corresponding result calculated for another distinct organism. The subtracted spectrum was plotted to demonstrate differences between sets of spectra from the two organisms and also to determine the critical discriminatory peak positions.

Recognition of the peaks was performed as described for single organisms in section 3.2.5.2.

A



B

Raman Shift (cm ⁻¹)	Compound/molecule
758	Phosphophenylpyruvate
780	Citidine, Uracil, Cytosine, Uracil ring stretching, Phosphophenylpyruvate, DNA Phosphodiester O-P-O stretching
903	Amylose
1000	Palmitic acid, D-(+)-Galactosamine
1100	Palmitic acid
1270	(not identified in literature)
1410	(not identified in literature)

Figure 3.9.: Subtraction of mean intensities (A) from a single whole experiment repeat (containing 30 spectra for each organism) for Top10 vs. 1457 and (B) Table representing the most characteristic peaks distinguishing between the two organisms, assigned to the life molecules according to the Table A.3.

3.2.5.4. Principal Component Analysis (PCA)

Following background removal sets of spectra were uploaded to PyChem, which offers the built-in PCA routine. The uploaded spectra were prepared for PCA through using the pre-processing protocols from the PyChem software including 'Normalisation of the

3. DEVELOPMENT OF RAMAN SPECTROSCOPY PROCEDURES FOR REPRODUCIBLE IDENTIFICATION OF BACTERIA

most intense bin to +1' and 'Scaling minimum to 0 and maximum to +1'.

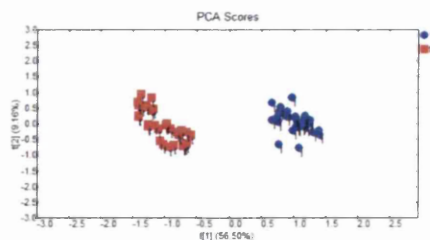


Figure 3.10.: Principal component analysis results in a form of clusters, of one whole experimental repeat consisting of 30 single sample repeat for each Top10 (red square) and 1457 (blue circle)

The PCA was conducted using the correlation matrix and NIPALS settings (Figure 3.10). The analysis was conducted up to the fourth principal component, where the main differences are observed.

3.2.5.5. Hierarchical Cluster Analysis (HCA)

Hierarchical clustering was performed using the standard tool available from PyChem software. Several options were available, however for the purpose of this project, HCA was performed on PC scores using hierarchical clustering as a clustering method with Euclidean distance measure and maximum linkage.

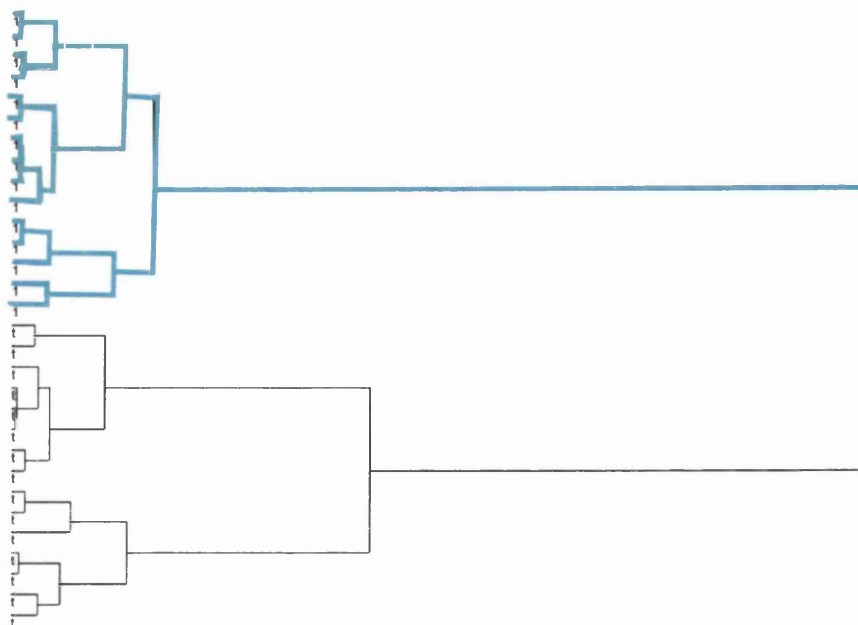


Figure 3.11.: Hierarchical cluster analysis for PC scores from a single whole experimental repeat (containing 15 single sample repeats of each sample) for *E. coli* Top10 (black) and *S. epidermidis* 1457 (cyan).

The results are in agreement with PCA clustering clearly separating two organisms into different groups, however HCA can offer additional information showing the relationship between clusters instead of just revealing the graphical distance between them.

3.2.5.6. T-test on individual principal components

The scores from PCA were extracted and the Student t-test was used to calculate a numerical value of the difference between the samples subjected to the PCA.

Calculations were performed on the extracted Principal Component (PC) Scores for each of the four PCs. The calculations were done based on standard t-test available from the R programming package. The normality of the sample was assumed.

In order to classify the results, they were divided into colour coded groups for easier comparison. The significance level was set to 0.05 therefore results higher than this value are considered to be not different and were not marked with any colour. Values lower than 0.05 but higher than and including 1×10^{-9} were marked with green colour, values within the range of 1×10^{-10} and 1×10^{-19} were marked with yellow colour, values between the numbers of 1×10^{-20} and 1×10^{-29} were marked with red colour. Finally, any value equal to or lower than 1×10^{-30} was marked with purple colour (Table 3.1). The t-tests values

3. DEVELOPMENT OF RAMAN SPECTROSCOPY PROCEDURES FOR REPRODUCIBLE IDENTIFICATION OF BACTERIA

reflect the results obtained from PCA and HCA, however it offers a numerical value. Thus findings can be compared in an unbiased way, and the 'amount' of difference quantified. Furthermore graphical representations alone may be interpreted subjectively.

Organism	Experiment number	T-test results value			
		PC1	PC2	PC3	PC4
Top10wt vs. 1457	1	8.58E-24	1.63E-02	7.90E-01	5.73E-01
	2	9.50E-34	1.53E-01	2.96E-01	6.57E-01
	3	2.95E-48	5.01E-01	6.71E-01	8.50E-01
	4	1.88E-37	2.59E-01	3.01E-01	9.32E-01

Table 3.1.: Results for t-test based on PC scores from the first four principal components calculated for comparison of four whole experimental repeats, each containing thirty single sample repeats of each Top10 and 1457.

3.2.6. Variation within and between experiments

In order to assess the validity of separation offered by PCA, the variation between single sample repeats sets taken on consecutive days (i.e. whole experimental repeats), were compared to each other using t-test and the highest variation between them, was assessed to be the threshold for the error and set as a non-significant difference (Table 3.2).

3. DEVELOPMENT OF RAMAN SPECTROSCOPY PROCEDURES FOR REPRODUCIBLE IDENTIFICATION OF BACTERIA

Table 3.2.: Comparison of the natural variation within the consecutive experimental sets of 30 spectra of Top10 (A) and 1457 (B).

A					
Organism	Experiment number	T-test results value			
		PC1	PC2	PC3	PC4
Top10wt	1vs.2	3.65E-01	2.23E-02	2.19E-01	5.61E-02
	1vs.3	1.15E-04	1.69E-04	2.62E-03	7.28E-01
	1vs.4	2.64E-03	2.90E-01	6.64E-01	1.72E-03
	2vs.3	1.12E-04	6.78E-01	2.45E-12	1.90E-01
	2vs.4	1.86E-07	9.93E-03	2.99E-02	8.57E-01
	3vs.4	5.62E-10	6.01E-01	6.84E-01	1.80E-02
B					
Organism	Experiment number	T-test results value			
		PC1	PC2	PC3	PC4
1457	1vs.2	1.38E-05	4.80E-03	3.81E-01	4.25E-01
	1vs.3	7.12E-01	6.12E-13	1.76E-03	6.73E-01
	1vs.4	1.22E-24	6.70E-01	6.80E-02	9.40E-01
	2vs.3	2.37E-04	2.17E-04	4.20E-01	2.29E-01
	2vs.4	2.55E-07	7.47E-03	8.77E-01	4.43E-01
	3vs.4	6.06E-19	6.68E-01	2.56E-01	4.48E-01

3.2.6.1. Rejection of single spectra within a single sample repeats set.

In order to conduct a reproducible experiment, 30 repeats were always attempted. However, some spectra were rejected, based on the reasons described in Table 3.3.

In cases when errors, poor quality or artefacts were noted during experiment, such as a spectrum being visibly different to the others taken during the experimental procedure, it was discarded and replaced with another repeated measurement.

However in some cases, rejection of a single sample repeat may not be detected by simple examination of spectra with the naked eye. These errors may only be detected later following PCA. Such case will cause separation of a single point from the whole cluster and obstruct the comparison as well as the t-test result. The arbitrarily chosen limit of acceptance was from -3 to +3 of PCA scale of PyChem software. These borders were based on majority of our data generated in a reproducible manner from various organisms.

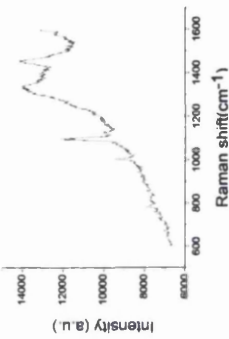
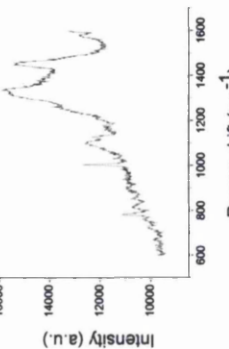
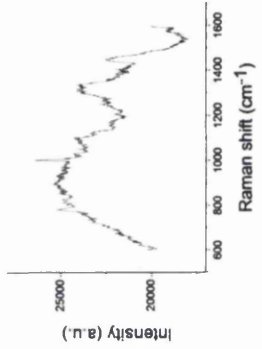
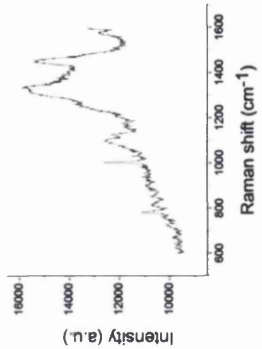
In order to maintain equal numbers of spectra within single sample repeat set, between all the samples tested, additional repeats of the spectra were performed to serve as spare

3. DEVELOPMENT OF RAMAN SPECTROSCOPY PROCEDURES FOR REPRODUCIBLE IDENTIFICATION OF BACTERIA

when the PCA shows the need for rejection of any of the repeats approved earlier in the analysis process.

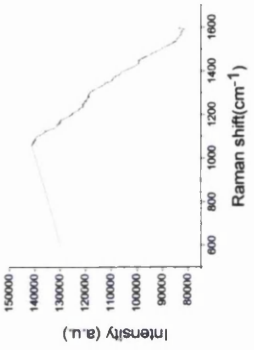
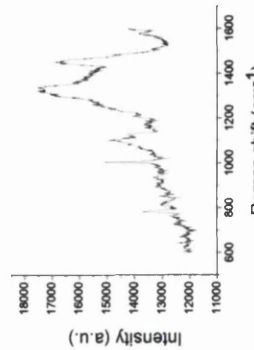
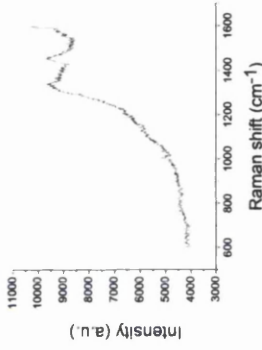
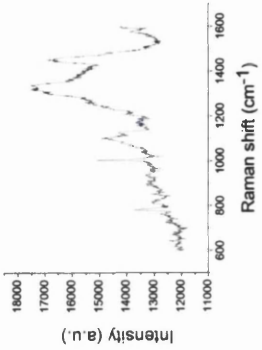
3. DEVELOPMENT OF RAMAN SPECTROSCOPY PROCEDURES FOR REPRODUCIBLE IDENTIFICATION OF BACTERIA

Table 3.3.: Selected reasons for rejection of single spectra.

Reason for rejection	Description	Inappropriate spectrum	Appropriate spectrum
Cosmic rays that cannot be instantly removed	Several cosmic rays may appear in one spectrum and overlap becoming too wide and the attempt to remove it using the 'zap' operation will have a dramatic effect on the spectrum possibly losing valuable information. Similarly, when cosmic rays are created on top of a peak, it is hard to distinguish the end of the peak and the base of the cosmic ray.		
High fluorescence signal	Very high fluorescence from either: sample, or substrate may interfere with important signal and even using background correction method can be futile		

3. DEVELOPMENT OF RAMAN SPECTROSCOPY PROCEDURES FOR REPRODUCIBLE IDENTIFICATION OF BACTERIA

Table 3.3.: (cont.) Selected reasons for rejection of single spectra.

Reason for rejection	Description	Inappropriate spectrum	Appropriate spectrum	Example
Saturation	Saturation can occur in any CCD image sensors when the finite charge capacity of individual photodiodes, or the maximum charge transfer capacity of the CCD, is reached. After too many electrons are delivered to a CCD pixel, the charge starts to spill into the adjoining pixels			
Poor focusing	Occasionally a single spectrum among the whole experiment can be of poor quality caused by focusing in the wrong area of a colony - either 'too high' on the top of very elevated colony, or 'on the side' where the density of a colony is very low and fluorescence or agar signal can drown/saturate the bacterial signal.			

3.2.6.2. Rejection of the single sample repeats within whole experimental repeats set

Due to high natural variations present within biological experiments, it was occasionally necessary to reject a single sample repeats set, containing a full collection of spectra done on one of the consecutive days. The decision was usually made after spectral analysis and comparison with the other measurements of the same samples. The possible reasons for the rejection of the single sample repeats set were summarised in Table 3.4. The criterion used for rejection of such inconsistent experiments was based on the high variability of spectra within the measured sample. The chosen limit of acceptance was from -3 to +3 of PCA scale of PyChem software.

3.2.7. Synergistic effect of the agar signal

In order to monitor the independence of the bacterial spectra from the background, a set of spectra taken from agar alone was determined and a mean value for each wavelength was calculated. These values were subtracted from each bacterial spectrum. This operation was applied post-RCF in order to avoid fluctuations in fluorescence.

The influence of the agar background was investigated to show how the subtraction of the agar spectra intensities results in the final clustering during the PCA. In order to achieve this, Top10 spectra obtained from experiments repeated over 4 consecutive days, each containing 30 spectra from 30 different colonies were compared before and after subtracting the agar background.

To investigate how the presence and absence of agar signal in the bacterial spectra affect the separation of organisms, Top10 and 1457 spectra obtained on four consecutive days with and without agar were compared for monitoring the differentiation.

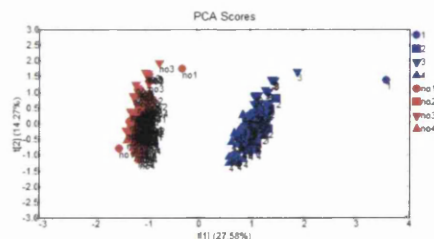


Figure 3.12.: Comparison of clustering for four whole experimental repeats for pre- (blue) and post- (red) agar spectra removal on Top10.

Thus with respect to effects on one strain Top 10 alone (Figure 3.12) clusters are tight

3. DEVELOPMENT OF RAMAN SPECTROSCOPY PROCEDURES FOR REPRODUCIBLE IDENTIFICATION OF BACTERIA

and distinct, suggesting the subtraction of agar background has no effect on the integrity of either of the spectra within a single experiment, as well as within the clustering of consecutive experimental repeats. However the clusters are separate, which indicates that the presence of agar signal does have an effect and is indeed recognised during Raman Spectroscopy. However, when distinction between organisms (Top 10 vs 1457) is assessed (Figure 3.13 and Table 3.5) removal of agar background has no effect on the separation of organisms (similarity between Table 3.1 no removal and Table 3.5 including removal), therefore it was neglected in further experiments within this project.

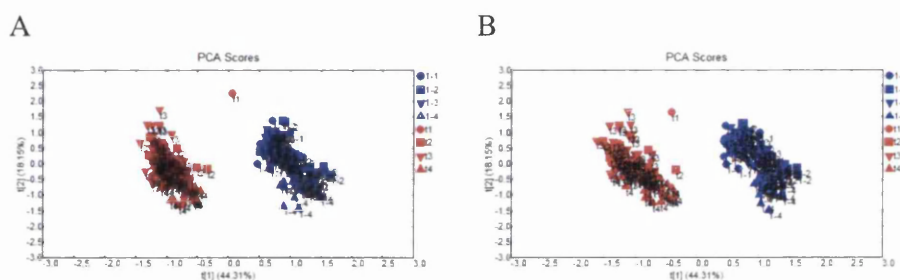
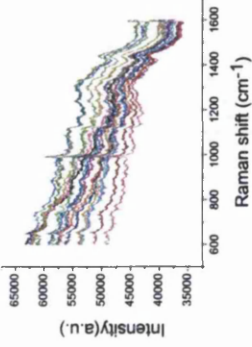



Figure 3.13.: Comparison of clustering between two different organisms pre- (A) and post- agar (B) spectra removal on 4 experimental sets of Top10wt (red) vs. 1457 (blue).

Table 3.4.: Comparison of results of t-tests performed on PCA scores of single experimental sets of Top10 and 1457 post- agar intensities removal.

T-test results value				Experiment number	Organism
PC1	PC2	PC3	PC4		
6.59E-34	7.79E-02	8.50E-01	6.51E-01	1	Top10wt vs. 1457
2.67E-32	5.10E-02	4.51E-01	5.92E-01	2	
1.43E-46	4.95E-01	5.19E-01	8.82E-01	3	
3.92E-29	1.33E-01	5.25E-01	9.16E-01	4	

Table 3.5.: Possible reasons for rejecting the complete experiments

Reason for rejection	Description	Example
Poor quality of the colonies	Colonies may show poor growth and low density resulting in high fluorescence through the whole experiment, however, repeats performed on consecutive days might have not been carrying the same burden.	
Poor quality of the agar	Occasionally the supplied CBA may be of low quality like the thinner layer deposited on the petri dish. When cut out, and placed on the microscopic slide, it may not be sufficient to quench the fluorescence from the glass	
Lysis of the agar	Blood-based agar is prone to lysis and therefore may result in producing not properly formed colonies (thinner and smaller) and have less effect in quenching the fluorescence.	

3.2.8. Assessing the correct sample size.

In order to prepare a proper comparison of the samples, the correct size of the single sample repeats set needed to be correctly assessed. For initial experiments, based on laboratory strains and transformed strains, spectra were collected in a set of 30 and repeated to obtain at least 3 whole experimental repeats.

It was important to verify whether the number of spectra in a single sample repeat set, as well as the number of whole experimental repeats in a set, was correct. In order to achieve this Top10 was compared to 1457 as well as to K12 to monitor samples that are representing the highest and lowest taxonomic difference.

Two parameters have been taken into account: the integrity within clusters and the quality of separation between organisms.

Comparison of two genera (Figure 3.14.A-I) showed that the clusters remain distinct and reasonably tight and is relatively independent of the number of repeats. The separation is noticeable already within the first 5 repeats (Figure 3.14.A) and maintained with increasing sample measurement up to 30 single sample repeats. Noticeably increasing the numbers of single sample repeats did not affect differentiation and close clustering was maintained even following 2, 3 and 4 experimental repeats (Figure 3.14.G-I).

When strains were compared: i.e. two *E. coli* strains (Figure 3.15), good distinction was maintained through the single experiments of 30 repeats (Figure 3.15.A-F). However, when experiments performed over consecutive days were compared, the separation between organisms became less distinct. (Figure 3.15.G-I)

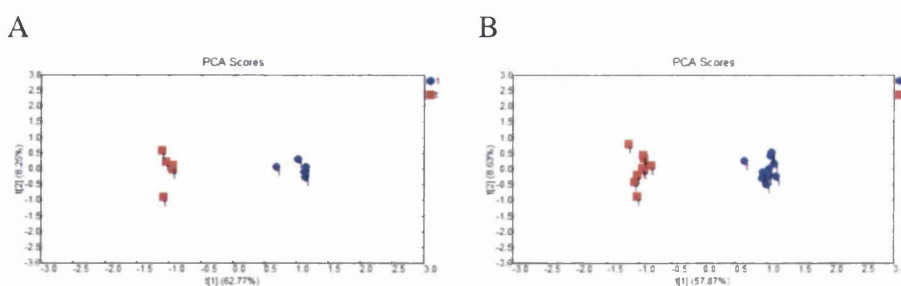


Figure 3.14.: Influence of sample size on separation and size and spatial distribution of clusters between Top10(red) and 1457(blue) containing: (A) 5; (B) 10; (C) 15; (D) 20; (E) 25; (F) 30 single samples repeats from a single experimental repeats and: (G) 2; (H) 3; (I) 4 whole experimental repeats for each organism containing 30 single sample repeats each.

3. DEVELOPMENT OF RAMAN SPECTROSCOPY PROCEDURES FOR REPRODUCIBLE IDENTIFICATION OF BACTERIA

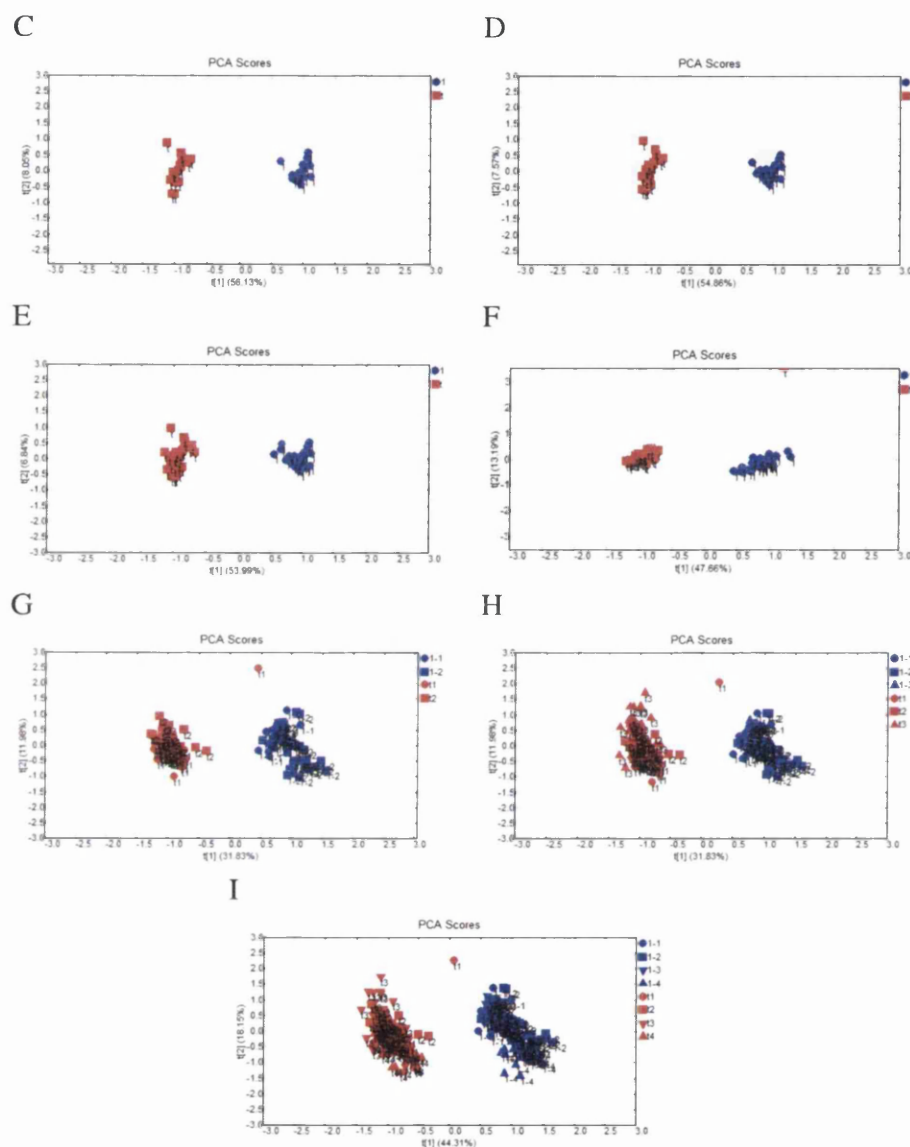


Figure 3.14.: (cont.) Influence of sample size on separation and size and spatial distribution of clusters between Top10(red) and 1457(blue) containing: (A) 5; (B) 10; (C) 15; (D) 20; (E) 25; (F) 30 single samples repeats from a single experimental repeats and: (G) 2; (H) 3; (I) 4 whole experimental repeats for each organism containing 30 single sample repeats each.

3. DEVELOPMENT OF RAMAN SPECTROSCOPY PROCEDURES FOR REPRODUCIBLE IDENTIFICATION OF BACTERIA

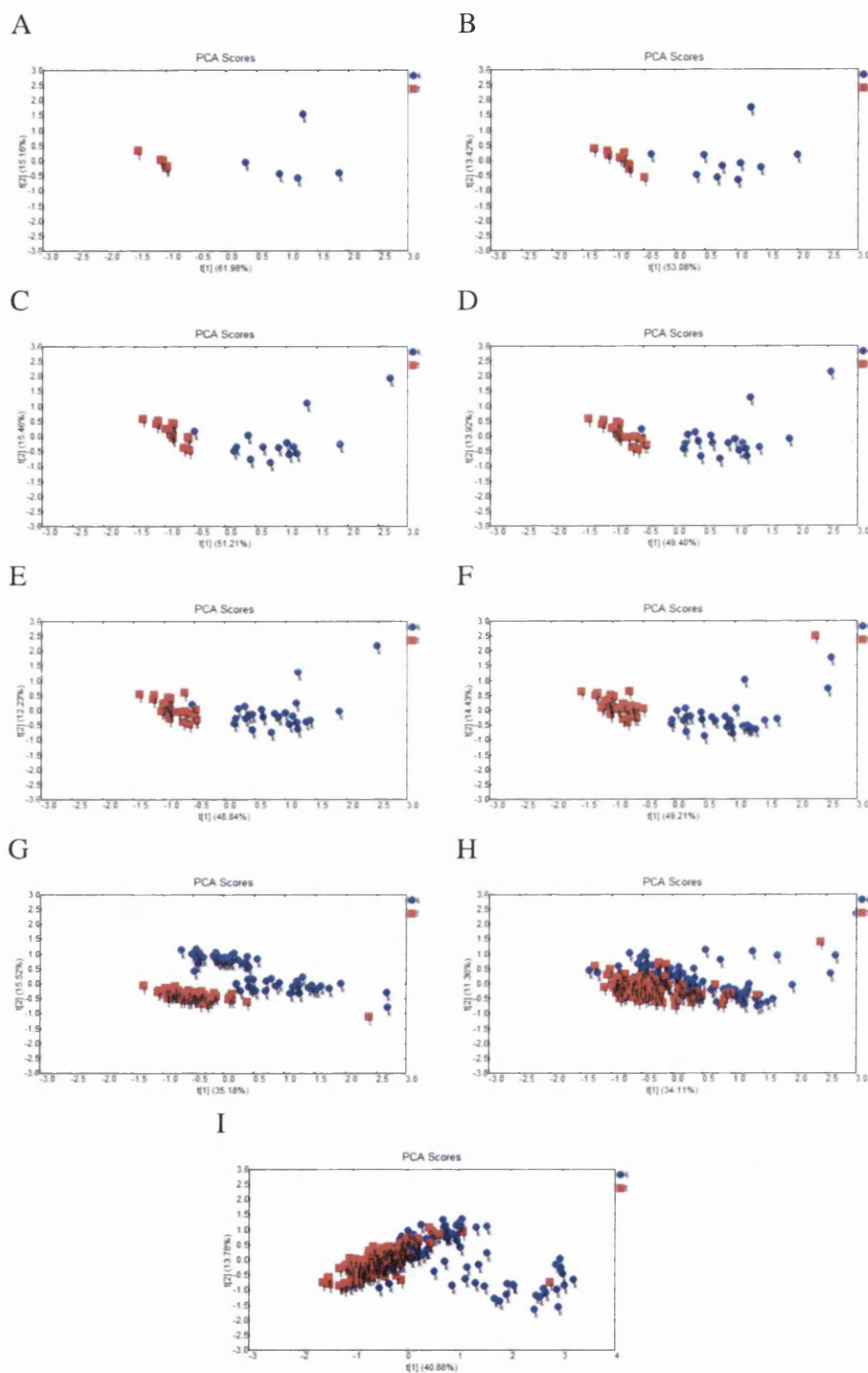


Figure 3.15.: Influence of sample size on separation, shape, and spatial distribution of clusters between Top10 (red) and K12 (blue) containing: (A) 5; (B) 10; (C) 15; (D) 20; (E) 25; (F) 30 single samples repeats from a single experimental repeats and: (G) 2; (H) 3; (I) 4 whole experimental repeats for each organism containing 30 single sample repeats each.

3.2.9. Selection of the regions of differences.

Comparing a whole spectrum may distort results, as the total signal may be burdened with unimportant information and noise. These unnecessary peaks could possibly distract from the factors that influence the differences between samples. We investigated this possibility.

3.2.9.1. Differentiation spectral regions into 6 life molecules peaks

The publication by De Gelder et al. (De Gelder, 2007) suggests using the database of biological molecules to divide a complete Raman spectrum from a live organism into sets of peaks assigned to a specific biomolecule(s). This was aimed to allow for easier and more thorough discrimination between organisms even at the strain level.

The selection was performed for: amino-acids (813; 828; 850-900; 1004; 1009; 1351; 1358; 1420-1500 cm^{-1}), DNA-RNA-bases (600-800 cm^{-1}), fats and fatty acids (800; 891-909; 910-970; 1050-1150; 1265; 1296; 1301; 1400-1500 cm^{-1}), primary metabolites (663-661; 723; 784; 787; 930-970; 973; 1034; 1395-1450 cm^{-1}), and saccharides (800-1500 cm^{-1}).

For each group of peaks, representing a particular 'life molecule' two instances have been taken into account: i) only the chosen peaks were selected for comparison and the rest of the spectrum was removed; ii) the peaks of interests have been removed and the remaining signal was compared.

Comparison of results performed for the Top10 vs. K12 (Figure 3.15.F vs. Figure 3.6.A-I), it was noted that excluding any part of the spectrum, whichever molecules it was related to, did not enhance the separation of clusters in a significant way. In fact, in most cases, removing certain peaks of the remaining signal caused a loss in the distinction between strains (amino-acids peaks; DNA and RNA bases peaks; fats and fatty acids peaks; and primary metabolites peaks) or the clusters became less tight (amino-acids peaks removed; and DNA and RNA bases peaks removed). The best results were the ones that had the greatest similarity to the whole-spectrum comparison i.e. containing the majority of the whole spectrum, since there is no better result represented by bigger separation or tighter clusters; those two examples are the selected peaks representing saccharides (Figure 3.6.H) and the whole spectrum with peaks representing primary metabolites removed (Figure 3.6.G).

3. DEVELOPMENT OF RAMAN SPECTROSCOPY PROCEDURES FOR REPRODUCIBLE IDENTIFICATION OF BACTERIA

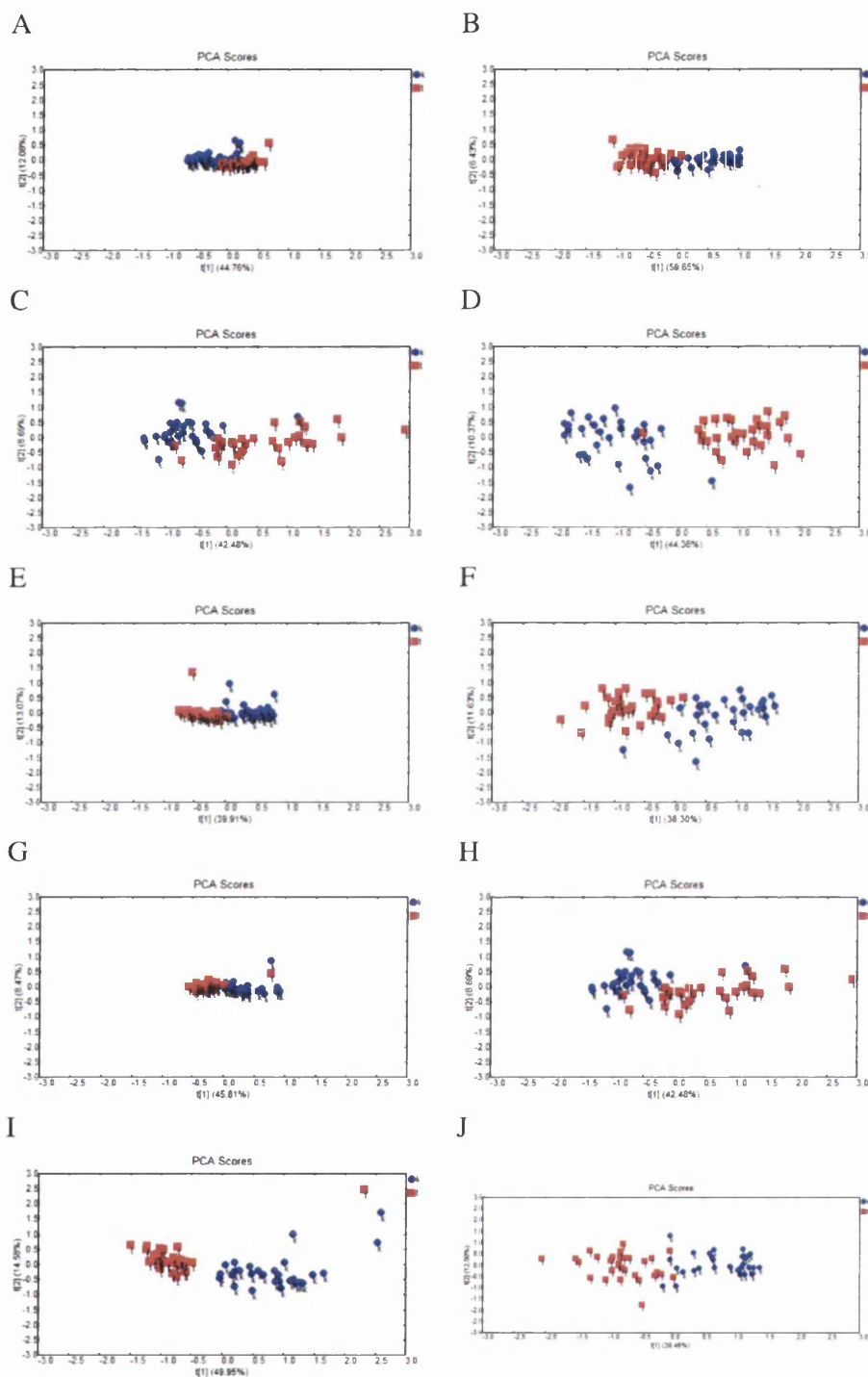


Figure 3.16.: Comparison of two single experiments of 30 repeats for each Top10 (red) and K12 (blue); (A) peaks associated to amino acids; (B) whole spectrum with peaks associated with amino acids removed; (C) peaks associated to DNA and RNA bases; (D) whole spectrum with peaks associated with DNA and RNA bases removed; (E) peaks associated to fats and fatty acids; (F) whole spectrum with peaks associated with fats and fatty acids removed; (G) peaks associated to primary metabolites; (H) peaks responsible for primary metabolites removed; (I) whole spectrum with peaks associated with saccharides; (J) peaks responsible for saccharides removed.

3.2.9.2. Comparing differences between values for each wavelength based on the t-test values

Specific comparison of peaks with significantly different intensities only, while the rest of the spectrum, including similar peaks and noise could be rejected was also investigated. The peaks intensities were compared after background correction to avoid the influence of possible fluorescence from the substrate or the sample.

The numerical values for the intensities from all 30 colonies, taken during a single experiment, were subjected to the Student t-test. The significance level was set to 5%, therefore, values lower than this threshold are considered to be significantly different and higher than 5% to be similar. This way the whole spectrum has been separated into intensities falling into two groups: significantly different and no different. Both were selected separately, subjected to PCA and clusters were prepared. When the Top10 and K12 measurements were compared, as expected, peaks of intensities calculated to show similarity $>5\%$ cluster together giving no separation between two organisms, while the intensities, selected for their significant differences showed separation when the PCA was applied (Figure 3.17). What is noteworthy is that this separation was not better than when the whole spectrum was taken into the analysis (Figure 3.17.B vs Figure 3.15.F).

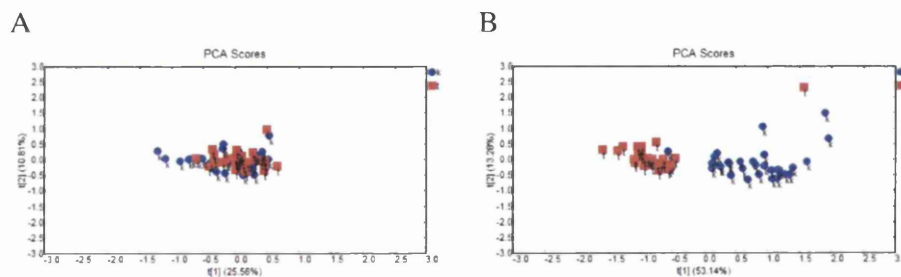


Figure 3.17.: Comparison of single whole experimental repeats containing 30 single sample repeats for each: Top10 (red) and K12 (blue) containing peaks of: (A) higher than 5% scored in the t-test; (B) lower than 5% scored in the t-test.

3.3. Discussion

The main issues that have been addressed in this chapter focused on establishing a system of procedures to obtain reproducible Raman spectra from bacteria.

Selecting appropriate settings for spectral acquisition is a crucial factor, especially in the clinical environment, when the data obtained from the sample should be as clear and as information-rich as possible, without compromising on the non-destructive qualities of Raman spectroscopy. According to the literature and our results, despite various systems used (Rösch et al., 2005) (Sengupta et al., 2006), different objectives (Maquelin et al., 2000), spectral ranges (Ciobot et al., 2010), and laser excitations (Goodwin, 2006) making it difficult to compare our system settings to all publications, Raman spectra can be obtained from bacteria with a variety of different settings.

Choosing the substrate is one of the most significant issues in the Raman spectroscopy based approach, since the literature varies greatly on this subject. It is important to remember that substrates can emit strong fluorescence signals, interfering and even obstructing the spectra of interest. In addition, if Raman spectroscopy is to be used as a diagnostic tool, the substrate should be easy to prepare, store and be inexpensive.

This chapter showed that agar was the optimum substrate for Raman spectroscopy of bacteria

The set-up closest to ours, was the use of micro-colonies, offering advantages in both: time and standard laboratory substrate. We have started investigating this idea and it is likely that given more time, we would have explored the area more. There are several publications offering alternative solutions: Harz et al (Harz et al., 2009) describes preliminary method of scanning single cells applied onto fused silica samples that was also tested for the patients cerebrospinal fluid. The results seem promising, however less is known specifically about the substrate and its influence on the sample.

Much of Raman spectroscopy-based bacterial research has focused on SERS, which offers significant signal enhancement, however, this approach inevitably relies on the use of specially prepared substrate, usually involving silver or gold nano-particles (Cam et al., 2009) (Jarvis et al., 2006) (Guicheteau & Christesen, 2010) (Premasiri et al., 2011) (Sengupta et al., 2006) (Jarvis & Goodacre, 2004b). Although authors claim the ease of SERS substrate preparation, it has also been stated that most of the time, the substrate has been monitored with either SEM or AFM for stability and reproducibility purposes. Such a step would not be welcome in the diagnostic laboratory. One way to avoid this could

involve buying ready-made SERS substrate, nevertheless to our knowledge there are no such possibilities currently and this would add to the costs of the diagnostic step.

Non-SERS approaches have claimed to reduce the time of sample preparation by applying bacterial biomass onto the CaF₂ windows (Kirschner et al., 2001) (Jarvis & Goodacre, 2004a) (Hutsebaut et al., 2006) or fused silica plate (Rösch et al., 2005) (Gaus et al., 2006) (Harz et al., 2005). Although these substrates seem easily available, it has not been clearly stated whether they can be re-used and therefore its cost efficiency can be questioned. In addition, most of the research involved preparation of the sample in laboratory conditions based on overnight growth and centrifuging bacterial suspension in order to obtain concentrated pellet. When we attempted to investigate such approaches with the use of gold coated slides, we experienced trouble focusing on concentrated pellet. In addition, growing a bacterial suspension concentrated enough to obtain sufficient amount of sample required additional incubation time, therefore this approach does not offer any time advantage over our methods. Furthermore there is also the requirement for purchasing different substrates, while we have used agar, a substrate already widely used in the hospital laboratories and by others. (Rösch et al., 2003).

The necessity of removing inappropriate spectra was assessed. It is only natural that biological systems involve some natural variation, even within replicates. In addition there may be some natural fluctuation related to the power of laser and error with focussing, especially when the elevation of the colony is taken into account, as the line mode of laser will not focus as well on the highly elevated as it would on flat surface. Including an experiment burdened with a general error will affect the final analysis and will be represented by wide spread of points in PC cluster representing the repeats for a single organism. Moreover, it could also falsely separate from other experimental repeats from the same organism and overlap with a different cluster, representing a different organism. This could bring a gross error and completely change the perception of the separation of two organisms. Such details have not been investigated in the current literature.

The importance of removing background signal is more popular in the Raman spectroscopy literature. A publication by Kourkoumelis et al. (Kourkoumelis et al., 2012) reviews the method based on the geometric definition of convex hull. The presented results are satisfying and authors inform that this method is semi-automated and requires input of only two variables. However promising the method is, it has not been applied to bacterial organisms and conclusions based only on paracetamol, prednisone acetate tablets and chondrocytes in cartilage cannot ensure it would be useful for diagnostic purposes.

3. DEVELOPMENT OF RAMAN SPECTROSCOPY PROCEDURES FOR REPRODUCIBLE IDENTIFICATION OF BACTERIA

Another available research incorporating background correction method was conducted by Huang et al. (Huang et al., 2010) and used Rolling Circle Filter with success. This confirms our choice in the method of background subtraction.

Many different tools for Raman spectra processing have been described in microbiology-related publications, especially when closely related and difficult to distinguish samples were examined. K-means clustering analysis has been criticised for not identifying the biochemical differences between regions and had to be used in conjunction with PCA (Bonnier & Byrne, 2012). Several other publications involving PCA have linked it with other techniques: Discriminant Function Analysis (DSF) (Nicolaou et al., 2011), cluster analysis (CA) (De Gelder et al., 2007c). PCA being an unsupervised method, similarly to factor analysis (FA) and CA does not require any previous knowledge about the sample and still offers grouping of the results, while supervised methods including multiple linear regression (MLR), principal component regression (PCR), partial least square regression (PLS) and linear discriminant analysis (LDA) require sets of well-characterised samples (Mobili & Londero, 2010), which may not be of desired quality for a diagnostic technique.

After investigating the most appropriate sample size, a conclusion can be drawn, that when comparing two organisms, one has to be very cautious with how many experimental repeats are included. When a high variation between experimental repeats is expressed, adding too many samples into the comparison may compromise the separation between distinct samples. This effect could possibly be investigated further in the future since the literature does not include any conclusive proof towards describing the most appropriate number of samples and varies to a great degree; from single bacteria (Ravindranath et al., 2011), to similar numbers of repeats as described by Jarvis and Goodacre (Jarvis & Goodacre, 2004b).

Assessing the influence of agar spectra in the bacterial signal was necessary. Although it seems that the signal from agar remains the general shape of the bacterial spectrum, it was shown that there is no influence on the clustering: neither within the single sample repeats, nor when different organisms were compared. However, when the agar signal is present, there is a single spectrum within the experiment 1 (blue round point marked with 1 - Figure 3.12) that does not belong with the cluster (and so was discarded), which is not visible when agar has been removed. In this project, such effects have minor implications and did not need to be investigated any further. These findings could not be compared with literature due to the lack of investigation in this field.

3. DEVELOPMENT OF RAMAN SPECTROSCOPY PROCEDURES FOR REPRODUCIBLE IDENTIFICATION OF BACTERIA

Our hypotheses about investigating only selected regions of spectra were shown to be incorrect for the purpose of this project. During PCA parts of the spectrum, responsible for the highest differentiation are automatically selected. In this case it is most likely the signal from fats and fatty acids. Therefore for differentiating between bacterial organisms, it is most appropriate when the whole spectrum is taken into account. It can be concluded that PCA focuses and prioritises only the regions of spectra that are responsible for significant differences and no selection of peaks is therefore necessary prior to the analysis.

In conclusion, this chapter assesses that *inVia* Raman system could serve as a novel analytical method for diagnosing bacterial diseases. The importance of optimising Raman procedures was presented in this chapter and has indicated the precision required when using this method. Its speed and ease of use may allow for important advancements in the diagnostic fields for patients that are in need of rapid care, while when combined with proper processing of the results, Raman micro-spectroscopy serves specificity and details in distinguishing between samples.

All the methods described in this chapter were applied in Chapters 4 - 6 (unless otherwise specified) which explore the possibilities of Raman spectroscopy for comparing bacterial organisms on different level of similarity: including different genus, within genus, different species, within species and even isogenic strains and clinical isolates.

3. DEVELOPMENT OF RAMAN SPECTROSCOPY PROCEDURES FOR REPRODUCIBLE IDENTIFICATION OF BACTERIA

4. DISCRIMINATION BETWEEN BACTERIAL SPECIES AND STRAINS USING RAMAN SPECTROSCOPY

4.1. Introduction

The literature offers wide variety of examples of comparison between genera and strains of bacteria, however, since various techniques and Raman enhancements are used it is difficult to compare results between different research groups.

Numerous studies have shown that diagnosing bacterial-caused infectious diseases in particular could profit from applying Raman spectroscopy with the examples being:

Esherichia coli, *Klebsiella pneumonia*, *Proteus* spp., *Klebsiella oxytoca*, *Proteus mirabilis*, *Enterococcus faecium*, *Enterococcus* spp., *Citrobacter freundii*, *Staphylococcus cohnii*, *Staphylococcus warneri*, *Staphylococcus epidermidis*, *Salmonella choleraesuis*, *Shigella flexneri*, *Micrococcus luteus*, *Rhodotorula mucilaginosa*, *Bacillus sphaericus*, *Pseudosomonas fluorescens*, *Helicobacter pylori*, *Staphylococcus aureus*, *Streptococcus pneumonia*, *Streptococcus agalactiae*, *Neisseria meningitides*, *Listeria monocytogenes*, *Shigella sonnei*, *Erwinia amylovora*, *Proteus vulgaris*, *Bacillus megaterium*, *Bacillus thuringiensis*, *Azohydromonas lata*, *Cupravidus necator*, *Acidophilium cryptum* (Ciobot et al., 2010). (Culha et al., 2010) (Hadjigeorgiou, 2009) (Jarvis et al., 2006) (Jarvis & Goodacre, 2004a) (Jarvis & Goodacre, 2004b) (Maquelin et al., 2000) (Mello et al., 2005) (Hadjigeorgiou, 2009) (Jarvis & Goodacre, 2004b) (Jarvis & Goodacre, 2004b) (Harz et al., 2005) (Harz et al., 2009) (Samek et al., 2008) (Mello et al., 2005) (Rösch et al., 2003)(Rsch et al., 2003) (Lin et al., 2009) (Jarvis et al., 2006) (Harz et al., 2009) Above references can be found in an easier to read format in Table A.2 in Appendix A.

Less is known about the discrimination between microorganisms and the key Raman shifts associated with each organism. In the previous chapter we demonstrated that Raman spectra could be successfully obtained from microorganisms in a reproducible fashion. This work forms our basic standard operating procedure which will now be applied with only slight modifications.

In this chapter Raman spectroscopy is used to

- identify species/strain related and species/strain specific Raman shifts
- discriminate between bacteria on different taxonomic levels
 - genus
 - species
 - strain

4. DISCRIMINATION BETWEEN BACTERIAL SPECIES AND STRAINS USING RAMAN SPECTROSCOPY

- generate a level of relatedness between strains
- identify the effects of storage on discrimination

4.2. Methods

4.2.1. Bacterial strains

This chapter describes experiments performed on the reference strains listed in Table 2.9.

4.2.2. Obtaining Raman spectra

Conditions for measuring and processing Raman spectra were described in Chapter 3

4.2.2.1. Comparing single sample repeats and whole experiment repeats

Reproducibility testing was performed for each of the strain used in this chapter according to Section 3.2.3.

4.2.2.2. Describing bacterial species

All of the strains used in this chapter were described by determining their crucial peaks as specified in Section 3.2.5.2.

4.2.2.3. Comparing bacterial spectra

Bacterial organisms were compared at each taxonomic level. Results were presented in a form of subtracted mean intensities, a table of peaks with suggested assignment from Table A.3 (according to Section 3.2.5.3), an example of PCA analysis (according to Section 3.2.5.4) based on one, randomly chosen whole experimental repeat and a table of t-test values calculated for all the whole experimental repeats performed for the first four principal components (according to Section 3.2.5.4).

4.2.3. Multiple strains comparison

All strains used in this chapter were compared together by calculating mean values of all the single spectral repeats within every whole experimental repeats and comparing the mean values by hierarchical cluster analysis according to the Section 3.2.5.5.

4.2.4. Assessing the influence of storage conditions on Raman spectroscopy measurements

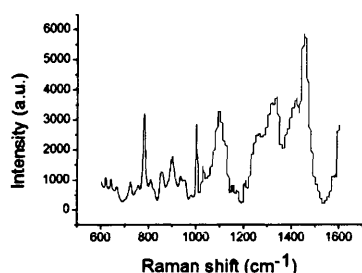
An overnight CBA plate containing colonies of Top10 or K12 was subjected to Raman spectroscopic measurements after: 0; 1; 2; 4; 8h. At least 15 spectra were taken from 15 different colonies at each time points. Pieces of agar containing the appropriate number of colonies were cut out of the plate and placed on a glass microscopic slide, while the plate with remaining colonies was immediately returned to either 4°C (standard fridge) or 25°C (room temperature) storage. After each time point a new fragment of agar was cut out of the original plate. The experiment was repeated on three consecutive days.

4.3. Results

4.3.1. Identifying the most crucial peaks for each bacterial strain

To determine which biological molecules are recognised by Raman spectroscopy, each strain used in this chapter was described separately and most significant peaks were identified using Table A.3.

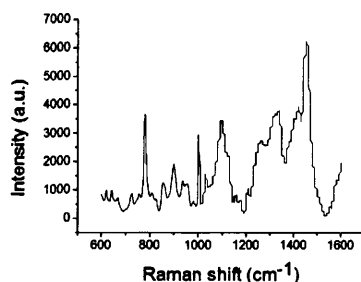
A



Raman shift (cm^{-1})	Compound/molecule
781	Citidine, Uracil, Cytosine, Uracil ring stretching, Phosphopyruvate, DNA Phosphodiester O-P-O stretching
900	Lactose
1000	Palmitic acid, D-(+)-Galactosamine
1100	Palmitic acid
1340	DNA/RNA(Guanine/Adenine), Proteins, Carbohydrates, Protein (Amide III)
1450	CH_2 scissoring, DNA, C-H bindings in lipids, Proteins, Carbohydrates, Bands of fatty acids, Deformation vibration CH_2 scissoring

Figure 4.1.: Plot and a table of most significant peaks with assigned molecules and bonds based on the mean spectra from all Raman measurements for (A) 1457; (B) 9142; (C) K12; (D) Strain B; (E) Top10; (F) 10418; (G) 6571; (H) Cowan 1

B

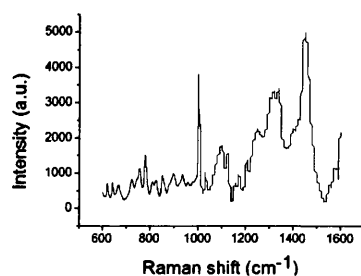


Raman shift (cm^{-1})	Compound/molecule
781	Citidine, Uracil, Cytosine, Uracil ring stretching, Phospho-phenylpyruvate, DNA Phosphodiester O-P-O stretching
900	Lactose
1000	Palmitic acid, D-(+)-Galactosamine
1100	Palmitic acid
1340	DNA/RNA(Guanine/Adenine), Proteins, Carbohydrates, Protein (Amide III)
1450	CH_2 scissoring, DNA, C-H bindings in lipids, Proteins, Carbohydrates, Bands of fatty acids, Deformation vibration CH_2 scissoring

Figure 4.1.: (cont.) Plot and a table of most significant peaks with assigned molecules and bonds based on the mean spectra from all Raman measurements for (A) 1457; (B) 9142; (C) K12; (D) Strain B; (E) Top10; (F) 10418; (G) 6571; (H) Cowan 1

4. DISCRIMINATION BETWEEN BACTERIAL SPECIES AND STRAINS USING RAMAN SPECTROSCOPY

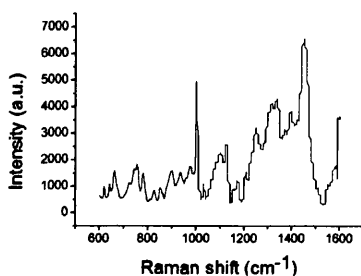
C



Raman shift (cm^{-1})	Compound/molecule
781	Citidine, Uracil, Cytosine, Uracil ring stretching, Phosphopyruvate, DNA Phosphodiester O-P-O stretching
1000	Palmitic acid, D-(+)-Galactosamine
1100	Palmitic acid
1340	DNA/RNA(Guanine/Adenine), Proteins, Carbohydrates, Protein (Amide III)
1450	CH_2 scissoring, DNA, C-H bindings in lipids, Proteins, Carbohydrates, Bands of fatty acids, Deformation vibration CH_2 scissoring

Figure 4.1.: (cont.) Plot and a table of most significant peaks with assigned molecules and bonds based on the mean spectra from all Raman measurements for (A) 1457; (B) 9142; (C) K12; (D) Strain B; (E) Top10; (F) 10418; (G) 6571; (H) Cowan 1

D

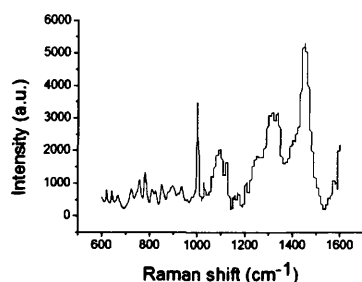


Raman shift (cm^{-1})	Compound/molecule
663	(not identified in literature, the closes signal is: Guanine)
756	Phosphophenylpyruvate
1000	Palmitic acid, D-(+)-Galactosamine
1120	D-(+)-Galactosamine, Acetyl coenzyme A
1340	DNA/RNA(Guanine/Adenine), Proteins, Carbohydrates, Protein (Amide III)
1450	CH_2 scissoring, DNA, C-H bindings in lipids, Proteins, Carbohydrates, Bands of fatty acids, Deformation vibration CH_2 scissoring

Figure 4.1.: (cont.) Plot and a table of most significant peaks with assigned molecules and bonds based on the mean spectra from all Raman measurements for (A) 1457; (B) 9142; (C) K12; (D) Strain B; (E) Top10; (F) 10418; (G) 6571; (H) Cowan 1

4. DISCRIMINATION BETWEEN BACTERIAL SPECIES AND STRAINS USING RAMAN SPECTROSCOPY

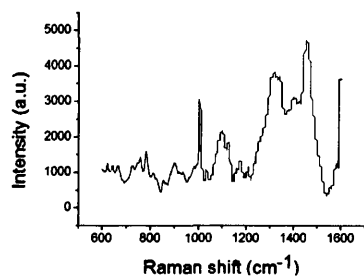
E



Raman shift (cm^{-1})	Compound/molecule
782	Citidine, Uracil, Cytosine, Uracil ring stretching, Phospho-phenylpyruvate, DNA Phosphodiester O-P-O stretching
1000	Palmitic acid, D-(+)-Galactosamine
1100	Palmitic acid
1340	DNA/RNA(Guanine/Adenine), Proteins, Carbohydrates, Protein (Amide III)
1450	CH_2 scissoring, DNA, C-H bindings in lipids, Proteins, Carbohydrates, Bands of fatty acids, Deformation vibration CH_2 scissoring

Figure 4.1.: (cont.) Plot and a table of most significant peaks with assigned molecules and bonds based on the mean spectra from all Raman measurements for (A) 1457; (B) 9142; (C) K12; (D) Strain B; (E) Top10; (F) 10418; (G) 6571; (H) Cowan 1

F

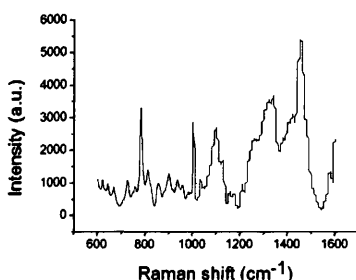


Raman shift (cm^{-1})	Compound/molecule
902	Amylose
1000	Palmitic acid, D-(+)-Galactosamine
1100	Palmitic acid
1340	DNA/RNA(Guanine/Adenine), Proteins, Carbohydrates, Protein (Amide III)
1420	CH_2 scissoring, DNA, C-H bindings in lipids, Proteins, Carbohydrates, Bands of fatty acids, Deformation vibration CH_2 scissoring

Figure 4.1.: (cont.) Plot and a table of most significant peaks with assigned molecules and bonds based on the mean spectra from all Raman measurements for (A) 1457; (B) 9142; (C) K12; (D) Strain B; (E) Top10; (F) 10418; (G) 6571; (H) Cowan 1

4. DISCRIMINATION BETWEEN BACTERIAL SPECIES AND STRAINS USING RAMAN SPECTROSCOPY

G

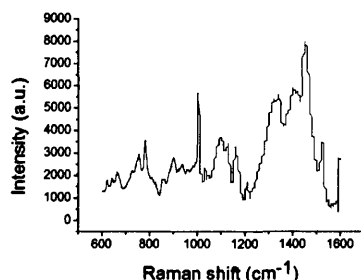


Raman shift (cm^{-1})	Compound/molecule
781	Citidine, Uracil, Cytosine, Uracil ring stretching, Phospho-phenylpyruvate, DNA Phosphodiester O-P-O stretching
1000	Palmitic acid, D-(+)-Galactosamine
1100	Palmitic acid
1340	DNA/RNA(Guanine/Adenine), Proteins, Carbohydrates, Protein (Amide III)
1450	CH_2 scissoring, DNA, C-H bindings in lipids, Proteins, Carbohydrates, Bands of fatty acids, Deformation vibration CH_2 scissoring

Figure 4.1.: (cont.) Plot and a table of most significant peaks with assigned molecules and bonds based on the mean spectra from all Raman measurements for (A) 1457; (B) 9142; (C) K12; (D) Strain B; (E) Top10; (F) 10418; (G) 6571; (H) Cowan 1

4. DISCRIMINATION BETWEEN BACTERIAL SPECIES AND STRAINS USING RAMAN SPECTROSCOPY

H



Raman shift (cm ⁻¹)	Compound/molecule
782	Citidine, Uracil, Cytosine, Uracil ring stretching, Phosphopyruvate, DNA Phosphodiester O-P-O stretching
1000	Palmitic acid, D-(+)-Galactosamine
1100	Palmitic acid
1450	CH ₂ scissoring, DNA, C-H bindings in lipids, Proteins, Carbohydrates, Bands of fatty acids, Deformation vibration CH ₂ scissoring

Figure 4.1.: (cont.) Plot and a table of most significant peaks with assigned molecules and bonds based on the mean spectra from all Raman measurements for (A) 1457; (B) 9142; (C) K12; (D) Strain B; (E) Top10; (F) 10418; (G) 6571; (H) Cowan 1

Table 4.1.: The summary of the Raman signal from all the reference (antibiotic susceptible) strains used in the project and showed separately in Figure 4.1

Raman shift	Organism							
	1457	9142	K12	Strain B	Top10	10418	6571	Cowan 1
663				x				
756				x				
781	x	x	x				x	
782					x			x
900	x	x						
902						x		
1000	x	x	x	x	x	x	x	x
1100		x	x		x	x	x	x
1120				x				
1340	x	x	x	x	x	x	x	
1420						x		
1450	x	x	x	x	x		x	

The presence of peak at the listed shift number is indicated by 'x'.

4.3.2. Similarity within experimental repeats

In order to investigate the ability of Raman spectroscopy to produce reproducible results, colonies of all the strains used in this chapter were subjected to Raman spectroscopy on consecutive days and the spectra were subjected to PCA (Figure 4.2). *S. epidermidis* (1457, 9142) and *E. coli* (K12, Strain B and Top10) strains showed tight clustering over the 3 day period suggesting high reproducibility and suggested the potential for simple discrimination between these species and strains. Less frequently used in laboratory strains of: *S. aureus* (6571 and Cowan1) and *E. coli* (10418) showed less clustering on respective days but maintained tight clusters on specific days. *E. coli* strain B had to be scanned 7 times to obtain 4 acceptable whole experimental repeats. This was due to reasons given in Table 3.5.

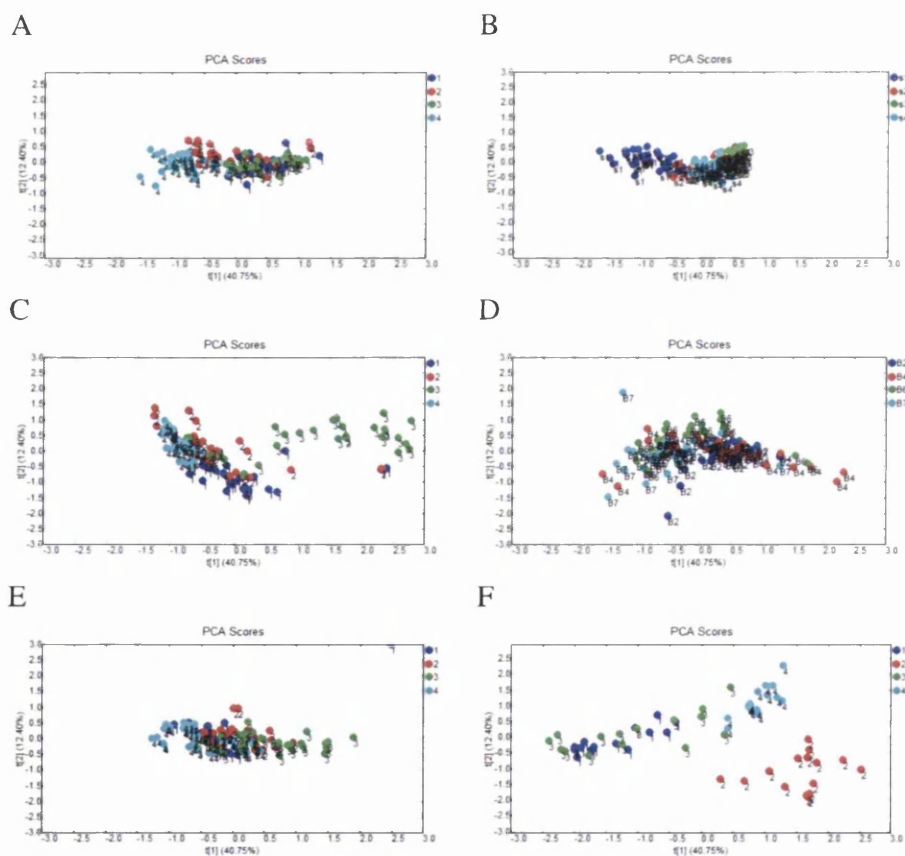


Figure 4.2.: PCA of whole experimental repeats performed for single strains used in the project; a) 1457; b)9142; c)K12; d) Strain B; e)Top10; f)10418; g) 6571; h)Cowan 1

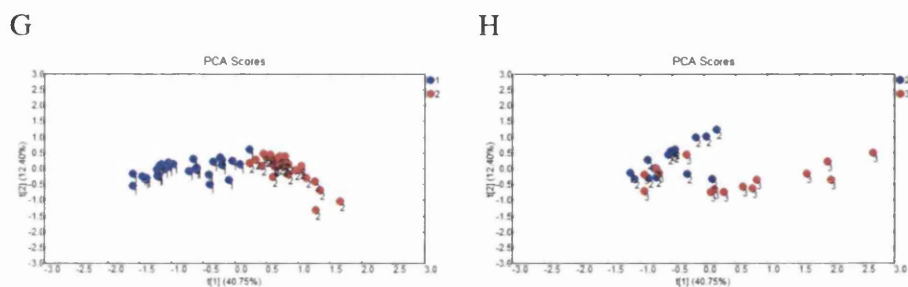


Figure 4.2.: (cont.) PCA of whole experimental repeats performed for single strains used in the project; a) 1457; b)9142; c)K12; d) Strain B; e)Top10; f)10418; g) 6571; h)Cowan 1

4.3.3. Comparison of organisms on different taxonomic levels

In order to determine whether Raman spectroscopy could distinguish between organisms at different taxonomic levels bacteria were compared in pairs.

4.3.3.1. Comparing different genera

The reproducibility experiments (Figure 4.2) confirmed our choice of strains at the genus level. The pairwise comparisons included the genera of *Esherichia* and *Staphylococcus* including *S. epidermidis* 1457 vs. *E. coli* Top10 (Figure 4.2), *S. epidermidis* 9142 vs. *E. coli* K12 (Figure 4.2) *S. aureus* 6571 vs. *E. coli* 10418 (Figure 4.2) and *S. aureus* Cowan1 vs. *E. coli* strain B (Figure 4.2). Comparisons showed many distinctive differences between the genera, which were visible upon subtraction of mean intensities values (A panel; blue curve on spectra) and represented by many Raman peaks (panel B; tables of signal) with defined shifts. Distinct separate PCA clusters (panel C; PCA plot) were confirmed by the very low probability values (high significance) following t-tests on individual PC scores (panel D; tables of t-test results). The signals identified are the result of DNA/RNA, amino acids and proteins. All of the comparisons show the peaks falling into the 778 - 785 cm^{-1} , which are all related strictly to molecules and bonds within the DNA.

4.3.3.2. Comparing different species within the same genera

The pairwise comparison of different species was carried out between *S. epidermidis* (strains 1457 and 9142) and *S. aureus* (6571 and Cowan1); specifically comparisons between *S. epidermidis* 1457 vs. *S. aureus* 6571 (Figure 4.2) and *S. epidermidis* 9142 vs. *S. aureus* Cowan1 (Figure 4.2). Overall, comparisons showed many distinctive differences between species, which were visible upon subtraction of mean intensities values

4. DISCRIMINATION BETWEEN BACTERIAL SPECIES AND STRAINS USING RAMAN SPECTROSCOPY

(A panel; blue curve on spectra) and represented by many Raman peaks (panel B; tables of signal) with defined shifts. Distinct separate PCA clusters (panel C; PCA plot) were confirmed by the low probability values (high significance) following t-tests on individual PC scores (panel D; tables of t-test results). Interestingly t-test scores were higher than for Figures 4.2 and 4.2 showing differences between genera. The most significant peaks have been assigned to similar signals as when different genera were compared.

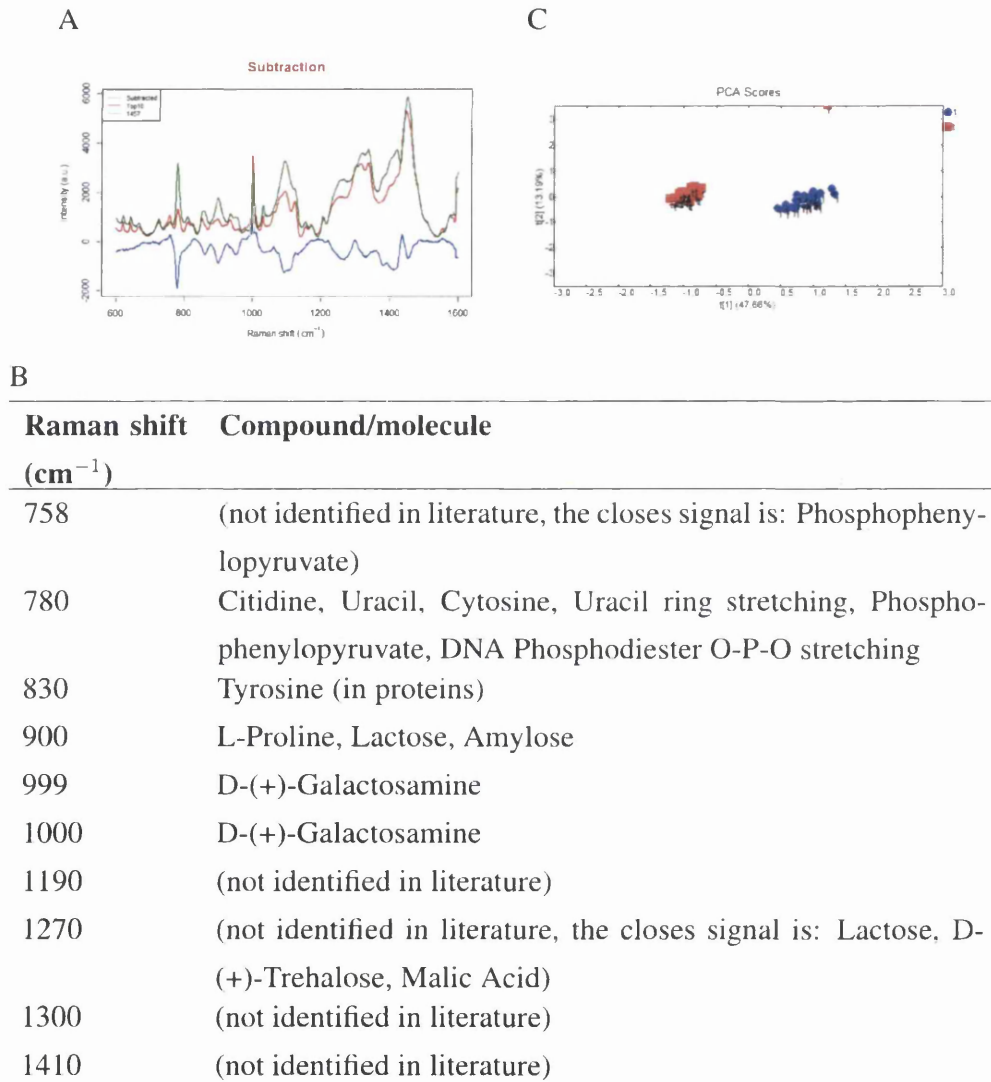


Figure 4.3.: The comparison of 1457 and Top10.; (A) plot of the means of all four whole experimental repeats (4 sets of 30 spectra) for each strain and a subtraction of these means; (B) the list or Raman peaks showing the most significant differences between the two organisms; (C) PCA comparing two single experiments; (D) table of t-test results comparing PC scores for each whole experimental repeats

4. DISCRIMINATION BETWEEN BACTERIAL SPECIES AND STRAINS USING RAMAN SPECTROSCOPY

D

Organism	Experiment number	T-test results value			
		PC1	PC2	PC3	PC4
Top10wt vs. 1457	1	8.58E-24	1.63E-02	7.90E-01	5.73E-01
	2	9.50E-34	1.53E-01	2.96E-01	6.57E-01
	3	2.95E-48	5.01E-01	6.71E-01	8.50E-01
	4	1.88E-37	2.59E-01	3.01E-01	9.32E-01

Figure 4.3.: (cont.) The comparison of 1457 and Top10.; (A) plot of the means of all four whole experimental repeats (4 sets of 30 spectra) for each strain and a subtraction of these means; (B) the list of Raman peaks showing the most significant differences between the two organisms; (C) PCA comparing two single experiments; (D) table of t-test results comparing PC scores for each whole experimental repeats

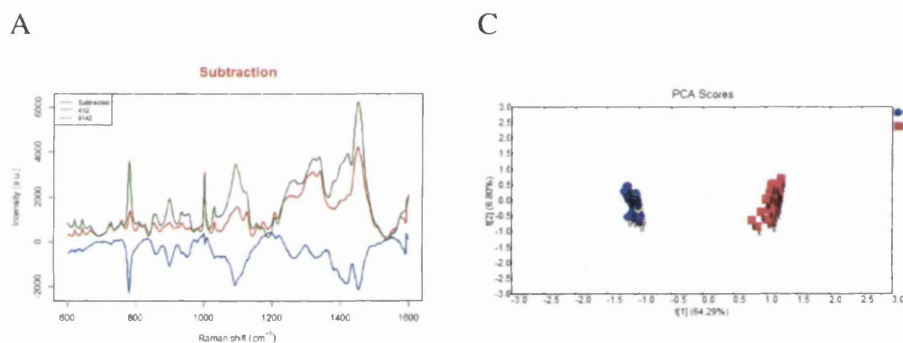


Figure 4.4.: The comparison of K12 and 9142; (A) plot of the means of all four whole experimental repeats (4 sets of 30 spectra) for each strain and a subtraction of these means; (B) the list of Raman peaks showing the most significant differences between the two organisms; (C) PCA comparing two single experiments (D) table of t-test results comparing PC scores for each whole experimental repeats.

4. DISCRIMINATION BETWEEN BACTERIAL SPECIES AND STRAINS USING RAMAN SPECTROSCOPY

B

Raman shift (cm^{-1})	Compound/molecule
781	Citidine, Uracil, Cytosine, Uracil ring stretching, Phospho-phenylpyruvate, DNA Phosphodiester O-P-O stretching
832	(not identified in literature, the closes signal is: Tyrosine (in proteins) exposed, L-Tryptophan
901	Amylose, Lactose
999	D-(+)-Galactosamine
1000	D-(+)-Galactosamine
1190	(not identified in literature)
1270	Amide III, DNA/RNA (Thymine, Adenine), Proteins (Amide III), Lipids
1450	CH_2 scissoring, DNA, C-H bindings in lipids, Proteins, Carbohydrates, Bands of fatty acids, Deformation vibration CH_2 scissoring
1550	(not identified in literature)
1600	(not identified in literature, the closes signal is: Tyrosine, Phenylalanine)

D

Organism	Experiment number	T-test results value			
		PC1	PC2	PC3	PC4
K12 vs. 9142	1	1.63E-31	4.24E-01	2.22E-01	5.71E-01
	2	1.03E-57	8.83E-01	8.16E-01	5.71E-01
	3	8.28E-49	5.75E-01	7.39E-01	6.35E-01
	4	5.70E-14	2.78E-04	8.47E-01	5.84E-01

Figure 4.4.: (cont.) The comparison of K12 and 9142; (A) plot of the means of all four whole experimental repeats (4 sets of 30 spectra) for each strain and a subtraction of these means; (B) the list of Raman peaks showing the most significant differences between the two organisms; (C) PCA comparing two single experiments (D) table of t-test results comparing PC scores for each whole experimental repeats.

4. DISCRIMINATION BETWEEN BACTERIAL SPECIES AND STRAINS USING RAMAN SPECTROSCOPY

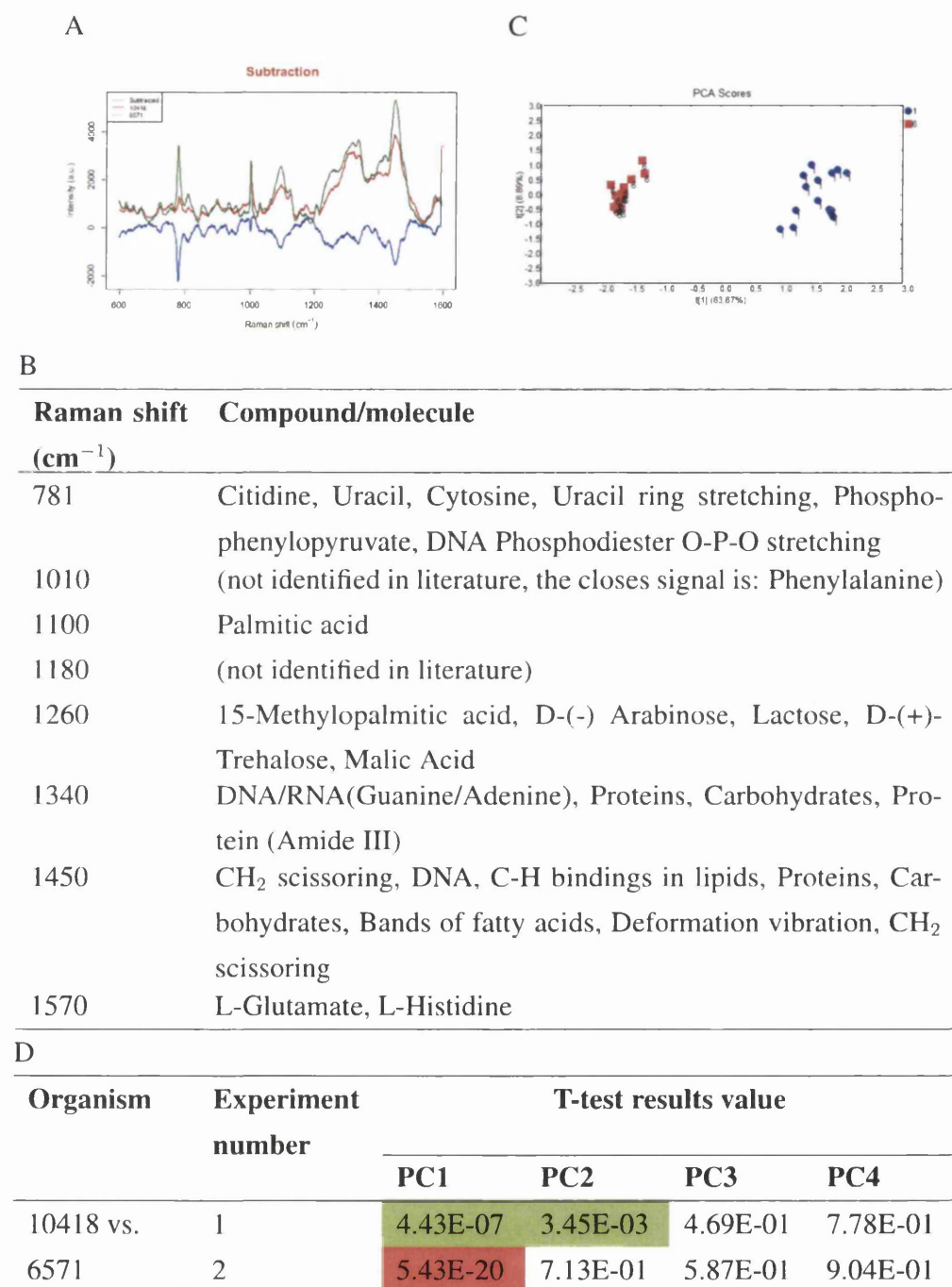


Figure 4.5.: The comparison of 10418 and 6571; (A) plot of the means of all two whole experimental repeats (2 sets of 15 spectra) for each strain and a subtraction of these means; (B) the list or Raman peaks showing the most significant differences between the two organisms; (C) PCA comparing two single experiments (D) table of t-test results comparing PC scores for each whole experimental repeats.

4. DISCRIMINATION BETWEEN BACTERIAL SPECIES AND STRAINS USING RAMAN SPECTROSCOPY

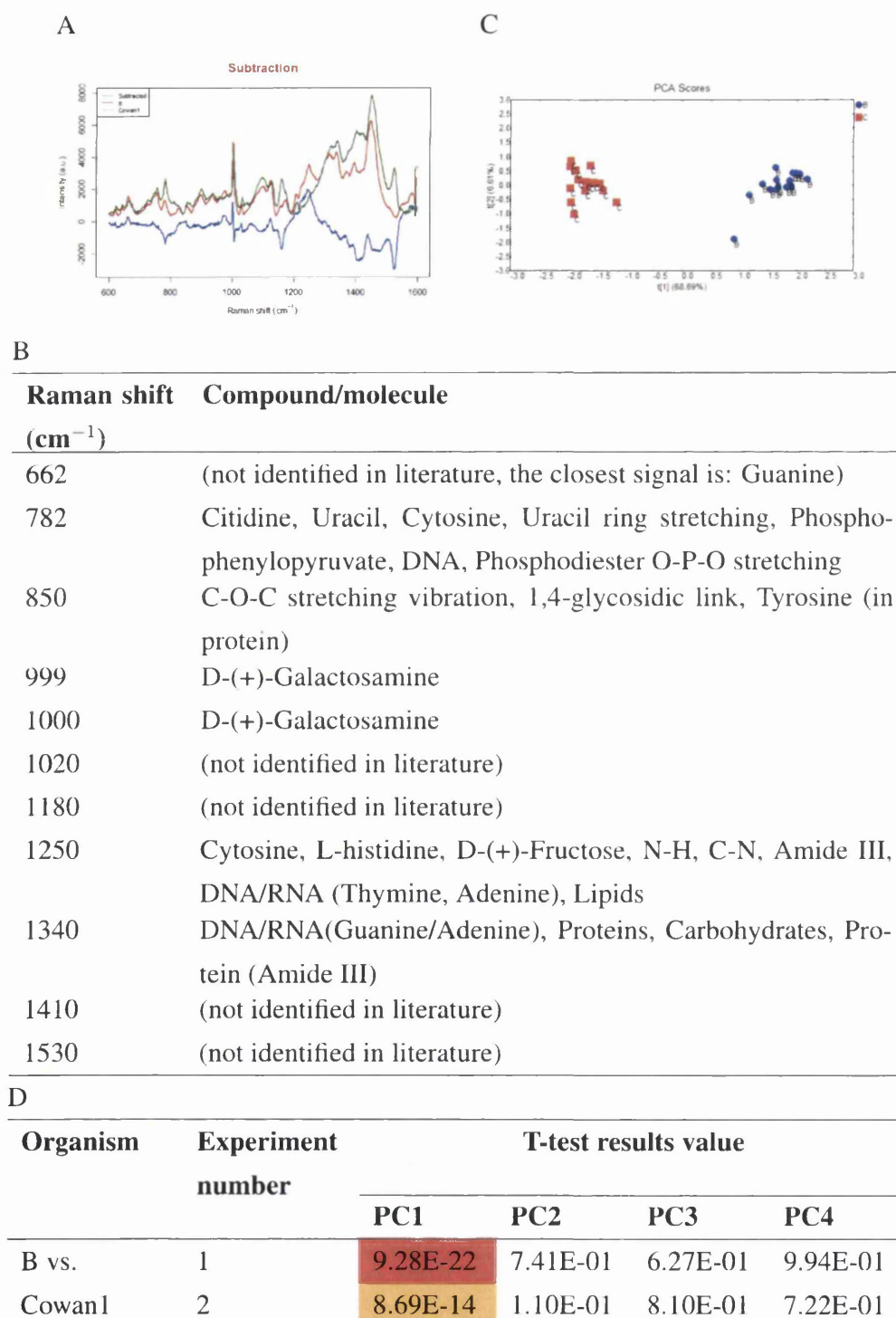


Figure 4.6.: The comparison of Strain B and Cowan 1; (A) plot of the means of all two whole experimental repeats (2 sets of 15 spectra) for each strain and a subtraction of these means; (B) the list of Raman peaks showing the most significant differences between the two organisms; (C) PCA comparing two single experiments (D) table of t-test results comparing PC scores for each whole experimental repeats.

4. DISCRIMINATION BETWEEN BACTERIAL SPECIES AND STRAINS USING RAMAN SPECTROSCOPY

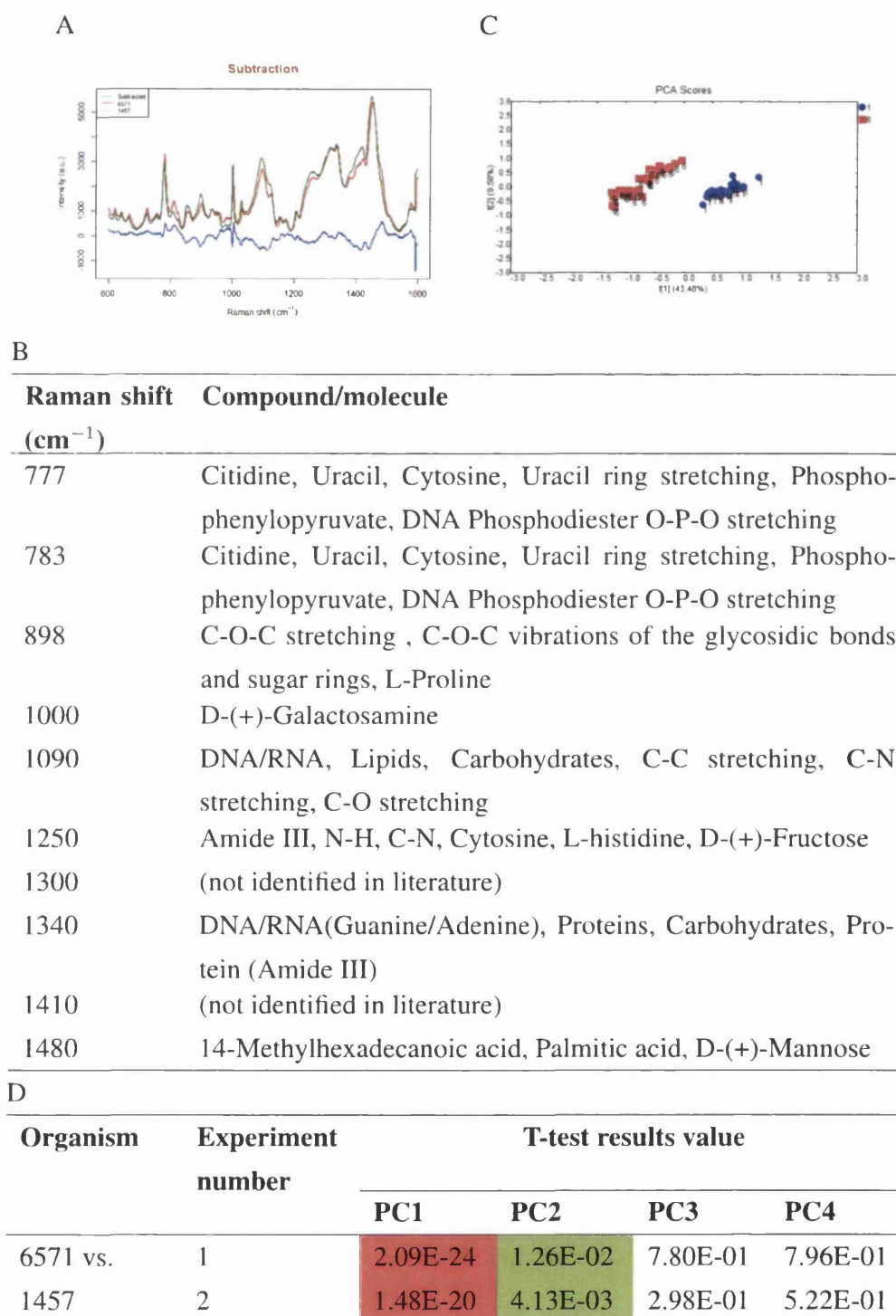


Figure 4.7.: The comparison of 1457 and 6571; (A) plot of the means of all two whole experimental repeats (2 sets of 15 spectra) for each strain and a subtraction of these means; (B) the list or Raman peaks showing the most significant differences between the two organisms; (C) PCA comparing two single experiments (D) table of t-test results comparing PC scores for each whole experimental repeats.

4. DISCRIMINATION BETWEEN BACTERIAL SPECIES AND STRAINS USING RAMAN SPECTROSCOPY

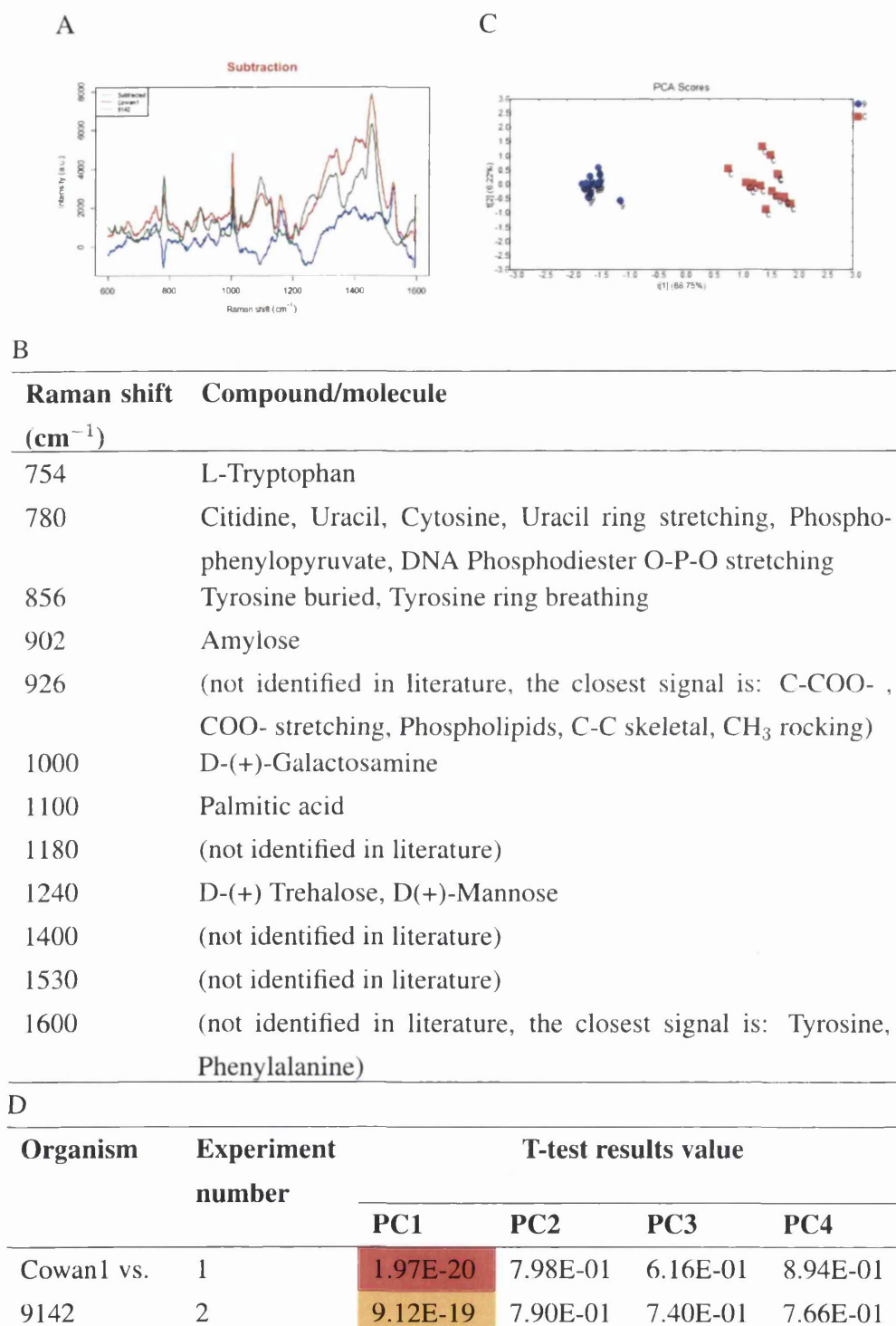


Figure 4.8.: The comparison of 9142 and Cowan1.; (A) plot of the means of all two whole experimental repeats (2 sets of 15 spectra) for each strain and a subtraction of these means; (B) the list of Raman peaks showing the most significant differences between the two organisms; (C) PCA comparing two single experiments (D) table of t-test results comparing PC scores for each whole experimental repeats.

4.3.3.3. Comparing different strains within the same species

In order to fully explore the abilities of Raman spectroscopy for precise differentiation between bacterial organisms, subtle comparisons between bacteria representing different strains of the same species were investigated. Thus in *S. epidermidis* strains 1457 and 9142 were compared (Figure 4.2). In *S. aureus* comparisons were made between strains 6571 vs. Cowan1 (Figure 4.2) was compared. In *E. coli* three further comparisons were made including K12 vs. Top10 (Figure 4.2), K12 vs. strain B (Figure 4.2) and Top10 vs. strain B (Figure 4.2).

Overall, comparisons showed many distinctive differences between species, which were visible upon subtraction of mean intensities values (A panel; blue curve on spectra) and represented by many Raman peaks (panel B; tables) with defined shifts. Distinct separate PCA clusters (panel C; PCA plot) were confirmed by the low probability values (high significance) following t-tests on individual PC scores (panel D; tables of t-test results). Interestingly t-test scores, especially within *E. coli* strains comparisons were higher than those shown for differences between genera.

Two organisms: 1457 and 9142 representing *S. epidermidis* strain, show very discrete differences when the mean intensities were subtracted, however still maintain well separated clusters and very low results of t-tests (Figure 4.2).

The comparison of two *S. aureus* species: 6571 and Cowan1 (Figure 4.2) although also contain the variation between the same species show very high differences of the mean intensities subtraction that could be compared to the differences between 9142 and Cowan1 or even Strain B and Cowan 1 and it is also supported by the results from t-tests. At this step of differentiation, there is a maintained trend of expressing DNA, proteins, carbohydrates, however there are more fatty acids and fats involved, therefore there is much higher variation in the assigned molecules and bonds.

4. DISCRIMINATION BETWEEN BACTERIAL SPECIES AND STRAINS USING RAMAN SPECTROSCOPY

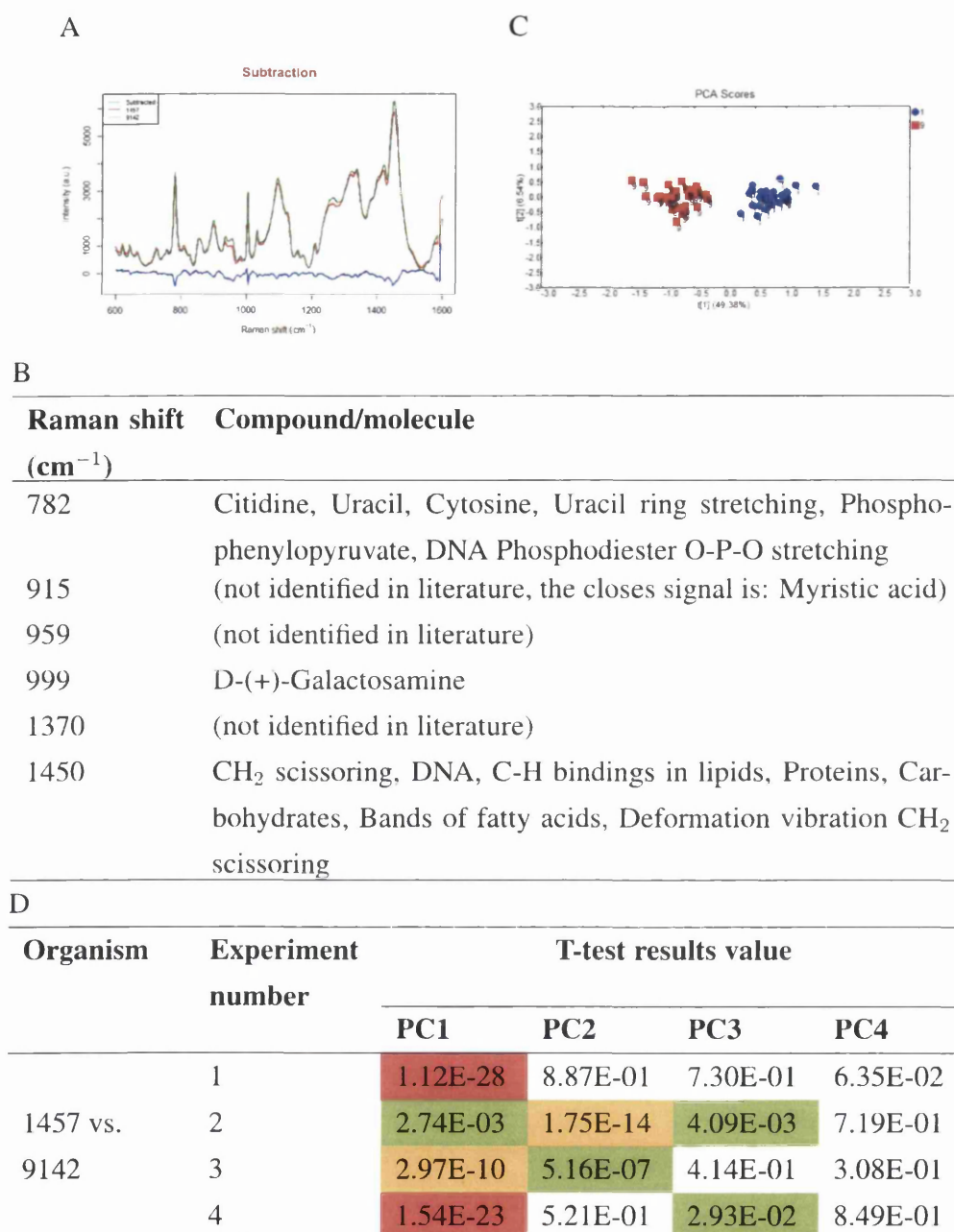


Figure 4.9.: The comparison of 1457 and 9142.; (A) plot of the means of all four whole experimental repeats (4 sets of 30 spectra) for each strain and a subtraction of these means; (B) the list or Raman peaks showing the most significant differences between the two organisms; (C) PCA comparing two single experiments; (D) table of t-test results comparing PC scores for each whole experimental repeats.

4. DISCRIMINATION BETWEEN BACTERIAL SPECIES AND STRAINS USING RAMAN SPECTROSCOPY

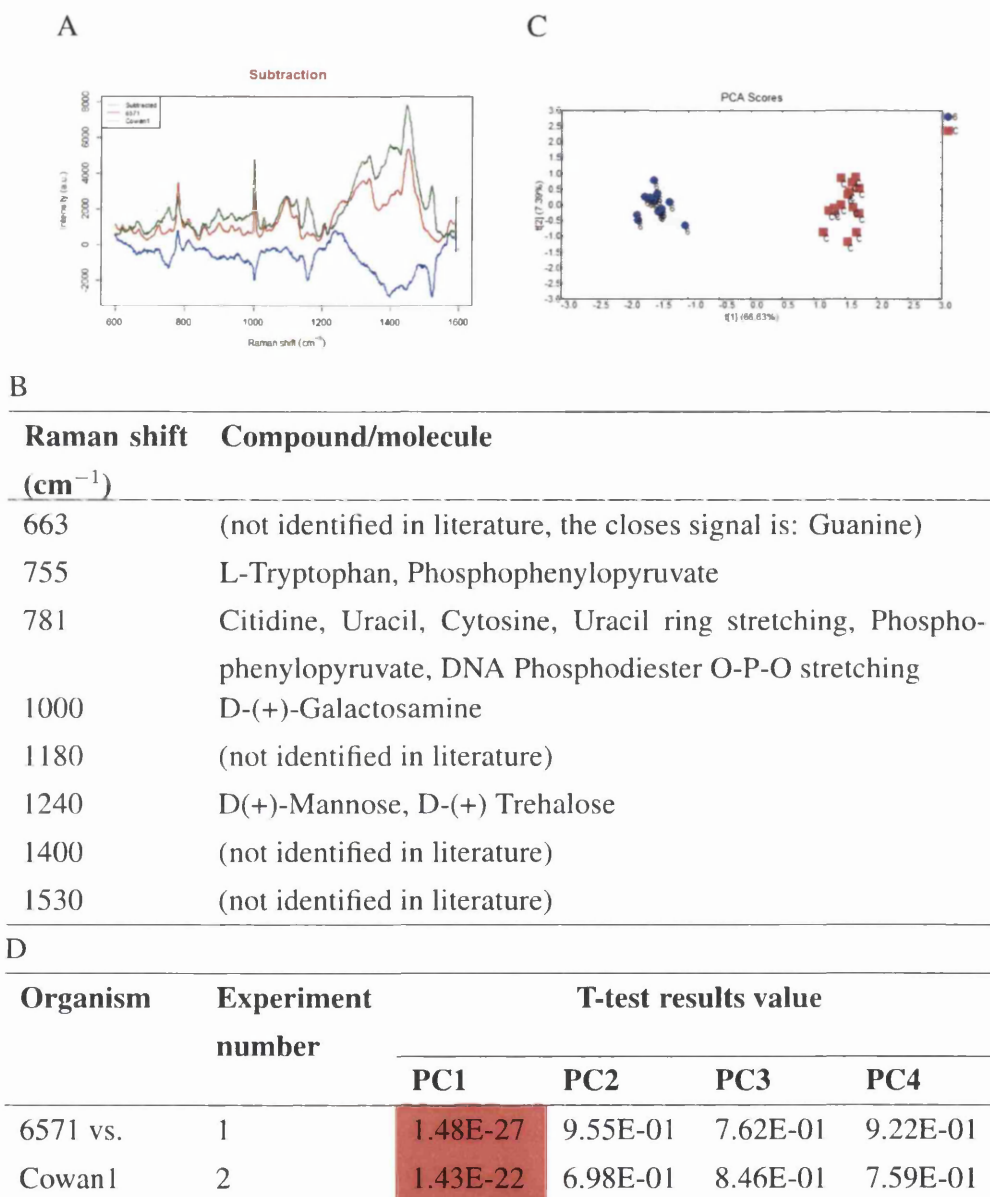


Figure 4.10.: The comparison of 6571 and Cowan1.; (A) plot of the means of all two whole experimental repeats (2 sets of 15 spectra) for each strain and a subtraction of these means; (B) the list of Raman peaks showing the most significant differences between the two organisms; (C) PCA comparing two single experiments; (D) table of t-test results comparing PC scores for each whole experimental repeats.

4. DISCRIMINATION BETWEEN BACTERIAL SPECIES AND STRAINS USING RAMAN SPECTROSCOPY

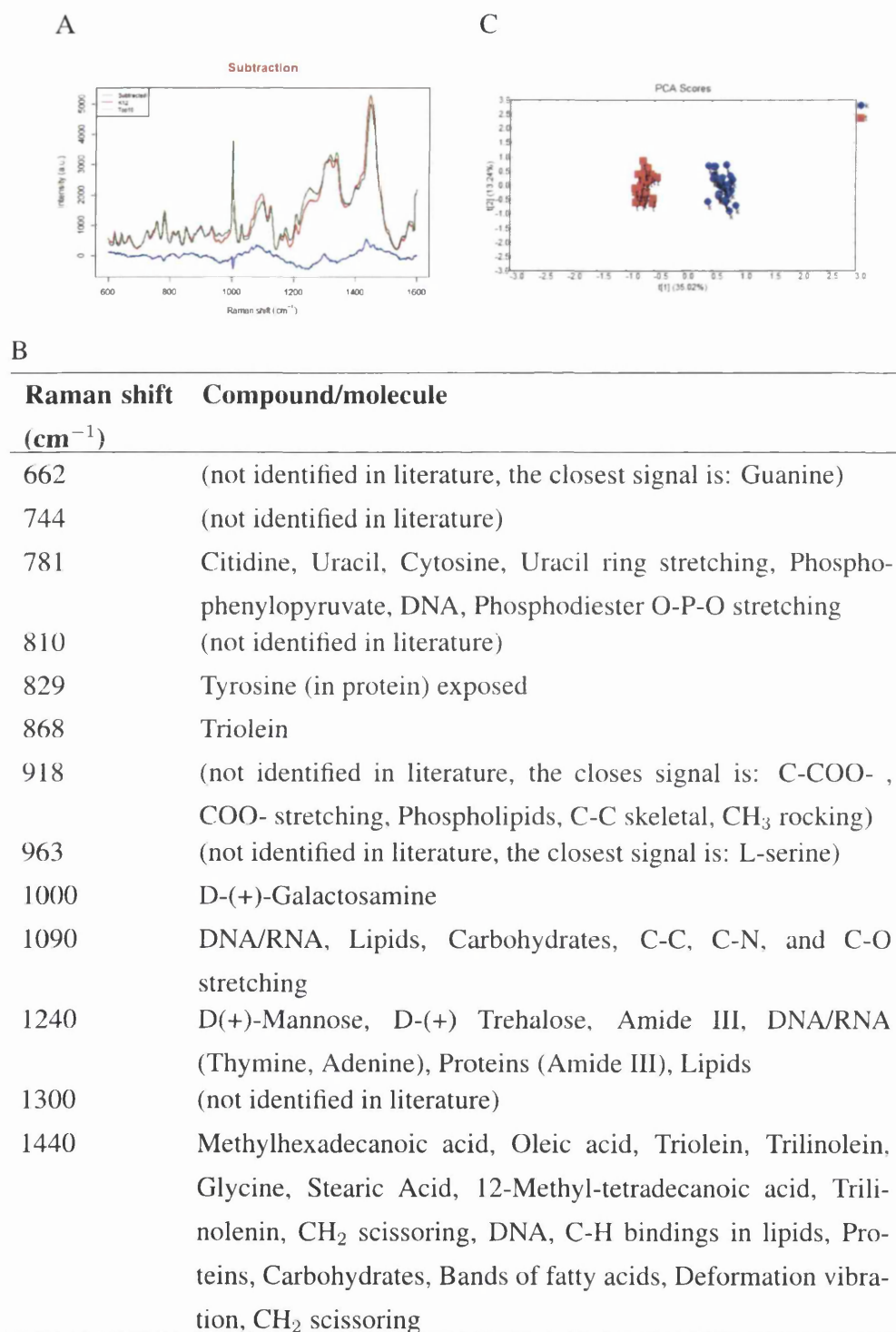


Figure 4.11.: The comparison of K12 and Top10; (A) plot of the means of all four whole experimental repeats (4 sets of 30 spectra) for each strain and a subtraction of these means; (B) the list or Raman peaks showing the most significant differences between the two organisms; (C) PCA comparing two single experiments; (D) table of t-test results comparing PC scores for each whole experimental repeats.

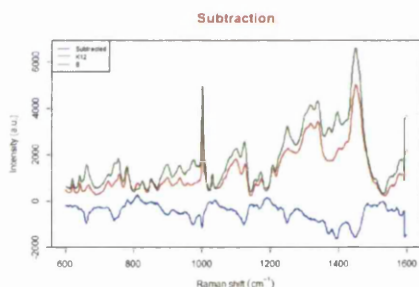
4. DISCRIMINATION BETWEEN BACTERIAL SPECIES AND STRAINS USING RAMAN SPECTROSCOPY

D

Organism	Experiment number	T-test results value			
		PC1	PC2	PC3	PC4
K12 vs.	1	4.04E-13	2.01E-03	1.11E-01	7.76E-02
Top10	2	3.49E-46	8.84E-01	7.08E-01	5.32E-01
	3	4.02E-01	4.38E-05	1.11E-07	7.66E-04
	4	1.46E-12	2.20E-01	1.50E-01	1.94E-01

Figure 4.11.: (cont.) The comparison of K12 and Top10; (A) plot of the means of all four whole experimental repeats (4 sets of 30 spectra) for each strain and a subtraction of these means; (B) the list or Raman peaks showing the most significant differences between the two organisms; (C) PCA comparing two single experiments; (D) table of t-test results comparing PC scores for each whole experimental repeats.

A



C

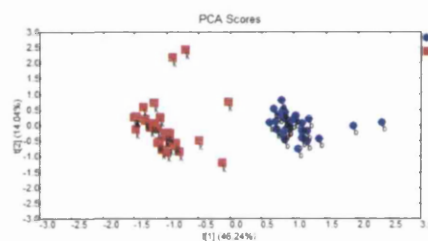


Figure 4.12.: The comparison of K12 and Strain B; (A) plot of the means of all four whole experimental repeats (4 sets of 30 spectra) for each strain and a subtraction of these means; (B) the list or Raman peaks showing the most significant differences between the two organisms; (C) PCA comparing two single experiments; (D) table of t-test results comparing PC scores for each whole experimental repeats.

4. DISCRIMINATION BETWEEN BACTERIAL SPECIES AND STRAINS USING RAMAN SPECTROSCOPY

B

Raman shift (cm^{-1})	Compound/molecule
663	(not identified in literature, the closes signal is: Guanine)
745	(not identified in literature)
811	(not identified in literature)
901	Lactose, Amylose
975	(not identified in literature, the closes signal is: C-C, Stretching of beta-sheet (proteins), C-H bending (lipids))
1120	D-(+)-Galactosamine, Acetyl coenzyme A
1190	(not identified in literature)
1250	Cytosine, L-histidine, D-(+)-Fructose, Amide III, N-H, C-N, Amide III, DNA/RNA (Thymine, Adenine), Proteins (Amide III), Lipids
1400	(not identified in literature)
1450	CH ₂ scissoring, DNA, C-H bindings in lipids, Proteins, Carbohydrates, Bands of fatty acids, Deformation vibration CH ₂ scissoring

D

Organism	Experiment number	T-test results value			
		PC1	PC2	PC3	PC4
K12 vs. B	1	2.73E-30	7.66E-01	2.67E-02	8.99E-01
	2	1.93E-01	7.20E-26	2.61E-02	4.59E-01
	3	4.99E-13	4.93E-04	4.11E-02	2.63E-01
	4	4.33E-08	3.19E-07	6.57E-03	5.43E-01

Figure 4.12.: (cont.) The comparison of K12 and Strain B; (A) plot of the means of all four whole experimental repeats (4 sets of 30 spectra) for each strain and a subtraction of these means; (B) the list or Raman peaks showing the most significant differences between the two organisms; (C) PCA comparing two single experiments; (D) table of t-test results comparing PC scores for each whole experimental repeats.

4. DISCRIMINATION BETWEEN BACTERIAL SPECIES AND STRAINS USING RAMAN SPECTROSCOPY

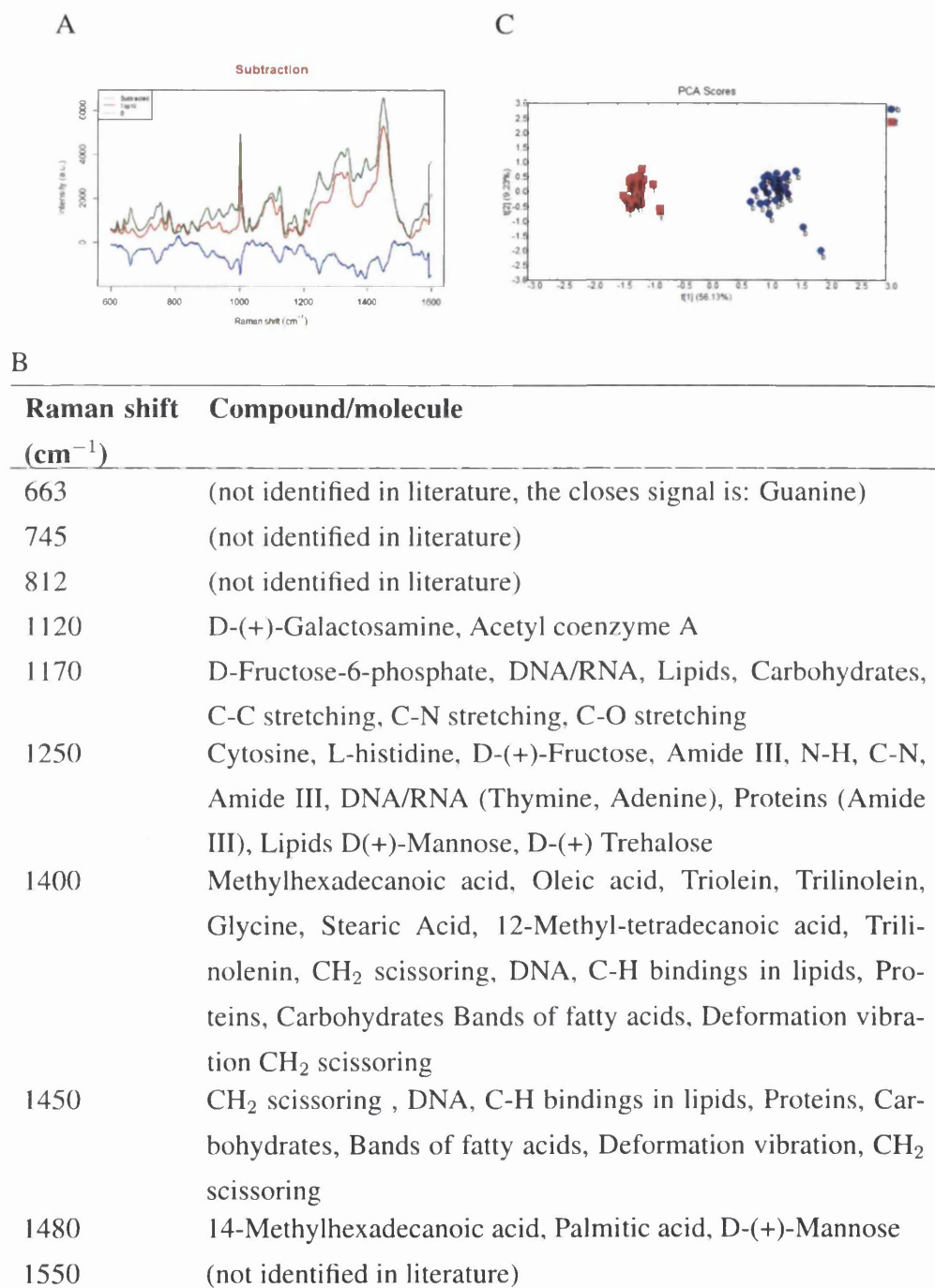


Figure 4.13.: The comparison of Top10 and Strain B; (A) plot of the means of all four whole experimental repeats (4 sets of 30 spectra) for each strain and a subtraction of these means; (B) the list or Raman peaks showing the most significant differences between the two organisms; (C) PCA comparing two single experiments; (D) table of t-test results comparing PC scores for each whole experimental repeats.

4. DISCRIMINATION BETWEEN BACTERIAL SPECIES AND STRAINS USING RAMAN SPECTROSCOPY

D

Organism	Experiment number	T-test results value			
		PC1	PC2	PC3	PC4
Top10 vs. B	1	1.62E-20	8.95E-04	1.55E-01	9.50E-01
	2	1.79E-41	7.04E-01	3.00E-01	9.48E-01
	3	1.71E-23	1.24E-01	7.43E-02	1.27E-01
	4	2.29E-16	1.35E-03	1.86E-01	6.86E-01

Figure 4.13.: (cont.) The comparison of Top10 and Strain B; (A) plot of the means of all four whole experimental repeats (4 sets of 30 spectra) for each strain and a subtraction of these means; (B) the list of Raman peaks showing the most significant differences between the two organisms; (C) PCA comparing two single experiments; (D) table of t-test results comparing PC scores for each whole experimental repeats.

4.3.3.4. Multiple strains comparison

In order to verify whether Raman can correctly assess the natural relationships between bacteria, a hierarchical cluster tree was designed (Figure 4.14).

It can be noted that majority of the strains cluster according to their taxonomic relationships: *E. coli* stay on one branch, with K12 and Top10 being the most closely related and with less proximity to strain B and even further from 10418. Among *Staphylococcus*, two *S. epidermidis*: 1457 and 9142 stay close together and the *S. aureus* strain 6571 on a separate branch. Another *S. aureus*, Cowan1 strain does not cluster with 6571 but stays completely separate from all other organisms.

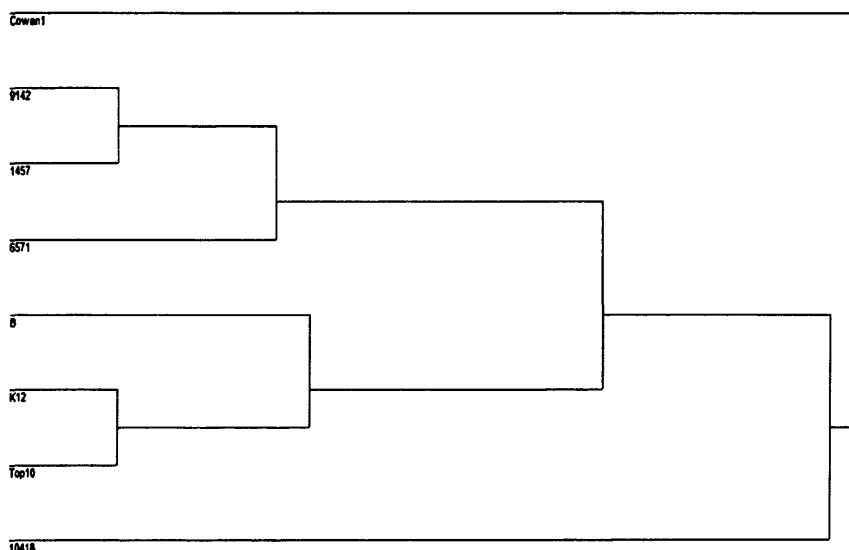


Figure 4.14.: The hierarchical cluster analysis tree of mean values calculated for each single sample repeat within all whole experimental repeats for the strains used in this chapter including: (A) Cowan1; (B) 9142; (C) 1457; (D) 6571; (E) Strain B; (F) K12; (G) Top10; (H) 10418.

4.3.3.5. Discrimination of *E. coli* following sample storage: effect of time and temperature

Raman spectroscopy has the potential to be used as a diagnostic technique for identification of causative agents during infectious disease. One challenge the technique would face in the clinical environment would be sample storage. Indeed, plated samples in a diagnostic laboratory may not be measured immediately and left overnight before analysis. Here, therefore metabolic changes/growth, that takes place during the storage time, were assessed for their influence on the discrimination of two *E. coli* strains (Top10 and K12) by Raman spectroscopy.

4.3.3.5.1 Maintaining the clustering within the repeats of the sample

In both cases of: Top10 and K12 (Figure 4.2 and 4.2 respectively) neither time nor temperature had clear visible effect on clustering of the sample repeats. There are minor changes in the shape of clusters as well as clustering between the single sample repeats and whole experimental repeats.

4.3.3.6. Influence of time and temperature on the ability to distinguish between two samples

The ability to distinguish between two organisms is an important factor for the diagnostic purposes. Figure 4.2 does not represent any noticeable differences in the clustering between Top10 and K12 neither under the influence of time, nor temperature.

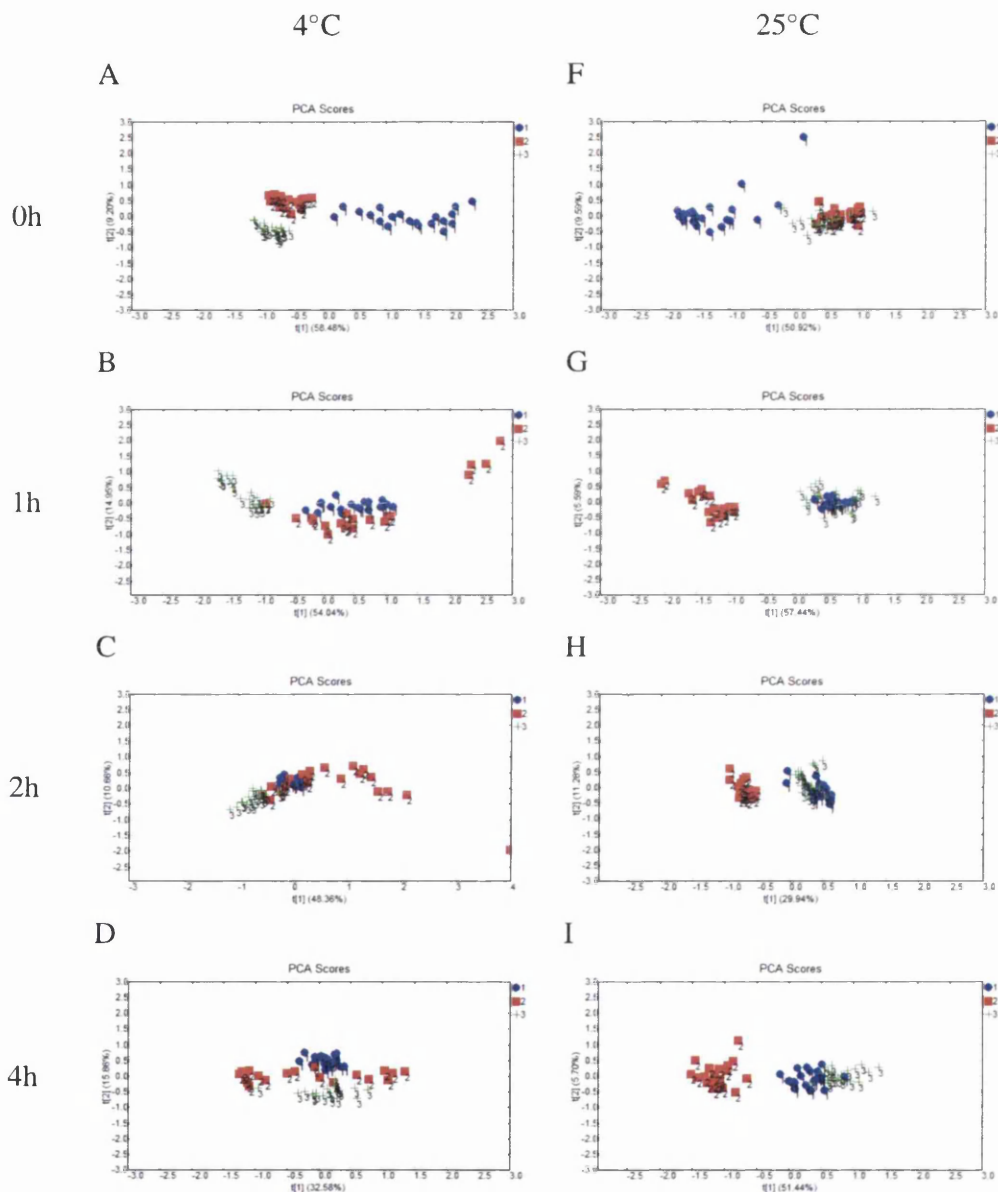


Figure 4.15.: Comparison of the influence of the temperature of storage in time on the clustering of Raman spectra for Top10 in (A-E) 4°C and (F-J) 25°C after (A and F)0; (B and G) 1; (C and H) 2; (D and I) 4; (E and J) 8 hours, including three experimental repeats (blue dot, red square and green cross for n=1; 2; and 3 respectively)

4. DISCRIMINATION BETWEEN BACTERIAL SPECIES AND STRAINS USING RAMAN SPECTROSCOPY

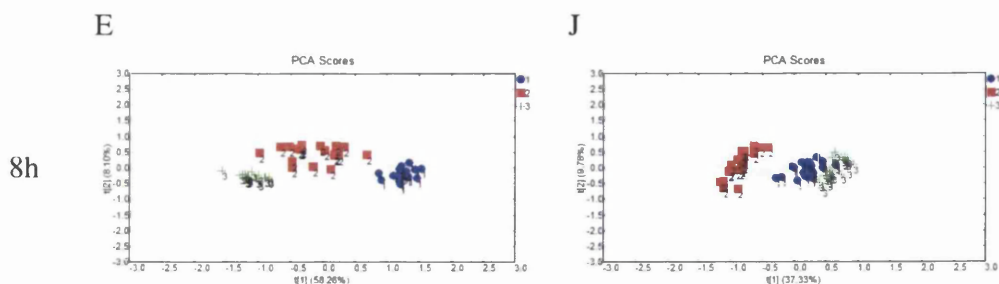


Figure 4.15.: (cont.) Comparison of the influence of the temperature of storage in time on the clustering of Raman spectra for Top10 in (A-E) 4°C and (F-J) 25°C after (A and F)0; (B and G) 1; (C and H) 2; (D and I) 4; (E and J) 8 hours, including three experimental repeats (blue dot, red square and green cross for n=1; 2; and 3 respectively)

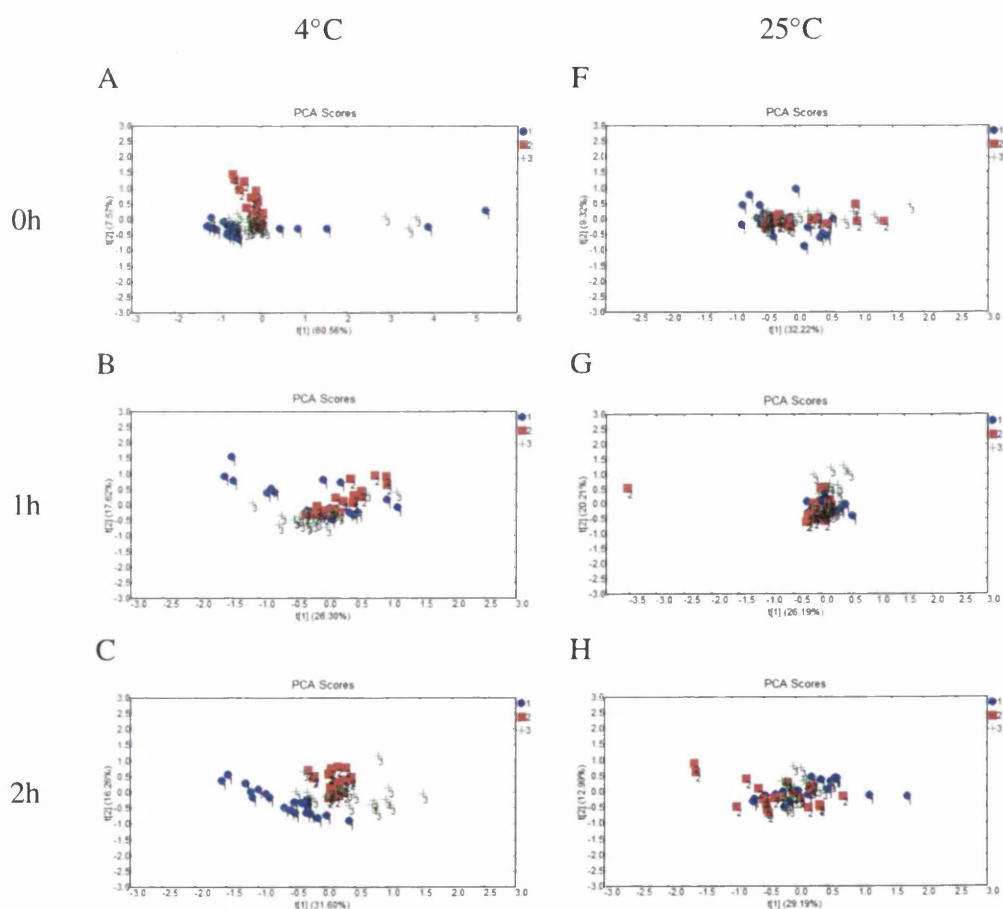


Figure 4.16.: Comparison of the influence of the temperature of storage in time on the clustering of Raman spectra for K12 in (A-E) 4°C and (F-J) 25°C after (A and F)0; (B and G) 1; (C and H) 2; (D and I) 4; (E and J) 8 hours, including three experimental repeats (blue dot, red square and green cross for n=1; 2; and 3 respectively)

4. DISCRIMINATION BETWEEN BACTERIAL SPECIES AND STRAINS USING RAMAN SPECTROSCOPY

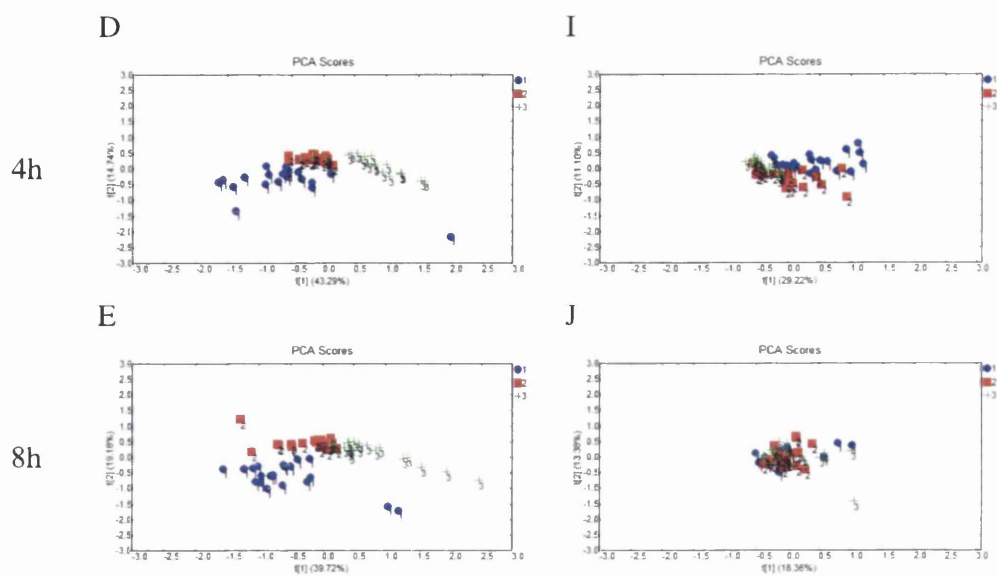


Figure 4.16.: (cont.) Comparison of the influence of the temperature of storage in time on the clustering of Raman spectra for K12 in (A-E) 4°C and (F-J) 25°C after (A and F)0; (B and G) 1; (C and H) 2; (D and I) 4; (E and J) 8 hours, including three experimental repeats (blue dot, red square and green cross for n=1; 2; and 3 respectively)

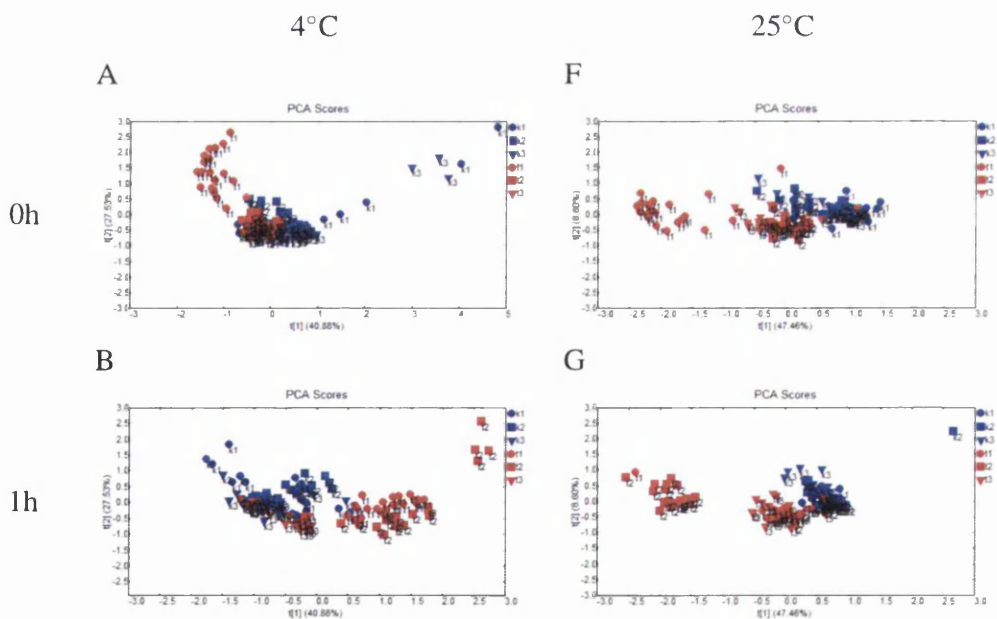


Figure 4.17.: Comparison of the influence of the temperature of storage in time on the differentiation between K12 (blue) and Top10 (red) spectra in (A-E) 4°C and (F-J) 25°C after (A and F)0; (B and G) 1; (C and H) 2; (D and I) 4; (E and J) 8 hours, including three experimental repeats for each organism (dot, square and triangle for n=1; 2; and 3 respectively)

4. DISCRIMINATION BETWEEN BACTERIAL SPECIES AND STRAINS USING RAMAN SPECTROSCOPY

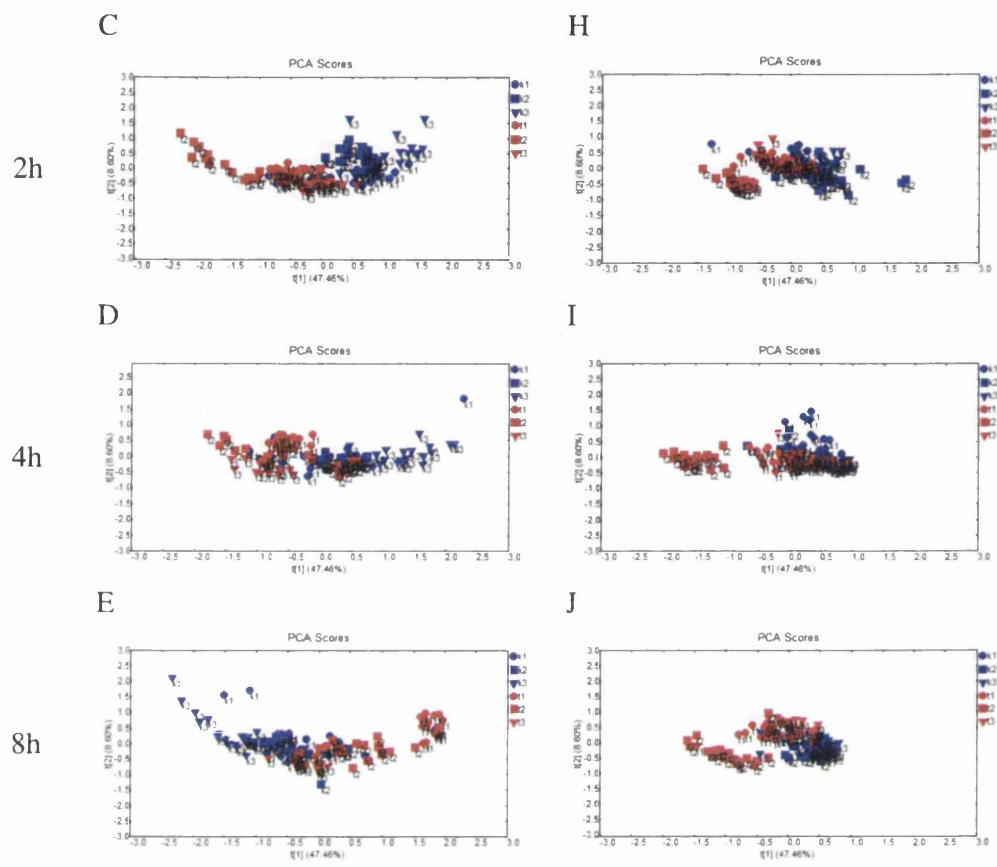


Figure 4.17.: (cont.) Comparison of the influence of the temperature of storage in time on the differentiation between K12 (blue) and Top10 (red) spectra in (A-E) 4°C and (F-J) 25°C after (A and F)0; (B and G) 1; (C and H) 2; (D and I) 4; (E and J) 8 hours, including three experimental repeats for each organism (dot, square and triangle for n=1; 2; and 3 respectively)

4.4. Discussion

Raman spectroscopy has gained a wide interest as a useful technique for successful distinguishing between bacterial organisms (Mariani et al., 2010) (Petry et al., 2003) (Downes & Elfick, 2010). However, here a broad extent of its abilities has been investigated, including various levels of taxonomic similarity, strains originating from two different environments: laboratory and clinical as well as the influence of possible metabolic changes dependant on the temperature and time of storage.

The ability of differentiation naturally follows the order of separation within: different genus >different species of the same genus >different strains of the same species.

An important effect can be seen between the comparisons involving Top10, K12 and Strain B spectra all representing to *E. coli* species. However, Top10 stems directly from the K12 strain, differing by only subtle genetic alternations that make it more suitable for transformation. Strain B descends from a separate isolate and as expected, should be less similar than Top10 and K12 when compared together (Schneider et al., 2002). Indeed as the Figure 4.2 shows, the differences both from mean intensities subtraction as well as from the t-tests results show lower variation in case of Top10 vs. K12 than between K12 and Strain B or Top10 and Strain B (Figure 4.2 and 4.2 respectively).

Other publications offer different but also very successful rate of differentiation between strains and species, including *Staphylococcus* spp. (Rösch et al., 2005) (Harz et al., 2005) and strains of *E. coli* (Jarvis & Goodacre, 2004b). The research that is the most similar, in terms of sample preparation and organisms used has been published by Maquelin et al. (Maquelin et al., 2000). It was possible to distinguish successfully between different genera; however, the results do not include sub-species classification.

We have observed that differences lay mainly within DNA and proteins with raising importance of fats and fatty acids towards the smaller degree of differentiation. This may lead towards the conclusion that the finer changes are dependant more on the outer bacterial envelope rather than genetic material and metabolites. The comparison of peaks from other publications confirms our assignment of peaks: namely DNA/RNA elements, proteins (Harz et al., 2005) (Maquelin et al., 2000) (Jarvis et al., 2004), however with very poor information on fats and fatty acids.

It is also worth noticing that the ability of differentiation between organisms rely to a certain extent on how well those organisms are characterised and whether they have been cultured for a longer period of time, i.e. K12, Top10, 1457 and 9142 showed much better

growth and therefore PCA clustering than Cowan1 and 10418. This fact was reflected both: when single sample repeats and whole experimental repeats were investigated.

Comparison of higher number of organisms contributed towards broader perspective analysis and investigation of relationships between all of the strains used in this chapter on one graph. The results from Figure 4.14 represent the naturally expected relationship between strains including the subtle relations between the Top10, K12 and strain B of *E. coli*. One exception is Cowan1, which is not related to any other organism, including another *S. aureus*: 6571. No Raman spectroscopy-based experiments of Cowan1 could be found and the only possible explanation could be that Cowan1 strains were of very poor quality, which might have influenced the final outcome. Therefore a preliminary conclusion could be drawn, that one has to be very rigorous when measuring the organisms and making sure the criterion of selection of the spectra should be very strictly determined.

Since this project evaluates the possibility of Raman spectroscopy to become a diagnostic technique, the fact that neither temperature, nor time of storage can influence the abilities of distinguishing between samples is of high importance. It would seem that this indicates that spectra do not reflect metabolic changes; however, this conclusion should not be drawn before more work is performed.

Despite the fact that there are several publications with regards to investigating bacterial biochemistry with Raman spectroscopy (Ciobot et al., 2010) (Palchaudhuri et al., 2011) (Jehlička et al., 2012), no information about the influence of storage of the biological material on the power of discrimination, could be found up-to-date.

The results obtained in this chapter allowed verifying that Raman spectroscopy can be considered as a very useful and consistent method in comparing bacterial organisms. The success of above investigation lead to the conclusion that the possibilities offered by the Raman spectroscopy could be investigated even further and more subtle differences, including different antibiotic resistance profile could be another step forward.

Chapter 5 will therefore be based on the application of Raman spectroscopy for distinguishing between antibiotic susceptible strains and their antibiotic resistant isogenic transformants.

4. DISCRIMINATION BETWEEN BACTERIAL SPECIES AND STRAINS USING RAMAN SPECTROSCOPY

5. DISCRIMINATION BETWEEN SUS-
CEPTIBLE STRAINS AND ISOGENIC
TRANSFORMANTS EXPRESSING AN-
TIBIOTIC RESISTANCE USING RAMAN
SPECTROSCOPY

5.1. Introduction

Antibiotic resistance is one of the major concerns associated with the treatment of infectious diseases today (Costelloe et al., 2010). It is responsible for increased mortality and morbidity among hospitalised patients as well as an increased healthcare burden (Carmeli et al., 1999) Common causes of antibiotic resistance are; the inappropriate use of antibiotics by over prescribing (Costelloe et al., 2010), use of sub-therapeutic amounts of antibiotics for growth promotion in animals, dusting of fruit for disease prophylaxis (Davies & Davies, 2010; Levy & Marshall, 2004).

Antibiotic resistance can be intrinsic (natural) (Yoneyama & Katsumata, 2006) or acquired through horizontal gene transfer (Stokes & Gillings, 2011) by mobile genetic elements including bacteriophages, plasmids, naked DNA and transposons (Sidjabat et al., 2006) or through sequential mutations in chromosomes (Levy & Marshall, 2004) (Giedraitien et al., 2011).

Antimicrobial susceptibility testing is now an essential step in Clinical Microbiology (Woodford & Sundsfjord, 2005). Currently several tests are routinely used in hospital laboratories, and include; i) broth dilution tests based on determining MIC for overnight bacterial suspension in the presence of different concentration of antibiotics; ii) M.I.C. Evaluator strips - based on placing a ready-made strip with dried antibiotic concentration gradient on an agar medium that has been inoculated with a standardised organism suspension; iii) disk diffusion test - based on placing antibiotic disks on an agar plate inoculated with bacterial suspension and measuring the growth inhibition zones around each of the disks; iv) automated instrumental systems, including: the MicroScan WalkAway that can analyse large numbers of microdilution trays in the set time, using photometric or fluorometric method for growth determination, the BD Phoenix Automated Microbiology System based on turbidometric and colorimetric growth detection of manually inoculated antibiotic doubling dilutions, the Vitek 1/2 System using plastic reagent cards with microliter quantities of antibiotic and test media monitoring growth defined incubation periods, the Sensititre ARIS 2X including standard microdilution plates on which growth is determined overnight by fluorescence measurements. Each of these automated systems relies on computer software for processing results. The strengths and weaknesses of these methods have been discussed, however the key factors influencing the success of an antimicrobial susceptibility test include: speed, accuracy and money efficiency (Jorgensen & Ferraro, 2009) (Richardson & Small, 1998)

To date relatively few studies have investigated the potential of Raman spectroscopy for antimicrobial susceptibility testing. They have used UVRR, portable Raman systems, micro-Raman and SERS approaches for screening responses to antibiotic treatment in *P. aeruginosa*, *E. coli*, *Klebsiella pneumonia*, *Proteus* spp., *S. aureus*, *C. jejuni* and Methicillin Resistant Coagulase Negative *Staphylococci* (López-Díez et al., 2005) (Neugebauer & Schmid, 2006) (Kastanos et al., 2008) (Liu et al., 2009) (Hadjigeorgiou, 2009) (Moritz et al., 2010a) (Willemse-Erix et al., 2010)

This chapter has two major aims; 1) to compare isogenic strains of *E. coli* sensitive and resistant to antibiotics using Raman spectroscopy; 2) to describe real-time monitoring of bacterial responses to antibiotics using Raman spectroscopy. This chapter uses the techniques of the previous chapters and addresses aims by:

1. Generating and characterising isogenic strains of *E. coli* Top10 (wild-type) with defined resistance (Top 10^A and Top 10^K)
2. Comparison of the Raman spectra of *E. coli* Top10 (wild-type) with transformed isogenic strains carrying resistance genes to ampicillin and kanamycin
3. Monitoring real-time responses of antibiotic through:
 - a. Flooding bacterial colonies with antibiotic solution
 - b. Transfer of bacterial colonies onto antibiotic containing plates

5.2. Methods

5.2.1. Transformation with electroporation

E. coli Top10 was transformed by electroporation with: a) pUC19 plasmid, carrying resistance to ampicillin and b) pET-26 plasmid, carrying resistance to kanamycin. Transformed bacteria grown and stored without antibiotics were referred to as Top10^{A/K} (for ampicillin/kanamycin respectively) and those grown and stored with antibiotics referred to as Top10^{AA/KK} (for ampicillin/kanamycin respectively). The details of the method of generating antibiotic resistant strains are described in Section 2.2.3.

5.2.2. Gel electrophoresis with restriction enzymes

The plasmid DNA was extracted using the PureYield Miniprep kit from transformed strains according to Section 2.2.6 and was subjected to restriction digestion and gel electrophoresis as described in Section 2.2.7 and 2.2.7.1 respectively.

5.2.3. Determination of Minimal Inhibitory Concentration (MIC)

MICs were determined using the limiting dilution method performed on a 96 well plate described in Section 2.2.4.

5.2.4. Temporal response to the action of antibiotics

Temporal responses of *E. coli* Top10, Top 10^A and Top 10^K to ampicillin and kanamycin respectively were determined as described previously in Section 2.2.5.

5.2.5. API 20E[®]

K12, Top10 and Top10^A were subjected to the API 20E test described in Section 2.2.8.

5.2.6. Quantification of *E. coli* viability using fluorescent microscopy

E. coli K12 were subjected to two viability assays described in Section 2.2.2.1 and 2.2.2.2 prior to examining them with confocal fluorescent microscopy.

5.2.7. Raman spectroscopy measurement

Transformed strains were subjected to Raman spectroscopy according to the conditions introduced in Section 2.2.9 and detailed in Chapter 3. Resistant strains were examined under three conditions; 1) grown, stored and measured in the absence of antibiotics referred to as Top10^A or Top10^K (for ampicillin or kanamycin resistant strains respectively) 2) grown and stored in the presence of antibiotics but measured in the absence of antibiotics and referred to as Top10^{AA} or Top10^{KK} (for ampicillin or kanamycin resistant strains respectively) and 3) grown, stored and measured in the presence of antibiotics and referred to as Top10^{AA}+Amp and Top10^{KK}+Kan (for ampicillin or kanamycin resistant strains respectively). The colonies in conditions 1) and 2) were measured on regular CBA plates, while the samples assigned to be tested in condition 3) were plated and measured on CBA plates containing ampicillin (100µg/ml) or kanamycin (50µg/ml).

5.2.8. Modifications of the standard Raman spectroscopy procedures

5.2.8.1. Whole plate flooding

Prior to the Raman measurement, 2ml of ampicillin (100µg/ml) was added onto the surface of agar plates containing *E. coli* Top10 colonies, and placed on a rocking platform until the solution absorbed or left for 3, 4, 6 hour treatment. The control sample was prepared using distilled water.

5.2.8.2. Single colony antibiotic flooding

Prior to the Raman measurement, 1µl of ampicillin (100µg/ml or 1mg/ml) was added directly onto the surface of single colonies of *E. coli* Top10 and then incubated at room temperature for 1, 3, or 17 hours.

5.2.8.3. Replica plating (Lederberg & Lederberg, 1952)

Top10 colonies were grown on two antibiotic-free plates (1 and 2) prior to transferring to the new plates using a sterile replica stamp. The colonies from plate 1 were transferred to a 1RA plate - a replica plate containing Ampicillin in the medium, while colonies from plate 2 were transferred to plate 2RN - a replica plate that was antibiotic free and used

as control (Figure 5.1). Stamped replica plates were incubated for an additional 24 hours and then subjected to Raman spectroscopy procedures.

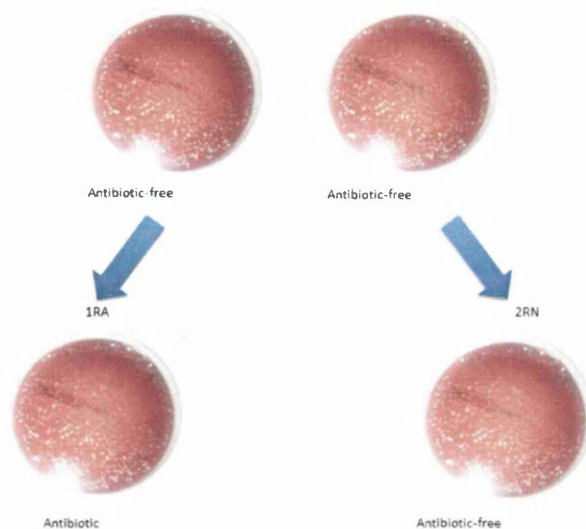


Figure 5.1.: Schematic representation of the replica plating method

5.2.8.4. Use of semi-permeable membranes

In order to select the most appropriate membrane, cellophane, immobylon, MCE, nitrocellulose, nylon, PES and PTFE were subjected to Raman spectroscopy alone, without colonies. The measurements (of N=6 for each: immobylon, MCE, nitrocellulose, nylon, PES and PTFE and N=9 for cellophane) were taken with standard settings directing the laser beam onto the membrane placed on a standard CBA plate. Colonies of *E. coli* Top10 were grown on semi-permeable membranes for 24h, after which the membrane was removed and cut in half. Then one part was transferred to a fresh plate containing antibiotic and other to a control plate with no antibiotic (Figure 5.2). Plates were incubated for 24 hours at 37°C and then subjected to standard Raman spectroscopy procedures.

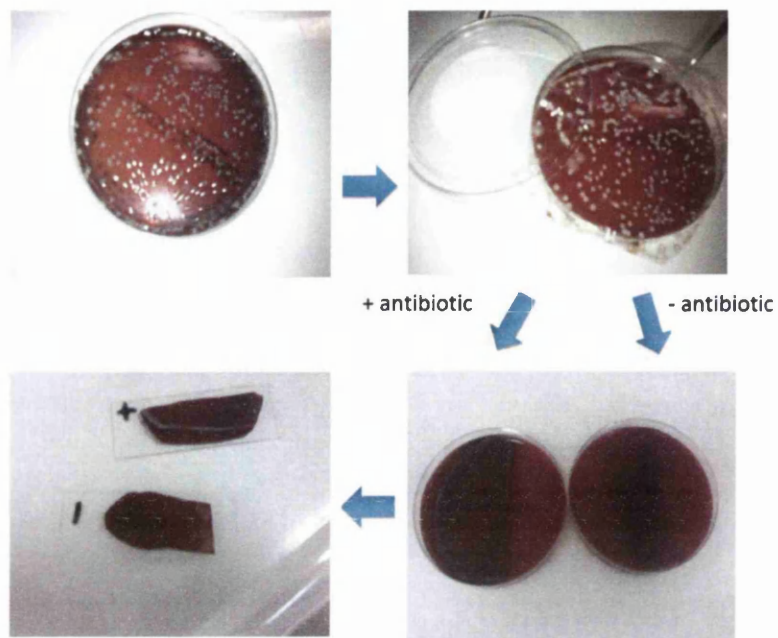


Figure 5.2.: Schematic representation of replication using membranes

5.3. Results

5.3.1. Generation of antibiotic resistant *E. coli* control strains

To characterise differences between antibiotic susceptible and resistant strains, positive controls expressing high levels of ampicillin (Top10^A) and kanamycin (Top10^K) resistance were generated. Gel electrophoresis of plasmid DNA isolated from the transformed Top10 cells and subjected to restriction enzymes revealed the presence of the band of the expected molecular weight: 2,686 bp for pUC-19 (Figure 5.3) and 5,360 bp for pET26 (Figure 5.4).

MIC for ampicillin against Top10wt was 32 µg/ml while it exceeded 1024 µg/ml for both Top10^A and Top10^{AA} indicating that the strains transformed with pUC-19 were resistant to the chosen antimicrobial agent (Table 5.1). The MIC for kanamycin against Top10wt was 64 µg/ml while it exceeded 1024 µg/ml for both Top10^K and Top10^{KK} indicating that the strains transformed with pET26 are resistant to the chosen antimicrobial agent whether it is present or not, suggesting that the plasmid is retained in the absence of antibiotic pressure (Table 5.2).

To further investigate the functional differences between susceptible and resistant strains, their temporal responses to antibiotics were studied (Figure 5.5). Decreased numbers of Top10wt were observed at 20-30 minutes following ampicillin treatment reaching significance at 120min when counts decreased from 2.28×10^{10} to 3.66×10^9 CFU/ml, while for kanamycin the numbers remained constant after 1 hour and were rapidly reduced after 2 hours from a starting concentration of 2.58×10^{10} to 2.00×10^9 CFU/ml. In contrast, antibiotic exposure did not decrease Top10^A and Top10^K viability. Furthermore, wild-type and isogenic mutants showed significant growth when antibiotic was not used.

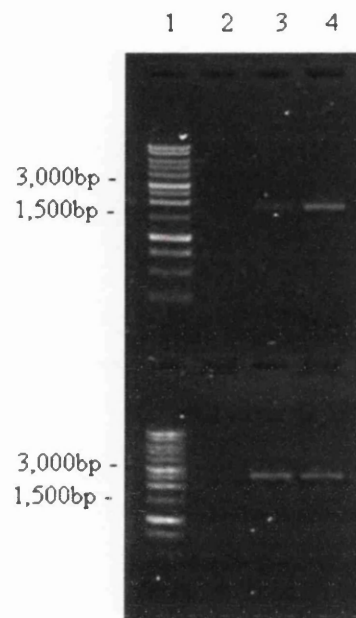


Figure 5.3.: Gel electrophoresis of plasmid DNA containing ampicillin resistance. Top gel contain uncut samples; 1-1kb ladder, 2-wild-type Top10, 3-Top10^A kept with no ampicillin, 4-Top10^{A.A} stored with 100 μg/ml ampicillin. Bottom gel contains samples cut with the XbaI restriction enzyme; 1-1kb ladder, 2-wild-type Top10, 3-Top10^A kept with no ampicillin, 4-Top10^{A.A} stored with 100 μg/ml ampicillin.

5. DISCRIMINATION BETWEEN SUSCEPTIBLE STRAINS AND ISOGENIC TRANSFORMANTS EXPRESSING ANTIBIOTIC RESISTANCE USING RAMAN SPECTROSCOPY

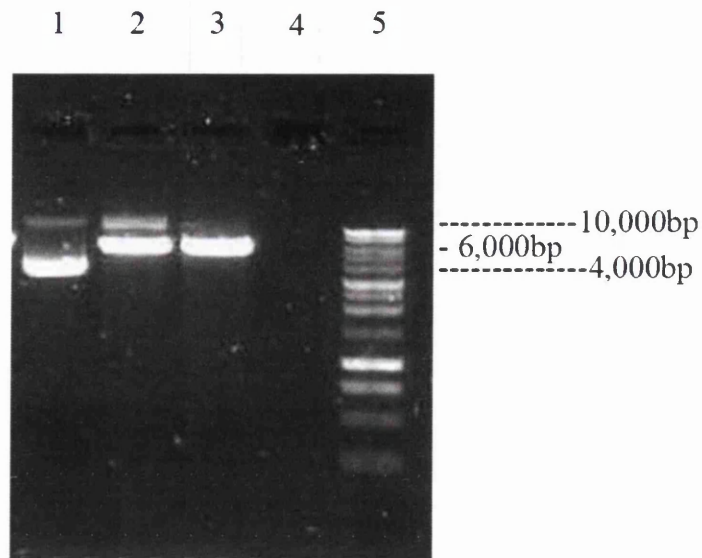


Figure 5.4.: Gel electrophoresis of plasmid DNA for three clones containing kanamycin resistance: 1-Top10^K uncut sample, 2- Top10^K cut with XhoI, 3- Top10^K cut with BamHI and 4- 1kb ladder.

Table 5.1.: Comparison of OD readings for untransformed Top10 with Top10^A and Top10^{AA} based on the results obtained from the plate-reader.

Dose of Amp [$\mu\text{g/ml}$]	Bacterial strain		
	Top10wt (n=11)	Top10 ^A (n=10)	Top10 ^{AA} (n=19)
1024	0.018	0.272	0.414
512	0.050	0.137	0.343
256	0.038	0.195	0.388
128	0.026	0.208	0.395
64	0.089	0.262	0.389
32	0.122	0.271	0.394
16	0.254	0.365	0.389
8	0.294	0.377	0.388
4	0.350	0.430	0.379
2	0.459	0.499	0.399
1	0.540	0.558	0.387
0	0.654	0.603	0.400

MIC indicated by the cyan line

5. DISCRIMINATION BETWEEN SUSCEPTIBLE STRAINS AND ISOGENIC
TRANSFORMANTS EXPRESSING ANTIBIOTIC RESISTANCE USING RAMAN
SPECTROSCOPY

Table 5.2.: Comparison of OD readings for untransformed Top10 with Top10^K and Top10^{KK} based on the results obtained from the plate-reader.

Dose of Kan [$\mu\text{g/ml}$]	Bacterial strain		
	Top10wt (n=12)	Top10 ^K (n=8)	Top10 ^{KK} (n=12)
1024	0.062	0.520	0.554
512	0.097	0.616	0.532
256	0.070	0.294	0.557
128	0.120	0.520	0.381
64	0.109	0.598	0.520
32	0.218	0.561	0.512
16	0.271	0.588	0.520
8	0.371	0.309	0.505
4	0.445	0.602	0.528
2	0.481	0.615	0.549
1	0.530	0.638	0.549
0	0.642	0.687	0.636

MIC indicated by the cyan line

5. DISCRIMINATION BETWEEN SUSCEPTIBLE STRAINS AND ISOGENIC TRANSFORMANTS EXPRESSING ANTIBIOTIC RESISTANCE USING RAMAN SPECTROSCOPY

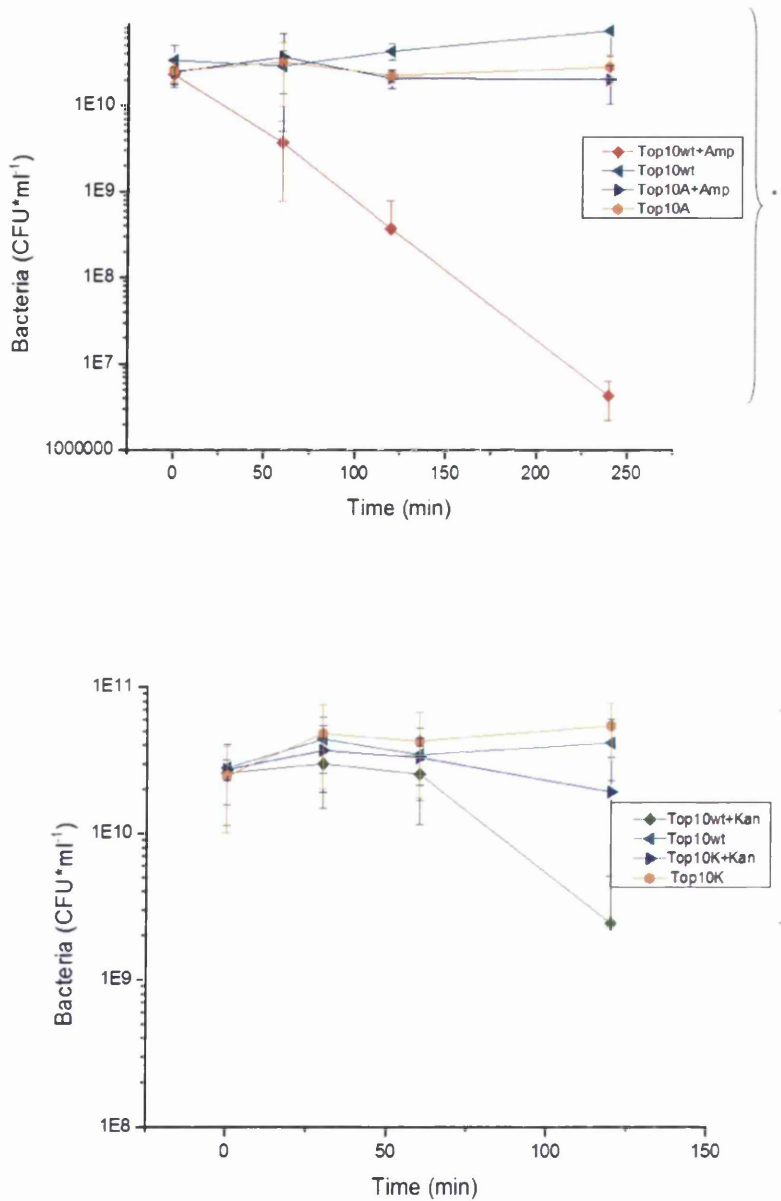


Figure 5.5.: Graph comparing the growth of bacteria after adding ampicillin (top) and kanamycin (bottom) in transformed and wild-type strains. There is a significant difference at 0.05 (*P=0.05) level between both transformants and wild type strains when subjected to antibiotic at the final time point (t=240 and t=120 min for ampicillin and kanamycin resistant transformants respectively). Both graphs are based on n=3 repeated experiments.

5.3.2. API 20E®

Identification using API 20E® was performed in order to verify that the transformed isogenic strain was not contaminated.

The results obtained directly from the test strips were: K12 - 5044552; Top10 - 4044550; Top10^A - 5044500 and after inserting them into the database, they all shared identity with *E. coli* of 99.8%; 51%; 97.3% respectively. Results for K12 and Top10^A were as expected, however the percentage for untransformed Top10 was considered low and warranted further investigation. After closer inspection the main reason for the difference was the first reaction: ONPG, which is catalysed by β -glucosidase and produced by the bacterial lac Operon. This gene sequence is normally present in *E. coli* and therefore can be found in K12 strains. Top10 however is strain a commercially prepared for transformation and for easier monitoring of the success of genetic manipulation, the lac Operon has been knocked out. Top10^A has a positive indicator for ONPG reaction since the lac Operon is present on pUC-19 plasmid, therefore, this experiment proves that similarity to *E. coli* is maintained and additionally exhibits that transformation with pUC-19 was successful and that the plasmid is expressed in Top10^A.

5.3.3. Comparison of Raman spectra from resistant and susceptible control strains

Raman spectra from CBA and CBA with ampicillin (100 μ g/ml) but without bacteria cluster together and overlap, suggesting that background signals from the agar and ampicillin are unlikely to contribute to discrimination between resistant and susceptible *E. coli* strains (Figure 5.6).

5. DISCRIMINATION BETWEEN SUSCEPTIBLE STRAINS AND ISOGENIC TRANSFORMANTS EXPRESSING ANTIBIOTIC RESISTANCE USING RAMAN SPECTROSCOPY

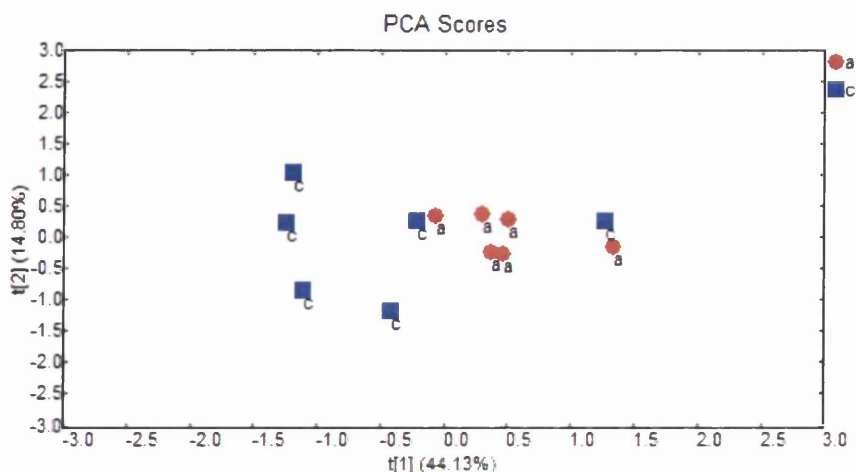


Figure 5.6.: Principal component analysis plot representing 6 single sample repeats from each: CBA (blue square) and CBA containing ampicillin (red circle).

Figures 5.3- 5.3 - show the comparison between antibiotic resistant and wild-type strains. The PCA analysis as well as the number of peaks from the signal subtractions confirms that in both case: ampicillin resistant and kanamycin resistant *E. coli*, there is a higher difference between the wild type strain and the transformant kept when the resistant strain was kept under the antibiotic pressure.

The identification of peaks responsible for the differences between the isogenic pairs allowed concluding what molecules are related to the antibiotic resistance when measured with Raman spectroscopy. The majority of signal is related to DNA and RNA as well as protein and amino acid components. With the increasing difference between the strains, there is more signal related to fats and fatty acids present.

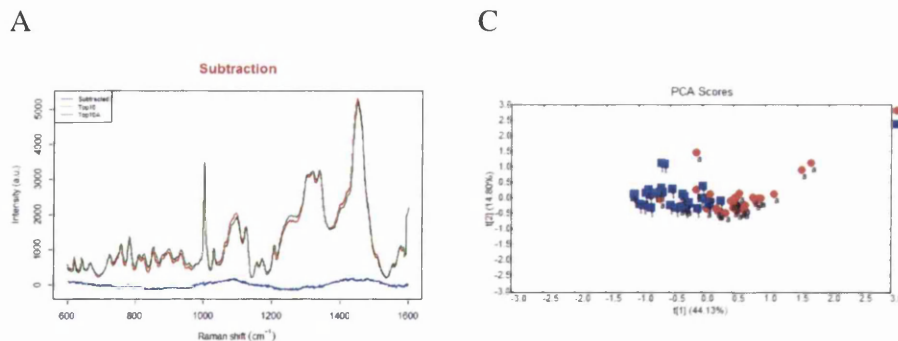


Figure 5.7.: The comparison of Top10 and Top10^A : (A) plot of the means of all four whole experimental repeats (4 sets of 30 spectra) for each strain and a subtraction of these means; (B) the list or Raman peaks showing the most significant differences between the two organisms; (C) PCA comparing two single experiments; (D) table of t-test results comparing PC scores for each whole experimental repeats.

B

Raman shift (cm^{-1})	Compound/molecule
755	Phosphophenylopyruvate, L-Tryptophan
780	Citidine, Uracil, Cytosine, Uracil ring stretching, Phosphophenylopyruvate, DNA, Phosphodiester, O-P-O stretching
840	L-Tryptophan, 12-methyl-tetradecanoic acid
944	Amylose
1260	15-Methylopalmitic acid, D(-) Arabinose, Lactose, D-(+)-Trehalose, Malic Acid
1440	Methylhexadecanoic acid, Oleic acid, Triolein, Trilinolein, Glycine, Stearic Acid, 12-Methyl-tetradecanoic acid, Trilinolenin, CH_2 scissoring, DNA, C-H bindings in lipids, Proteins, Carbohydrates, Bands of fatty acids, Deformation vibration CH_2 scissoring

D

Organism	Experiment number	T-test results value			
		PC1	PC2	PC3	PC4
	1	1.62E-06	5.30E-04	2.26E-01	4.03E-02
Top10wt vs.	2	4.44E-11	4.36E-01	4.45E-01	6.73E-01
Top10 ^A	3	9.74E-01	7.41E-01	6.56E-01	6.64E-02
	4	5.54E-01	1.50E-01	4.88E-01	2.49E-01

Figure 5.7.: (cont.) The comparison of Top10 and Top10^A: (A) plot of the means of all four whole experimental repeats (4 sets of 30 spectra) for each strain and a subtraction of these means; (B) the list of Raman peaks showing the most significant differences between the two organisms; (C) PCA comparing two single experiments; (D) table of t-test results comparing PC scores for each whole experimental repeats.

5. DISCRIMINATION BETWEEN SUSCEPTIBLE STRAINS AND ISOGENIC TRANSFORMANTS EXPRESSING ANTIBIOTIC RESISTANCE USING RAMAN SPECTROSCOPY

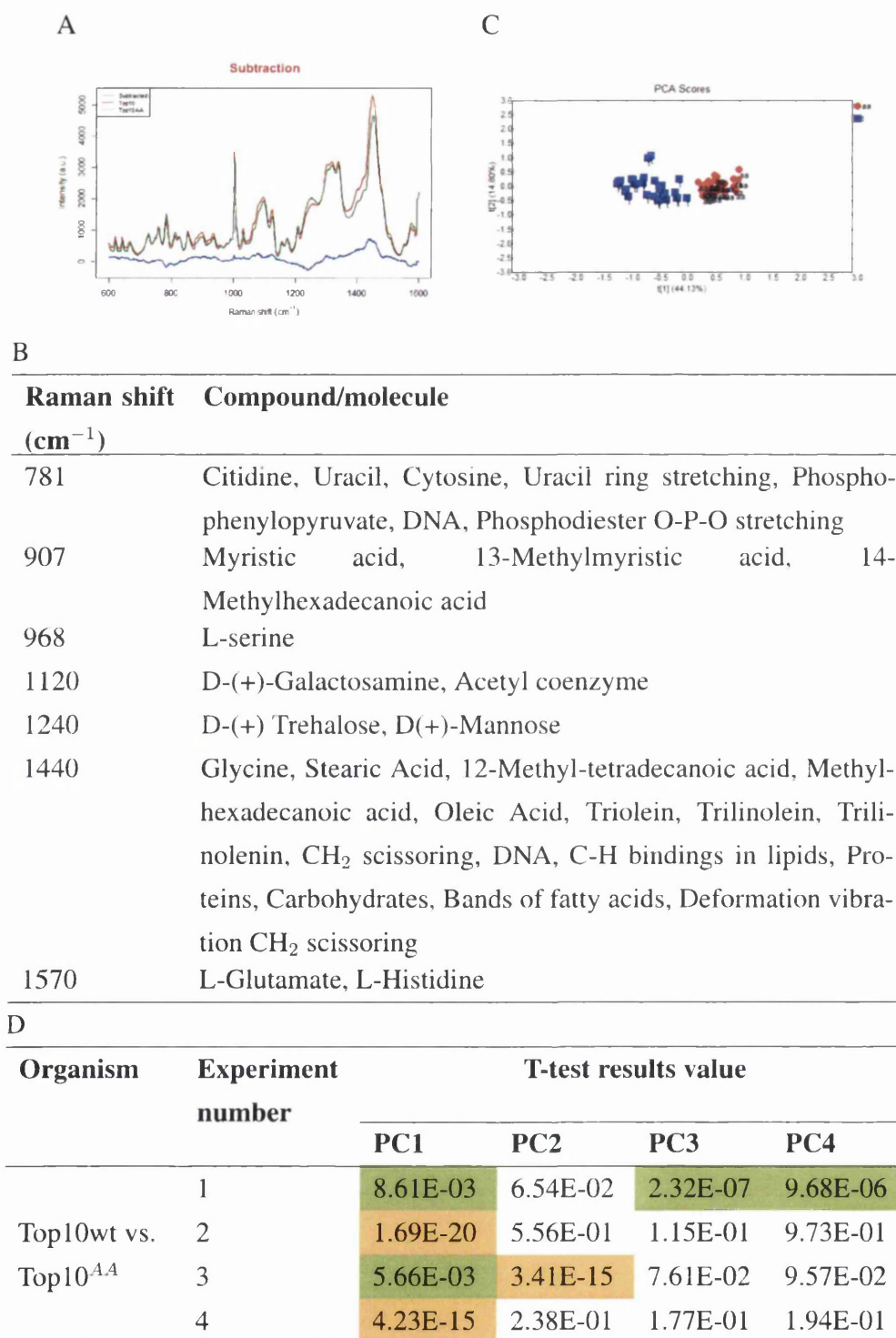


Figure 5.8.: The comparison of Top10 and Top10^{AA} : (A) plot of the means of all four whole experimental repeats (4 sets of 30 spectra) for each strain and a subtraction of these means; (B) the list of Raman peaks showing the most significant differences between the two organisms; (C) PCA comparing two single experiments; (D) table of t-test results comparing PC scores for each whole experimental repeats.

5. DISCRIMINATION BETWEEN SUSCEPTIBLE STRAINS AND ISOGENIC TRANSFORMANTS EXPRESSING ANTIBIOTIC RESISTANCE USING RAMAN SPECTROSCOPY

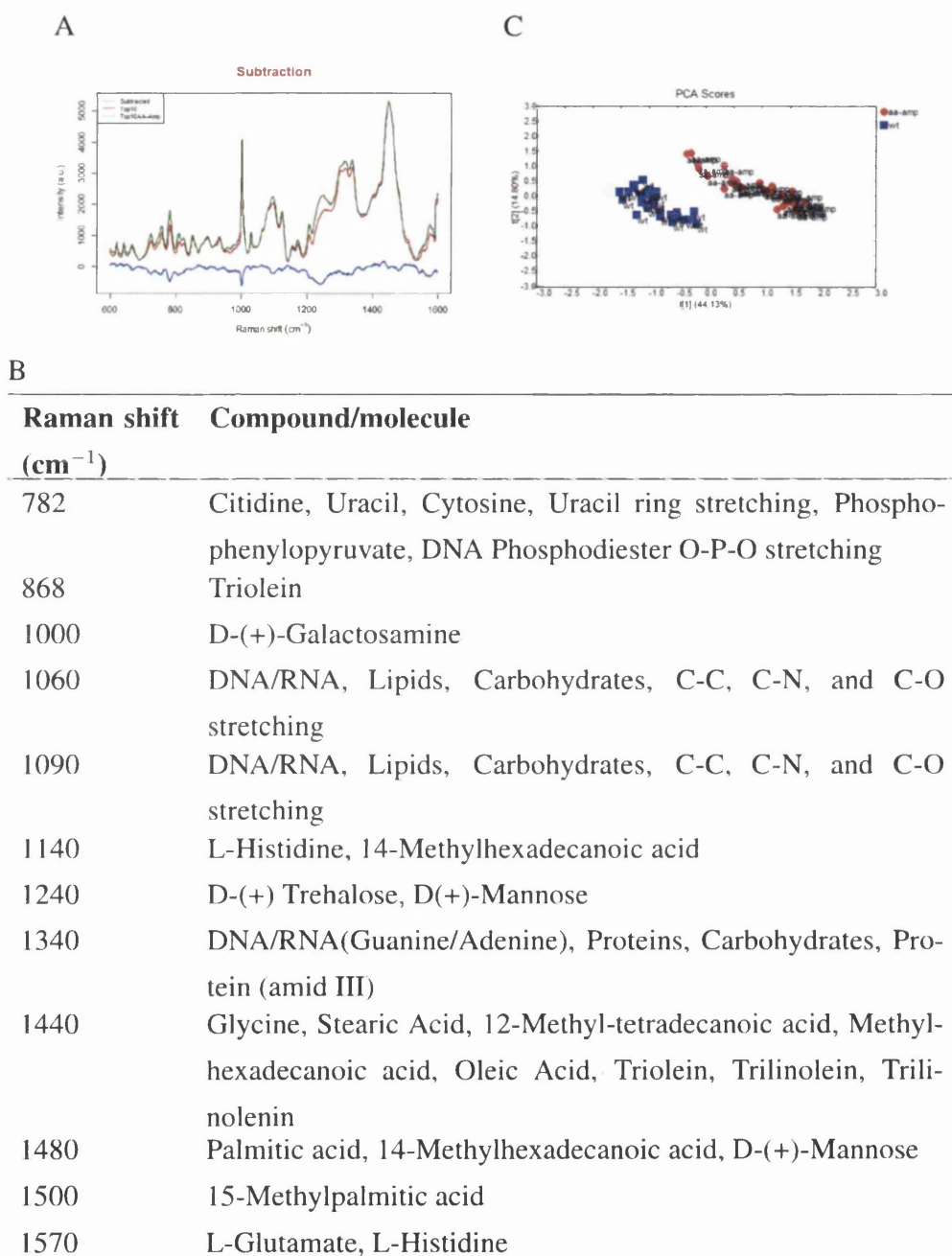


Figure 5.9.: The comparison of Top10 and Top10^{A-A} on ampicillin containing plate: (A) plot of the means of all four whole experimental repeats (4 sets of 30 spectra) for each strain and a subtraction of these means; (B) the list of Raman peaks showing the most significant differences between the two organisms; (C) PCA comparing two single experiments; (D) table of t-test results comparing PC scores for each whole experimental repeats.

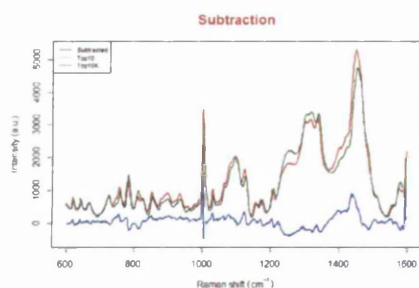
5. DISCRIMINATION BETWEEN SUSCEPTIBLE STRAINS AND ISOGENIC TRANSFORMANTS EXPRESSING ANTIBIOTIC RESISTANCE USING RAMAN SPECTROSCOPY

D

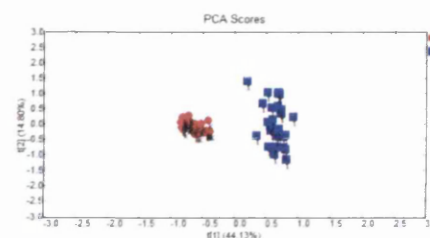
Organism	Experiment number	T-test results value			
		PC1	PC2	PC3	PC4
Top10wt vs. Top10 ^{AA}	1	5.25E-05	4.34E-07	1.50E-01	3.23E-01
	2	8.92E-05	1.44E-02	6.86E-01	1.38E-04
CBAmp	3	2.15E-01	3.18E-27	5.59E-01	5.93E-01
	4	1.18E-17	4.59E-04	8.04E-01	4.01E-01

Figure 5.9.: (cont.) The comparison of Top10 and Top10^{AA} on ampicillin containing plate: (A) plot of the means of all four whole experimental repeats (4 sets of 30 spectra) for each strain and a subtraction of these means; (B) the list of Raman peaks showing the most significant differences between the two organisms; (C) PCA comparing two single experiments; (D) table of t-test results comparing PC scores for each whole experimental repeats.

A



C



B

Raman shift (cm ⁻¹)	Compound/molecule
756	Phosphophenyloxyruvate, L-Tryptophan
784	Citidine, Uracil, Cytosine, Uracil ring stretching, Phosphophenyloxyruvate, DNA Phosphodiester O-P-O stretching
1000	D-(+)-Galactosamine
1070	D-Fructose-6-phosphate, DNA/RNA, Lipids, Carbohydrates, C-C stretching, C-N stretching, C-O stretching
1250	Cytosine, Amide III, N-H, C-N, L-Histidine, D-(+)-Fructose
1440	Glycine, Stearic Acid, 12-Methyl-tetradecanoic acid, Methyl-hexadecanoic acid, Oleic Acid, Triolein, Trilinolein, Trilinolenin
1480	Palmitic acid, 14-Methylhexadecanoic acid, D-(+)-Mannose

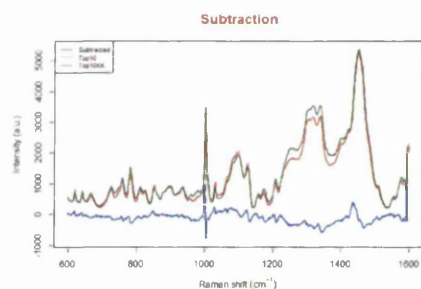
Figure 5.10.: The comparison of Top10 and Top10^K: (A) plot of the means of all four whole experimental repeats (4 sets of 30 spectra) for each strain and a subtraction of these means; (B) the list of Raman peaks showing the most significant differences between the two organisms; (C) PCA comparing two single experiments; (D) table of t-test results comparing PC scores for each whole experimental repeats.

D

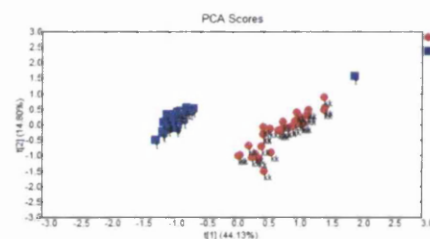
Organism	Experiment number	T-test results value			
		PC1	PC2	PC3	PC4
Top10wt vs.	1	1.60E-13	5.24E-04	3.49E-03	2.44E-01
	2	8.50E-19	1.18E-02	1.93E-02	7.35E-01
Top10 ^K	3	2.59E-12	1.06E-04	1.20E-01	1.55E-01
	4	6.60E-09	8.58E-01	3.16E-10	8.78E-01

Figure 5.10.: (cont.) The comparison of Top10 and Top10^K: (A) plot of the means of all four whole experimental repeats (4 sets of 30 spectra) for each strain and a subtraction of these means; (B) the list of Raman peaks showing the most significant differences between the two organisms; (C) PCA comparing two single experiments; (D) table of t-test results comparing PC scores for each whole experimental repeats.

A



C



B

Raman shift (cm ⁻¹)	Compound/molecule
784	Citidine, Uracil, Cytosine, Uracil ring stretching, Phosphophenylpyruvate, DNA, Phosphodiester O-P-O stretching
847	L-Tryptophan, 15-Methylpalmitic acid
999	D-(+)-Galactosamine
1130	CH ₂ deformation, =C-C= in unsaturated fatty acids in lipids
1350	Malic Acid, L-Valine, L-Proline
1440	Glycine, Stearic Acid, 12-Methyl-tetradecanoic acid, Methyl-hexadecanoic acid, Oleic Acid, Triolein, Trilinolein, Trilinolenin
1470	13-Methylmyristic acid, D-(+)-Trehalose, D-(-)-Fructose

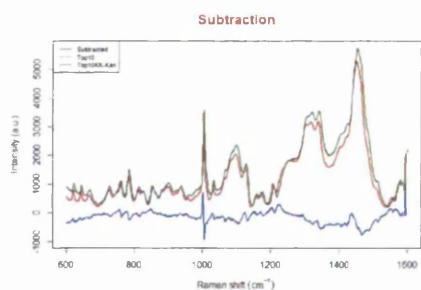
Figure 5.11.: The comparison of Top10 and Top10^K: (A) plot of the means of all four whole experimental repeats (4 sets of 30 spectra) for each strain and a subtraction of these means; (B) the list of Raman peaks showing the most significant differences between the two organisms; (C) PCA comparing two single experiments; (D) table of t-test results comparing PC scores for each whole experimental repeats.

D

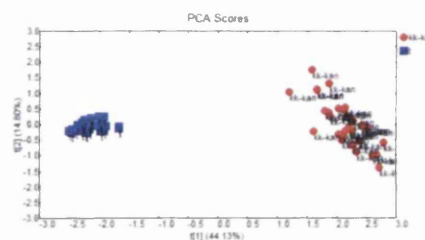
Organism	Experiment number	T-test results value			
		PC1	PC2	PC3	PC4
Top10wt vs. Top10 ^{KK}	1	3.17E-18	9.76E-04	4.90E-02	9.73E-01
	2	1.65E-16	2.93E-01	1.70E-02	6.13E-01
	3	4.59E-28	2.73E-02	8.69E-01	8.10E-01
	4	3.39E-19	7.64E-01	2.66E-03	3.98E-01

Figure 5.11.: (cont.) The comparison of Top10 and Top10^{KK}: (A) plot of the means of all four whole experimental repeats (4 sets of 30 spectra) for each strain and a subtraction of these means; (B) the list of Raman peaks showing the most significant differences between the two organisms; (C) PCA comparing two single experiments; (D) table of t-test results comparing PC scores for each whole experimental repeats.

A



C



B

Raman shift (cm ⁻¹)	Compound/molecule
754	L-Tryptophan
784	Citidine, Uracil, Cytosine, Uracil ring stretching, Phosphophenylpyruvate, DNA Phosphodiester O-P-O stretching
847	L-Tryptophan, 15-Methylpalmitic acid
900	L-Proline, Lactose, Amylose
999	D-(+)-Galactosamine
1110	L-Histidine, Glycerol
1230	Amide III, DNA/RNA (Thymine, Adenine), Proteins (Amide III), Lipids
1350	Malic acid, L-ValineL-Proline
1470	13-Methylmyristic acid, D-(+)-TrehaloseD-(-)-Fructose

Figure 5.12.: The comparison of Top10 and Top10^{KK} on kanamycin containing plate: (A) plot of the means of all four whole experimental repeats (4 sets of 30 spectra) for each strain and a subtraction of these means; (B) the list of Raman peaks showing the most significant differences between the two organisms; (C) PCA comparing two single experiments; (D) table of t-test results comparing PC scores for each whole experimental repeats.

D

Organism	Experiment number	T-test results value			
		PC1	PC2	PC3	PC4
Top10wt vs. Top10 ^{KK}	1	4.40E-03	1.20E-08	6.50E-08	7.98E-01
	2	3.37E-12	6.10E-01	1.98E-07	7.17E-01
CBA-Kan	3	1.49E-14	1.02E-05	7.17E-01	3.78E-01
	4	1.98E-43	5.07E-01	9.46E-01	6.49E-01

Figure 5.12.: (cont.) The comparison of Top10 and Top10^{KK} on kanamycin containing plate: (A) plot of the means of all four whole experimental repeats (4 sets of 30 spectra) for each strain and a subtraction of these means; (B) the list of Raman peaks showing the most significant differences between the two organisms; (C) PCA comparing two single experiments; (D) table of t-test results comparing PC scores for each whole experimental repeats.

5.3.4. Multiple strains comparison

To further identify the relationship between the wild type (Top10), ampicillin resistant (Top10^A, Top10^{AA} and Top10^{AA} + Amp), kanamycin resistant (Top10^K, Top10^{KK} and Top10^{KK} + Kan) strains the average spectra (4 experiments) were subjected to hierarchical cluster analysis with the results presented as a tree (Figure 5.13). Strain B and K12 were included as controls and confirmed the close relationship between Top10 or K12. Strains transformed with kanamycin resistance cluster together, with Top10^{KK} grown on Kan plates, placed on a different branch as it expresses the highest level of resistance to kanamycin. Top10^{AA} and Top10^{AA} + Amp cluster together with K12, while Top10^A clusters with Top10. Naturally Top10 does not contain the *lac* Operon, however transformants express from the plasmid, therefore isogenic strains become more similar to K12 rather than K12 after electroporation. Those results confirm conclusions drawn from the API E20[®] identification test were ampicillin strains cluster more closely with K12.

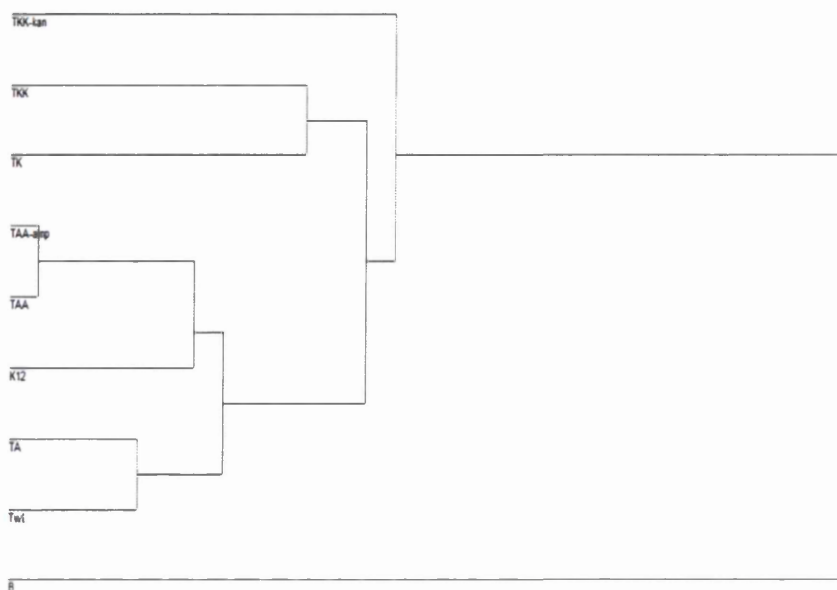


Figure 5.13.: Hierarchical analysis tree based on means from all the whole experimental repeats performed for: (A) Top10^{KK} grown on Kan plates (TKK-kan); (B) Top10^{KK} (TKK); (C) Top10^K (TK); (D) Top10^{AA} grown on Amp plates (TAA-amp); (E) Top10^{AA} (TAA); (F) K12 (K12); (G) Top10^A (TA); (H) Top10 (Twt); (I) strain B. Top10^{KK} grown on Kan plates (TKK-kan).

5.3.5. Real time monitoring of the bacterial response to antibiotics by Raman spectroscopy.

To extend the results of the previous sections showing that Raman spectroscopy can determine a resistant phenotype in strains of *E. coli*, we investigated whether the technique is also applicable to measuring bacterial responses to antibiotic treatment in real-time on bacterial colonies. Two methods of antibiotic exposure to bacterial colonies were investigated, namely ‘antibiotic flooding’ and replica-plating.

5.3.5.1. Antibiotic flooding

5.3.5.1.1 Applying antibiotic solution onto the whole plate containing bacterial colonies

Comparison of non-flooded, water flooded and antibiotic flooded colonies showed distinct clustering of the three groups (Figure 5.14a). Flooding colonies appeared to elongate clusters suggesting larger differences within treatment groups. Repeating the experiment (Figure 5.14b) however did not confirm these results and suggested that this method may

present inconsistencies.

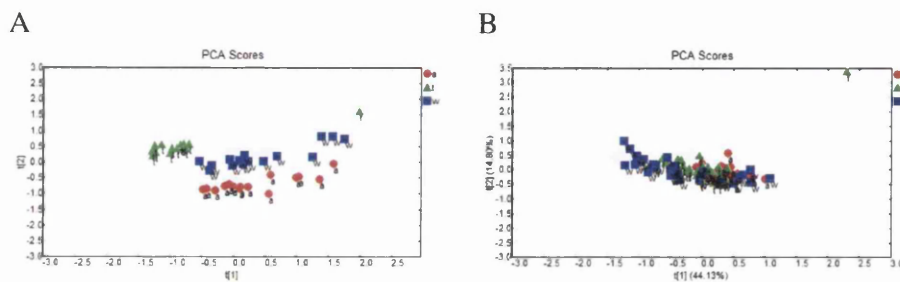


Figure 5.14.: Principal component analysis scores of Raman spectra from Top10wt colonies subjected to different solutions and repeated on two consecutive days: (A) day one; (B) day two; red circles: colonies flooded with 2ml of 100 μ g/ml ampicillin; blue squares: colonies flooded with 2ml distilled water; green triangles: not flooded sample.

Next the time of exposure to the action of antibiotic was investigated (Figure 5.15). There was no distinct PCA clustering between colonies exposed to antibiotic solution for 3h, 4h and 6h, suggesting that time has no influence on the rate of dying of the cells. Therefore a conclusion can be drawn that the portion of the colony, that is being measured by the Raman spectroscopy is affected by antibiotic in time less than 3h and additional time has no influence on it.

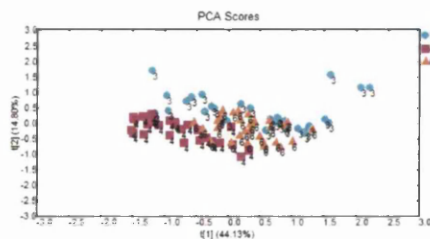


Figure 5.15.: Principal component analysis scores of Raman spectra from Top10 colonies subjected to 2ml of 100 μ g/ml ampicillin for different periods of time; cyan circle: 3 hours, magenta square: 4 hours, orange cross: 6 hours.

5.3.5.1.2 Applying antibiotic solution directly onto single bacterial colonies

Figure 5.16a. shows the initial experiment. There is a very distinct clustering separating the colonies with antibiotic solution from these with just water applied onto and the non-flooded samples. However, when the results were repeated with the same dose and exactly the same time of exposure, situation was similar as with the whole plate flooding experiment - there was much lower difference, especially between the antibiotic flooded sample and the non-flooded colonies (Figure 5.16b).

5. DISCRIMINATION BETWEEN SUSCEPTIBLE STRAINS AND ISOGENIC TRANSFORMANTS EXPRESSING ANTIBIOTIC RESISTANCE USING RAMAN SPECTROSCOPY

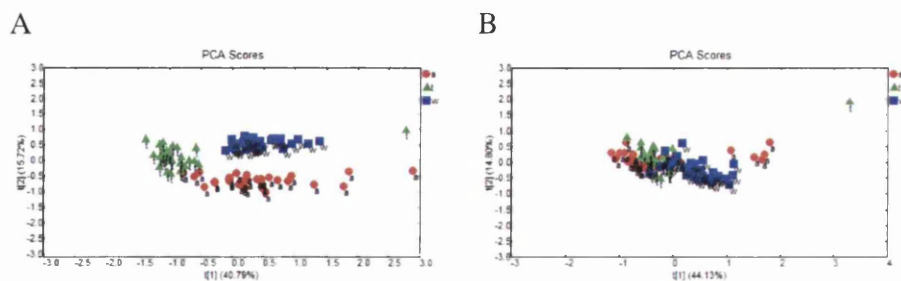


Figure 5.16.: Raman spectra from Top10wt colonies subjected for 3 hours to $1\mu\text{l}$ performed on two consecutive days: a) day one; b) day two. Red dot $100\mu\text{g/ml}$ ampicillin, blue square: distilled water, green triangle: colonies not flooded.

Figure 5.17a shows the same experiment performed with higher dose of antibiotic: $1000\mu\text{g/ml}$ in the same exposure time, i.e. 3 hours. The results, when compared to the Figure 5.16, show no effect due to the increased dose, there is no separation between neither antibiotic and water flooded sample, nor the non-flooded colonies. Figures 5.17b and 5.17c show the same dose of antibiotic ($1000\mu\text{l/ml}$) but applied left on the surface of bacterial colonies for 1 and 17 hours (respectively) prior to the Raman spectroscopy measurement. In both cases, the colonies flooded with water show very little difference from the ones flooded with antibiotic, while the non-flooded sample is separate. Only several spectra from the water-affected sample in the Figure 5.17b are closer to the non-flooded sample, however this is not representative enough to draw any positive conclusion about the effectiveness of this method.

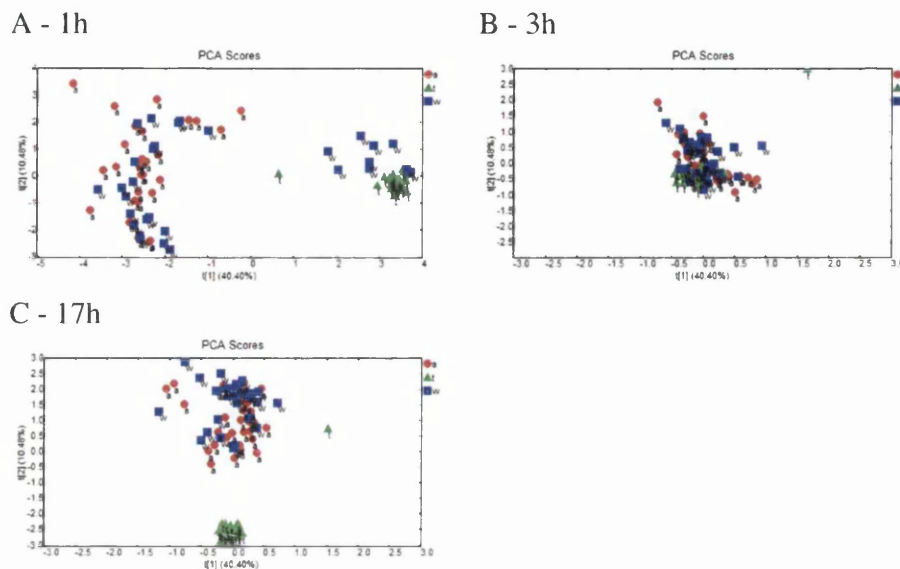


Figure 5.17.: Principal component analysis scores of Raman spectra from Top10wt colonies flooded with $1\mu\text{l}$ of $1000\mu\text{g/ml}$ of ampicillin for: (A)3 hours; (B)1 hour; (C) 17 hours. Red circle: ampicillin; blue square: water; green triangle: not flooded sample.

5.3.5.2. Transfer of colonies onto antibiotic containing media

An alternative method of monitoring the Raman signal from bacterial colonies following the application of antibiotics was developed by moving the live, fully grown colonies onto a substrate containing the antibiotic of interest.

5.3.5.2.1 Transfer using replica plating

After the comparison, PCA results in Figure 5.18 show that transferred samples grown without antibiotics clusters together with the colonies from the original plate (even though sample 2RN was grown from plate 2-not included in the PCA - and not plate 1), while the transferred samples grown on antibiotic containing plate make up a distant cluster. This demonstrates again that Raman spectroscopy can show the difference between samples that express antibiotic resistance and those that do not.

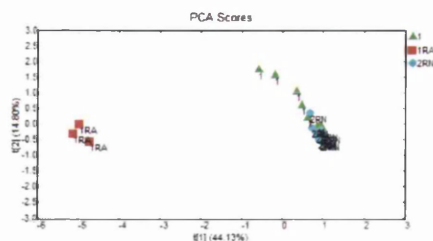


Figure 5.18.: Principal component analysis scores of Raman spectra from Top10^{4.4} plated on an original plate (green triangle) and moved to: 1RA - new plate containing antibiotic (red square); 2RN-control plate without antibiotic (cyan circle).

5.3.5.2.2 Transfer using membranes

Several different membrane types were tested (Table 2.3). Most of the membranes exhibit very strong Raman peaks, however PVDF was rejected as the first one since it caused full saturation, which most likely would not be quenched even with very thick colonies.

Figure 5.19 shows the clustering of the spectra from all the membranes placed on CBA (except for PVDF). All of them produce tight, distinct clusters, except for nylon and immobylon, which cluster together.

The growth of colonies was poorer on the membranes than without in all cases. However the two membranes, MEC and nitrocellulose, showed the best colonies and were investigated further.

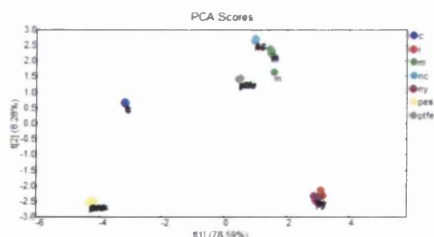


Figure 5.19.: Raman spectra (n=6) from the membranes on CBA plates: blue - cellophane; red - immobylon; green - MCE; cyan - nitrocellulose; purple - nylon; yellow - PES; grey - PTFE

The initial experiment was performed using MCE membrane in order to verify the influence of membrane signal on the experimental outcome. Figure 5.20 shows clear differences between spectra taken from colonies grown without membrane and the initial plate containing colonies grown with membrane. It is noteworthy that the spectra from MCE on CBA without bacteria are closer to the clusters from colonies on the membrane than to the colonies without membrane. This can have strong implications that the membrane

can obstruct the spectra in a meaningful way since its signal is included in the bacterial spectra.

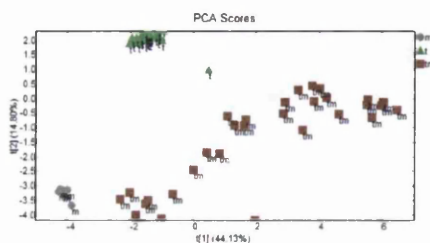


Figure 5.20.: Principal component analysis scores of: Top10wt plated on CBA plates containing MCE membrane (brown square); Top10wt plated on a CBA without the membrane (green triangle); membrane itself (grey circle).

Further experiment based on MCE membrane included comparing the spectra from original plate containing bacterial colonies grown on the membrane, which was then transferred onto an antibiotic containing plate and a control plate (according to Figure 5.2). The results from Figure 5.21 do not show any separation between the samples: spectra from the original plate cluster together with both transfer plates and none of them is tight, therefore exhibiting high variation and poor reproducibility of single sample repeats.

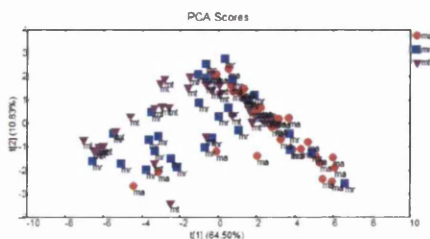


Figure 5.21.: Principal component analysis scores of Top10wt plated on CBA plates containing MCE membrane: purple triangle - the initial plate; red circle - moved onto antibiotic containing plate and measured after 24 hours; blue square - moved onto non-antibiotic containing plate and measured after 24 hours.

Figure 5.22 show the antibiotic dose influence on the growth of colonies on a nitrocellulose membrane. The results show difference between colonies transferred onto medium containing 500 or 1000 μ g/ml of ampicillin and those moved onto antibiotic free agar serving as control for each of the experiments. Colonies transferred onto 100 μ g/ml of ampicillin clustered closer to the colonies transferred onto the antibiotic free plate than those transferred on media containing. This suggested a clear dose response relationship.

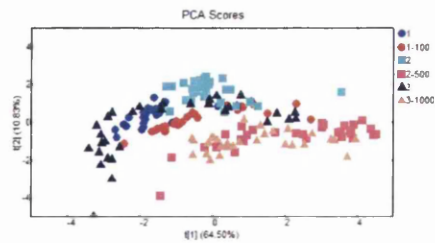


Figure 5.22.: Comparison of the influence of antibiotic dose on the CBA plates on the spectra of Top10wt grown on nitrocellulose membrane and moved onto the new plates. Red dot -100 μ g/ml of ampicillin, blue dot- control for this experiment; pink square- 500 μ g/ml ampicillin, cyan square - control for this experiment; orange triangle - 1000 μ g/ml ampicillin, navy triangle - control for this experiment.

5.4. Discussion

Antibiotic screening is an important stage of infectious-diseases diagnosis. In this chapter we have successfully created and described isogenic strains expressing resistance to two different antibiotics: ampicillin and kanamycin and compared them to the susceptible strains.

Our methods of preparation of isogenic transformants were similar to the protocol described by Walter et al. (Walter et al., 2011), therefore we have carefully investigated the functionality of the resistant strains as well as the antibiotic.

For both: pUC19 and pET-26 we were able to determine their presence in the *E. coli* through the agarose gel electrophoresis. In both cases it was essential to use the restriction enzyme, as uncut fragments were of lower molecular weight than expected, indicating that the DNA fragment might have been in a supercoiled configuration.

In order to describe the functionality of the plasmid within the transformants, MICs were calculated. There was no difference in the level of resistance between the strains harvested with- and without antibiotic neither for ampicillin, nor for kanamycin resistant strains and both were higher than for the un-transformed strains.

Resistant strains behaved in a different way to the susceptible Top10 when the temporal response to antibiotic was tested. No difference could be noticed in Top10^A upon addition of antibiotic and in control solution, whereas the susceptible strain counts dropped significantly. Top10^K on the other hand did show less resistance to the action of kanamycin in time, however it was not a significant decrease in numbers, while the susceptible Top10 lowered the CFU in a meaningful way. This clearly shows differences between the action of antibiotics, therefore it was significant to test at least the two different antimicrobials for Raman spectroscopic measurements.

We were able to determine that Raman spectroscopy recognises the differences between those controls and further analysis allowed to determine that these fluctuations in the signal come mainly from the DNA/RNA, proteins and lipids, therefore concluding that Raman spectroscopy recognises resistance profiles based on the genetic material and bacterial envelope.

The differences between the resistance to ampicillin and kanamycin were also noticed: there is more variation in terms of the amount of peaks, and value of PC scores results between the Top10^A, Top10^{AA} and Top10^{AA} measured on ampicillin medium than there is between respective strains transformed to express kanamycin resistance, which seem

slightly more stable and uniform. This may be caused by the ability of *E. coli* to lose the pUC-19 plasmid unless the ampicillin pressure is maintained, while pET-26 may be more persistent. This effect could be the reason for characteristic grouping in Figure 5.3 where strains exhibiting kanamycin resistance are set on one branch, separate from the susceptible strains. Top10^A however is very close to the untransformed strains while Top10^{AA} and Top10^{AA} measured on ampicillin medium are separated. This effect, to some extent may resemble the API E20 test, where wild-type Top10 was recognised as *E. coli* in much lower percentage than Top10^A. In case of the hierarchical tree it is possible that Top10 and Top10^A are less related to K12, which clusters closer to Top10^{AA} and Top10^{AA} measured on ampicillin medium most likely because of the tendency of Top10^A to dropping the plasmid and acting like untransformed Top10, i.e. not containing lac Operon, a fragment of DNA delivered in the plasmid, maintained in all other transformed strains as well as in K12. It is possible that Raman spectroscopy could recognise this subtle change.

Real-time monitoring of responses to antibiotic actions were performed including antibiotic flooding and transfer of bacterial colonies onto the antibiotic-free and antibiotic-containing media. The reasoning behind this strategy was based on the fact that antibiotic flooding could serve as a simple way of the real-time monitoring of responses to antibacterial agent and could assist in differentiating between the resistant and susceptible strains. Unfortunately whole-plate flooding did effect in washing off a large portion of colonies, while the point-flooding was more tedious and time consuming, which would not be a welcome quality for a potential new diagnostic technique. In addition it was difficult to describe the most appropriate time of antibiotic exposure and dose; even though the time needed for ampicillin action against Top10 was proven to be less than 30 minutes and MIC to be equal to 32 µg/ml, our standard procedure for Raman spectroscopy involved screening colonies, in which case the dose and time of antibiotic penetration were difficult to determine. Therefore; neither, the whole-flooding, nor the point-flooding were applicable, since they did not prove successful in determining the differences between the live and dead cells, or sufficient reproducibility.

Replica plating was used as a very simple method of transferring colonies onto a fresh petri plate with or without antibiotics. Transferred colonies serve as precursors for the new colonies that grow overnight enough to be able to give decent Raman spectra, however they cannot be viewed instantly due to insufficient thickness resulting in too much background signal from the underlying agar. Therefore additional time for growth was

required. However, even after allowing 24h more, poorer quality colonies were grown resulting in a very limited number of spectra.

Semi-permeable membranes were investigated for their ability to transfer bacterial colonies to an antibiotic containing media. To be functional, the membrane should allow diffusion of the nutrients from the substrate, including the antibiotic, to the bacteria. Thus colonies were subjected to the action of the antimicrobial factor after moving to the new plate. The success of this technique involved correctly identified correlation of the response to the dose of antibiotic used and separation between affected and control strain, therefore this approach might potentially be used for monitoring of the real-time antibiotic action however; care should be taken to choose a correct membrane and dose of antibiotic. More time would be required to investigate this approach in full.

Techniques based on the need for bacterial replication raised many concerns and showed limited success while also exhibiting the disadvantage, of increasing the time necessary for the colonies to grow after transfer to a new plate. This would extend the time of diagnosis to at least 48 hours which would be undesirable for clinical application.

Work performed by other research teams and published in this subject to-date varies to a high degree. Most of the projects have focused mainly on monitoring the bacterial response to antibiotics in susceptible strains but without comparing them with the resistant organisms (Hadjigeorgiou, 2009; Lin et al., 2012; Liu et al., 2009; López-Díez et al., 2005; Moritz et al., 2010a; Neugebauer & Schmid, 2006; Willemsse-Erix et al., 2010) did test the resistant strains, however it has not been directly compared with the susceptible strains. The most comprehensive study was published by Walter et al. (Walter et al., 2011) presenting methods similar to ours in terms of generating resistant strains while comparing them to untransformed bacteria. Despite using different strain of *E. coli* transformed with different plasmid than investigated by us, results discussed in the publications are in agreement with findings presented in this chapter also addressing the problem of lowering content of plasmid in ampicillin non-challenged cultures. There is also a similarity in the spectral peaks that were identified as responsible for the separation, which were assigned to DNA/RNA.

It was difficult to compare findings when different Raman enhancements (López-Díez et al., 2005; Neugebauer & Schmid, 2006) than the ones used by us in this chapter and therefore consult the Raman shifts identified since the different wavelengths and excitations were used.

To our best knowledge, there were no attempts for utilising neither antibiotic flooding

nor replication techniques in the Raman spectroscopy based literature, which is still very limited in terms of antibiotic resistance studies.

We conclude that based on our findings and some of the suggestions from the research published to-date, the fastest and most efficient approach would be creating a universal library of microorganisms including all the possible antibiotic-resistant samples that could serve as reference for comparison with any hospital sample tested with Raman spectroscopy. With the use of properly designed software this step should be fast and easy delivering much needed result.

In Chapter 6 we applied our methods to a set of archived clinical samples of *E. coli* expressing extended-spectrum beta-lactamases. Raman spectroscopy was investigated for its ability to distinguish between the subtle differences exhibited by different antibiotic resistance profiles as well as for assigning the organisms to the determined phylogenetic groups.

6. CHARACTERISATION OF CLINICAL ISOLATES OF *Escherichia coli* EXPRESSING EXTENDED SPECTRUM β -LACTAMASES, USING RAMAN SPECTROSCOPY

6.1. Introduction

Multiresistance in bacteria is becoming a key issue, influencing administration and limiting the options of the correct treatment strategies.

Escherichia coli strains have been reported to emerge with the ability to produce extended spectrum β -lactamases (ESBLs). Over 75 ESBLs present in gram negative bacteria are able to inactivate many currently available advanced-generation cephalosporins and penicillins that were promised to be the safest and the most affective antibiotics.

TEM-1 and SHV-1 are the most common β -lactamases found in enteric bacilli (Bonomo, 2000) and most ESBLs emerged from TEM and SHV enzymes (Woodford et al., 2004) but CTX-M enzymes are becoming more important. Among the family of >110 ESBLs, CTX-M-15 and CTX-M-14 are the most common CTX-Ms (Woodford et al., 2011).

The occurrence of CTX-M producers can cause serious public health implications mainly related to designing an appropriate therapy (Woodford et al., 2004).

In the previous chapters it has been proven that Raman spectroscopy can identify between bacterial organisms and is able to successfully differentiate between isogenic mutants obtained in our laboratory and wild type reference strains.

To assess the abilities of Raman spectroscopy to become a diagnostic technique useful in the hospital laboratories its capability of recognising hospital isolates has been included in this chapter. In addition, taking into account the growing problem of antibiotic resistance and emergence of multiresistant strains, the organisms that were used in this part of the project were confirmed to express extended spectrum β -lactamases.

6.2. Methods

6.2.1. Polymerase Chain Reaction

PCR was performed according to Section 2.2.6 and the results were obtained from agarose gel electrophoresis described in Section 2.2.7.

6.2.2. Phylogenetic classification

Phylogenetic classification has been performed according to (Clermont et al., 2000) using the results from Polymerase Chain Reaction revealed after agarose gel electrophoresis. In cases where no strains were present, strains were marked as 'NO' and not classified as belonging to any of the phylogenetic groups. In cases when the results were inconclusive, the experiments were repeated.

6.2.3. Raman spectroscopy measurements

ESBL expressing clinical isolates were subjected to procedures described in Chapter 3. At least 15 single sample repeats were taken for each strain. The PCA was performed using the mean result for intensities from the single sample repeat for each strain and arranged according to the resistance group the strain belonged to (Table 2.12)

6.3. Results

6.3.1. Polymerase Chain Reaction

In order to classify the clinical isolates into phylogenetic groups, each of them was subjected to the triplex PCR using ChuA.1, ChuA.2, YjaA.1, YjaA.2, YjaA.2, YjaA.2, TspE4C2.1, TspE4C2.2 primers.

Phylogenetic group A was confirmed by the presence of YjaA band at 211kbp; group B1 was confirmed by the presence of TspE4C2 band at 159kpb; group B2 was confirmed by the presence of either two bands for both: ChuA and YjaA at 279 and 211kpb or by all three bands representing each gene, while group D was confirmed by the presence of ChuA band at 279kpb alone or together with TspE4C2 at 152kpb.

The verification of the method was performed using standard strains for each phylogenetic group (Figure 6.1). The standards for group A were K12 and Top10, for group B1 was ECOR33, for group B2 was strain B and ECOR59, for group D was ECOR50. All these groups were recognised correctly.

The comparison off all the strains, including their resistance group and number of strains in every phylogenetic group can be seen in Figure 6.2.

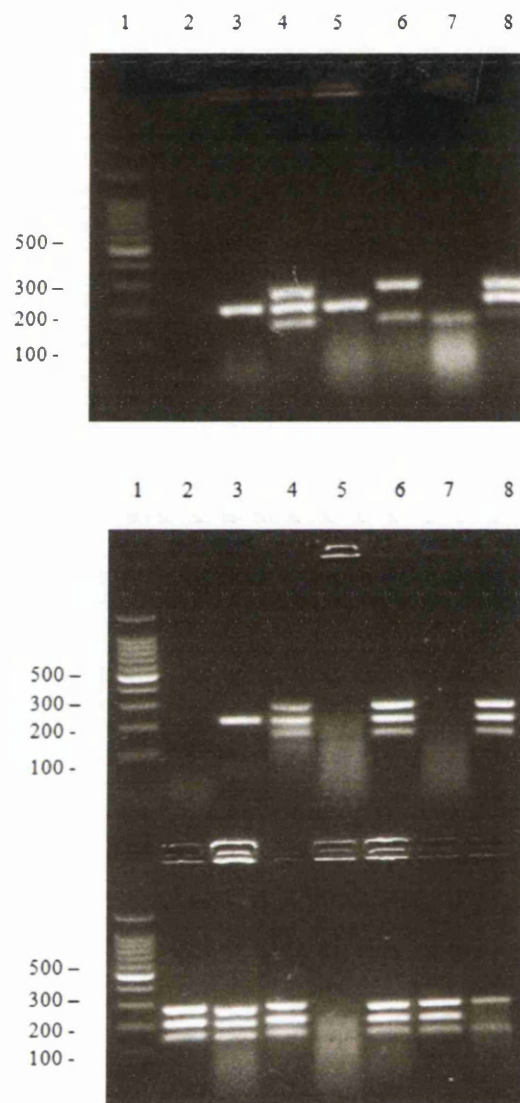


Figure 6.1.: The results of triplex PCR; a) 1: 100kb molecular marker, 2: empty, 3: Top10, 4: StrainB, 5: K12, 6: ECOR50 (standard for phylogenetic group D), 7: ECOR33 (standard for phylogenetic group B1), 8: ECOR59 (standard for phylogenetic group B2); b) strains from different groups

6. CHARACTERISATION OF CLINICAL ISOLATES OF *ESCHERICHIA COLI* EXPRESSING EXTENDED SPECTRUM β -LACTAMASES, USING RAMAN SPECTROSCOPY

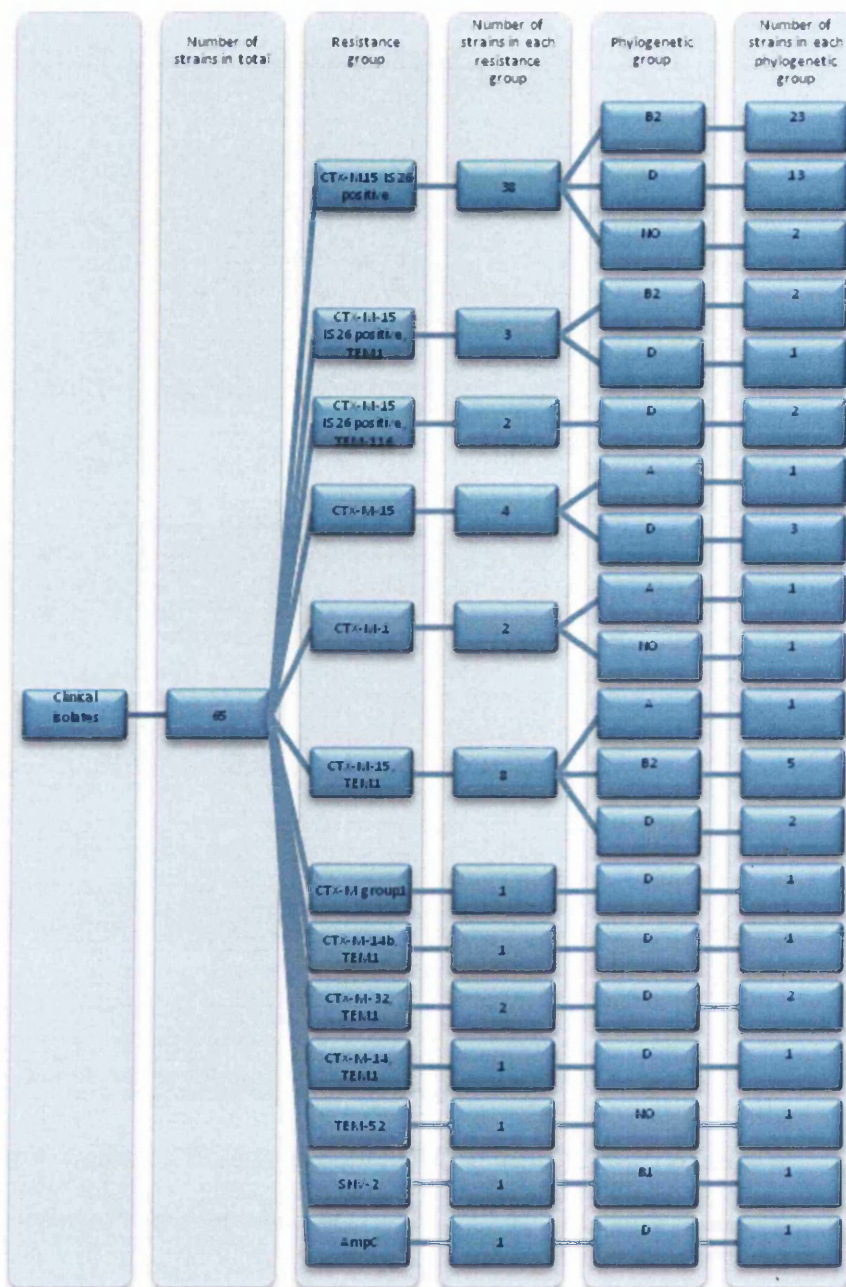


Figure 6.2.: The collection of clinical isolates expressing ESBLs with phylogenetic groups assigned to them.

6.3.2. Raman spectroscopy

All ESBL strains from the collection of clinical isolates have been tested with Raman spectroscopy. Figures 6.3 and 6.4 represent the groups with the highest number of strains:

CTX-M15, TEM-1 and CTX-M15 IS 26 positive respectively.

Figure 6.3 clearly shows that spectra within the CTX-M15, TEM-1 cluster according to their phylogenetic groups. The phylogenetic tree confirms the result presented that there is a closer relation between the strains from B2 and A group than between group D.

Strains within CTX-M15 IS 26 positive are more diverse. There are two separate clusters present, both including mixture of strains for B2 and D group and each contains a single strain that did not show any bands after PCR.

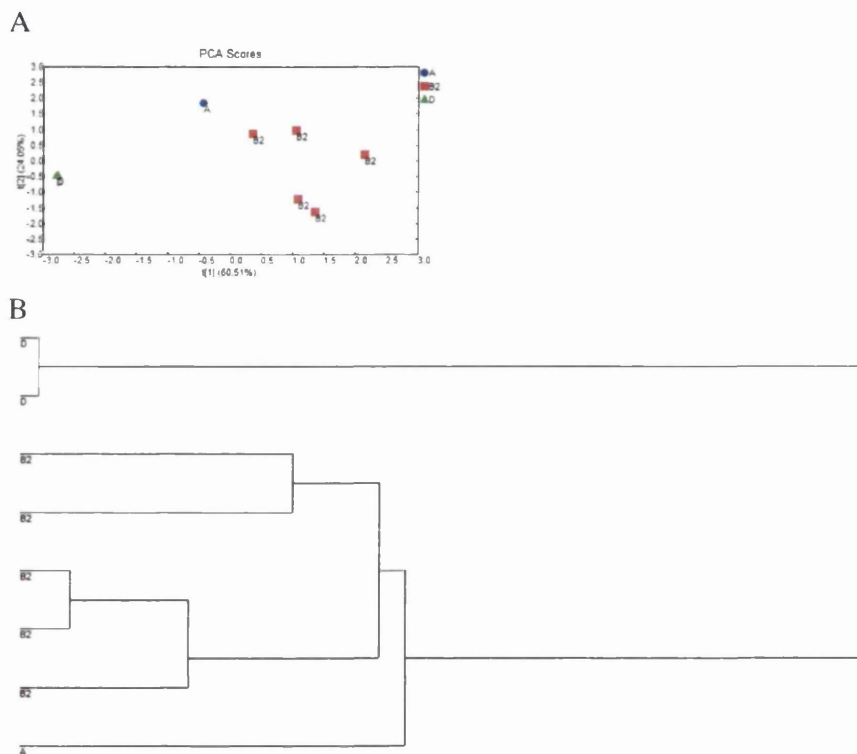


Figure 6.3.: Results based Raman spectra for the collection of clinical strains expressing CTX-M-15, TEM-1, A) PCA clusters, strains belonging to phylogenetic group A: blue circle; strains belonging to phylogenetic group B2: red square; strains belonging to phylogenetic group D: green triangle; B) hierarchical tree showing the relationship between the strains; two top branches: strains belonging to phylogenetic group D, bottom branch: strain belonging to phylogenetic group A, five middle branches: strains belonging to phylogenetic group B2

6. CHARACTERISATION OF CLINICAL ISOLATES OF *ESCHERICHIA COLI* EXPRESSING EXTENDED SPECTRUM β -LACTAMASES, USING RAMAN SPECTROSCOPY

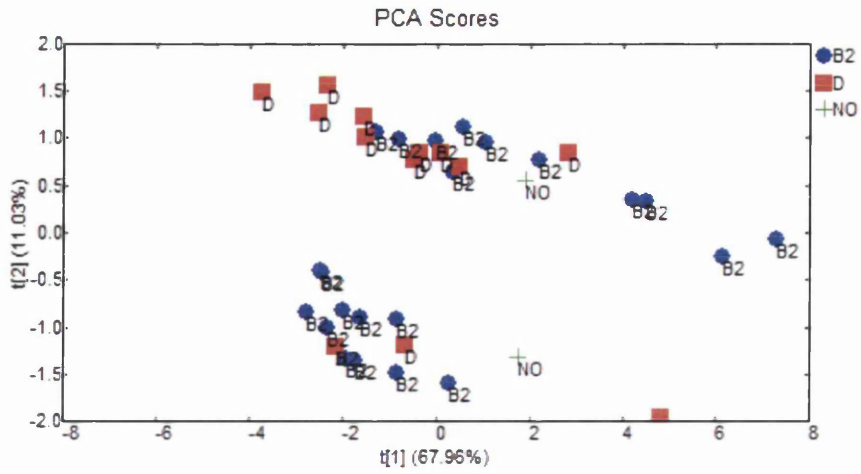


Figure 6.4.: PCA clusters based on Raman spectra for the collection of clinical strains expressing CTX-M-15IS26 positive; strains belonging to phylogenetic group B2: blue circle, strains belonging to phylogenetic group D: red square, strains that did not show any bands after PCR: green cross

6.4. Discussion

This chapter has proven that it was possible to assign organisms within groups expressing different extended spectrum β -lactamases profiles to different phylogenetic groups as well as to classify strains within these groups using Raman spectroscopy.

To our knowledge this is the first study involving that broad number of ESBL strains measured with Raman spectroscopy. In addition, the phylogenetic classification was verified as well therefore Raman spectroscopy was used for assessing bacteria phenotypically, genetically and phylogenetically. Our work could therefore be a pioneer attempt to broaden the uses of Raman spectroscopy for investigating multi-resistant strains concerning the public health nowadays as well as for epidemiological studies of *Enterobacteriaceae*.

This work has based the phylogenetic classification on the methods presented by Clermont et al. (Clermont et al., 2000) and the results are in agreement with the published findings. The article does not mention cases in which the bands were not present, which has happened in this project with 4 strains and the result was consistent in repeated experiments. Yet another problematic issue was the difficulty in distinguishing between B2 and D strains in several cases. This was caused by the fact that TspE4C2 band at 152pb was very faint and it was the decisive band differentiating between B2 and D groups. This may be the reason for the diversity in the two PCA clusters of CTX-M15 IS 26 positive Raman spectra. Normally it would be expected to obtain separate clusters for B2 and D groups since these are the biggest phylogenetic groups within this ESBL collection. However, the lack of uniformity within those clusters may possibly be caused by the incorrect recognition between B2 and D groups.

A publication by Doumith et al. (Doumith et al., 2012) addresses the problem of polymorphic nucleotides revealed for the three original primers. In order to avoid the situation, it was suggested to use 281-, 216-, and 158- bp fragments instead of 279-, 211- and 152-bp respectively. The new set also contained a 373bp fragment for *gadA*.

In this project we did not have the opportunity to test this modification of the original method, however, according to the publication, strains that were considered to be in D group after using Clermont et al. method were recognised as B2 with the new approach. Trusting these results we did make an attempt to change the phylogenetic group of the strains which were inconclusive in at least one of the experimental repeats from D to B2 hoping that it would clarify the existence of two clusters within the CTX-M15 IS 26

positive group. Unfortunately the effect was not as expected.

It can be concluded that this chapter gave an important insight into the capabilities of Raman spectroscopy and proves that it can be used for many purposes including classification of the multiresistant strains according to their antibiotic profile as well as to their phylogenetic group.

7. FINAL DISCUSSION AND FUTURE PERSPECTIVES

7. FINAL DISCUSSION AND FUTURE PERSPECTIVES

Infectious diseases have influenced human lives for centuries, with examples of pandemics and epidemics able to destroy entire civilisations and cause death over broad regions of the world (Brachman, 2003; Morens et al., 2004; Tatem et al., 2006). Infectious diseases remain major threats and are related to mortality, morbidity as well as an economical burden (Gubler, 1998). Attempts to counteract infectious diseases and to prevent their spread have focused on i) basic science to further knowledge about the disease-causing vectors; ii) development of immunity against the infectious factors by producing vaccines (Stern & Markel, 2005); iii) discovery of therapeutic agents in the form of antibiotics (Aminov, 2010; Gensini et al., 2007; Longworth, 2008) and iv) advances in diagnosis, such as PCR.

Development of antibiotic resistance through exchanging genetic information has clearly decreased the effectiveness of progress to address infectious disease (Davies & Davies, 2010). Several factors have enhanced the spread of antibiotic resistance mechanisms such as overuse of antimicrobials, especially those with broad spectrum action (ampicillin), poorly designed treatment, inclusion of antibiotics in animal feed which allows access to soil and groundwater, leading bacteria to develop mechanisms of defence against antimicrobials (Levy & Marshall, 2004; Yoshikawa et al.). Furthermore bacterial organisms also gain resistance to multiple groups of antibiotics, termed multiple drug resistance, amplifying the problems for human health. Thus cutting edge clinical microbiology now requires identification and determination of antimicrobial susceptibility before fully instigating a treatment regime.

There are a variety of diagnostic methods available currently, including traditional phenotype-based testing, metabolic activity investigation, automated systems including antibiotic profiling as well as techniques involving molecular biology (Kim et al., 2008; Woodford & Sundsfjord, 2005). However, many of these methods are still not cost effective and rarely used in hospital laboratories, resulting in them being dependent on culturing methods incorporating a cascade of steps usually lasting 8-24h each, extending time of diagnosis to several days (Petersen & McMillan, 1998). This can have serious adverse effects on patients survival rate especially in severe cases like septicaemia or acute meningitis where the delay in the initiation of correct anti-microbial therapy is linked to mortality (Tunkel et al., 2004)(Tunkel et al., 2004). This thesis recognised the urgent need for a new, rapid, and cost effective diagnostic method which could be incorporated into the natural diagnostic process within hospital laboratories.

Raman spectroscopy has previously been used for analytical purposes in chemistry and

physics (Gerrard, 1994) but gradually gained popularity in various different fields including art, archaeology (Marcolli & Wiedemann, 2001) (Vandenabeele et al., 2007a), forensics (Salahioğlu & Went, 2012) (Cho, 2007), pharmaceuticals (Fini, 2004) (Vankeirsbilck et al., 2002), as well as the bio-medical field (Downes & Elfick, 2010) (Petry et al., 2003). Raman spectroscopy possesses several important advantages that could make it a useful diagnostic tool, namely: it is non-destructive, able to investigate spectra in an aqueous environment, inexpensive, and the signal has the potential to be enhanced (Pappas et al., 2000) (Fabian & Anzenbacher, 1993).

We have made the efforts of investigating previously suggested approaches with more focus on the diagnostic application, therefore: this project aims to determine whether Raman spectroscopy has the qualities including: the cost effectiveness, reproducibility and ease of use but does not compromise on the specificity and ability to distinguish between very similar organisms and bacteria of different antibiotic profile. Our work had a strict clinical oriented interest.

This thesis assesses the potential of Raman spectroscopy to address two major problems in clinical microbiology, namely bacterial identification and determination of antimicrobial susceptibility. The thesis results begin with a basic science approach to characterise the Raman system and assess reproducibility of Raman spectra of bacteria (Chapter 3). Then the thesis addresses the potential of Raman spectroscopy to discriminate between species and strains of bacteria (Chapter 4). In the next chapter the ability to detect laboratory produced resistant strains of bacteria is assessed (Chapter 5). Then finally the potential of Raman spectroscopy to identify and characterise 65 strains of multidrug resistant *E. coli* was assessed (Chapter 6).

In Chapter 3 we designed procedures for reproducible spectra collection and data processing. For collecting spectra, all experiments were performed on the *inVia*Raman system calibrated for silicon sample and set up to: 10 seconds of 1 accumulation, with laser power of 50%, using the 785nm red laser. The range chosen for the experiments was 600-1600 cm^{-1} and we have established that the best results can be obtained with 15-30 spectra using the whole spectrum, not just its fragments, as also mentioned in our previous work. (Almarashi et al., 2012).

Experiments were performed on fully grown bacterial colonies on solid growth medium (Columbia Blood Agar) as the substrate of choice. Agar had no influence on the quality of the spectra and being commonly used in the clinical environment, is an advantage for its future use alongside current procedures in the hospital laboratory. Additionally,

our approach does not extend the time suggested by most other publications using alternative substrates, including CaF_2 . They were based on bacterial suspensions grown overnight/24h or on solid medium, but involved scraping part of a colony and moving it onto a different substrate (Jarvis et al., 2006) (Rösch et al., 2005) (Kirschner et al., 2001) (Maquelin et al., 2000). Therefore our method, involving scanning colonies directly on the agar growth medium, allows one step to be omitted in the procedure (no extra transfer). Moreover, it has been suggested (Maquelin & Kirschner, 2003) (Maquelin & Choo-Smith, 2002) that it may be possible to decrease the time of bacterial growth to 6-8h using microcolonies before Raman measurement. This has met with some success by other members of our group (Almarashi et al., 2012) and in this way the procedure here could be enhanced even further by reducing the time to an 'identification' decision.

Processing of the spectra was an important step. The initial step included background removal which was an essential practice and should not be omitted due to the natural fluorescence observed in biological samples, as well as many common substrates, when subjected to Raman spectroscopy (Fabian & Anzenbacher, 1993) (Huang et al., 2010) (Escoriza et al., 2006). There are several methods of background correction suggested in the literature, including geometric approaches (Kourkoumelis et al., 2012) and polynomial regression model baseline correction De Wael et al. (2008). However, after investigating three further methods which included background subtraction available from PyChem, AirPLS, and Rolling Circle Filter we confirmed that the RCF delivered the most reliable results. This is supported by others using the method for analysis of Raman-based research (Huang et al., 2010) (Samek et al., 2010a,b,c).

For the most efficient differentiation between bacterial organisms it was also essential to choose an appropriate method for spectral comparison. This is applicable for both closely related samples (Wagner, 2009) (Jehlička et al., 2012) with more complex comparisons, involving samples exhibiting more subtle differences, requiring more advanced spectral processing methods. Among many techniques covered in the literature (Zhu et al., 2004) (Rösch et al., 2005) this work focused on Principal Component Analysis (Jarvis & Goodacre, 2004b) (Ciobot et al., 2010) (Jarvis et al., 2006) with Hierarchical Clustering (Kirschner et al., 2001). In addition selecting the most significant peaks when comparing samples to each other (Maquelin et al., 2003) and assigning the identified values to the library of Raman signals of biological molecules was a useful addition of our analysis (Ivleva et al., 2008) (Samek et al., 2008) (Maquelin et al., 2002) (De Gelder, 2007) (Schuster et al., 2000) (Samek et al., 2010a,b,c). Such procedures tested and de-

scribed in Chapter 3 allowed the development of a standard operating procedure (SOP) that was applied in all following chapters.

In Chapter 4 the Raman SOP was applied to distinguish between bacterial samples in order to verify possible applications of the technique to the clinical field. Collections of strains including *E. coli* (Top10, K12, Strain B), *S. epidermidis* (1457 and 9142) and *S. aureus* (10418 and 6571) were tested. The results allowed us to conclude that distinction between bacteria using Raman spectroscopy is associated with taxonomic differences, Thus the differences detected between organisms decrease in the order genus > strain > sub-strain. Similar findings confirming our conclusions can be found in other publications including the comparison of different organisms and even the same species (Rossi et al., 2012) (Kahraman et al., 2009).

Our method was also able to identify and discriminate very fine differences. For example the comparison between *E. coli* strains Top10, K12 and Strain B. Here the system could identify that Top10 and K12 are more closely related than strain B-indeed Top10 was derived from K12. Raman spectra exhibited close relations between the *E. coli* strain which are following the natural trend (Andreishcheva & Vann, 2006) (Schneider et al., 2002).

The approach of identifying significant Raman peaks when comparing samples enabled us to identify the biological molecules responsible for the separation of the organisms and was also used successfully to monitor the composition of single bacterial cells (Schuster et al., 2000). We identified that DNA and RNA bases, as well as protein and amino-acids were the main discriminatory signals when comparing at the genus level, while more closely related bacteria are differentiated by additional peaks associated with sugars, fats and fatty acids. These findings lead to the conclusion that Raman spectroscopy recognises major taxonomic differences based on genes and the expressed proteins. However, when investigating between more subtle relationships; the outer bacterial envelope has more influence on the differentiation.

Another important factor, especially for the clinical setting, was the investigation of the influence of both temperature and storage time on the quality of spectra and on the ability of Raman spectroscopy to differentiate between samples. Based on our findings we managed to draw conclusions that neither the temperature nor the time of the storage, up to 8 hours, can have a visible influence on the quality of separation between the strains, nor on the shape of the clusters. This experiment adds to the qualities of Raman spectroscopy as a potential diagnostic technique, since, due to the working hours of the hospital labo-

7. FINAL DISCUSSION AND FUTURE PERSPECTIVES

ratories, samples sometimes have to be stored before testing. This would not affect the diagnosis. To our knowledge and surprise this has not been investigated in the literature to date.

In Chapter 5 we focused on determining the abilities of Raman spectroscopy to identify antibiotic resistance mechanisms. In order to examine this premise we generated and characterised isogenic strains of *E. coli* Top10 resistant to ampicillin (Top10^{AA} and Top10^A) and kanamycin (Top10^{KK} and Top10^K). Growth curves and MIC determination confirmed the sensitive and resistant phenotypes. Characterised strains, were subjected to Raman spectroscopy and compared to the susceptible wild-type strain. Results suggested that there were differences in antibiotic resistance based on the presence of antibiotic i.e. resistant strains kept under the antibiotic pressure and tested on agar containing the antibiotic showed the most distant PCA clusters when compared to untransformed strains. The differences between transformants and the wild-type strains were gradually decreasing with the level of antibiotic exposure; therefore they were the lowest for Top10^A and Top10^K respectively. However, even in those instances, samples were easy to distinguish. Interestingly comparable findings using a similar transformation strategy (but different plasmid, pDrive) were described by Walter et al. (Walter et al., 2011), who identified the major differences to be dependent on the DNA/RNA and cytochrome content.

Additionally, it was also noticed that ampicillin resistant strains were more prone to losing the plasmid expression than strains transformed with pET-26 plasmid. This conclusion was drawn upon building the hierarchical tree clustering, which grouped all the kanamycin resistant strains together but the pUC19 bearing bacteria were divided; Top10^A grouped closer to the Top10 but away from the K12, while Top10^{AA} and Top10^{AA}+Amp are situated near K12 and in close proximity to all kanamycin resistant Transformants.

We have concluded that the reason may be due to the fact that Top10, unlike K12, does not contain functioning lac Operon, however, this gene cluster's function can be gained due to transformation with plasmid containing lac Operon genes and therefore become more similar to K12 than to the untransformed Top10. Top10^A maintains on a branch close to Top10 wild-type, which may indicate that the plasmid containing lac Operon could be lost, due to the lack of ampicillin pressure. Therefore Raman spectroscopy may be able to distinguish the persistence of resistance factors within bacterial cells.

Chapter 6 was devoted entirely to the clinical applications for Raman spectroscopy. A collection of hospital isolates of *E. coli* expressing extended spectrum beta lactamases (ESBLs) characterised previously for their detailed antibiotic profiles was used for this

section. Additionally we tested a novel approach of confronting Raman spectroscopy with phylogenetic classification. Using the triplex PCR methods involving 3 sets of primers: ChuA.1, ChuA.2, YjaA.1, YjaA.2, YjaA.2, YjaA.2, TspE4C2.1, TspE4C2.2 we assigned each of the 65 strains in the collection to one of 4 major phylogenetic groups: A, B1, B2 and D, based on the approach introduced by Clermont et al. (Clermont et al., 2000).

The results varied in a high degree with majority of the strains falling into B2 or D group with three strains of different antibiotic profiles, which could not be assigned to any of the phylogenetic group. No direct link between the antibiotic resistance profile and the phylogenetic groups could be identified.

After subjecting strains from two most numerous ESBL groups: CTX-M-15, TEM-1 and CTX-M-15IS26 positive, to Raman spectroscopy, it could be noticed that there were separate, phylogenetic group dependant clusters within the first ESBL group. The latter one did divide into two clusters, however they both contained B2 and D strains. There were chances that our phylogenetic classification might have had some flaws and the results from the CTX-M-15IS26 positive group may confirm this assumption. Our suspicions are confirmed Doumith et al. (Doumith et al., 2012) criticizing the effectiveness of Clermont's premise and suggesting an alternative solution. Unfortunately due to the lack of time we were not able to perform the experiments as suggested there.

This project has raised numerous important points that warrant further investigation and could benefit from future modifications and improvements.

One of the main limitations, that could prevent Raman spectroscopy from being used as the ultimate diagnostic tool in infectious diseases, would be the inability to scan patients sample directly.

Possible approach could involve single-cell analysis excluding completely the incubation period. We made initial attempts towards this idea when testing the best possible substrate. We did not manage to obtain any valuable signal from bacterial suspension, which was burdened by the fluorescence.

Another technique attempted was SERS for which we prepared silver nanoparticles as described in the literature (Jarvis et al., 2008, 2004, 2006). Preparing the substrate was indeed rapid, inexpensive and easy, however the authors recommend testing the substrate with Atomic Force Microscopy, which we did not manage to obtain. Additionally the SERS papers cited here, use the bacterial samples grown overnight, therefore it would not decrease the time of diagnosis, that our project offers, but add at least one step to the procedure.

7. FINAL DISCUSSION AND FUTURE PERSPECTIVES

An interesting effect was obtained when using optical tweezers and this could possibly be the next step worth exploring (Moritz et al., 2010a,b; Wagner, 2009).

Other problematic factor was the variation within the samples involving hospital isolates, especially the Extended Spectrum β -lactamases *E. coli*. The colonies often exhibited poorer growth resulting in lower quality spectra. Presence of such errors could seriously obstruct the correct diagnosis. Within the literature records, most authors seem rather positive about their results when using Raman spectroscopy for identifying hospital strains, therefore more practice on our side and possible collaborations with other laboratories could decrease the issue.

Another improvement to our project could be delivered by using more sophisticated methods of spectra processing. There are various different techniques used and to test them, could possibly profit in obtaining even better, more detailed information from Raman spectra serving the diagnostic purposes. T-tests used for determining the significance of difference between corresponding Principal Components have raised some questions over the course of this project. Sadly, no alternative has been suggested to-date. Literature mentioned before dictates using certain techniques serving as post-analysis procedures, however the limited time and access to professional statisticians' advice made it impossible to explore include more elaborate results within this thesis.

Using Raman spectroscopy for phylogenetic investigations offered so far only limited results. This fact was related again: to the poor repetitiveness of ESBLs as well as to limited time. This attempt was a very novel approach within our laboratory and could possibly allow for other project based on the principle to follow if more time and funds were allocated.

This thesis has produced a comprehensive body of work on the potential use of Raman spectroscopy for diagnosing bacterial-associated infectious disease. The work has focused on taxonomic identification and discrimination between bacteria. Furthermore work has suggested the possible use of Raman for identifying antibiotic resistant phenotypes. Our original hypothesis outlining the potential of Raman spectroscopy for diagnosis of infectious disease has been confirmed in the basic science laboratory and has yielded promising results. The major goal is the steps needed for application in hospital laboratories. At this stage it may seem that there is a very long way to go for Raman spectroscopy before it could be commonly used for medical purposes, however experience on Phoenix systems or even Mass spectroscopy confirm that there could be profit in developing phenotypic assays and Raman spectroscopy has the potential to complement

them.

For Raman spectroscopy to become a method commonly used in clinical laboratories, more effort should be done, especially in terms of unifying the variety of methods and integrating them for clinical use. One major advance should definitely be the development of an easily accessible Raman signal database for both: single molecules, as well as for the whole bacterial organisms. Therefore any spectra received by the laboratory technician or through an automated procedure, could instantly be compared to the standard and a diagnosis could be delivered.



Appendices



A. SUPPLEMENTARY INFORMATION

A. SUPPLEMENTARY INFORMATION

Table A.1.: Approaches have been used for studying microorganisms with Raman spectroscopy

Method	References
Fully grown colonies	(Samek et al., 2008) (Rösch et al., 2003)
microcolonies	(Maquelin et al., 2000) (Maquelin et al., 2002) (Maquelin & Kirschner, 2003) (Goodwin, 2006)
bacterial biomass	(Kirschner et al., 2001) (Choo-Smith, 2001) (Hutsebaut et al., 2006) (De Gelder et al., 2007a) (Ivleva et al., 2009) (Hall et al., 2011) (Willemse-Erix et al., 2009) (Escoriza et al., 2006)
single cells	(Schuster et al., 2000) (Guicheteau et al., 2010) (Harz et al., 2009) (Rösch et al., 2005)

A. SUPPLEMENTARY INFORMATION

Table A.2.: Different microorganisms studied using Raman spectroscopy.

microorganism	References
<i>Esherichia coli</i>	(Culha et al., 2010) (Hadjigeorgiou, 2009) (Jarvis et al., 2006) (Jarvis & Goodacre, 2004a) (Jarvis & Goodacre, 2004b) (Maquelin et al., 2000) (Mello et al., 2005)
<i>Klebsiella pneumonia</i> <i>Klebsiella oxytoca</i> <i>Proteus spp</i>	(Jarvis & Goodacre, 2004a) (Hadjigeorgiou, 2009) (Jarvis & Goodacre, 2004b)
<i>Enterococcus spp.</i>	(Maquelin et al., 2000) (Jarvis & Goodacre, 2004a) (Jarvis & Goodacre, 2004b)
<i>Citrobacter freundii</i>	(Jarvis & Goodacre, 2004b)
<i>Staphylococcus cohnii</i> <i>Staphylococcus warneri</i>	(Harz et al., 2005) (Harz et al., 2009)
<i>Staphylococcus epidermidis</i>	(Maquelin et al., 2000) (Harz et al., 2005) (Harz et al., 2009) (Samek et al., 2008)
<i>Salmonella choleraesuis</i> <i>Shigella flexneri</i>	(Mello et al., 2005)
<i>Micrococcus luteus</i> <i>Rhodotorula mucilaginosa</i> <i>Bacillus sphericus</i> <i>Pseudosomonas fluorescens</i>	(Rösch et al., 2003)
<i>Helicobacter pylori</i>	(Lin et al., 2009)
<i>Staphylococcus aureus</i>	(Jarvis et al., 2006) (Maquelin et al., 2000)
<i>Streptococcus pneumonia</i> <i>Streptococcus agalactiae</i> <i>Neisseria meningitides</i> <i>Listeria monocytogenes</i>	(Harz et al., 2009)
<i>Shigella sonnei</i> <i>Erwinia amylovora</i> <i>Proteus vulgaris</i>	(Culha et al., 2010)
<i>Bacillus megaterium</i> <i>Acidophilium cryptum</i> <i>Cupravidus necator</i> <i>Azohydromonas lata</i> <i>Bacillus thuringiensis</i>	(Ciobot et al., 2010)

A. SUPPLEMENTARY INFORMATION

Table A.3.: Characteristic peaks obtained from Raman spectroscopy of biological samples according to: (De Gelder, 2007; Ivleva et al., 2008; Maquelin et al., 2002; Samek et al., 2008, 2010b; Schuster et al., 2000)

Raman Shift(cm⁻¹)	Bond/Molecule
561	C-O-C glycosidic ring deformation Polysaccharide COO- wagging C-C skeletal
620	Phenylalanine
640-643	Tyrosine
665	Guanine
720-723	Adenine
734	Glycosidic ring Polysaccharide CH ₂
755	L-tryptophan
756	Phosphophenylopyruvate
778-785	Citidine Uracil Cytosine Uracil ring stretching Phosphophenylopyruvate DNA Phosphodiester O-P-O stretching
829-830	Tyrosine (in protein) exposed
840	L-Tryptophan 12-methyl-tetradecanoic acid
841	Beta-D-Glucose, Alpha-D-Glucose
846	15-Methylpalmitic acid
848	L-tryptophan
850	C-O-C stretching vibration 1,4-glycosidic link

Table A.3.: (cont.) Characteristic peaks obtained from Raman spectroscopy of biological samples according to: (De Gelder, 2007; Ivleva et al., 2008; Maquelin et al., 2002; Samek et al., 2008, 2010b; Schuster et al., 2000)

Raman Shift(cm⁻¹)	Bond/Molecule
	Tyrosine (in protein)
852-855	Tyrosine buried
	Tyrosine ring breathing
858	C-C stretching
	C-O-C
	1,4 glycosidic link
869	Triolein
897	C-O-C stretching , C-O-C vibrations of the glycosidic bonds and sugar rings
899	L-Proline
900	Lactose
901	Amylose
906	14-Methylhexadecanoic acid
907	13-Methylmyristic acid
908	Myristic acid
923	C-COO-
	COO- stretching
	Phospholipids
	C-C skeletal
	CH ₃ rocking
932	C-C
	Stretching of alpha helix
	C-O-H glycosides (carbohydrates)
937	C-O-C stretching vibration
	Glycosidic link
944	Amylose
968	L-serine
980	C-C
	Stretching of beta-sheet (proteins)
	C-H bending (lipids)
999	D-(+)-Galactosamine

A. SUPPLEMENTARY INFORMATION

Table A.3.: (cont.) Characteristic peaks obtained from Raman spectroscopy of biological samples according to: (De Gelder, 2007; Ivleva et al., 2008; Maquelin et al., 2002; Samek et al., 2008, 2010b; Schuster et al., 2000)

Raman Shift(cm⁻¹)	Bond/Molecule
1002	Phenylalanine
1003	Phenylalanine C-CH ₃ Carotenoids
1004	Phenylalanine
1030	Phenylalanine C-H in plane Carbohydrates
1060-1096	DNA/RNA Lipids Carbohydrates C-C stretching C-N stretching C-O stretching
1071	D-Fructose-6-phosphate
1088	C-C stretching C-O-C Glycosidic ring Polysaccharide
1098	C-O-C stretching vibrations Glycosidic link C-C skeletal
1099	Palmitic acid
1110	Glycerol
1111	L-Histidine
1121	D-(+)-Galactosamine Acetyl coenzyme A
1127	C-C stretching C-O-C Glycosidic ring breathing Symmetrical polycacharides

Table A.3.: (cont.) Characteristic peaks obtained from Raman spectroscopy of biological samples according to: (De Gelder, 2007; Ivleva et al., 2008; Maquelin et al., 2002; Samek et al., 2008, 2010b; Schuster et al., 2000)

Raman Shift(cm⁻¹)	Bond/Molecule
	C-N amino acids
1129	CH ₂ deformation
1130	=C-C= in unsaturated fatty acids in lipids
1140	L-Histidine
	14-Methylhexadecanoic acid
1145	C-C
	C-O breath asymmetric polysaccharide
	NH ₂ twist amino acids
1152	C-C stretching
	Carotenoids
1158	Proteins
1220-1295	Amide III
	DNA/RNA (Thymine, Adenine)
	Proteins (Amide III)
	Lipids
1233-1237	Amide III
1239	D(+)-Mannose
1240	D-(+) Trehalose
1249	Amide III
	N-H
	C-N
1250	Cytosine
	L-histidine
	D-(+)-Fructose
1258	AmideIII
1259	15-Methylpalmitic acid
	D(-) Arabinose
1261	Lactose
	D-(+)-Trehalose
	Malic Acid
1320-1340	DNA/RNA(Guanine/Adenine)

A. SUPPLEMENTARY INFORMATION

Table A.3.: (cont.) Characteristic peaks obtained from Raman spectroscopy of biological samples according to: (De Gelder, 2007; Ivleva et al., 2008; Maquelin et al., 2002; Samek et al., 2008, 2010b; Schuster et al., 2000)

Raman Shift(cm ⁻¹)	Bond/Molecule
	Proteins
	Carbohydrates
	Protein (Amide III)
1336	Amide III
	O-H
	C-O-H
	H-C-O
	H-C-C deformation polysaccharide
	C-H deformation
1350	L-Proline
1351	Malic acid
	L-Valine
1382	COO- stretching symmetric
1440	Methylhexadecanoic acid
	Oleic acid
	Triolein
	Trilinolein
1441	Glycine
	Stearic Acid
	12-Methyl-tetradecanoic acid,
	Trilinolenin
1440-1460	CH ₂ scissoring
	DNA
	C-H bindings in lipids
	Proteins
	Carbohydrates
	Bands of fatty acids
	Deformation vibration CH ₂ scissoring
1448	CH ₂ deformation
1469	13-Methylmyristic acid
	D-(+)-Trehalose

Table A.3.: (cont.) Characteristic peaks obtained from Raman spectroscopy of biological samples according to: (De Gelder, 2007; Ivleva et al., 2008; Maquelin et al., 2002; Samek et al., 2008, 2010b; Schuster et al., 2000)

Raman Shift(cm⁻¹)	Bond/Molecule
1471	D-(-)-Fructose
1479	14-Methylhexadecanoic acid
1481	Palmitic acid
	D-(+)-Mannose
1501	15-Methylpalmitic acid
1502	C=C stretching carotenoids
1512	C=C stretching carotenoids
	Amide III
1570	L-Glutamate
1571	L-Histidine
1573	C=C
1575	Guanine and adenine ring stretching
1581	A, G ring stretching
1585	COO- stretching asymmetric
1605-1615	Tyrosine
	Phenylalanine
1640-1680	Amide I
	Lipids
1655	Amide I

B. R-CODE

B.1. Subtracting agar

```
$ int = read.table(file.choose())
$ sample = read.table(file.choose())
$ sub=array()
$ for (i in 1:30) {sub[i]=(sample[,i]-int)}
$ write.table(sub, file = "noAgar.txt", quote=FALSE,
sep = "\t", row.names = FALSE, col.names=FALSE)
```

B.2. Calculating t-tests from PCA scores

```
$ PCA = read.table(file.choose())
$ A = PCA[1:30,]
$ B = PCA[31:60,]
$ PCA2 = cbind(A,B)
$ mat=matrix(ncol=1,nrow=4)
$ for(i in 1:4) {mat[i]=(t.test(PCA2[,i],PCA2[,i+4])
[["p.value"]])}
$ print(mat)
$ for (i in (mat)) {if(i<0.05)print
("significant difference") else print ("not different")}
$ mat1=function(mat){for (i in (mat)) {if(i<0.05)
print("significant difference")
else print("not different")}}
$ mat1(mat)
$ write(mat,file = "PCA_t-test.txt", ncol=1)
$ #PCA2t=t.test (PCA2[,1],PCA2[,5]))
```

B.3. Subtracting mean spectra intensities in a form of a graph

```
$ merInt = read.table(file.choose())
$ A = merInt[,1:120]
```

```
$ B = merInt[,121:240]
$ meanA = rowMeans(A)
$ meanB = rowMeans(B)
$ newSpec = meanA-meanB
$ wave = read.table(file.choose())
$ wavel = wave[,1]
$ g_range = range(0, newSpec, meanA, meanB)
$ g_range
$ plot_colours = c("blue","red","forestgreen")
$ png(filename="C:/Users/mack2/Desktop/Natalia-Raman
/subtract.png", height=600, width=600, bg="white")
$ plot(wavel, newSpec, type="l", col=plot_colours[1],
ylim = g_range, ann=FALSE, cex.axis=2, lwd=2)
$ lines(wavel, meanA, type="l", pch=28,
col=plot_colours[2], lwd=2)
$ lines(wavel, meanB, type="l", pch=28,
col=plot_colours[3], lwd=2)
$ title(main="Subtraction", col.main="red", cex.main=3)
$ title(xlab= expression("Raman shift" ~ (cm^{-1})),
col.lab=rgb(0,0.1,0), cex.lab=2)
$ title(ylab= "Intensity (a.u.)", col.lab=rgb(0,0.1,0),
cex.lab=2)
$ legend(600,5000, c("Subtracted","Top10","B"), cex=1,
col=plot_colors, lty=1)
$ final=cbind(meanA,meanB,newSpec)
$ write.table(final, file = "subtract.txt", col.names=NA,
sep="\t")
$ dev.off()
```


C. PUBLICATION BASED ON RESULTS INCLUDED IN THIS THESIS

Hindawi Publishing Corporation
Spectroscopy: An International Journal
Volume 27 (2012), Issue 5-6, Pages 361–365
doi:10.1155/2012/540490

Raman Spectroscopy of Bacterial Species and Strains Cultivated under Reproducible Conditions

Jamal F. M. Almarashi,¹ Natalia Kapel,² Thomas S. Wilkinson,² and Helmut H. Telle¹

¹Department of Physics, Swansea University, Swansea SA2 8PP, UK

²Department of Medical Microbiology and Infectious Diseases, Institute of Life Science, Swansea University, Swansea SA2 8PP, UK

Correspondence should be addressed to Helmut H. Telle, h.h.telle@swansea.ac.uk

Copyright © 2012 Jamal F. M. Almarashi et al. This is an open access article distributed under the Creative Commons Attribution License, which permits unrestricted use, distribution, and reproduction in any medium, provided the original work is properly cited.

Abstract. Rapid and reproducible discrimination between bacterial pathogens is a clear goal in microbiological laboratories when processing infected clinical samples. In this study Raman spectra were taken from at least 30 colonies of four strains of bacteria including *Staphylococcus epidermidis* (1457 and 9142) and *Escherichia coli* (K12 and Top 10) using the Renishaw *in Via* Raman microscope system. Analysis based on principal components suggests that even strain differentiation (e.g., 1457 versus 9142 or K12 versus Top10) is possible.

Keywords: Raman spectroscopy, bacterial identification, principal component analysis

1. Introduction

Reproducible and robust bacterial identification is the key to cutting-edge clinical microbiology. Current methodologies for determining the identity of unknown bacteria in a clinical specimen include traditional methods based on biochemistry (e.g., API test), specific activities (e.g., agglutination), or growth requirements (e.g., high NaCl concentration). More modern approaches have now automated biochemical tests (Phoenix) and developed specific assaying methodologies that identify bacteria from their DNA (Polymerase chain reaction) or protein (MALDI-TOF); see, for example, [1, 2].

During the last 10 years or so, Raman spectroscopy has gained a wider acceptance as a method for bacterial identification. Studies have demonstrated that Raman spectra generated from bacterial colonies give sufficient information to identify and differentiate medically relevant microorganisms, including *Staphylococcus* spp., *Candida* spp. and *Escherichia coli* (see e.g., [3, 4]). We have also used Raman spectroscopy to identify bacterial species and have suggested, specifically, that in some instances it may be a useful technique to detect biofilm formation [5]. Others have demonstrated that, provided that the Raman signal can be enhanced, through surface-enhanced (SERS) or tip-enhanced (TERS)

Raman spectroscopy, spectra can also be generated from single bacteria (see e.g., [6]); this leads to the possibility that microorganisms may be traced and identified directly in biological fluids.

Thus, previous work has confirmed the potential of Raman spectroscopy to identify bacteria. Less work has focused on the limits and reproducibility of this method—the true measure of clinical usefulness. We have analysed numerous colonies resulting from the same bacterial specimen so that clear limitations and sensitivities can be determined and the potential of Raman spectroscopy in routine clinic diagnostics can be gauged.

2. Instrumentation and Methodology

The instrument used in our experiments is the Renishaw *in Via* system with a charge-coupled device (CCD) detector and a Leica DM2500 microscope. The microscope is supplied with a motorised sample stage. The microscope is equipped with 5x, 20x, 50x, and 100x objective lenses, and Windows-based Raman Environment software (*WiRE3.2*) is used for controlling the system for data acquisition. Two laser devices are coupled to the *in Via* Raman system, operating at excitation wavelengths of 532 nm and 785 nm; for the work reported here we exclusively used the NIR laser excitation source at 785 nm.

A number of bacterial specimen, namely, *S. epidermidis* 1457 and 9142, and *E. coli* Top10 and K12 were cultivated separately for 24 hours in an incubator at 37°C, from frozen stock supplies spread onto Petri dishes of Columbia blood (Horse) agar (CBA). After 24 hours, pieces of Agar containing bacterial colonies were cut from the Petri dish and placed on a microscope slide.

Samples were positioned directly under the 50x microscope objective and the laser spot focused sequentially on the (central) top of each individual bacterial colony. The acquisition parameters used for each single measurement included a laser power on the target of ~110 mW and a (static) exposure time of 10 s (72 s for a complete single-spectrum scan). The spectral range was extended to 600–1600 cm⁻¹ to cover the most relevant bacterial Raman features using the system's SynchroScan mode for single spectrum accumulation; the total time of measurement for a series of 30 individual colonies normally was less than two hours (this includes the time for homing in individual colonies and exchanging samples).

The Raman spectra were treated with a Savitzky-Golay coupled advanced rolling filter-*SCARF*-background removal routine (see, e.g., [7]), and then analysed using a standard multivariate principle-component program *PyChem* [8]; further, discriminant analysis steps are not included here.

3. Results

To assess the reproducibility of Raman spectroscopy, we inoculated Columbia blood agar plates with *S. epidermidis* 1457, 9142 or *E. coli* Top10, K12, and collected data from a minimum of 30 colonies using the Renishaw *in Via* Raman system. Typical (raw) spectra are shown in Figure 1(a). Chemometric principal component analysis of these spectra generated clusters of data points, from which the reproducibility of the measurement could be analysed. This type of data could be used to compare bacteria at both the species and strain level and allowed us to investigate the influence of successive principal components on the ability to differentiate between bacteria and their strains.

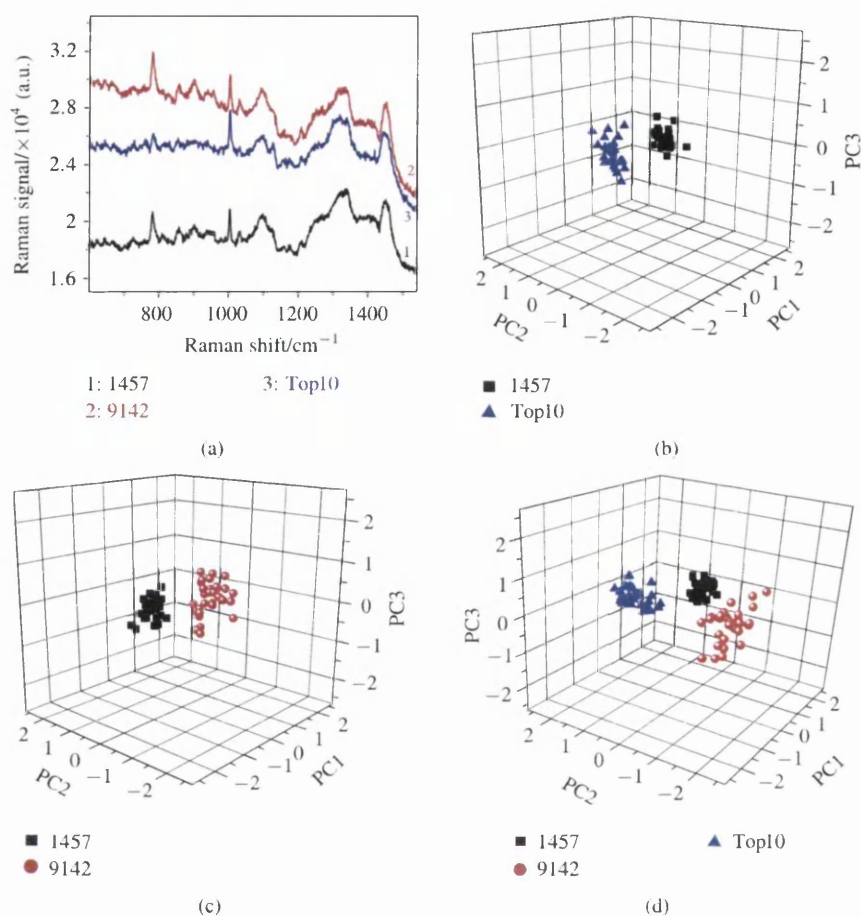


Figure 1: Analysis of repeat measurements of different colonies of the same bacteria, cultured for 24 hours, exemplified for two *S. epidermidis* (1457 and 9142) and one *E. coli* (Top10WT) strains. Typical Raman spectra from individual bacterial colonies are shown in (a); the related 3D plots of principle component relations for 30 repeat measurements compare (b) two bacteria types (c) two bacteria strains and (d) bacteria types and strains.

In order to investigate the reproducibility to differentiate between bacterial species, we compared the first five principal components (PCs) generated from Raman spectra taken from 30 colonies of *S. epidermidis* 1457 and *E. coli* Top10, respectively (see Figure 1(b)). In Figure 1 PC1 to PC3 are displayed in a 3D-plot; evidently, these three components seem to be sufficient to define and contain all of the variability in two clear clusters. Equally, a PC-plot, generated from 30 colonies of *S. epidermidis* 1457 and 9142, respectively, demonstrates that one also is able to differentiate between bacterial strains (see Figure 1(c)). We like to mention that a similarly defined distinction resulted from the comparison of the two *E. coli* strains Top10WT and K12 although these data are not included in the figure for brevity.

Finally, in Figure 1(d) all bacteria and strains shown in Figures 1(b) and 1(c) are included; the distinctive clustering is maintained although the relative cluster orientation is altered. This is a typical behaviour of principle component analysis when additional data sets are added to the evaluation. While the three PCs shown here are sufficient to provide clear distinction in this specific case, additional PCs may be necessary to achieve unique cluster association. Notably this is required when additional, closely-related strains of a bacteria species are included in the overall comparison. Specifically further bacteria strains—requires that additional PCs may be necessary to result in unique cluster association.

4. Conclusion

Our results from replicate measurements show that colonies of the same bacterial species and/or strains cluster together rather well; the exact nature of clustering is now under investigation. The most likely cause for cluster scatter is associated with the difficulty of measuring colonies at the same central location each time; but in addition there is evidence that the subtle phenotype differences in colonies on an agar plate contribute as well. Thus, the spread in clustering is associated with the variability in the measurement of a biological sample and carries the requirement for multiple measurements to define a bacterial population within a species or strain. Variability away from the cluster's centre will aid in defining the false positive rate, which is a parameter we are currently investigating. These findings are consistent with the research of Choo-Smith and coworkers who observed heterogeneity in microcolony analysis [9].

This study also underlines the importance of pinpointing the contributions made by individual principal component in the analysis. Understanding the key bacterial structures responsible for the Raman shifts (for a first library collection, see, e.g., [10])—defined within the first few, significant principal components—looks to be essential to assess the strengths and limitations of using this technique for routine discrimination of bacteria.

The exact understanding of the origin of individual spectral contributions is still in its infancy, but further comparisons of spectra from other sample specimens are now under way, with the hope that this should aid in the quest for full strain discrimination.

We also commenced to apply the methodology described in this study to other problems in clinical microbiology, such as antibiotic susceptibility testing, analysis of microcolonies and single cells, and the understanding of bacterial metabolism.

Acknowledgments

The authors thank Professor D. Mack for the archived bacterial samples. N. Kapel was supported by a PhD studentship of the Centre of NanoHealth, Swansea University; J. F. M. Almarashi was funded by Taibah University, Saudi Arabia.

References

- [1] G. Jannes and D. De Vos, "A review of current and future molecular diagnostic tests for use in the microbiology laboratory," *Methods in Molecular Biology*, vol. 345, pp. 1–21, 2006.

- [2] M. Kemp, K. H. Jensen, R. Dargis, and J. J. Christensen, "Routine ribosomal PCR and DNA sequencing for detection and identification of bacteria," *Future Microbiology*, vol. 5, no. 7, pp. 1101–1107, 2010.
- [3] C. Kirschner, K. Maquelin, P. Pina et al., "Classification and identification of enterococci: a comparative phenotypic, genotypic, and vibrational spectroscopic study," *Journal of Clinical Microbiology*, vol. 39, no. 5, pp. 1763–1770, 2001.
- [4] K. Maquelin, L. P. Choo-Smith, H. P. Endtz, H. A. Bruining, and G. J. Puppels, "Rapid identification of *Candida* species by confocal raman microspectroscopy," *Journal of Clinical Microbiology*, vol. 40, no. 2, pp. 594–600, 2002.
- [5] O. Samek, J. F. M. Al-Marashi, and H. H. Telle, "The potential of Raman spectroscopy for the identification of biofilm formation by *Staphylococcus epidermidis*," *Laser Physics Letters*, vol. 7, no. 5, pp. 378–383, 2010.
- [6] M. Harz, M. Kiehntopf, S. Stöckel et al., "Direct analysis of clinical relevant single bacterial cells from cerebrospinal fluid during bacterial meningitis by means of micro-Raman spectroscopy," *Journal of Biophotonics*, vol. 2, no. 1-2, pp. 70–80, 2009.
- [7] A. G. González, A. G. Ureña, R. J. Lewis, and G. Van Der Zwan, "Spectroscopy and kinetics of tyrosinase catalyzed trans-resveratrol oxidation," *Journal of Physical Chemistry B*, vol. 116, no. 8, pp. 2553–2560, 2012.
- [8] R. M. Jarvis, D. Broadhurst, H. Johnson, N. M. O'Boyle, and R. Goodacre, "PYCHEM: a multivariate analysis package for python," *Bioinformatics*, vol. 22, no. 20, pp. 2565–2566, 2006.
- [9] L. P. Choo-Smith, K. Maquelin, T. Van Vreeswijk et al., "Investigating microbial (Micro)colony heterogeneity by vibrational spectroscopy," *Applied and Environmental Microbiology*, vol. 67, no. 4, pp. 1461–1469, 2001.
- [10] J. De Gelder, K. De Gussem, P. Vandenabeele, and L. Moens, "Reference database of Raman spectra of biological molecules," *Journal of Raman Spectroscopy*, vol. 38, no. 9, pp. 1133–1147, 2007.

BIBLIOGRAPHY

- Almarashi, J. F. M., Kapel, N., Wilkinson, T. S., & Telle, H. H. Raman Spectroscopy of Bacterial Species and Strains Cultivated under Reproducible Conditions. *Spectroscopy: An International Journal*, 27(5-6):361–365, 2012. ISSN 0712-4813. doi: 10.1155/2012/540490. URL <http://www.hindawi.com/journals/spectroscopy/2012/540490/>.
- Alvarez, A. M. Integrated approaches for detection of plant pathogenic bacteria and diagnosis of bacterial diseases. *Annual review of phytopathology*, 42:339–66, January 2004. ISSN 0066-4286. doi: 10.1146/annurev.phyto.42.040803.140329. URL <http://www.ncbi.nlm.nih.gov/pubmed/15283670>.
- Aminov, R. I. A brief history of the antibiotic era: lessons learned and challenges for the future. *Frontiers in microbiology*, 1(December):134, January 2010. ISSN 1664-302X. doi: 10.3389/fmicb.2010.00134. URL <http://www.pubmedcentral.nih.gov/articlerender.fcgi?artid=3109405&tool=pmcentrez&rendertype=abstract>.
- Andreishcheva, E. & Vann, W. Gene products required for de novo synthesis of polysialic acid in Escherichia coli K1. *Journal of bacteriology*, 188(5):1786–1797, 2006. doi: 10.1128/JB.188.5.1786. URL <http://jbs.asm.org/content/188/5/1786.short>.
- Basiev, T., a.a. Sobol, Zverev, P., Ivleva, L., Osiko, V., & Powell, R. Raman spectroscopy of crystals for stimulated Raman scattering. *Optical Materials*, 11(4):307–314, March 1999. ISSN 09253467. doi: 10.1016/S0925-3467(98)00030-5. URL <http://linkinghub.elsevier.com/retrieve/pii/S0925346798000305>.
- Beier, B. D., Quivey, R. G., & Berger, A. J. Identification of different bacterial species in biofilms using confocal Raman microscopy. *Journal of biomedical optics*, 15(6):066001, 2010. ISSN 1560-2281. doi: 10.1117/1.

BIBLIOGRAPHY

3505010. URL <http://www.pubmedcentral.nih.gov/articlerender.fcgi?artid=3014224&tool=pmcentrez&rendertype=abstract>.

Bellot-Gurlet, L., Pages-Camagna, S., & Coupry, C. Raman spectroscopy in art and archaeology. In *Journal of raman spectroscopy*, pages 962–965, 2006. doi: 10.1002/jrs. URL <http://onlinelibrary.wiley.com/doi/10.1002/jrs.1217/abstract>.

Bonnier, F. & Byrne, H. J. Understanding the molecular information contained in principal component analysis of vibrational spectra of biological systems. *The Analyst*, 137(2):322–32, January 2012. ISSN 1364-5528. doi: 10.1039/c1an15821j. URL <http://www.ncbi.nlm.nih.gov/pubmed/22114757>.

Bonomo, R. Multiple antibiotic-resistant bacteria in long-term-care facilities: an emerging problem in the practice of infectious diseases. *Clinical infectious diseases*, pages 1414–1422, 2000. URL <http://cid.oxfordjournals.org/content/31/6/1414.short>.

Brachman, P. S. Infectious diseases—past, present, and future. *International Journal of Epidemiology*, 32(5):684–686, October 2003. ISSN 1464-3685. doi: 10.1093/ije/dyg282. URL <http://www.ije.oupjournals.org/cgi/doi/10.1093/ije/dyg282>.

Buijtsels, P. C. a. M., Willemse-Erix, H. F. M., Petit, P. L. C., Endtz, H. P., Puppels, G. J., Verbrugh, H. a., van Belkum, a., van Soolingen, D., & Maquelin, K. Rapid identification of mycobacteria by Raman spectroscopy. *Journal of clinical microbiology*, 46(3):961–5, March 2008. ISSN 1098-660X. doi: 10.1128/JCM.01763-07. URL <http://www.pubmedcentral.nih.gov/articlerender.fcgi?artid=2268361&tool=pmcentrez&rendertype=abstract>.

Cam, D., Keseroglu, K., Kahraman, M., Sahin, F., & Culha, M. Multiplex identification of bacteria in bacterial mixtures with surface-enhanced Raman scattering. *Journal of Raman Spectroscopy*, 41(5):484–489, October 2009. ISSN 03770486. doi: 10.1002/jrs.2475. URL <http://doi.wiley.com/10.1002/jrs.2475>.

Cançado, L. G., Hartschuh, A., & Novotny, L. Tip-enhanced Raman spectroscopy of carbon nanotubes. *Journal of Raman Spectroscopy*, 40(10):1420–1426, October 2009. doi: 10.1002/jrs.2448.

- Cantón, R. & Coque, T. M. The CTX-M beta-lactamase pandemic. *Current opinion in microbiology*, 9(5):466–75, October 2006. ISSN 1369-5274. doi: 10.1016/j.mib.2006.08.011. URL <http://www.ncbi.nlm.nih.gov/pubmed/16942899>.
- Cantón, R., Morosini, M. I., Martin, O., Maza, S. D., & Pedrosa, E. G. G. D. IRT and CMT b-lactamases and inhibitor resistance. 14:53–62, 2008.
- Carbonnelle, E., Mesquita, C., Bille, E., Day, N., Dauphin, B., Beretti, J.-L., Ferroni, A., Gutmann, L., & Nassif, X. MALDI-TOF mass spectrometry tools for bacterial identification in clinical microbiology laboratory. *Clinical biochemistry*, 44(1):104–9, January 2011. ISSN 1873-2933. doi: 10.1016/j.clinbiochem.2010.06.017. URL <http://www.ncbi.nlm.nih.gov/pubmed/20620134>.
- Carmeli, Y., Troillet, N., Karchmer, A., & Samore, M. Health and Economic Outcomes of Antibiotic Resistance in *Pseudomonas aeruginosa*. *Archives of International Medicine*, 159:1127–1132, 1999.
- Carroll, K. C., Glanz, B. D., Borek, A. P., Burger, C., Bhally, H. S., Henciak, S., & Flayhart, D. C. Evaluation of the BD Phoenix automated microbiology system for identification and antimicrobial susceptibility testing of staphylococci and enterococci. *Journal of clinical microbiology*, 44(6):2072–7, June 2006a. ISSN 0095-1137. doi: 10.1128/JCM.02636-05. URL <http://www.pubmedcentral.nih.gov/articlerender.fcgi?artid=1489426&tool=pmcentrez&rendertype=abstract>
<http://www.pubmedcentral.nih.gov/articlerender.fcgi?artid=1594749&tool=pmcentrez&rendertype=abstract>.
- Carroll, K. C., Glanz, B. D., Borek, A. P., Burger, C., Bhally, H. S., Henciak, S., & Flayhart, D. C. Evaluation of the BD Phoenix automated microbiology system for identification and antimicrobial susceptibility testing of Enterobacteriaceae. *Journal of clinical microbiology*, 44(6):2072–7, June 2006b. ISSN 0095-1137. doi: 10.1128/JCM.02636-05. URL <http://www.pubmedcentral.nih.gov/articlerender.fcgi?artid=1489426&tool=pmcentrez&rendertype=abstract>
<http://www.pubmedcentral.nih.gov/articlerender.fcgi?artid=1594749&tool=pmcentrez&rendertype=abstract>.

BIBLIOGRAPHY

- Chaplin, T. D., Clark, R. J. H., & Beech, D. R. Comparison of genuine (1851-1852 AD) and forged or reproduction Hawaiian Missionary stamps using Raman microscopy. *Journal of Raman Spectroscopy*, 33(6):424–428, June 2002. ISSN 1097-4555. doi: 10.1002/jrs.874. URL <http://dx.doi.org/10.1002/jrs.874>.
- Chen, J., Conache, G., Pistol, M.-E., Gray, S. M., Borgström, M. T., Xu, H., Xu, H. Q., Samuelson, L., & Håkanson, U. Probing strain in bent semiconductor nanowires with Raman spectroscopy. *Nano letters*, 10(4):1280–6, April 2010. ISSN 1530-6992. doi: 10.1021/nl904040y. URL <http://www.ncbi.nlm.nih.gov/pubmed/20192231>.
- Cho, L. Identification of textile fiber by Raman microspectroscopy. *Forensic Science Journal*, 6(1):55–62, 2007. URL <http://scholar.google.com/scholar?hl=en&btnG=Search&q=intitle:Identification+of+textile+fiber+by+Raman+microspectroscopy\#2>.
- Choo-Smith, L.-P., Edwards, H. G. M., Endtz, H. P., Kros, J. M., Heule, F., Barr, H., Robinson, J. S., Bruining, H. a., & Puppels, G. J. Medical applications of Raman spectroscopy: from proof of principle to clinical implementation. *Biopolymers*, 67(1): 1–9, January 2002. ISSN 0006-3525. doi: 10.1002/bip.10064. URL <http://www.ncbi.nlm.nih.gov/pubmed/11842408>.
- Choo-Smith, L. Investigating microbial (micro) colony heterogeneity by vibrational spectroscopy. ...*microbiology*, 2001. doi: 10.1128/AEM.67.4.1461. URL <http://aem.asm.org/content/67/4/1461.short>.
- Ciobot, V., Burkhardt, E.-M., Schumacher, W., Rösch, P., Küsel, K., & Popp, J. The influence of intracellular storage material on bacterial identification by means of Raman spectroscopy. *Analytical and bioanalytical chemistry*, 397(7):2929–37, August 2010. ISSN 1618-2650. doi: 10.1007/s00216-010-3895-1. URL <http://www.ncbi.nlm.nih.gov/pubmed/20582405>.
- Clermont, O., Bonacorsi, S., & Bingen, E. Rapid and simple determination of the Escherichia coli phylogenetic group. *Applied and environmental microbiology*, 66(10):4555–8, October 2000. ISSN 0099-2240. URL <http://www.pubmedcentral.nih.gov/articlerender.fcgi?artid=92342&tool=pmcentrez&rendertype=abstract>.

- Codeço, C. T. Endemic and epidemic dynamics of cholera: the role of the aquatic reservoir. *BMC infectious diseases*, 1:1, January 2001. ISSN 1471-2334. URL <http://www.pubmedcentral.nih.gov/articlerender.fcgi?artid=29087&tool=pmcentrez&rendertype=abstract>.
- Cohen, M. L. Resurgent and emergent disease in a changing world. *British medical bulletin*, 54(3):523–32, January 1998. ISSN 0007-1420. URL <http://www.ncbi.nlm.nih.gov/pubmed/10326281>.
- Costelloe, C., Metcalfe, C., Lovering, a., Mant, D., & Hay, a. D. Effect of antibiotic prescribing in primary care on antimicrobial resistance in individual patients: systematic review and meta-analysis. *Bmj*, 340(may18 2):c2096–c2096, May 2010. ISSN 0959-8138. doi: 10.1136/bmj.c2096. URL <http://www.bmj.com/cgi/doi/10.1136/bmj.c2096>.
- Culha, M., Kahraman, M., Çam, D., Sayn, I., & Keserolu, K. Rapid identification of bacteria and yeast using surface-enhanced Raman scattering. *Surface and Interface Analysis*, 42(6-7):462–465, March 2010. ISSN 01422421. doi: 10.1002/sia.3256. URL <http://doi.wiley.com/10.1002/sia.3256>.
- Davies, J. & Davies, D. Origins and evolution of antibiotic resistance. *Microbiology and molecular biology reviews : MMBR*, 74(3):417–33, September 2010. ISSN 1098-5557. doi: 10.1128/MMBR.00016-10. URL <http://www.pubmedcentral.nih.gov/articlerender.fcgi?artid=2937522&tool=pmcentrez&rendertype=abstract>.
- Davis, M. a., Baker, K. N. K., Orfe, L. H., Shah, D. H., Besser, T. E., & Call, D. R. Discovery of a gene conferring multiple-aminoglycoside resistance in *Escherichia coli*. *Antimicrobial agents and chemotherapy*, 54(6): 2666–9, June 2010. ISSN 1098-6596. doi: 10.1128/AAC.01743-09. URL <http://www.pubmedcentral.nih.gov/articlerender.fcgi?artid=2876372&tool=pmcentrez&rendertype=abstract>.
- De Beer, T., Burggraeve, a., Fonteyne, M., Saerens, L., Remon, J. P., & Vervaet, C. Near infrared and Raman spectroscopy for the in-process monitoring of pharmaceutical production processes. *International journal of pharmaceutics*, 417(1-2):32–47, September 2011. ISSN 1873-3476. doi: 10.1016/j.ijpharm.2010.12.012. URL <http://www.ncbi.nlm.nih.gov/pubmed/21167266>.

BIBLIOGRAPHY

- De Gelder, J. Reference database of Raman spectra of biological molecules. ...*Spectroscopy*, (April):1133–1147, 2007. doi: 10.1002/jrs. URL <http://onlinelibrary.wiley.com/doi/10.1002/jrs.1734/abstract>.
- De Gelder, J., De Gussem, K., Vandenabeele, P., De Vos, P., & Moens, L. Methods for extracting biochemical information from bacterial Raman spectra: an explorative study on *Cupriavidus metallidurans*. *Analytica chimica acta*, 585(2):234–40, March 2007a. ISSN 1873-4324. doi: 10.1016/j.aca.2006.12.050. URL <http://www.ncbi.nlm.nih.gov/pubmed/17386670>.
- De Gelder, J., De Gussem, K., Vandenabeele, P., Vancanneyt, M., De Vos, P., & Moens, L. Methods for extracting biochemical information from bacterial Raman spectra: focus on a group of structurally similar biomolecules–fatty acids. *Analytica chimica acta*, 603(2):167–75, November 2007b. ISSN 1873-4324. doi: 10.1016/j.aca.2007.09.049. URL <http://www.ncbi.nlm.nih.gov/pubmed/17963837>.
- De Gelder, J., Scheldeman, P., Leus, K., Heyndrickx, M., Vandenabeele, P., Moens, L., & De Vos, P. Raman spectroscopic study of bacterial endospores. *Analytical and bioanalytical chemistry*, 389(7-8):2143–51, December 2007c. ISSN 1618-2650. doi: 10.1007/s00216-007-1616-1. URL <http://www.ncbi.nlm.nih.gov/pubmed/17962923>.
- De Wael, K., Lepot, L., Gason, F., & Gilbert, B. In search of blood–detection of minute particles using spectroscopic methods. *Forensic science international*, 180(1):37–42, August 2008. ISSN 1872-6283. doi: 10.1016/j.forsciint.2008.06.013. URL <http://www.ncbi.nlm.nih.gov/pubmed/18706777>.
- Deckert, V. Tip-Enhanced Raman Spectroscopy. *Journal of Raman Spectroscopy*, 40 (10):1336–1337, October 2009. ISSN 03770486. doi: 10.1002/jrs.2452. URL <http://doi.wiley.com/10.1002/jrs.2452>.
- Doumith, M., Day, M. J., Hope, R., Wain, J., & Woodford, N. Improved multiplex PCR strategy for rapid assignment of the four major *Escherichia coli* phylogenetic groups. *Journal of clinical microbiology*, 50(9):3108–10, September 2012. ISSN 1098-660X. doi: 10.1128/JCM.01468-12. URL <http://www.pubmedcentral.nih.gov/articlerender.fcgi?artid=3421818&tool=pmcentrez&rendertype=abstract>.

- Downes, A. & Elfick, A. Raman spectroscopy and related techniques in biomedicine. *Sensors (Basel, Switzerland)*, 10(3):1871–89, January 2010. ISSN 1424-8220. doi: 10.3390/s100301871. URL <http://www.pubmedcentral.nih.gov/articlerender.fcgi?artid=3000600&tool=pmcentrez&rendertype=abstract>.
- Dudovich, N., Oron, D., & Silberberg, Y. Single-pulse coherently controlled nonlinear Raman spectroscopy and microscopy. *Nature*, 418(6897):512–4, August 2002. ISSN 0028-0836. doi: 10.1038/nature00933. URL <http://www.ncbi.nlm.nih.gov/pubmed/12152073>.
- Dutta, R., Sharma, P., & Pandey, A. Surface enhanced Raman spectra of Escherichia Coli cell using ZnO nanoparticles. *Dig. J. Nanomater. Biostruct*, 4(1):83–87, 2009. URL <http://chalcogen.ro/1RanuDutta.pdf>.
- Efrima, S. & Zeiri, L. Understanding SERS of bacteria. *Journal of Raman Spectroscopy*, 40(3):277–288, March 2009. ISSN 03770486. doi: 10.1002/jrs.2121. URL <http://doi.wiley.com/10.1002/jrs.2121>.
- Escoriza, M. F., VanBriesen, J. M., Stewart, S., Maier, J., & Treado, P. J. Raman spectroscopy and chemical imaging for quantification of filtered waterborne bacteria. *Journal of microbiological methods*, 66(1):63–72, July 2006. ISSN 0167-7012. doi: 10.1016/j.mimet.2005.10.013. URL <http://www.ncbi.nlm.nih.gov/pubmed/16325947>.
- Essack, S. Y. The development of beta-lactam antibiotics in response to the evolution of beta-lactamases. *Pharmaceutical research*, 18(10):1391–9, October 2001. ISSN 0724-8741. URL <http://www.ncbi.nlm.nih.gov/pubmed/11697463>.
- Eydmann, M., Ball, D., Sadler, G., & Wilks, M. Introduction of MALDI-TOF : a revolution in diagnostic. *Mass Spectroscopy*, pages 1–4, 2011. URL <http://www.bartsandthelondon.nhs.uk/assets/ilibrary/Our-Services/Pathology/Introduction-of-MALDI-TOF.pdf>.
- Fabian, H. & Anzenbacher, P. New developments in Raman spectroscopy of biological systems. *Vibrational Spectroscopy*, 4(2):125–148, January 1993. ISSN 09242031. doi: 10.1016/0924-2031(93)87032-O. URL <http://linkinghub.elsevier.com/retrieve/pii/0924203193870320>.

BIBLIOGRAPHY

- Fan, C., Hu, Z., Mustapha, A., & Lin, M. Rapid detection of food- and waterborne bacteria using surface-enhanced Raman spectroscopy coupled with silver nanosubstrates. *Applied microbiology and biotechnology*, 92(5):1053–61, December 2011. ISSN 1432-0614. doi: 10.1007/s00253-011-3634-3. URL <http://www.ncbi.nlm.nih.gov/pubmed/22005743>.
- Ferreira, L., Sánchez-Juanes, F., González-Avila, M., Cembrero-Fuciños, D., Herrero-Hernández, A., González-Buitrago, J. M., & Muñoz Bellido, J. L. Direct identification of urinary tract pathogens from urine samples by matrix-assisted laser desorption ionization-time of flight mass spectrometry. *Journal of clinical microbiology*, 48(6):2110–5, June 2010. ISSN 1098-660X. doi: 10.1128/JCM.02215-09. URL <http://www.pubmedcentral.nih.gov/articlerender.fcgi?artid=2884468&tool=pmcentrez&rendertype=abstract>.
- Fini, G. Applications of Raman spectroscopy to pharmacy. *Journal of Raman Spectroscopy*, 35(5):335–337, May 2004. ISSN 0377-0486. doi: 10.1002/jrs.1161. URL <http://doi.wiley.com/10.1002/jrs.1161>.
- Fleming, A. & Maclean, I. On the Occurrence of Influenza Bacilli in the Mouths of Normal Persons. *British journal of experimental pathology*, 1930. URL <http://www.ncbi.nlm.nih.gov/pmc/articles/PMC2048086/>.
- Gaus, K., Rösch, P., & Petry, R. Classification of lactic acid bacteria with UV-resonance Raman spectroscopy. ..., 82:286–290, 2006. doi: 10.1002/bip. URL <http://onlinelibrary.wiley.com/doi/10.1002/bip.20448/full>.
- Gensini, G. F., Conti, A. A., & Lippi, D. The contributions of Paul Ehrlich to infectious disease. *Journal of Infection*, 54(3):221–224, 2007. URL <http://www.sciencedirect.com/science/article/pii/S0163445306000557>.
- Gerrard, D. L. Raman spectroscopy. *Analytical chemistry*, 66(12):547R–557R, June 1994. ISSN 0003-2700. URL <http://www.ncbi.nlm.nih.gov/pubmed/8092477>.
- Giedraitien, A., Vitkauskien, A., Naginien, R., & Pavidonis, A. Antibiotic resistance mechanisms of clinically important bacteria. *Medicina (Kaunas, Lithuania)*, 47(3): 137–46, January 2011. ISSN 1648-9144. URL <http://www.ncbi.nlm.nih.gov/pubmed/21822035>.

- Gniadkowski, M., Schneider, I., Pal, A., Mikiewicz, B., & Bauernfeind, A. Cefotaxime-Resistant Enterobacteriaceae Isolates from a Hospital in Warsaw , Poland : Identification of a New CTX-M-3 Cefotaxime-Hydrolyzing β -Lactamase That Is Closely Related to the CTX-M-1 / MEN-1 Enzyme Cefotaxime-Resistant Enterobacteriaceae Isolate. 1998.
- Goodwin, J. Raman spectroscopic study of the heterogeneity of microcolonies of a pigmented bacterium. ... *of Raman Spectroscopy*, 37:932–936, 2006. URL <http://onlinelibrary.wiley.com/doi/10.1002/jrs.1523/abstract>.
- Grow, A. E., Wood, L. L., Claycomb, J. L., & Thompson, P. a. New biochip technology for label-free detection of pathogens and their toxins. *Journal of Microbiological Methods*, 53(2):221–233, May 2003. ISSN 01677012. doi: 10.1016/S0167-7012(03)00026-5. URL <http://linkinghub.elsevier.com/retrieve/pii/S0167701203000265>.
- Gubler, D. J. Resurgent vector-borne diseases as a global health problem. *Emerging infectious diseases*, 4(3):442–50, 1998. ISSN 1080-6040. doi: 10.3201/eid0403.980326. URL <http://www.pubmedcentral.nih.gov/articlerender.fcgi?artid=2640300&tool=pmcentrez&rendertype=abstract>.
- Guicheteau, J. & Christesen, S. Bacterial mixture identification using Raman and surface-enhanced Raman chemical imaging. *Journal of Raman ...*, 41(12):1632–1637, December 2010. doi: 10.1002/jrs.2601. URL <http://onlinelibrary.wiley.com/doi/10.1002/jrs.2601/full>.
- Guicheteau, J., Christesen, S., Emge, D., & Tripathi, A. Bacterial mixture identification using Raman and surface-enhanced Raman chemical imaging. *Journal of Raman Spectroscopy*, 41(12):1632–1637, December 2010. ISSN 03770486. doi: 10.1002/jrs.2601. URL <http://doi.wiley.com/10.1002/jrs.2601>.
- Hadjigeorgiou, K. Raman spectroscopy for UTI diagnosis and antibiogram. ... *and Applications in ...*, (November):5–7, 2009. URL http://ieeexplore.ieee.org/xpls/abs_all.jsp?arnumber=5394425.
- Hagrasy, A. E., Chang, S.-y., Desai, D., & Kiang, S. Application of Raman Spectroscopy for Quantitative In-Line Monitoring of Tablet. (February):1–4, 2006.

BIBLIOGRAPHY

- Haider, S., Wagner, M., Schmid, M. C., Sixt, B. S., Christian, J. G., Häcker, G., Pichler, P., Mechtler, K., Müller, A., Baranyi, C., Toenshoff, E. R., Montanaro, J., & Horn, M. Raman microspectroscopy reveals long-term extracellular activity of Chlamydiae. *Molecular microbiology*, 77(3):687–700, August 2010. ISSN 1365-2958. doi: 10.1111/j.1365-2958.2010.07241.x. URL <http://www.ncbi.nlm.nih.gov/pubmed/20545842>.
- Hall, E. K., Singer, G. a., Pözl, M., Hämmerle, I., Schwarz, C., Daims, H., Maixner, F., & Battin, T. J. Looking inside the box: using Raman microspectroscopy to deconstruct microbial biomass stoichiometry one cell at a time. *The ISME journal*, 5(2):196–208, March 2011. ISSN 1751-7370. doi: 10.1038/ismej.2010.115. URL <http://www.pubmedcentral.nih.gov/articlerender.fcgi?artid=3105696&tool=pmcentrez&rendertype=abstract>.
- Hall, M. L.-v. & Fluit, A. BD Phoenix, VITEK 1, and VITEK 2 automated instruments for detection of extended-spectrum beta-lactamases in multiresistant *Escherichia coli* and *Klebsiella* spp. *Journal of clinical ...*, 40(10):3703–3711, 2002. doi: 10.1128/JCM.40.10.3703. URL <http://jcm.asm.org/content/40/10/3703.short>.
- Hanlon, E. B., Manoharan, R., Koo, T. W., Shafer, K. E., Motz, J. T., Fitzmaurice, M., Kramer, J. R., Itzkan, I., Dasari, R. R., & Feld, M. S. Prospects for in vivo Raman spectroscopy. *Physics in medicine and biology*, 45(2):R1–59, February 2000. ISSN 0031-9155. URL <http://www.ncbi.nlm.nih.gov/pubmed/10701500>.
- Haque, M. S., Naseem, H. a., Shultz, J. L., Brown, W. D., Lal, S., & Gangopadhyay, S. Comparison of infrared, Raman, photoluminescence, and x-ray photoelectron spectroscopy for characterizing arc-jet-deposited diamond films. *Journal of Applied Physics*, 83(8):4421, 1998. ISSN 00218979. doi: 10.1063/1.367201. URL <http://link.aip.org/link/JAPIAU/v83/i8/p4421/s1&Agg=doi>.
- Harhay, G. & Siragusa, G. HYDROGEN-DEUTERIUM EXCHANGE AND ULTRAVIOLET RESONANCE RAMAN SPECTROSCOPY OF BACTERIA IN A COMPLEX FOOD MATRIX1. *...of Rapid Methods & Automation in ...*, 7(402):25–38, 1999. URL <http://onlinelibrary.wiley.com/doi/10.1111/j.1745-4581.1999.tb00369.x/abstract>.
- Harz, M., Rösch, P., Peschke, K.-D., Ronneberger, O., Burkhardt, H., & Popp, J. Micro-Raman spectroscopic identification of bacterial cells of the genus *Staphylococcus* and

- dependence on their cultivation conditions. *The Analyst*, 130(11):1543–50, November 2005. ISSN 0003-2654. doi: 10.1039/b507715j. URL <http://www.ncbi.nlm.nih.gov/pubmed/16222378>.
- Harz, M., Kiehntopf, M., Stöckel, S., Rösch, P., Straube, E., Deufel, T., & Popp, J. Direct analysis of clinical relevant single bacterial cells from cerebrospinal fluid during bacterial meningitis by means of micro-Raman spectroscopy. *Journal of biophotonics*, 2(1-2):70–80, February 2009. ISSN 1864-0648. doi: 10.1002/jbio.200810068. URL <http://www.ncbi.nlm.nih.gov/pubmed/19343686>.
- Horstkotte, M. A., Knobloch, J. K., Rohde, H., Dobinsky, S., & Mack, D. Evaluation of the BD PHOENIX automated microbiology system for detection of methicillin resistance in coagulase-negative staphylococci. *J Clin Microbiol*, 42(11):5041–5046, 2004. doi: 42/11/5041[pii]10.1128/JCM.42.11.5041-5046.2004. URL <http://jcm.asm.org/content/42/11/5041.short><http://www.ncbi.nlm.nih.gov/pubmed/15528693>.
- Huang, Y. Y., Beal, C. M., Cai, W. W., Ruoff, R. S., & Terentjev, E. M. Micro-Raman spectroscopy of algae: composition analysis and fluorescence background behavior. *Biotechnology and bioengineering*, 105(5):889–98, April 2010. ISSN 1097-0290. doi: 10.1002/bit.22617. URL <http://www.ncbi.nlm.nih.gov/pubmed/19998275>.
- Hutsebaut, D., Vandroemme, J., Heyrman, J., Dawyndt, P., Vandenabeele, P., Moens, L., & de Vos, P. Raman microspectroscopy as an identification tool within the phylogenetically homogeneous 'Bacillus subtilis' group. *Systematic and applied microbiology*, 29(8):650–60, December 2006. ISSN 0723-2020. doi: 10.1016/j.syapm.2006.02.001. URL <http://www.ncbi.nlm.nih.gov/pubmed/16564151>.
- Isenberg, H. & Berkman, J. Microbial diagnosis in a general hospital. *Annals of the New York Academy of...*, 1962. URL <http://onlinelibrary.wiley.com/doi/10.1111/j.1749-6632.1962.tb30587.x/abstract>.
- Ivleva, N. P., Wagner, M., Horn, H., Niessner, R., & Haisch, C. In situ surface-enhanced Raman scattering analysis of biofilm. *Analytical chemistry*, 80(22):8538–44, November 2008. ISSN 1520-6882. doi: 10.1021/ac801426m. URL <http://www.ncbi.nlm.nih.gov/pubmed/18947197>.

BIBLIOGRAPHY

- Ivleva, N. P., Wagner, M., Horn, H., Niessner, R., & Haisch, C. Towards a nondestructive chemical characterization of biofilm matrix by Raman microscopy. *Analytical and bioanalytical chemistry*, 393(1):197–206, January 2009. ISSN 1618-2650. doi: 10.1007/s00216-008-2470-5. URL <http://www.ncbi.nlm.nih.gov/pubmed/18979092>.
- Jarvis, R., Law, N., & Shadi, I. Surface-enhanced Raman scattering from intracellular and extracellular bacterial locations. *Analytical ...*, 80(17):6741–6746, 2008. doi: 10.1039/b705973f.(25). URL <http://pubs.acs.org/doi/abs/10.1021/ac800838v>.
- Jarvis, R. M. & Goodacre, R. Ultra-violet resonance Raman spectroscopy for the rapid discrimination of urinary tract infection bacteria. *FEMS microbiology letters*, 232(2): 127–32, March 2004a. ISSN 0378-1097. doi: 10.1016/S0378-1097(04)00040-0. URL <http://www.ncbi.nlm.nih.gov/pubmed/15033230>.
- Jarvis, R. M. & Goodacre, R. Discrimination of bacteria using surface-enhanced Raman spectroscopy. *Analytical chemistry*, 76(1):40–7, January 2004b. ISSN 0003-2700. doi: 10.1021/ac034689c. URL <http://www.ncbi.nlm.nih.gov/pubmed/22577658>.
- Jarvis, R. M. & Goodacre, R. Characterisation and identification of bacteria using SERS. *Chemical Society reviews*, 37(5):931–6, May 2008. ISSN 0306-0012. doi: 10.1039/b705973f. URL <http://www.ncbi.nlm.nih.gov/pubmed/18443678>.
- Jarvis, R. M., Brooker, A., & Goodacre, R. Surface-enhanced Raman spectroscopy for bacterial discrimination utilizing a scanning electron microscope with a Raman spectroscopy interface. *Analytical chemistry*, 76(17):5198–202, September 2004. ISSN 0003-2700. doi: 10.1021/ac049663f. URL <http://www.ncbi.nlm.nih.gov/pubmed/15373461>.
- Jarvis, R. M., Brooker, A., & Goodacre, R. Surface-enhanced Raman scattering for the rapid discrimination of bacteria. *Faraday Discussions*, 132(0):281, 2006. ISSN 1359-6640. doi: 10.1039/b506413a. URL <http://xlink.rsc.org/?DOI=b506413a>.
- Jehlička, J., Oren, A., & Víték, P. Use of Raman spectroscopy for identification of compatible solutes in halophilic bacteria. *Extremophiles : life under extreme conditions*,

- 16(3):507–14, May 2012. ISSN 1433-4909. doi: 10.1007/s00792-012-0450-3. URL <http://www.ncbi.nlm.nih.gov/pubmed/22527044>.
- Johnson, J. R. Virulence factors in *Escherichia coli* urinary tract infection. *Clinical microbiology reviews*, 4(1):80–128, January 1991. ISSN 0893-8512. URL <http://www.pubmedcentral.nih.gov/articlerender.fcgi?artid=358180&tool=pmcentrez&rendertype=abstract>.
- Jones, C. *No TitleMolecular epidemiology of extended-spectrum B-lactamase (ESBL) carrying Enterobacteriaceae at ABM University Health Board*. PhD thesis, Swansea University, 2012. URL <https://ifind.swan.ac.uk/discover/Record/626623#.U9WIHvldXKM>.
- Jorgensen, J. H. & Ferraro, M. J. Antimicrobial susceptibility testing: a review of general principles and contemporary practices. *Clinical infectious diseases : an official publication of the Infectious Diseases Society of America*, 49(11):1749–55, December 2009. ISSN 1537-6591. doi: 10.1086/647952. URL <http://www.ncbi.nlm.nih.gov/pubmed/19857164>.
- Kahraman, M., Yazici, M. M., Sahin, F., & Culha, M. Convective assembly of bacteria for surface-enhanced Raman scattering. *Langmuir : the ACS journal of surfaces and colloids*, 24(3):894–901, February 2008. ISSN 0743-7463. doi: 10.1021/la702240q. URL <http://www.ncbi.nlm.nih.gov/pubmed/18179261>.
- Kahraman, M., Zamaleeva, A. I., Fakhrullin, R. F., & Culha, M. Layer-by-layer coating of bacteria with noble metal nanoparticles for surface-enhanced Raman scattering. *Analytical and bioanalytical chemistry*, 395(8):2559–67, December 2009. ISSN 1618-2650. doi: 10.1007/s00216-009-3159-0. URL <http://www.ncbi.nlm.nih.gov/pubmed/19795108>.
- Kailer, A., Nickel, K. G., & Gogotsi, Y. G. Raman microspectroscopy of nanocrystalline and amorphous phases in hardness indentations. *Journal of Raman Spectroscopy*, 30(10):939–946, October 1999. ISSN 1097-4555. doi: 10.1002/(SICI)1097-4555(199910)30:10<939::AID-JRS460>3.0.CO;2-C. URL [http://dx.doi.org/10.1002/\(SICI\)1097-4555\(199910\)30:10<939::AID-JRS460>3.0.CO2-C](http://dx.doi.org/10.1002/(SICI)1097-4555(199910)30:10<939::AID-JRS460>3.0.CO2-C).

BIBLIOGRAPHY

- Kastanos, E., Kyriakides, A., Hadjigeorgiou, K., & Pitris, C. Identification and Antibiotic Sensitivity of UTI Pathogens Using Raman Spectroscopy. *cdn.intechweb.org*, 2008. URL <http://cdn.intechweb.org/pdfs/20574.pdf>.
- Kastanos, E., Kyriakides, A., Hadjigeorgiou, K., & Pitris, C. A Novel Method for Bacterial UTI Diagnosis Using Raman Spectroscopy. *International Journal of Spectroscopy*, 2012:1–13, 2012. ISSN 1687-9449. doi: 10.1155/2012/195317. URL <http://www.hindawi.com/journals/ijss/2012/195317/>.
- Khorasaninejad, M., Adachi, M. M., Walia, J., Karim, K. S., & Saini, S. S. Raman spectroscopy of core/shell silicon nanowires grown on different substrates. *Physica Status Solidi (a)*, 5:n/a–n/a, November 2012. ISSN 18626300. doi: 10.1002/pssa.201228235. URL <http://doi.wiley.com/10.1002/pssa.201228235>.
- Kim, M., Heo, S. R., Choi, S. H., Kwon, H., Park, J. S., Seong, M.-W., Lee, D.-H., Park, K. U., Song, J., & Kim, E.-C. Comparison of the MicroScan, VITEK 2, and Crystal GP with 16S rRNA sequencing and MicroSeq 500 v2.0 analysis for coagulase-negative Staphylococci. *BMC microbiology*, 8: 233, January 2008. ISSN 1471-2180. doi: 10.1186/1471-2180-8-233. URL <http://www.pubmedcentral.nih.gov/articlerender.fcgi?artid=2633347&tool=pmcentrez&rendertype=abstract>.
- Kirschner, C., Maquelin, K., & Pina, P. Classification and identification of enterococci: a comparative phenotypic, genotypic, and vibrational spectroscopic study. *Journal of clinical ...*, 39(5):1763–1770, 2001. doi: 10.1128/JCM.39.5.1763. URL <http://jcm.asm.org/content/39/5/1763.short>.
- Knauer, M., Ivleva, N. P., Niessner, R., & Haisch, C. A flow-through microarray cell for the online SERS detection of antibody-captured E. coli bacteria. *Analytical and bioanalytical chemistry*, 402(8):2663–7, March 2012. ISSN 1618-2650. doi: 10.1007/s00216-011-5398-0. URL <http://www.ncbi.nlm.nih.gov/pubmed/21947437>.
- Kneipp, K., Kneipp, H., Itzkan, I., Dasari, R. R., & Feld, M. S. Ultrasensitive chemical analysis by Raman spectroscopy. *Chemical reviews*, 99(10):2957–76, October 1999. ISSN 1520-6890. URL <http://www.ncbi.nlm.nih.gov/pubmed/11749507>.

- Kniggendorf, A.-K. & Meinhardt-Wollweber, M. Of microparticles and bacteria identification—(resonance) Raman micro-spectroscopy as a tool for biofilm analysis. *Water research*, 45(15):4571–82, October 2011. ISSN 1879-2448. doi: 10.1016/j.watres.2011.06.007. URL <http://www.ncbi.nlm.nih.gov/pubmed/21741670>.
- Kniggendorf, A.-K., Gaul, T. W., & Meinhardt-Wollweber, M. Effects of ethanol, formaldehyde, and gentle heat fixation in confocal resonance Raman microscopy of purple nonsulfur bacteria. *Microscopy research and technique*, 74(2):177–83, February 2011. ISSN 1097-0029. doi: 10.1002/jemt.20889. URL <http://www.ncbi.nlm.nih.gov/pubmed/20544803>.
- Kourkoumelis, N., Polymeros, A., & Tzaphlidou, M. Background Estimation of Biomedical Raman Spectra Using a Geometric Approach. *Spectroscopy: An International Journal*, 27(5-6):441–447, 2012. ISSN 0712-4813. doi: 10.1155/2012/530791. URL <http://www.hindawi.com/journals/spectroscopy/2012/530791/>.
- Krause, M. & Radt, B. The investigation of single bacteria by means of fluorescence staining and Raman spectroscopy. ... of *Raman Spectroscopy*, (March):369–372, 2007. doi: 10.1002/jrs. URL <http://onlinelibrary.wiley.com/doi/10.1002/jrs.1721/abstract>.
- Krause, M., Rösch, P., Radt, B., & Popp, J. Localizing and identifying living bacteria in an abiotic environment by a combination of Raman and fluorescence microscopy. *Analytical chemistry*, 80(22):8568–75, November 2008. ISSN 1520-6882. doi: 10.1021/ac8014559. URL <http://www.ncbi.nlm.nih.gov/pubmed/18847286>.
- Kumar, A., Roberts, D., Wood, K. E., Light, B., Parrillo, J. E., Sharma, S., Suppes, R., Feinstein, D., Zanotti, S., Taiberg, L., Gurka, D., Kumar, A., & Cheang, M. Duration of hypotension before initiation of effective antimicrobial therapy is the critical determinant of survival in human septic shock. *Critical care medicine*, 34(6):1589–96, June 2006. ISSN 0090-3493. doi: 10.1097/01.CCM.0000217961.75225.E9. URL <http://www.ncbi.nlm.nih.gov/pubmed/16625125>.
- Lederberg, J. & Lederberg, E. M. Replica plating and indirect selection of bacterial mutants. *Journal of bacteriology*, 63(3):399–406, March 1952. ISSN 0021-9193. URL <http://www.pubmedcentral.nih.gov/articlerender.fcgi?artid=1203627&tool=pmcentrez&rendertype=abstract>.

BIBLIOGRAPHY

- Lepot, L., De Wael, K., Gason, F., & Gilbert, B. Application of Raman spectroscopy to forensic fibre cases. *Science & justice : journal of the Forensic Science Society*, 48(3): 109–17, September 2008. ISSN 1355-0306. doi: 10.1016/j.scijus.2007.09.013. URL <http://www.ncbi.nlm.nih.gov/pubmed/18953798>.
- Levy, S. B. & Marshall, B. Antibacterial resistance worldwide: causes, challenges and responses. *Nature medicine*, 10(12 Suppl):S122–9, December 2004. ISSN 1078-8956. doi: 10.1038/nm1145. URL <http://www.ncbi.nlm.nih.gov/pubmed/15577930>.
- Lin, C.-c., Yang, Y.-m., & Chang, H.-c. Raman discrimination of *Helicobacter pylori* fingerprint in dielectrophoresis chip. *2009 4th IEEE International Conference on Nano/Micro Engineered and Molecular Systems*, (I):793–796, 2009. doi: 10.1109/NEMS.2009.5068697. URL <http://ieeexplore.ieee.org/lpdocs/epic03/wrapper.htm?arnumber=5068697>.
- Lin, H.-H., Li, Y.-C., Chang, C.-H., Liu, C., Yu, A. L., & Chen, C.-H. Single nuclei Raman spectroscopy for drug evaluation. *Analytical chemistry*, 84(1):113–20, January 2012. ISSN 1520-6882. doi: 10.1021/ac201900h. URL <http://www.ncbi.nlm.nih.gov/pubmed/22053782>.
- Liu, T.-T., Lin, Y.-H., Hung, C.-S., Liu, T.-J., Chen, Y., Huang, Y.-C., Tsai, T.-H., Wang, H.-H., Wang, D.-W., Wang, J.-K., Wang, Y.-L., & Lin, C.-H. A high speed detection platform based on surface-enhanced Raman scattering for monitoring antibiotic-induced chemical changes in bacteria cell wall. *PLoS one*, 4(5):e5470, January 2009. ISSN 1932-6203. doi: 10.1371/journal.pone.0005470. URL <http://www.pubmedcentral.nih.gov/articlerender.fcgi?artid=2674953&tool=pmcentrez&rendertype=abstract>.
- Livermore, D. M., Canton, R., Gniadkowski, M., Nordmann, P., Rossolini, G. M., Arlet, G., Ayala, J., Coque, T. M., Kern-Zdanowicz, I., Luzzaro, F., Poirel, L., & Woodford, N. CTX-M: changing the face of ESBLs in Europe. *The Journal of antimicrobial chemotherapy*, 59(2):165–74, February 2007. ISSN 0305-7453. doi: 10.1093/jac/dkl483. URL <http://www.ncbi.nlm.nih.gov/pubmed/17158117>.
- Longworth, D. L. Update in infectious disease treatment. *Cleveland Clinic journal of medicine*, 75(8):584–90, August 2008. ISSN 0891-1150. URL <http://www.ncbi.nlm.nih.gov/pubmed/21474210>.

- Lopez, F. J., Givan, U., Connell, J. G., & Lauhon, L. J. Silicon nanowire polytypes: identification by Raman spectroscopy, generation mechanism, and misfit strain in homostructures. *ACS nano*, 5(11):8958–66, November 2011. ISSN 1936-086X. doi: 10.1021/nn2031337. URL <http://www.ncbi.nlm.nih.gov/pubmed/22017649>.
- López-Díez, E. C., Winder, C. L., Ashton, L., Currie, F., & Goodacre, R. Monitoring the mode of action of antibiotics using Raman spectroscopy: investigating subinhibitory effects of amikacin on *Pseudomonas aeruginosa*. *Analytical chemistry*, 77(9):2901–6, May 2005. ISSN 0003-2700. doi: 10.1021/ac048147m. URL <http://www.ncbi.nlm.nih.gov/pubmed/15859609>.
- Luo, B. S. & Lin, M. a Portable Raman System for the Identification of Foodborne Pathogenic Bacteria. *Journal of Rapid Methods & Automation in Microbiology*, 16(3): 238–255, September 2008. ISSN 10603999. doi: 10.1111/j.1745-4581.2008.00131.x. URL <http://doi.wiley.com/10.1111/j.1745-4581.2008.00131.x>.
- Mack, D., Siemssen, N., & Laufs, R. Parallel induction by glucose of adherence and a polysaccharide antigen specific for plastic-adherent *Staphylococcus epidermidis*: evidence for functional relation to intercellular adhesion. *Infection and immunity*, 60(5):2048–57, May 1992. ISSN 0019-9567. URL <http://www.pubmedcentral.nih.gov/articlerender.fcgi?artid=257114&tool=pmcentrez&rendertype=abstract>.
- Manoharan, R., Ghiamati, E., Dalterio, R., Britton, K., Nelson, W., & Sperry, J. UV resonance Raman spectra of bacteria, bacterial spores, protoplasts and calcium dipicolinate. *Journal of Microbiological Methods*, 11(1):1–15, February 1990. ISSN 01677012. doi: 10.1016/0167-7012(90)90042-5. URL <http://www.sciencedirect.com/science/article/pii/0167701290900425>.
- Maquelin, K. & Choo-Smith, L. Rapid identification of *Candida* species by confocal Raman microspectroscopy. *Journal of clinical ...*, 40(2):594–600, 2002. doi: 10.1128/JCM.40.2.594. URL <http://jcm.asm.org/content/40/2/594.short>.
- Maquelin, K. & Kirschner, C. Prospective study of the performance of vibrational spectroscopies for rapid identification of bacterial and fungal pathogens recovered from blood cultures. *Journal of clinical ...*, 2003. doi: 10.1128/JCM.41.1.324. URL <http://jcm.asm.org/content/41/1/324.short>.

BIBLIOGRAPHY

- Maquelin, K., Choo-Smith, L. P., van Vreeswijk, T., Endtz, H. P., Smith, B., Bennett, R., Bruining, H. a., & Puppels, G. J. Raman spectroscopic method for identification of clinically relevant microorganisms growing on solid culture medium. *Analytical chemistry*, 72(1):12–9, January 2000. ISSN 0003-2700. URL <http://www.ncbi.nlm.nih.gov/pubmed/10655628>.
- Maquelin, K., Kirschner, C., Choo-Smith, L.-P., van den Braak, N., Endtz, H. P., Naumann, D., & Puppels, G. J. Identification of medically relevant microorganisms by vibrational spectroscopy. *Journal of microbiological methods*, 51(3):255–71, November 2002. ISSN 0167-7012. URL <http://www.ncbi.nlm.nih.gov/pubmed/12223286>.
- Maquelin, K., Kirschner, C., Vreeswijk, T. V., Stämmeler, M., Endtz, H. P., Bruining, H. A., Naumann, D., & Puppels, G. J. Prospective Study of the Performance of Vibrational Spectroscopies for Rapid Identification of Bacterial and Fungal Pathogens Recovered from Blood Cultures Prospective Study of the Performance of Vibrational Spectroscopies for Rapid Identification of Bact. 2003. doi: 10.1128/JCM.41.1.324.
- Maquelin, K., Hoogenboezem, T., Jachtenberg, J.-W., Dumke, R., Jacobs, E., Puppels, G. J., Hartwig, N. G., & Vink, C. Raman spectroscopic typing reveals the presence of carotenoids in *Mycoplasma pneumoniae*. *Microbiology (Reading, England)*, 155 (Pt 6):2068–77, June 2009. ISSN 1350-0872. doi: 10.1099/mic.0.026724-0. URL <http://www.ncbi.nlm.nih.gov/pubmed/19383695>.
- Marcolli, C. & Wiedemann, H. Distinction of Original and Forged Lithographs by Means of Thermogravimetry and Raman Spectroscopy. *Journal of Thermal Analysis and Calorimetry*, 64(3):987–1000, June 2001. doi: 10.1023/A:1011587316504. URL <http://dx.doi.org/10.1023/A:1011587316504>.
- Mariani, M. M., Day, P. J. R., & Deckert, V. Applications of modern micro-Raman spectroscopy for cell analyses. *Integrative biology : quantitative biosciences from nano to macro*, 2(2-3):94–101, March 2010. ISSN 1757-9708. doi: 10.1039/b920572a. URL <http://www.ncbi.nlm.nih.gov/pubmed/20473387>.
- Mello, C., Ribeiro, D., Novaes, F., & Poppi, R. J. Rapid differentiation among bacteria that cause gastroenteritis by use of low-resolution Raman spectroscopy and PLS

- discriminant analysis. *Analytical and bioanalytical chemistry*, 383(4):701–6, October 2005. ISSN 1618-2642. doi: 10.1007/s00216-005-0017-6. URL <http://www.ncbi.nlm.nih.gov/pubmed/16158301>.
- Méric, G., Kemsley, E. K., Falush, D., Siggers, E. J., & Lucchini, S. Phylogenetic distribution of traits associated with plant colonization in *Escherichia coli*. *Environmental microbiology*, 15(2):487–501, February 2013. ISSN 1462-2920. doi: 10.1111/j.1462-2920.2012.02852.x. URL <http://www.ncbi.nlm.nih.gov/pubmed/22934605>.
- Mobili, P. & Londero, A. Multivariate analysis of Raman spectra applied to microbiology: Discrimination of microorganisms at the species level. *Revista mexicana de ...*, 56(5):378–385, 2010. URL http://www.scielo.org.mx/scielo.php?pid=S0035-001X2010000500004&script=sci_arttext&tlng=pt.
- Morens, D. M., Folkers, G. K., & Fauci, A. S. The challenge of emerging and re-emerging infectious diseases. *Nature*, 430(6996):242–9, July 2004. ISSN 1476-4687. doi: 10.1038/nature02759. URL <http://www.ncbi.nlm.nih.gov/pubmed/15241422>.
- Moritz, T. J., Polage, C. R., Taylor, D. S., Krol, D. M., Lane, S. M., & Chan, J. W. Evaluation of *Escherichia coli* cell response to antibiotic treatment by use of Raman spectroscopy with laser tweezers. *Journal of clinical microbiology*, 48(11):4287–90, November 2010a. ISSN 1098-660X. doi: 10.1128/JCM.01565-10. URL <http://www.pubmedcentral.nih.gov/articlerender.fcgi?artid=3020843&tool=pmcentrez&rendertype=abstract>.
- Moritz, T. J., Taylor, D. S., Polage, C. R., Krol, D. M., Lane, S. M., & Chan, J. W. Effect of cefazolin treatment on the nonresonant Raman signatures of the metabolic state of individual *Escherichia coli* cells. *Analytical chemistry*, 82(7):2703–10, April 2010b. ISSN 1520-6882. doi: 10.1021/ac902351a. URL <http://www.ncbi.nlm.nih.gov/pubmed/20196565>.
- Muldrew, K. L. Molecular diagnostics of infectious diseases. *Current opinion in pediatrics*, 21(1):102–11, February 2009. ISSN 1531-698X. doi: 10.1097/MOP.0b013e328320d87e. URL <http://www.ncbi.nlm.nih.gov/pubmed/19242246>.

BIBLIOGRAPHY

- Nari, B. GenBank Accession #: L09137 pUC19 is a small, high-copy number. URL http://www.neb.com/~media/NebUs/PageImages/ToolsandResources/InteractiveTools/DNASequencesandMaps/pUC19_map.pdf.
- Neugebauer, U. & Schmid, U. Characterization of bacterial growth and the influence of antibiotics by means of UV resonance Raman spectroscopy. ..., 82:306–311, 2006. doi: 10.1002/bip. URL <http://onlinelibrary.wiley.com/doi/10.1002/bip.20447/full>.
- Nicolaou, N., Xu, Y., & Goodacre, R. Fourier transform infrared and Raman spectroscopies for the rapid detection, enumeration, and growth interaction of the bacteria *Staphylococcus aureus* and *Lactococcus lactis* ssp. *cremoris* in milk. *Analytical chemistry*, 83(14):5681–7, July 2011. ISSN 1520-6882. doi: 10.1021/ac2008256. URL <http://www.ncbi.nlm.nih.gov/pubmed/21639098>.
- Novagen. pET-26b (+) Restriction Map. URL http://pef.aibn.uq.edu.au/wordpress/wp-content/blogs.dir/1/files/Support/Bacteria/Vectors/pET/pET_26+.pdf.
- Ovsyannikov, S. V., Shchennikov, V. V., Ponosov, Y. S., Gudina, S. V., Guk, V. G., Skipetrov, E. P., & Mogilenskikh, V. E. Application of the high-pressure thermoelectric technique for characterization of semiconductor microsamples: PbX-based compounds. *Journal of Physics D: Applied Physics*, 37(8): 1151–1157, April 2004. ISSN 0022-3727. doi: 10.1088/0022-3727/37/8/002. URL <http://stacks.iop.org/0022-3727/37/i=8/a=002?key=crossref.694b7bb65f13d9f0e9a26a145619d72f>.
- Palchadhuri, S., Rehse, S. J., Hamasha, K., Syed, T., Kurtovic, E. E., & Stenger, J. Raman spectroscopy of xylitol uptake and metabolism in Gram-positive and Gram-negative bacteria. *Applied and environmental microbiology*, 77(1): 131–7, January 2011. ISSN 1098-5336. doi: 10.1128/AEM.01458-10. URL <http://www.pubmedcentral.nih.gov/articlerender.fcgi?artid=3019703&tool=pmcentrez&rendertype=abstract>.
- Pappas, D., Smith, B. W., & Winefordner, J. D. Raman spectroscopy in bioanalysis. *Talanta*, 51(1):131–44, January 2000. ISSN 1873-3573. URL <http://www.ncbi.nlm.nih.gov/pubmed/18967845>.

- Patel, I. & Premasiri, W. Barcoding bacterial cells: a SERS-based methodology for pathogen identification. *Journal of Raman ...*, (October):1660–1672, 2008. doi: 10.1002/jrs. URL <http://onlinelibrary.wiley.com/doi/10.1002/jrs.2064/abstract><http://onlinelibrary.wiley.com/doi/10.1002/jrs.2064/full>.
- Peláez, F. The historical delivery of antibiotics from microbial natural products—can history repeat? *Biochemical pharmacology*, 71(7):981–90, March 2006. ISSN 0006-2952. doi: 10.1016/j.bcp.2005.10.010. URL <http://www.ncbi.nlm.nih.gov/pubmed/16290171>.
- Pereira, L., Sousa, A., Coelho, H., Amado, A. M., & Ribeiro-Claro, P. J. Use of FTIR, FT-Raman and ¹³C-NMR spectroscopy for identification of some seaweed phyco-colloids. *Biomolecular Engineering*, 20(4-6):223–228, July 2003. ISSN 13890344. doi: 10.1016/S1389-0344(03)00058-3. URL <http://linkinghub.elsevier.com/retrieve/pii/S1389034403000583>.
- Petersen, K. & McMillan, W. Toward next generation clinical diagnostic instruments: scaling and new processing paradigms. *Biomedical ...*, pages 71–79, 1998. URL <http://link.springer.com/article/10.1023/A:1009986407026>.
- Petrov, G. I., Arora, R., Yakovlev, V. V., Wang, X., Sokolov, A. V., & Scully, M. O. Comparison of coherent and spontaneous Raman microspectroscopies for noninvasive detection of single bacterial endospores. *Proceedings of the National Academy of Sciences of the United States of America*, 104(19):7776–9, May 2007. ISSN 0027-8424. doi: 10.1073/pnas.0702107104. URL <http://www.pubmedcentral.nih.gov/articlerender.fcgi?artid=1876523&tool=pmcentrez&rendertype=abstract>.
- Petry, R., Schmitt, M., & Popp, J. Raman spectroscopy—a prospective tool in the life sciences. *Chemphyschem : a European journal of chemical physics and physical chemistry*, 4(1):14–30, January 2003. ISSN 1439-4235. doi: 10.1002/cphc.200390004. URL <http://www.ncbi.nlm.nih.gov/pubmed/12596463>.
- Pfaller, M. a. & Herwaldt, L. a. The clinical microbiology laboratory and infection control: emerging pathogens, antimicrobial resistance, and new technology. *Clinical infectious diseases : an official publication of the Infectious Diseases Society of America*,

BIBLIOGRAPHY

- 25(4):858–70, October 1997. ISSN 1058-4838. URL <http://www.ncbi.nlm.nih.gov/pubmed/9356802>.
- Piscanec, S., Cantoro, M., Ferrari, a., Zapien, J., Lifshitz, Y., Lee, S., Hofmann, S., & Robertson, J. Raman spectroscopy of silicon nanowires. *Physical Review B*, 68(24): 241312, December 2003. ISSN 0163-1829. doi: 10.1103/PhysRevB.68.241312. URL <http://link.aps.org/doi/10.1103/PhysRevB.68.241312>.
- Premasiri, W. R., Gebregziabher, Y., & Ziegler, L. D. On the difference between surface-enhanced raman scattering (SERS) spectra of cell growth media and whole bacterial cells. *Applied spectroscopy*, 65(5):493–9, May 2011. ISSN 1943-3530. doi: 10.1366/10-06173. URL <http://www.ncbi.nlm.nih.gov/pubmed/21513591>.
- Ravindranath, S. P., Henne, K. L., Thompson, D. K., & Irudayaraj, J. Surface-enhanced Raman imaging of intracellular bioreduction of chromate in *Shewanella oneidensis*. *PloS one*, 6(2):e16634, January 2011. ISSN 1932-6203. doi: 10.1371/journal.pone.0016634. URL <http://www.pubmedcentral.nih.gov/articlerender.fcgi?artid=3045368&tool=pmcentrez&rendertype=abstract>.
- Ravindranath, S. P., Kadam, U. S., Thompson, D. K., & Irudayaraj, J. Intracellularly grown gold nanoislands as SERS substrates for monitoring chromate, sulfate and nitrate localization sites in remediating bacteria biofilms by Raman chemical imaging. *Analytica chimica acta*, 745:1–9, October 2012. ISSN 1873-4324. doi: 10.1016/j.aca.2012.07.037. URL <http://www.ncbi.nlm.nih.gov/pubmed/22938600>.
- Reuben, J., Bachur, N., Novak, R., Armstrong, R., Sullivan, T., & Borgoyne, T. Preliminary Evaluation and Overview of Phoenix , A New Automated ID / AST System ABSTRACT. (March), 1999.
- Richardson, H. & Small, F. Recent Advances Medical Microbiology. *Journal of the Royal Society of Medicine*, pages 1060–1062, 1998. URL <http://www.ncbi.nlm.nih.gov/pmc/articles/PMC1902277/>.
- Rivers, E. P., McIntyre, L., Morro, D. C., & Rivers, K. K. Early and innovative interventions for severe sepsis and septic shock: taking advantage of a window of opportunity. *CMAJ : Canadian Medical Association journal = journal de l'Association medicale canadienne*, 173(9):1054–65, October 2005. ISSN 1488-2329. doi: 10.1503/cmaj.

050632. URL <http://www.pubmedcentral.nih.gov/articlerender.fcgi?artid=1266331&tool=pmcentrez&rendertype=abstract>.
- Robert, B. Resonance Raman spectroscopy. *Photosynthesis research*, 101(2-3):147–55, 2009. ISSN 1573-5079. doi: 10.1007/s11120-009-9440-4. URL <http://www.ncbi.nlm.nih.gov/pubmed/19568956>.
- Rösch, P., Schmitt, M., Kiefer, W., & Popp, J. The identification of microorganisms by micro-Raman spectroscopy. *Journal of Molecular Structure*, 661-662:363–369, December 2003. ISSN 00222860. doi: 10.1016/j.molstruc.2003.06.004. URL <http://linkinghub.elsevier.com/retrieve/pii/S0022286003005106>.
- Rösch, P., Harz, M., & Schmitt, M. Chemotaxonomic identification of single bacteria by micro-Raman spectroscopy: application to clean-room-relevant biological contaminations. *Applied and ...*, 71(3):1626–1637, 2005. doi: 10.1128/AEM.71.3.1626. URL <http://aem.asm.org/content/71/3/1626.short>.
- Rossi, E. E., Pinheiro, A. L. B., Baltatu, O. C., Pacheco, M. T. T., & Silveira, L. Differential diagnosis between experimental endophthalmitis and uveitis in vitreous with Raman spectroscopy and principal components analysis. *Journal of photochemistry and photobiology. B, Biology*, 107:73–8, February 2012. ISSN 1873-2682. doi: 10.1016/j.jphotobiol.2011.12.001. URL <http://www.ncbi.nlm.nih.gov/pubmed/22209031>.
- Rubino, S., Cappuccinelli, P., & Kelvin, D. J. Escherichia coli (STEC) serotype O104 outbreak causing haemolytic syndrome (HUS) in Germany and France. *Journal of infection in developing countries*, 5(6):437–40, June 2011. ISSN 1972-2680. URL <http://www.ncbi.nlm.nih.gov/pubmed/21727641>.
- Salahioglu, F. & Went, M. J. Differentiation of lipsticks by Raman spectroscopy. *Forensic science international*, 223(1-3):148–52, November 2012. ISSN 1872-6283. doi: 10.1016/j.forsciint.2012.08.018. URL <http://www.ncbi.nlm.nih.gov/pubmed/22959771>.
- Samek, O., Telle, H., Harris, L., Bloomfield, M., & Mack, D. Raman spectroscopy for rapid discrimination of Staphylococcus epidermidis clones related to medical device-associated infections. *Laser Physics Letters*, 5(6):465–470, June 2008. ISSN

BIBLIOGRAPHY

16122011. doi: 10.1002/lapl.200810011. URL <http://doi.wiley.com/10.1002/lapl.200810011>.

Samek, O., Al-Marashi, J., & Telle, H. The potential of Raman spectroscopy for the identification of biofilm formation by *Staphylococcus epidermidis*. *Laser Physics Letters*, 7(5):378–383, May 2010a. ISSN 16122011. doi: 10.1002/lapl.200910154. URL <http://doi.wiley.com/10.1002/lapl.200910154>.

Samek, O., Al-Marashi, J. F. M., & Telle, H. H. The potential of Raman spectroscopy for the identification of biofilm formation by *Staphylococcus epidermidis*. *Laser Physics Letters*, 7(5):378–383, May 2010b. ISSN 16122011. doi: 10.1002/lapl.200910154. URL <http://doi.wiley.com/10.1002/lapl.200910154>.

Samek, O., Jonáš, A., Pilát, Z., & Zemánek, P. Raman microspectroscopy of individual algal cells: sensing unsaturation of storage lipids in vivo. *Sensors*, 2010c. doi: 10.3390/s100x0000x. URL <http://www.mdpi.com/1424-8220/10/9/8635/> [htmhttp://www.mdpi.com/1424-8220/10/9/8635/pdf](http://www.mdpi.com/1424-8220/10/9/8635/pdf).

Schneider, D., Duperchy, E., Depeyrot, J., Coursange, E., Lenski, R., & Blot, M. Genomic comparisons among *Escherichia coli* strains B, K-12, and O157:H7 using IS elements as molecular markers. *BMC microbiology*, 2:18, July 2002. ISSN 1471-2180. URL <http://www.pubmedcentral.nih.gov/articlerender.fcgi?artid=117601&tool=pmcentrez&rendertype=abstract>.

Schuster, K. C., Urlaub, E., & Gapes, J. R. Single-cell analysis of bacteria by Raman microscopy: spectral information on the chemical composition of cells and on the heterogeneity in a culture. *Journal of microbiological methods*, 42(1):29–38, September 2000. ISSN 0167-7012. URL <http://www.ncbi.nlm.nih.gov/pubmed/11000428>.

Sengupta, A., Mujacic, M., & Davis, E. J. Detection of bacteria by surface-enhanced Raman spectroscopy. *Analytical and bioanalytical chemistry*, 386(5):1379–86, November 2006. ISSN 1618-2642. doi: 10.1007/s00216-006-0711-z. URL <http://www.ncbi.nlm.nih.gov/pubmed/16933128>.

Sidjabat, H. E., Townsend, K. M., Hanson, N. D., Bell, J. M., Stokes, H. W., Gobius, K. S., Moss, S. M., & Trott, D. J. Identification of bla(CMY-7) and associated plasmid-mediated resistance genes in multidrug-resistant *Escherichia coli* isolated from dogs at

- a veterinary teaching hospital in Australia. *The Journal of antimicrobial chemotherapy*, 57(5):840–8, May 2006. ISSN 0305-7453. doi: 10.1093/jac/dkl057. URL <http://www.ncbi.nlm.nih.gov/pubmed/16524894>.
- Smith, J. P. & Hinson-Smith, V. Probing single molecules in living cells. *Analytical chemistry*, 72(23):732A, December 2000. ISSN 0003-2700. URL <http://www.ncbi.nlm.nih.gov/pubmed/11128953>.
- Smith, R. D. & Coast, J. Antimicrobial resistance: a global response. *Bulletin of the World Health Organization*, 80(2):126–33, January 2002. ISSN 0042-9686. URL <http://www.pubmedcentral.nih.gov/articlerender.fcgi?artid=2567729&tool=pmcentrez&rendertype=abstract>.
- Starbuck, C., Spartalis, A., Wai, L., Wang, J., Fernandez, P., Lindemann, C. M., Zhou, G. X., & Ge, Z. Process Optimization of a Complex Pharmaceutical Polymorphic System via In Situ Raman Spectroscopy. *Crystal Growth & Design*, 2(6):515–522, November 2002. ISSN 1528-7483. doi: 10.1021/cg025559k. URL <http://pubs.acs.org/doi/abs/10.1021/cg025559k>.
- Stefaniuk, E., Mrówka, A., & Hryniewicz, W. Susceptibility testing and resistance phenotypes detection in bacterial pathogens using the VITEK 2 System. *Polish journal of microbiology / Polskie Towarzystwo Mikrobiologów = The Polish Society of Microbiologists*, 54(4):311–6, January 2005. ISSN 1733-1331. URL <http://www.ncbi.nlm.nih.gov/pubmed/16599303>.
- Stern, A. M. & Markel, H. The history of vaccines and immunization: familiar patterns, new challenges. *Health affairs (Project Hope)*, 24(3):611–21, 2005. ISSN 0278-2715. doi: 10.1377/hlthaff.24.3.611. URL <http://www.ncbi.nlm.nih.gov/pubmed/15886151>.
- Stöckel, S., Schumacher, W., Meisel, S., Elschner, M., Rösch, P., & Popp, J. Raman spectroscopy-compatible inactivation method for pathogenic endospores. *Applied and environmental microbiology*, 76(9):2895–907, May 2010. ISSN 1098-5336. doi: 10.1128/AEM.02481-09. URL <http://www.pubmedcentral.nih.gov/articlerender.fcgi?artid=2863453&tool=pmcentrez&rendertype=abstract>.

BIBLIOGRAPHY

- Stockle, R. M., Suh, Y. D., Deckert, V., & Zenobi, R. Nanoscale chemical analysis by tip-enhanced Raman spectroscopy. (February):131–136, 2000.
- Stokes, H. W. & Gillings, M. R. Gene flow, mobile genetic elements and the recruitment of antibiotic resistance genes into Gram-negative pathogens. *FEMS microbiology reviews*, 35(5):790–819, September 2011. ISSN 1574-6976. doi: 10.1111/j.1574-6976.2011.00273.x. URL <http://www.ncbi.nlm.nih.gov/pubmed/21517914>.
- Takeuchi, H., Hashimoto, S., & Harada, I. Simple and Efficient Method to Eliminate Spike Noise from Spectra Recorded on Charge-Coupled Device Detectors. *Appl. Spectrosc.*, 47(1):129–131, 1993. URL <http://as.osa.org/abstract.cfm?URI=as-47-1-129>.
- Tallury, P., Malhotra, A., Byrne, L. M., & Santra, S. Nanobioimaging and sensing of infectious diseases. *Advanced drug delivery reviews*, 62(4-5):424–37, March 2010. ISSN 1872-8294. doi: 10.1016/j.addr.2009.11.014. URL <http://www.ncbi.nlm.nih.gov/pubmed/19931579>.
- Tang, H., Yao, H., Wang, G., Wang, Y., Li, Y.-Q., & Feng, M. NIR Raman spectroscopic investigation of single mitochondria trapped by optical tweezers. *Optics express*, 15(20):12708–16, October 2007. ISSN 1094-4087. URL <http://www.ncbi.nlm.nih.gov/pubmed/19550539>.
- Tang, Y. W., Procop, G. W., & Persing, D. H. Molecular diagnostics of infectious diseases. *Clinical chemistry*, 43(11):2021–38, November 1997. ISSN 0009-9147. URL <http://www.ncbi.nlm.nih.gov/pubmed/9365385>.
- Tatem, A. J., Rogers, D. J., & Hay, S. I. Global transport networks and infectious disease spread. *Advances in parasitology*, 62(05):293–343, January 2006. ISSN 0065-308X. doi: 10.1016/S0065-308X(05)62009-X. URL <http://www.pubmedcentral.nih.gov/articlerender.fcgi?artid=3145127&tool=pmcentrez&rendertype=abstract>.
- Triebold, S., Luvizotto, G. L., Tolosana-Delgado, R., Zack, T., & Eynatten, H. Discrimination of TiO₂ polymorphs in sedimentary and metamorphic rocks. *Contributions to Mineralogy and Petrology*, 161(4):581–596, July 2010. ISSN 0010-7999. doi: 10.1007/s00410-010-0551-x. URL <http://www.springerlink.com/index/10.1007/s00410-010-0551-x>.

- Troop, P. Health Protection in the 21st Century. Technical report, Health Protection Agency, London, 2005.
- Tunkel, A. R., Hartman, B. J., Kaplan, S. L., Kaufman, B. a., Roos, K. L., Scheld, W. M., & Whitley, R. J. Practice guidelines for the management of bacterial meningitis. *Clinical infectious diseases : an official publication of the Infectious Diseases Society of America*, 39(9):1267–84, November 2004. ISSN 1537-6591. doi: 10.1086/425368. URL <http://www.ncbi.nlm.nih.gov/pubmed/15494903>.
- Tzouveleakis, L. S., Tzelepi, E., Tassios, P. T., & Legakis, N. J. CTX-M-type beta-lactamases: an emerging group of extended-spectrum enzymes. *International journal of antimicrobial agents*, 14(2):137–42, March 2000. ISSN 0924-8579. URL <http://www.ncbi.nlm.nih.gov/pubmed/10720804>.
- Vandenabeele, P., Edwards, H. G. M., & Moens, L. A decade of Raman spectroscopy in art and archaeology. *Chemical reviews*, 107(3):675–86, March 2007a. ISSN 0009-2665. doi: 10.1021/cr068036i. URL <http://www.ncbi.nlm.nih.gov/pubmed/17315936>.
- Vandenabeele, P., Ortega-Avilès, M., Castilleros, D. T., & Moens, L. Raman spectroscopic analysis of Mexican natural artists' materials. *Spectrochimica acta. Part A, Molecular and biomolecular spectroscopy*, 68(4):1085–8, December 2007b. ISSN 1386-1425. doi: 10.1016/j.saa.2007.01.031. URL <http://www.ncbi.nlm.nih.gov/pubmed/17347030>.
- Vankeirsbilck, T., Vercauteren, A., & Baeyens, W. Applications of Raman spectroscopy in pharmaceutical analysis. 21(12), September 2002. ISSN 0513-4870. URL <http://144.206.159.178/ft/987/78523/1324542.pdf>.
- Waghorn, D. J. Serological testing in a microbiology laboratory of specimens from patients with suspected infectious disease. *Journal of clinical pathology*, 48(4):358–63, April 1995. ISSN 0021-9746. URL <http://www.pubmedcentral.nih.gov/articlerender.fcgi?artid=502556&tool=pmcentrez&rendertype=abstract>.
- Wagner, M. Single-cell ecophysiology of microbes as revealed by Raman microspectroscopy or secondary ion mass spectrometry imaging. *Annual review of microbiol-*

BIBLIOGRAPHY

ogy, 63:411–29, January 2009. ISSN 1545-3251. doi: 10.1146/annurev.micro.091208.073233. URL <http://www.ncbi.nlm.nih.gov/pubmed/19514853>.

Walter, A., Reinicke, M., Bocklitz, T., Schumacher, W., Rösch, P., Kothe, E., & Popp, J. Raman spectroscopic detection of physiology changes in plasmid-bearing *Escherichia coli* with and without antibiotic treatment. *Analytical and bioanalytical chemistry*, 400(9):2763–73, July 2011. ISSN 1618-2650. doi: 10.1007/s00216-011-4819-4. URL <http://www.ncbi.nlm.nih.gov/pubmed/21424521>.

Weldon, M. K., Morris, M. D., Harris, a. B., & Stoll, J. K. Surface enhanced Raman spectroscopic monitor of *P. acnes* lipid hydrolysis in vitro. *Journal of lipid research*, 39(9):1896–9, September 1998. ISSN 0022-2275. URL <http://www.ncbi.nlm.nih.gov/pubmed/9741703>.

Wiegand, I., Geiss, H. K., Mack, D., Stürenburg, E., & Seifert, H. Detection of extended-spectrum beta-lactamases among Enterobacteriaceae by use of semiautomated microbiology systems and manual detection procedures. *Journal of clinical microbiology*, 45(4):1167–74, April 2007. ISSN 0095-1137. doi: 10.1128/JCM.01988-06. URL <http://www.pubmedcentral.nih.gov/articlerender.fcgi?artid=1865808&tool=pmcentrez&rendertype=abstract>.

Willemse-Erix, D. F. M., Scholtes-Timmerman, M. J., Jachtenberg, J.-W., van Leeuwen, W. B., Horst-Kreft, D., Bakker Schut, T. C., Deurenberg, R. H., Puppels, G. J., van Belkum, A., Vos, M. C., & Maquelin, K. Optical fingerprinting in bacterial epidemiology: Raman spectroscopy as a real-time typing method. *Journal of clinical microbiology*, 47(3):652–9, March 2009. ISSN 1098-660X. doi: 10.1128/JCM.01900-08. URL <http://www.pubmedcentral.nih.gov/articlerender.fcgi?artid=2650950&tool=pmcentrez&rendertype=abstract>.

Willemse-Erix, H. F. M., Jachtenberg, J., Barutçi, H., Puppels, G. J., van Belkum, a., Vos, M. C., & Maquelin, K. Proof of principle for successful characterization of methicillin-resistant coagulase-negative staphylococci isolated from skin by use of Raman spectroscopy and pulsed-field gel electrophoresis. *Journal of clinical microbiology*, 48(3):736–40, March 2010. ISSN 1098-660X. doi: 10.1128/JCM.01153-09. URL <http://www.pubmedcentral.nih.gov/articlerender.fcgi?artid=2832465&tool=pmcentrez&rendertype=abstract>.

- Woodford, N., Ward, M. E., Kaufmann, M. E., Turton, J., Fagan, E. J., James, D., Johnson, a. P., Pike, R., Warner, M., Cheasty, T., Pearson, a., Harry, S., Leach, J. B., Loughrey, a., Lowes, J. a., Warren, R. E., & Livermore, D. M. Community and hospital spread of *Escherichia coli* producing CTX-M extended-spectrum beta-lactamases in the UK. *The Journal of antimicrobial chemotherapy*, 54(4):735–43, October 2004. ISSN 0305-7453. doi: 10.1093/jac/dkh424. URL <http://www.ncbi.nlm.nih.gov/pubmed/15347638>.
- Woodford, N. & Sundsfjord, A. Molecular detection of antibiotic resistance: when and where? *The Journal of antimicrobial chemotherapy*, 56(2):259–61, August 2005. ISSN 0305-7453. doi: 10.1093/jac/dki195. URL <http://www.ncbi.nlm.nih.gov/pubmed/15967769>.
- Woodford, N., Turton, J. F., & Livermore, D. M. Multiresistant Gram-negative bacteria: the role of high-risk clones in the dissemination of antibiotic resistance. *FEMS microbiology reviews*, 35(5):736–55, September 2011. ISSN 1574-6976. doi: 10.1111/j.1574-6976.2011.00268.x. URL <http://www.ncbi.nlm.nih.gov/pubmed/21303394>.
- Xie, C. & Li, Y.-q. Confocal micro-Raman spectroscopy of single biological cells using optical trapping and shifted excitation difference techniques. *Journal of Applied Physics*, 93(5):2982, 2003. ISSN 00218979. doi: 10.1063/1.1542654. URL <http://link.aip.org/link/JAPIAU/v93/i5/p2982/s1\&Agg=doi>.
- Xie, C., Nguyen, N., Zhu, Y., & Li, Y.-q. Detection of the Recombinant Proteins in Single Transgenic Microbial Cell Using Laser Tweezers and Raman Spectroscopy lactin was inserted into two different expression vectors. 79(24):9269–9275, 2007.
- Yamamoto, T., Yamagata, S., Horii, K., & Yamagishi, S. Comparison of transcription of beta-lactamase genes specified by various ampicillin transposons. *Journal of bacteriology*, 150(1):269–76, April 1982. ISSN 0021-9193. URL <http://www.pubmedcentral.nih.gov/articlerender.fcgi?artid=220109\&tool=pmcentrez\&rendertype=abstract>.
- Yang, X., Gu, C., Qian, F., Li, Y., & Zhang, J. Z. Highly sensitive detection of proteins and bacteria in aqueous solution using surface-enhanced Raman scattering and optical fibers. *Analytical chemistry*, 83(15):5888–94, August 2011. ISSN 1520-6882.

BIBLIOGRAPHY

doi: 10.1021/ac200707t. URL <http://www.ncbi.nlm.nih.gov/pubmed/21692506>.

Yoneyama, H. & Katsumata, R. Antibiotic resistance in bacteria and its future for novel antibiotic development. *Bioscience, biotechnology, and biochemistry*, 70(5):1060–75, May 2006. ISSN 0916-8451. URL <http://www.ncbi.nlm.nih.gov/pubmed/16717405>.

Yoshikawa, T. T., Editor, S., & Bonomo, R. A. Multiple Antibiotic Resistant Bacteria in Long-Term-Care Facilities : An Emerging Problem in the Practice of Infectious Diseases. pages 1414–1422.

Zhou, A., McEwen, G., & Wu, Y. Combined AFM/Raman microspectroscopy for characterization of living cells in near physiological conditions. pages 515–522, 2010. URL <http://www.formatex.info/microscopy4/515-522.pdf>.

Zhu, Q., Quivey, R. G., & Berger, A. J. Measurement of bacterial concentration fractions in polymicrobial mixtures by Raman microspectroscopy. *Journal of biomedical optics*, 9(6):1182–6, 2004. ISSN 1083-3668. doi: 10.1117/1.1803844. URL <http://www.ncbi.nlm.nih.gov/pubmed/15568938>.

